Research Topics

Effect of disturbance on natural forest regeneration in a changing tropical environment

Edited by
Donald Mlambo, Munesh Kumar, Stephen Syampungani
and Uttam Kumar Sahoo

Published in
Frontiers in Forests and Global Change

ISSN 1664-8714
ISBN 978-2-8325-3475-5
DOI 10.3389/978-2-8325-3475-5

About Frontiers

Frontiers is more than just an open access publisher of scholarly articles: it is a pioneering approach to the world of academia, radically improving the way scholarly research is managed. The grand vision of Frontiers is a world where all people have an equal opportunity to seek, share and generate knowledge. Frontiers provides immediate and permanent online open access to all its publications, but this alone is not enough to realize our grand goals.

Frontiers journal series

The Frontiers journal series is a multi-tier and interdisciplinary set of open-access, online journals, promising a paradigm shift from the current review, selection and dissemination processes in academic publishing. All Frontiers journals are driven by researchers for researchers; therefore, they constitute a service to the scholarly community. At the same time, the *Frontiers journal series* operates on a revolutionary invention, the tiered publishing system, initially addressing specific communities of scholars, and gradually climbing up to broader public understanding, thus serving the interests of the lay society, too.

Dedication to quality

Each Frontiers article is a landmark of the highest quality, thanks to genuinely collaborative interactions between authors and review editors, who include some of the world's best academicians. Research must be certified by peers before entering a stream of knowledge that may eventually reach the public - and shape society; therefore, Frontiers only applies the most rigorous and unbiased reviews. Frontiers revolutionizes research publishing by freely delivering the most outstanding research, evaluated with no bias from both the academic and social point of view. By applying the most advanced information technologies, Frontiers is catapulting scholarly publishing into a new generation.

What are Frontiers Research Topics?

Frontiers Research Topics are very popular trademarks of the *Frontiers journals series*: they are collections of at least ten articles, all centered on a particular subject. With their unique mix of varied contributions from Original Research to Review Articles, Frontiers Research Topics unify the most influential researchers, the latest key findings and historical advances in a hot research area.

Find out more on how to host your own Frontiers Research Topic or contribute to one as an author by contacting the Frontiers editorial office: frontiersin.org/about/contact

Effect of disturbance on natural forest regeneration in a changing tropical environment

Topic editors
Donald Mlambo — National University of Science and Technology, Zimbabwe
Munesh Kumar — Hemwati Nandan Bahuguna Garhwal University, India
Stephen Syampungani — Copperbelt University, Zambia
Uttam Kumar Sahoo — Mizoram University, India

Citation
Mlambo, D., Kumar, M., Syampungani, S., Sahoo, U. K., eds. (2023). *Effect of disturbance on natural forest regeneration in a changing tropical environment*. Lausanne: Frontiers Media SA. doi: 10.3389/978-2-8325-3475-5

Table of contents

frontiers | Frontiers in Forests and Global Change

TYPE Editorial
PUBLISHED 20 October 2023
DOI 10.3389/ffgc.2023.1289315

OPEN ACCESS

EDITED AND REVIEWED BY
Geertje M. F. Van Der Heijden,
University of Nottingham, United Kingdom

*CORRESPONDENCE
Donald Mlambo
✉ dmlambo8@gmail.com

RECEIVED 05 September 2023
ACCEPTED 05 October 2023
PUBLISHED 20 October 2023

CITATION
Mlambo D, Kumar M, Sahoo UK and Syampungani S (2023) Editorial: Effect of forest disturbances on natural forest regeneration in a changing tropical environment.
Front. For. Glob. Change 6:1289315.
doi: 10.3389/ffgc.2023.1289315

Editorial: Effect of forest disturbances on natural forest regeneration in a changing tropical environment

Donald Mlambo[1]*, Munesh Kumar[2], Uttam Kumar Sahoo[3] and Stephen Syampungani[4]

[1]Department of Forest Resources and Wildlife Management, Faculty of Environmental Science, National University of Science and Technology, Bulawayo, Zimbabwe, [2]Department of Forestry and Natural Resources, Hemvati Nandan Bahuguna Garhwal University (A Central University), Srinagar, Uttarakhand, India, [3]Department of Forestry, Mizoram University, Aizawl, India, [4]Department of Plant and Environmental Science, Copperbelt University, Kitwe, Zambia

KEYWORDS

disturbance, forest regeneration, tropical environment, nutrient cycling, carbon storage

Editorial on the Research Topic
Effect of forest disturbances on natural forest regeneration in a changing tropical environment

Introduction

In tropical forests, the human footprint continues to expand and recent estimates show that ∼82% of the remaining tropical forest ecosystems are degraded (Watson et al., 2018). Disturbances are predicted to increase in tropical forests due to human activities such as agricultural expansion, timber extraction, charcoal production, livestock grazing, and infrastructure development (Vancutsem et al., 2021; Baumann et al., 2022). These activities threaten the survival of many species and reduce the ability of the forests to provide ecosystem goods and services to local communities. Forest regeneration in tropical forests is a dynamic and intricate process influenced by a myriad of interrelated elements. Understanding the effect of disturbances on natural regeneration is crucial for effective forest management and conservation, as well as fostering resilient and diverse tropical ecosystems. By unraveling the effects of disturbances on natural regeneration, we can develop strategies to support the long-term sustainability of tropical forests that are known to harbor more than half of the world's terrestrial floral and faunal species (Pillay et al., 2022).

The objective of this Research Topic was to gain a better understanding of the effects of disturbances on natural forest regeneration in a changing tropical environment. This editorial highlights the key findings of the seven papers submitted under this topic and contextualizes them in terms of disturbance implications on natural regeneration. Contributions to this topic can help conservationists and policymakers develop strategies to improve tropical forest ecosystem recovery and long-term sustainability in the face of continuous environmental issues. We acknowledge that the topic is complex and multifaceted because natural forest regeneration is controlled by a number of interconnected elements such as light availability, soil conditions, climate, nutrient availability, competition, herbivory, and seed predation.

Effect of forest disturbance on seed regeneration

Forest disturbances can trigger successional processes, leading to changes in vegetation composition and structure (Poorter et al., 2023). As the forest recovers, early successional species may be gradually replaced by later successional species with different seed regeneration strategies. Zhou et al. simulated the effect of light in canopy gaps on the growth rates of seedlings from early-, mid-, and late-successional stages in tropical montane forest in Hainan Island, China. These authors showed that light conditions under small canopy gaps (10–15% full sunlight) and large canopy gaps (40–50% full sunlight) induced greater growth rates for seedlings from early- and mid-successional stages than from late-successional stage. Their findings have important implications for the management of disturbed tropical forests because they show that canopy gaps created by disturbances (e.g., cyclones and wildfires) create a benign environment for seedlings of light-demanding tree species but not for seedlings of deep shade-adapted tree species.

Effect of forest disturbance on natural regeneration, soil carbon, and nutrient cycling

Forest disturbances such as wildfires, logging, or natural events can affect key ecosystem processes that support natural regeneration including soil carbon and nutrient cycling. A summary of several studies accepted under this topic reveals that tropical forests are undergoing alterations in carbon and nitrogen biogeochemical cycles, which may impair natural regeneration processes. A study by Tiwari et al. showed that human disturbance in the montane forests of the Garhwal Himalaya in India altered plant species composition, soil properties, and carbon stock. Their results indicate that some species may be more resilient to disturbances and have adaptations that allow them to thrive in disturbed environments, while others may be more susceptible to mortality. Tiwari et al. further highlighted that human pressures in tropical forests can accelerate soil erosion, which can transfer carbon-rich topsoil away from the site. According to Saleem et al., agroforestry can provide numerous benefits in terms of minimizing the effects of disturbances in tropical forests and helping in ecosystem restoration. Their findings highlight how the presence of trees in agroforestry systems may provide additional sources of organic matter via litterfall, which adds to soil nutrient inputs and organic matter.

The contribution of fine roots to soil organic matter through mortality is frequently underestimated in tropical forests. Awasthi et al. and Pandey et al. found that fine roots play an important role in soil organic matter accumulation and nutrient return to soil. Although these studies suggest that human disturbances can increase root turnover in tropical forests, detailed studies are required to address the effect of anthropogenic disturbances such as fire and logging on fine root mortality and decomposition and nutrient release to the soil. Depending on the severity and frequency of the disturbance, as well as the unique characteristics of the forest ecosystem, disturbances are anticipated to have varying impacts on fine root turnover in tropical forests.

George-Chacon et al. used chronosequence data, satellite observations, and a carbon cycle model to determine woody carbon dynamics in two dry forest ecotypes (semi-deciduous and semi-evergreen) in Yucatán, Mexico. The study demonstrated that the rate and extent of carbon storage and sequestration can vary depending on various factors including species composition, environmental conditions, and ecological processes. The study provided important insights on how woody biomass stocks can change under different disturbance frequencies. This study predicted that increases in temperature and declines in precipitation reduce the capacity of dry forests to regenerate and store carbon. Such predictions are useful for effective forest management, climate change mitigation, and conservation of carbon-rich tropical forests.

Yaseen et al. studied responses of plant functional traits in tropical dwarf forest on Hainan Island and highlighted that plant functional traits can be used to predict soil nutrients and ecosystem functioning. This study provided a better understanding of the importance of selecting different species across multiple trait axes in the restoration of degraded tropical forests. However, further studies are needed to explore the soil properties and their association with plant functional features and their role in ecosystem functioning.

Conclusion

The seven papers presented have enhanced our understanding on the effect of disturbances on natural forest regeneration in tropical environments thus far but there are still some research gaps that need to be addressed. First, there is need for studies that investigate the long-term effects of different types of disturbances (e.g., logging, fire, and climate change) on natural regeneration processes in tropical forests. Second, because tropical forests are exposed to several disturbances at the same time, the interacting effects of multiple disturbances on natural regeneration need to be investigated. Third, studies are scarce in the tropical region that demonstrate the role of different tree species and their regeneration strategies in post-disturbance recovery. Fourth, it is crucial to examine the effect of landscape (e.g., proximity to undisturbed forests or edge effects) on natural regeneration processes. Fifth, few studies in the tropical region have evaluated the effectiveness of different management strategies (e.g., active restoration or passive natural regeneration) in promoting forest recovery after disturbances. Lastly, there is a need for research that integrates socio-economic factors into forest regeneration studies. This includes understanding the impacts of local communities, land tenure systems, and economic incentives on forest regeneration outcomes.

Author contributions

DM: Writing—review and editing. MK: Writing—original draft, Writing—review and editing. US: Writing—original

draft, Writing—review and editing. SS: Writing—review and editing.

Funding

The author(s) declare that no financial support was received for the research, authorship, and/or publication of this article.

Acknowledgments

We are grateful to the editorial board of Frontiers for supporting this Research Topic. We deeply thank all the authors and reviewers who have participated in this Research Topic.

Conflict of interest

The authors declare that the research was conducted in the absence of any commercial or financial relationships that could be construed as a potential conflict of interest.

Publisher's note

References

Baumann, M., Gasparri, I., Buchadas, A., Oeser, J., Meyfroidt, P., Levers, C., et al. (2022). Frontier metrics for a process-based understanding of deforestation dynamics. *Environ. Res. Lett.* 17, 095010. doi: 10.1088/1748-9326/ac8b9a

Pillay, R., Venter, M., Aragon- Osejo, J., González-del-Pliego, P., Hansen, A. J., Watson, J. E. M., et al. (2022). Tropical forests are home to over half of the world's vertebrate species. *Front Ecol. Environ.* 20, 10–15. doi: 10.1002/fee.2420

Poorter, L., Amissah, L., Bongers, F., Hordijk, I., Kok, J., Laurance, S. G. W., et al. (2023). Successional theories. *Biol. Rev.* doi: 10.1111/brv.12995 [Epub ahead of print].

Vancutsem, C., Achard, F., Pekel, J.-F., Vieilledent, G., Carboni, S., Simonetti, D., et al. (2021). Long-term (1990–2019) monitoring of forest cover changes in the humid tropics. *Sci. Adv.* 7, eabe1603. doi: 10.1126/sciadv.abe1603

Watson, J. E. M., Evans, T., Venter, O., Williams, B., Tulloch, A., Stewart, C., et al. (2018). The exceptional value of intact forest ecosystems. *Nat. Ecol. Evol.* 2, 599–610. doi: 10.1038/s41559-018-0490-x

frontiers | Frontiers in Forests and Global Change

TYPE Original Research
PUBLISHED 13 September 2022
DOI 10.3389/ffgc.2022.1008939

OPEN ACCESS

EDITED BY
Munesh Kumar,
Hemwati Nandan Bahuguna Garhwal University, India

REVIEWED BY
Satish Garkoti,
Jawaharlal Nehru University, India
Amit Kumar,
Nanjing University of Information Science and Technology, China

*CORRESPONDENCE
Surendra Singh Bargali
surendrakiran@rediffmail.com

SPECIALTY SECTION
This article was submitted to Forest Disturbance, a section of the journal Frontiers in Forests and Global Change

RECEIVED 01 August 2022
ACCEPTED 24 August 2022
PUBLISHED 13 September 2022

CITATION
Awasthi P, Bargali K, Bargali SS and Khatri K (2022) Nutrient return through decomposing *Coriaria nepalensis* litter in degraded hills of Kumaun Himalaya, India.
Front. For. Glob. Change 5:1008939.
doi: 10.3389/ffgc.2022.1008939

Nutrient return through decomposing *Coriaria nepalensis* litter in degraded hills of Kumaun Himalaya, India

Pankaj Awasthi, Kiran Bargali, Surendra Singh Bargali* and Kavita Khatri

Department of Botany, DSB Campus, Kumaun University, Nainital, Uttarakhand, India

Coriaria nepalensis, a nitrogen-fixing actinorhizal shrub, is a prominent and successful colonizer of bare rocks and landslide affected degraded lands. Field experiments were conducted to determine the differences in biomass decomposition and nutrient release pattern of different plant parts of *C. nepalensis* using litter bag technique. Results showed that the leaves decomposed completely within 6 months while only 46.55% of the lateral roots were decomposed with slowest decomposition rate of 0.14% day^{-1}. The decomposition rate was in the order: Leaves > Reproductive parts > Twigs (< 5 mm) > Twigs (> 5 mm) > Bark > Fine roots > Lateral roots. The decay rate coefficient was highest (0.003–0.014) for leaves and lowest (0.001–0.002) for lateral roots. During the decomposition cycle (364 days), overall increase was reported in nitrogen and phosphorus concentration, while potassium concentration decreased continuously in residual litters. The nutrient mobility was in the order: K > P > N. Climatic factors like temperature, relative humidity and rainfall significantly affected the decomposition process and among these factors, rainfall pattern emerged as a most effective environmental driver. Thus, taking into account initial nutrient content, nutrient release and decay rates, the leaves and reproductive parts of *C. nepalensis* proved to be more important as nutrient source than other components.

KEYWORDS

decomposition, decay coefficient, degraded lands, litter bags, litter types, nutrient dynamics

Introduction

Decomposition of plant litter is a fundamental biogeochemical process and plays vital role in soil organic matter accumulation and nutrient cycling (Bargali et al., 2015a; Li et al., 2022). It plays major role in regeneration, conserving biological diversity, ensuring plant nutrition, maintaining air and water quality, and preserving soil resilience (Steffen et al., 2015; Turmel et al., 2015), thus any disturbance that affects the decomposition can have pervasive effects on ecosystem functioning. Nutrient release pattern varies with nutrient types and exhibits the different immobilizing patterns which pose different impacts on forest ecosystem functions (Bargali, 1996).

According to the prevalent conceptual model of litter decomposition, climate, litter quality and decomposer species are the key influencers that regulate the rate of decomposition (Bradford et al., 2017; Manral et al., 2022). These controls are thought to work in a hierarchical manner in space, with climate and litter quality co-dominant at regional to global dimensions but decomposers acting solely as the local control with minor effects at larger scales (Makkonen et al., 2012; Santonja et al., 2015; Guo et al., 2019). Over the last three decades, it has been demonstrated that litter decay is influenced by a variety of chemical properties of the litter, including the litter N (Hobbie et al., 2012; Karki et al., 2022; Li et al., 2022), P and K concentrations and lignin content (Liu et al., 2022). However, Monroy et al. (2022) suggested that in temperate regions, chemical properties may not be a good predictor of litter decomposability. Climatic factors like temperature, humidity and rainfall regulate the decomposition processes (Sanderman and Amundson, 2005; Kumar et al., 2021) and among these drivers rainfall pattern assert decomposition more than any other environmental drivers (Bradford et al., 2016; Steidinger et al., 2019).

Coriaria nepalensis (Coriariaceae) is commonly known as Masuri berry, Rikhola, Makhaul, Tanner's tree, or Masuri shrub (Awasthi et al., 2022a). It is evergreen non-leguminous nitrogen fixing actinorhizal shrub with root nodules formed by *Frankia* and arbuscular mycorrhizal fungi (Santi et al., 2013). It is prominent and successful colonizer of bare rocks and landslide affected areas. Being a nodulated species (actinorhizal), it is very helpful in nitrogen fixation in eroded soil and able to replenish the deficiency of nitrogen for associate nearby growing species (Bargali et al., 2015a; Mourya et al., 2019).

Active restoration of degraded lands can be achieved through reactivation of biogeochemical nutrient cycles via litter decomposition. Lanuza et al. (2019) reported that the litter decomposition of nitrogen-fixing plants improve the nutrient release and nutrient deposition to support vegetation development and recover soil properties signifying that *C. nepalensis* should be used for recovering nutrient cycling in retrieval of degraded hills. Most of the studies on decomposition of litter generally consider leaf component only because it represent 50–90% of the total litter fall (Farooq et al., 2022), but in an ecosystem where leaf litter represents only 50% of the total litter fall, it is very vital to consider rest 50% of the litter for decomposition as well (Awasthi et al., 2022b). This study was conducted with the hypothesis that (i) the responses of different litter components of same species differ in weight loss and nutrient release pattern due to differences in initial nutrient content and (ii) in relatively short periods of time *C. nepalensis* litter can improve soil nutrient (N, P, and K) availability through decomposition of nutrient rich litter and therefore, suitable for the restoration of degraded hills.

Assessment of the periodic monitoring of nutrient cycling in the present climate changing scenario could help in better understanding the alteration in litter decomposition processes and nutrient recycling, if any. However, the available literature about the decomposition of *C. nepalensis* litter is very old and has not been assessed with respect to the present rising temperature and changing rainfall pattern, which modify the interconnected environmental variables of any region. The nitrogen fixing potential of *C. nepalensis* possesses nursing effect which encourages other associated species to grow and stabilize the degraded lands for longer period of time and reduces the probability of land degradation, biodiversity loss and landslides in those areas. So, a complete account of information about the contribution of *C. nepalensis* in nutrients (N, P, and K) recycling would be essential for the proper management and restoration of degraded lands in current climate changing circumstances. Therefore, the objective of this study was to analyse the decomposition rate and associated nutrient dynamics of different plant components of *C. nepalensis* as a key strategy to reactivate biogeochemical nutrient cycles and thus, improve soil quality in degraded lands of Kumaun Himalaya, India.

Materials and methods

The climate of the study area is monsoon warm temperate (Singh and Singh, 1992). It is characterized by summer (March to mid-June), rainy (mid-June to October) and very cold winter from November to February or sometimes till mid-March. Climatic data of the study site was obtained from the ARIES (Aryabhatta Research Institute of Observational Sciences, Manora peak, Nainital), which is within the aerial distance of 2 km from the study site. During the study period (September 2017 to March 2019), minimum temperature ranged between 7 and 23°C while maximum temperature ranged between 19 and 32°C. The lowest annual rainfall in the region was recorded as 0 mm (November 2017), whereas, highest rainfall was observed as 944.7 mm (August 2018) (**Figure 1**). About 75% of the total rainfall occurs during the 3 months, *i.e.,* mid-June to mid-September.

Decomposition processes

The detailed description of the litter fall estimation of the *C. nepalensis* dominated sites is given in Awasthi et al. (2022b). For the assessment of the decomposition rate and nutrient dynamics of the different components of the

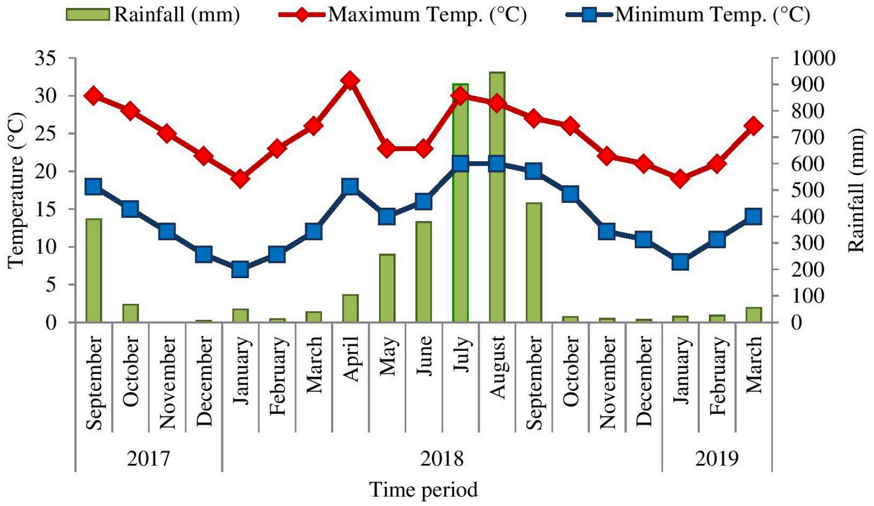

FIGURE 1
Meteorological data of Nainital (study sites) during September 2017 to March 2019 (Source: ARIES, Nainital).

same, litter bag technique, which is a direct method of measuring decomposition rate, was used to observe the litter decomposition (Awasthi et al., 2022c). Nearly senesced but attached plant leaves, twigs (twigs < 5 mm and twigs > 5 mm), bark, fine roots, lateral roots, and reproductive parts were collected from the plant and air dried till the constant weight was not achieved. Nylon litter bags (20 cm × 20 cm with 1 mm mesh size) were prepared and filled with 10 g air dried litter samples, separately. To permit the movement of microbes and other litter decomposing agents, 1 mm mesh size was considered sufficient (Robertson and Paul, 1999). Before deciding on the necessary number of duplicates, variations in the microenvironment of the stand, the diversity of the overstory and understory, and the quality of the litter were taken into account (the phytodiversity of all the sites is given in Awasthi et al., 2022a). A total of 378 litter bags (7 components × 3 replicates × 18 months) were randomly placed on the forest floor in the month of August 2017 in such a way that they were very close to soil without disturbing the forest floor vegetation. This made it possible to characterize the decay curve in a more reliable way. To compare the sample mass of the pre and post decomposition stages, collected litter bags were oven dried as well. All the samples in the litter bags for decomposition were placed at Rusi (1,756 m asl) which is located between 29°21′57′′N latitude 79°27′23′′E longitude. As the site was very steep in nature, small plain surfaces under *C. nepalensis* plant had been chosen to put litter bags with different litter components after removing the pre-existing debris. No disturbance rather than removing the debris had been made. To protect the litter bags from washing out from the steep site, a boundary of large gravels around the litter bags had been created. Further details about the study site were given in Awasthi et al. (2022b).

Three litter bags of each sample for 18 months (544 days) were monthly recovered. The recovered litter samples were kept in polyethylene bags individually and brought to laboratory, where the samples after separating from the litter bags were carefully washed with water to remove soil particles and dried at 60°C to constant weight and weighed.

Rate of decomposition (% R)

The weight loss of litter was expressed as the percentage remaining after a given time and was calculated as (Petersen and Cummins, 1974; Smeti et al., 2019):

$$\%\ \mathrm{R}\ \left(\%\ \mathrm{day}^{-1}\right) = \frac{\mathrm{W}(\mathrm{t_x})}{\mathrm{W}\ (\mathrm{t_i})} \times 100$$

Where, $\mathrm{W}(\mathrm{t_x})$ is the dry weight (g) of the litter after time ($\mathrm{t_x}$), and $\mathrm{W}(\mathrm{t_i})$ is the initial weight of the litter. In the present study, % R was calculated monthly as well as for the entire period.

Decay rate coefficient (k) was computed following Ndagurwa et al. (2015) as:

$$\mathrm{k} = \ln \frac{\%\ \mathrm{R}}{100 \times \mathrm{t}}$$

Where, *t* is the time in days.

Relative decomposition rate (RDR) was calculated following Bargali et al. (2015b) as:

$$\mathrm{RDR}\ \left(\mathrm{g\ g^{-1} day^{-1}}\right) = \ln \frac{(\mathrm{W_1} - \mathrm{W_0})}{(\mathrm{t_1} - \mathrm{t_0})}$$

Where, $\mathrm{W_0}$ = litter mass at time $\mathrm{t_0}$, $\mathrm{W_1}$ = litter mass at time $\mathrm{t_1}$, $\mathrm{t_1} - \mathrm{t_0}$ = sampling interval (days).

The mass loss over time was fitted to a simple negative exponential model (Olson, 1963; Tan et al., 2021):

$$k_t = \ln\frac{X_t}{X_0}$$

Where, X_0 is the original litter mass, X_t the amount of litter remaining after time *t*, *t* the time (days), and k is the decomposition rate (day^{-1}). The time required for 50% and 95% mass loss was calculated as $t_{50} = 0.693/k$ and $t_{95} = 3/k$, respectively.

Chemical analysis of litter

Collected litter material was grounded and passed through a 0.5 mm sieve for chemical analysis. All analyses were carried out in triplicate. Total Nitrogen (N) concentration was determined by the micro-Kjeldahl method (Jackson, 1958; Kumar et al., 2022). Phosphorous (P) concentration was estimated by the Olsen's method (Olsen et al., 1954; Wieczorek et al., 2022) using spectrophotometer and the potassium, *i.e.*, exchangeable potassium was determined by flame photometer (Black, 1965; Banerjee and Prasad, 2020) in Soil testing laboratory, Tea Development Board, Bhowali, Nainital.

Nutrient release pattern of decomposing litter

The release pattern of nutrients (N, P, and K) from the litter was calculated monthly by determining the differences in nutrient quantities between two successive months and the net release was calculated by summing nutrient release for the entire period (Wang et al., 2014).

$$\text{Nutrient release} = (Wt_2 \times Xt_2) - (Wt_1 \times Xt_1)$$

Where, Wt_2 is the dry weight of component litter at time t_2, Xt_2 is the nitrogen/phosphorus/potassium concentration of components at time t_2, Wt_1 is the weight of component at time t_1 and Xt_1 is the concentration of nitrogen/phosphorus/potassium of component at time t_1.

Results

Weight loss pattern

There is no benchmark for the beginning of decomposition of litter that is detached from the living plant. During decomposition, litter samples lost their natural color and turned black by the time, got fragmented into various pieces except twigs > 5 mm (544 days), which may be because of the formation of hardwood or secondary growth in twigs > 5 mm. For all the litter components, higher decomposition was recorded during the period between the placement of the litter bags (August) and first two collections (After 30 and 61 days). Among all the components, leaves decomposed within 6 months of the placement on the site because of its high surface area and thinness of leaves (0.54% day^{-1}), whereas lateral roots decomposed only 46.55% with the slowest decomposition rate (0.14% day^{-1}) (Table 1). The order of decomposition

TABLE 1 Rate of decomposition (% day^{-1}) for different components of *Coriaria nepalensis* ($n = 3$).

Days elapsed	**Components**						
	Leaves	**Reproductive parts**	**Twigs < 5 mm**	**Twigs > 5 mm**	**Bark**	**Lateral roots**	**Fine roots**
30	0.27	0.16	0.27	0.26	0.26	0.11	0.15
62	0.60	0.35	0.39	0.27	0.23	0.11	0.15
91	0.60	0.58	0.44	0.30	0.26	0.16	0.12
123	0.62	0.49	0.38	0.24	0.23	0.17	0.15
151	0.58	0.47	0.32	0.21	0.22	0.17	0.14
182		0.45	0.27	0.19	0.19	0.14	0.12
211		0.42	0.28	0.18	0.18	0.13	0.13
244			0.26	0.18	0.17	0.11	0.13
273			0.24	0.17	0.15	0.13	0.12
299			0.22	0.16	0.15	0.14	0.14
331			0.20	0.16	0.15	0.14	0.17
364			0.19	0.15	0.15	0.15	0.18
392			0.19	0.16	0.16	0.14	0.17
425			0.19	0.16	0.18	0.14	0.17
452			0.19	0.16	0.19	0.13	0.16
480			0.18	0.15	0.18	0.13	0.16
511			0.17	0.14	0.17	0.12	0.15
544			0.16	0.14	0.16	0.12	0.15
Average	0.54	0.42	0.25	0.19	0.19	0.14	0.15

Where, % day^{-1} = Percentage per day.

rate of the different components was: Leaves > Reproductive parts > Twigs (<5 mm) > Twigs (>5 mm) > Bark > Fine roots > Lateral roots.

The decay coefficient of all components is given in Table 2. It was highest for leaves (0.003–0.014) and lowest for lateral roots (0.001–0.002). Relative decomposition rate for leaves, reproductive parts, twigs < 5 mm, twigs > 5 mm, bark, lateral roots and fine roots was ranged from 0.001 to 0.017, 0.000–0.024, 0.000–0.0227, 0.001–0.011, 0.000–0.011, 0.000–0.037, and 0.001–0.026 g g^{-1} day^{-1}, respectively (Table 3). t_{50} and t_{95} of respective components is given in Table 4.

TABLE 2 Decay coefficients (−*k*) of different components for *Coriaria nepalensis* (*n* = 3).

Days elapsed	Components						
	Leaves	Reproductive parts	Twigs < 5 mm	Twigs > 5 mm	Bark	Lateral roots	Fine roots
30	0.003	0.002	0.003	0.003	0.003	0.001	0.002
62	0.008	0.004	0.004	0.003	0.003	0.001	0.002
91	0.009	0.008	0.006	0.004	0.003	0.002	0.001
123	0.012	0.008	0.005	0.003	0.003	0.002	0.002
151	0.014	0.008	0.004	0.003	0.003	0.002	0.002
182		0.009	0.004	0.002	0.002	0.002	0.001
211		0.010	0.004	0.002	0.002	0.002	0.002
244			0.004	0.002	0.002	0.001	0.002
273			0.004	0.002	0.002	0.002	0.002
299			0.004	0.002	0.002	0.002	0.002
331			0.003	0.002	0.002	0.002	0.003
364			0.003	0.002	0.002	0.002	0.003
392			0.003	0.002	0.002	0.002	0.003
425			0.004	0.003	0.003	0.002	0.003
452			0.004	0.003	0.004	0.002	0.003
480			0.004	0.003	0.004	0.002	0.003
511			0.004	0.003	0.004	0.002	0.003
544			0.004	0.002	0.004	0.002	0.003

TABLE 3 Relative decomposition rate (g g^{-1} day^{-1}) for different components of *Coriaria nepalensis* (*n* = 3).

Days elapsed	Components						
	Leaves	Reproductive parts	Twigs < 5 mm	Twigs > 5 mm	Bark	Lateral roots	Fine roots
30	0.007	0.024	0.007	0.008	0.009	0.037	0.026
62	0.017	0.008	0.008	0.002	0.007	0.016	0.013
91	0.006	0.013	0.005	0.001	0.000	0.003	0.018
123	0.006	0.002	0.003	0.011	0.008	0.004	0.003
151	0.001	0.001	0.023	0.010	0.004	0.005	0.009
182	0.001	0.000	0.009	0.007	0.011	0.026	0.010
211		0.001	0.001	0.006	0.006	0.008	0.004
244		0.000	0.004	0.002	0.004	0.021	0.003
273			0.006	0.007	0.010	0.000	0.005
299			0.013	0.005	0.003	0.003	0.001
331			0.007	0.003	0.002	0.001	0.001
364			0.003	0.003	0.003	0.001	0.001
392			0.003	0.001	0.001	0.003	0.003
425			0.000	0.001	0.001	0.003	0.002
452			0.002	0.004	0.000	0.008	0.007
480			0.006	0.006	0.004	0.004	0.001
511			0.004	0.005	0.005	0.003	0.006
544			0.004	0.004	0.007	0.003	0.003

Where, g g^{-1} day^{-1} = gram per gram per day.

TABLE 4 Decomposition parameters for nutrients and time required for various levels of nutrient release (n = 3).

Components	Mass loss (days)		N-Stock loss (days)		P-Stock loss (days)		K-Stock loss (days)	
	t_{50}	t_{95}	t_{50}	t_{95}	t_{50}	t_{95}	t_{50}	t_{95}
Leaves	50	216	364	1574	206	893	285	1235
Reproductive Parts	57	248	350	1517	228	989	221	958
Twigs < 5 mm	215	931	316	1370	349	1512	356	1542
Twigs > 5 mm	314	1361	352	1524	483	2090	191	828
Bark	323	1400	333	1440	441	1910	296	1281
Lateral roots	327	1414	525	2273	549	2376	368	1595
Fine roots	246	1063	551	2386	571	2472	761	3296

Where, t_{50} = 50% nutrient release, t_{95} = 95% nutrient release, N = nitrogen, P = phosphorus, K = potassium.

Changes in nutrient concentration in decomposing litter

N and P concentration in the different litter component was generally increased throughout the study period but concentration of K decreased in residual litter in the entire decomposition cycle (364 days). N concentration in bark and fine roots and P concentration in bark and lateral roots slightly decreases sometimes in the later stage of decomposition. Concentration of N was more than twice of initial concentration during the study period in both types of twigs and bark (**Figures 2A–C**). $t_{50\text{and}}$ t_{95} for N, P, and K stock loss for all respective components is given in **Table 4**.

Nutrient release pattern

During first 123 days, about 71% of nitrogen was released from leaves followed by reproductive parts (50.36%) and twigs < 5 mm (27.74%). The slowest release of nitrogen in the first 123 days was in lateral roots (0.35%) followed by fine roots (2.70%). In case of bark the absolute amount of nitrogen increased by 1.61% within 123 days of the study. In the first month of the study (0–30 days) the maximum release in nitrogen was in reproductive parts (37.60%), whereas, minimum was in twigs > 5 mm (7.55%). Except leaf litter, no other component continuously decreased in absolute amount of nitrogen throughout the study. At the end of the study (364 days), percent N release ranged from 14.97% (Twigs < 5 mm) to 83.05% (Leaves) (**Figure 3**).

The release of phosphorus was faster in comparison to nitrogen except in the case of leaf litter. The pattern of phosphorus release was fastest in leaves (78.92%) in the first 151 days of the study, followed by reproductive parts (67.13%) and lateral roots (19.61%). None of the selected components surpassed the initial absolute amount of phosphorus except bark that surpassed the absolute amount of phosphorus by maximum 11.01%. At the end of the study, release of phosphorus was observed between 24.73% (Bark) and 79.92% (Leaves). Except leaf and reproductive parts, no other component continuously decreased in absolute amount of phosphorus throughout the study period (**Figure 4**).

The release of potassium was faster in comparison to nitrogen and phosphorus. Continuous release occurred in all the components except in bark and lateral roots. The pattern of potassium release was fastest in leaves (91.19%) in the first 151 days of the study, followed by reproductive parts (88.62%) and twigs < 5 mm (64.52%). At the end of the study, release of potassium was observed between 93.41% (Reproductive parts) and 77.21% (Lateral roots) (**Figure 5**).

Discussion

The order of the different components on the basis of decomposition rate was: Leaves > Reproductive parts > Twigs (< 5 mm) > Twigs (> 5 mm) > Bark > Fine roots > Lateral roots. Among all the components, leaves decomposed within 6 months of the sample placement on site because of its high surface area and thinness of leaves (0.54% day^{-1}), whereas lateral roots only decomposed 46.55% with the slowest decomposition rate (0.14% day^{-1}). High value of decay rate coefficient (k) indicates high rate of decomposition. The higher values of k for leaves (0.003–0.014) and reproductive parts (0.002–0.010) indicated that these components decomposed faster while lowest values of k reported for lateral roots (0.001–0.002) indicated its slow decomposition.

Decomposition and mass loss

It has been shown that the labile fractions of litter provide a readily available source of energy for the decomposer; moreover, the nutrients are easily leached. Nutrient concentration should therefore, be most influential in determining the rate of decomposition in the initial days (Siqueira et al., 2022). On

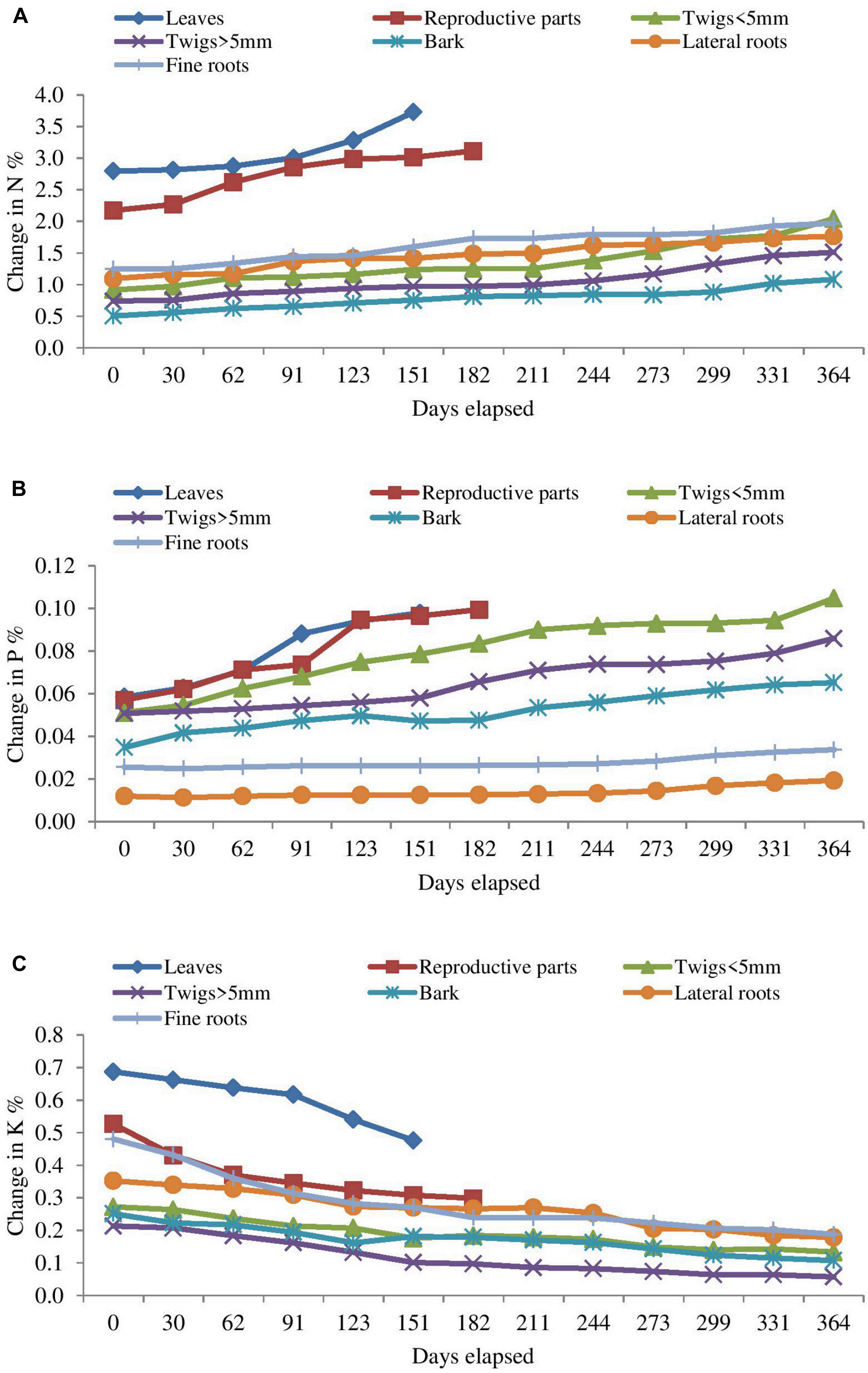

FIGURE 2
Changes in **(A)** Nitrogen, **(B)** Phosphorus, and **(C)** Potassium concentration in different components of decomposing *Coriaria nepalensis* litter ($n = 3$).

the sites where understory vegetation is available in ample amount, it helps soil to retain moisture for longer period of time and eventually helps microbes responsible for decomposition to flourish (Su et al., 2022). Differences in the rate of decomposition of leaf have been reported by several authors, e.g., Bargali S. S. et al. (2015) and Joshi and Garkoti (2020) (**Table 5**).

In conformity to earlier studies among all the components (Marchante et al., 2019; Akoto et al., 2022), the higher weight loss was recorded during rainy season followed by

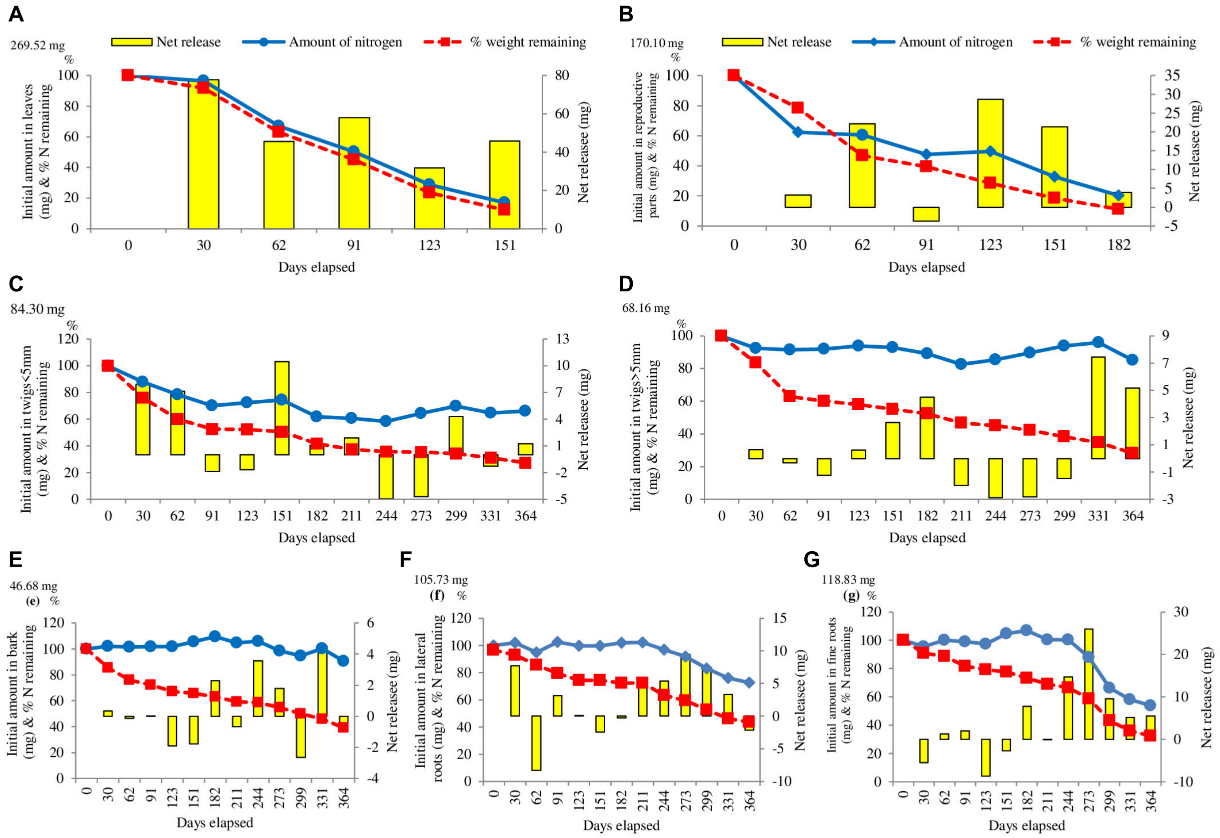

FIGURE 3
Changes in the absolute amount of nitrogen in **(A)** leaves, **(B)** reproductive parts, **(C)** twigs < 5 mm, **(D)** twigs > 5 mm, **(E)** bark, **(F)** lateral roots, **(G)** fine roots mass in litter. The initial mass of nitrogen is given on the left side of the Y-axis. The columns indicate the net change between the measurements (right Y-axis). The broken lines indicate the percentage weight remaining of litter (n = 3).

summer and winter season. The greater decomposition in rainy season may be due to the presence of pronounced microbial activity under favorable conditions, *i.e.,* availability of ample moisture and optimum temperature that accentuated due to rainfall (Krishna and Mohan, 2017; Tamura et al., 2017). They also stated that indirectly, climate could affect the litter decomposition by interacting with plant physiology and nutrients re-absorption, thus, modulating the chemical composition of plant litter at its formative stages. Decomposition of litter continued throughout the study period because of microbial activity depending on the conditions available for them. Actinomycetes, bacteria, algae and fungi may be the major soil fauna and microbes which directly affect the litter decomposition (Berg and McClaugherty, 2014) and their abundance and hierarchy in the soil would be very vital for their role on decomposition rate (Bargali S. S. et al., 2015).

Decomposition rate is markedly affected by water soluble compounds and leachable substances and nutrients in fresh litter. In the present study, components like leaves and reproductive parts showed similar pattern while twigs and roots follow almost different pattern. Overall this species showed higher decomposition rate as compared to the other species of the region.

t_{50} and t_{95} for different components ranged from 50 to 327 and 216–1,414 days, respectively (**Table 4**) as it depends on various factors such as biochemistry of components, behavior of soil and edaphic factors. The higher t_{50} and t_{95} reported by Bohara et al. (2019) were 456–569 and 3,289–4,125, respectively, in shrubland of Taihang Mountain, North China; Yang et al. (2021) reported 880–1,529 for t_{50} and 3,938–6,563 days for t_{95} and Huang et al. (2011) reported 324–511 days for t_{50} and 1,405–2,119 days for t_{95}. Caliman et al. (2020) reported 84–284 days for t_{50} days and 372–1,230 days for t_{95} for multipurpose trees in Central India, which was lower than reported in the present study. Presence of favorable condition for decomposition may reduce the t_{50} and t_{95} time and lower value of t_{50} and t_{95} depicts that the site has a very active cycling of nutrients and dry matter.

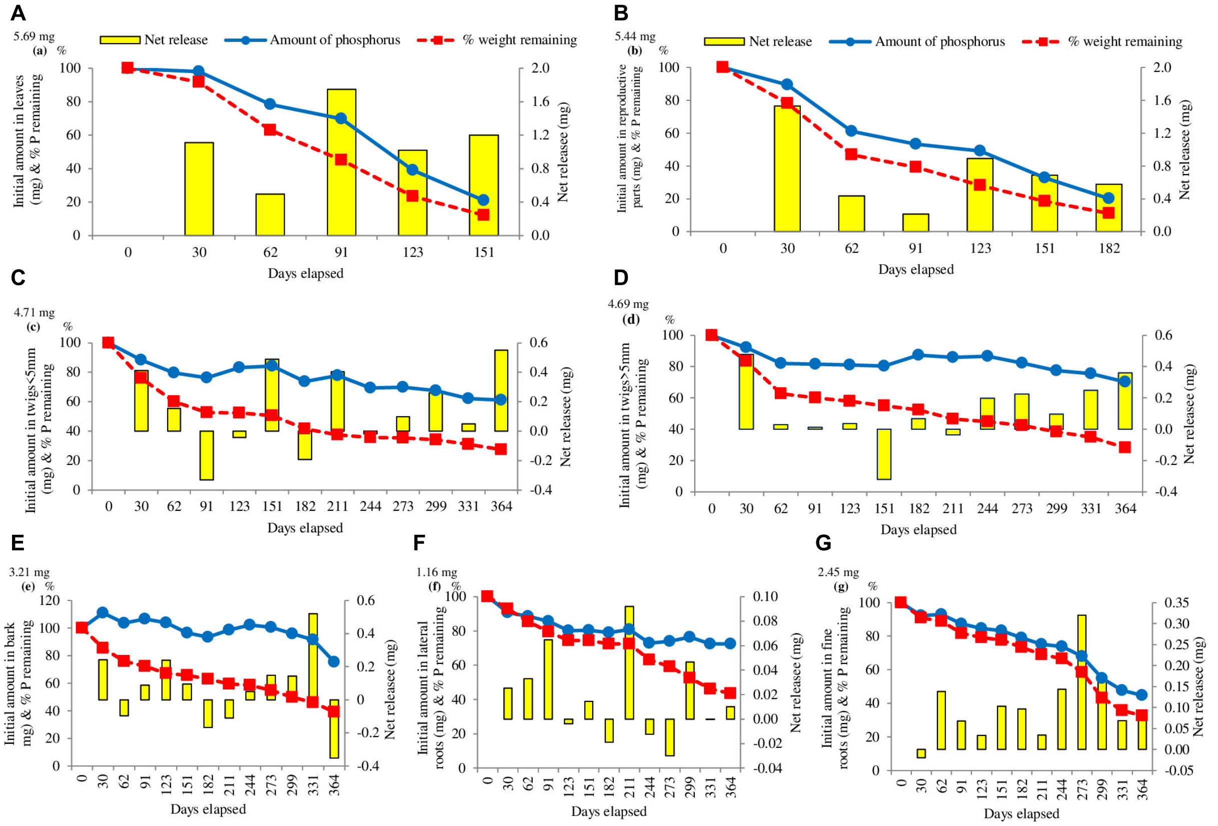

FIGURE 4

Changes in the absolute amount of phosphorus in **(A)** leaves, **(B)** reproductive parts, **(C)** twigs < 5 mm, **(D)** twigs > 5 mm, **(E)** bark, **(F)** lateral roots, **(G)** fine roots mass enclosed in litter. The initial mass of phosphorus is given on the left side of the Y-axis. The columns indicate the net change between the measurements (right Y-axis). The broken lines indicate the percentage weight remaining of litter (*n* = 3).

To determine the temporal pattern of weight loss, the percent weight remaining was regressed against the time (days) elapsed (Table 6). A negative relationship between percent weight remaining and time elapsed was recorded for all the components.

Nutrient dynamics of decomposing litter

N and P concentrations (%) generally increased during different months till the termination of the experiment while the N and P content (mg) decreased due to release of nutrients during decomposition process (Figure 2). About 13–85% N and 22–75% P remained at the end of experiment for all litter types with highest release observed in the leaves. During the litter decomposition, K is released in accordance with the gradual process of leaching. The release of nutrients may contribute to nutrient conservation in degraded nutrient-poor sites (Manral et al., 2020). The observed pattern of initial N accumulation led to a net N release after 330 days, suggesting that immobilization of N was needed in this shrub until a critical concentration for decomposition was reached. The N and P immobilization indicate that leaching is not important for these two nutrients, whereas K has the significant leaching ability. By analyzing the nutrients remaining at the end of the decomposition process, the mobility of K was high followed by P and N in different components as also reported by Li et al. (2007) and Yang et al. (2022). Akoto et al. (2022) observation on a wide-ranging pattern of nutrient release from decomposing litter components includes an early immobilization of N and P often followed by net nutrient discharge. In contrast to our findings, an initial release phase followed by net accumulation for N and P was reported by Gaisie et al. (2016) in multipurpose trees.

Controlling factors

The decomposition during first 2 months was rapid because the molecules are easy to breakdown and rich in energy and

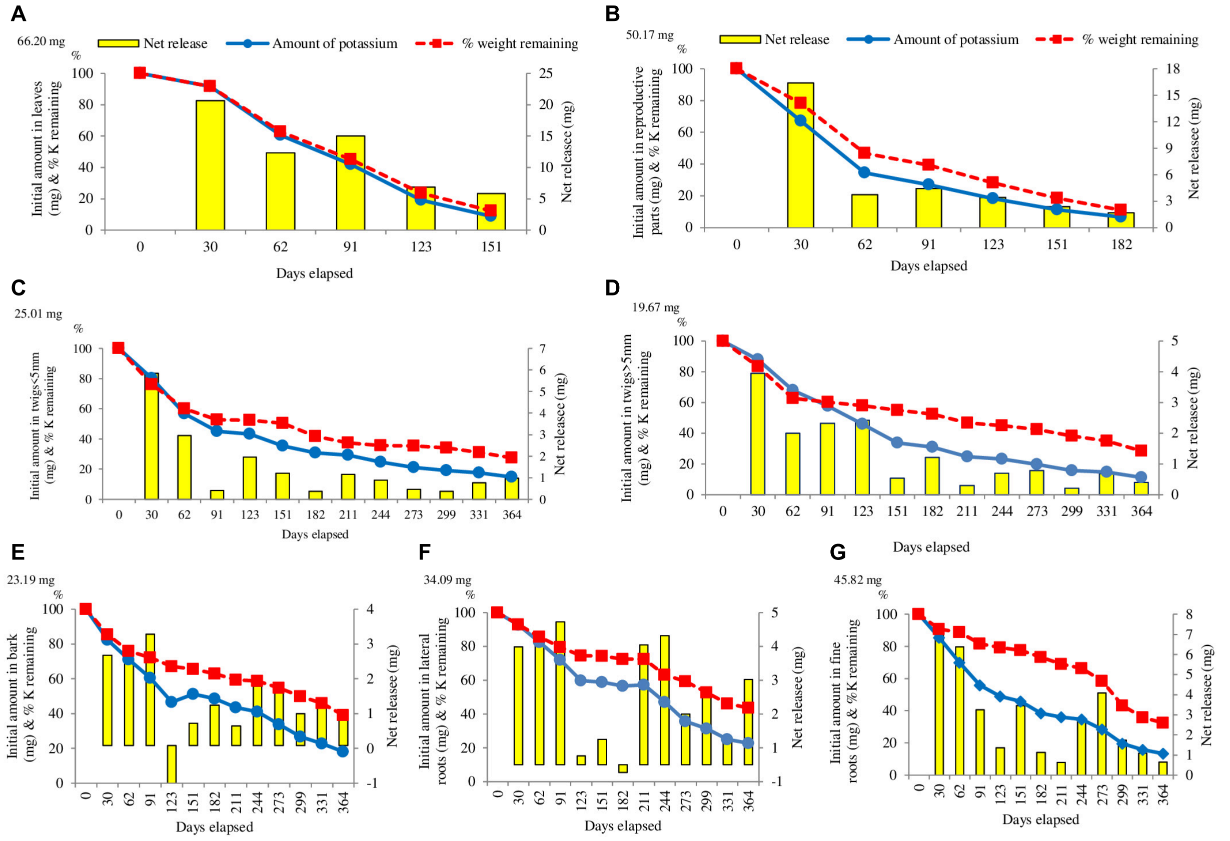

FIGURE 5

Changes in the absolute amount of potassium in **(A)** leaves, **(B)** reproductive parts, **(C)** twigs < 5 mm, **(D)** twigs > 5 mm, **(E)** bark, **(F)** lateral roots, **(G)** fine roots mass enclosed in litter. The initial mass of Potassium is given on the left side of the Y-axis. The columns indicate the net change between the measurements (right Y-axis). The broken lines indicate the percentage weight remaining of litter ($n = 3$).

the period of incubation was monsoon season (August) and the rainfall influenced the rate of decomposition by enhancing the activities of microorganisms. The greater weight loss recorded during rainy season may be due to optimum moisture, soil temperature and leaching of water soluble substances from the litter mass. Lower weight loss during winter season may be due to cool and dry conditions. However, in the later stages of litter decomposition, weight loss was decreased because the breakdown of lignin was much slower (due to very large and complex molecules) and the period of decomposition was post monsoon, *i.e.,* winter and summer seasons where precipitation was not enough to support decomposition. The positive correlation between the weight remaining with rainfall temperature, humidity and rainfall also supported these finding (**Table 6**). Among the three environmental drivers, the litter decomposition was most affected by rainfall as compared to the other two drivers, *i.e.,* relative humidity and temperature.

TABLE 5 Comparative account of decomposition rate of leaf litter in different studies.

Forests/ Plantations	Locality	Decomposition rate (% day^{-1})	References
Chir pine	India	0.09–0.28	Majila et al. (2005)
Himalayan alpine ecosystem	India	0.001–0.03	Rawat et al. (2010)
Q. semecarpifolia	India	0.08	Rai (2012)
R. companulatum	India	0.08	
Madhuca indica	India	0.21	Bargali S. S. et al. (2015)
Quercus leucotrichophora	India	0.01	Joshi and Garkoti (2020)
Alnus nepalensis	India	0.02	

The components of *C. nepalensis* released nutrients (N, P, and K) at different rates, depending on their initial N, P, and K concentration (**Figure 2**). As compared to other components, leaves and reproductive parts with high N concentration showed fast decomposition. Previous studies (Lv et al., 2013; Zhang et al., 2021) also reported lower initial nitrogen content for

TABLE 6 Correlation coefficient between weight remaining, days elapsed, relative humidity, temperature, and rainfall.

X vs Y	Components	Intercept (a)	Slope (b)	Correlation coefficient (r)*
WR vs DE	Leaves	10.15	−0.06	0.98*
	Reproductive parts	9.92	−0.04	0.96*
	Twigs < 5 mm	8.13	−0.01	0.90**
	Twigs > 5 mm	9.08	−0.01	0.97*
	Bark	9.63	−0.02	0.97*
	Lateral roots	9.76	−0.01	0.97**
	Fine roots	10.30	−0.02	0.97*
WR vs R	Leaves	1.99	0.03	0.87**
	Reproductive parts	2.39	0.02	0.80*
	Twigs < 5 mm	3.77	0.01	0.85**
	Twigs > 5 mm	5.33	0.01	0.72*
	Bark	4.96	0.02	0.63**
	Lateral roots	6.35	0.01	0.79*
	Fine roots	5.96	0.01	0.83*
WR vs RH	Leaves	−8.19	0.21	0.93**
	Reproductive parts	−6.28	0.19	0.96*
	Twigs < 5 mm	1.91	0.04	0.78*
	Twigs > 5 mm	4.55	0.02	0.82*
	Bark	4.44	0.01	0.60
	Lateral roots	5.94	0.01	0.70*
	Fine roots	6.21	−0.01	0.70*
WR vs T	Leaves	−10.65	0.73	0.97**
	Reproductive parts	−8.09	0.61	0.63*
	Twigs < 5 mm	0.85	0.16	0.83*
	Twigs > 5 mm	2.92	0.12	0.80*
	Bark	1.32	0.19	0.86**
	Lateral roots	4.40	0.09	0.66*
	Fine roots	3.48	0.11	0.75*

Where, *Significant at $p < 0.05$, **Significant at $p < 0.01$, WR = weight remaining (g), DE = days elapsed, RH = relative humidity (%), R = rainfall (mm), T = temperature (°C).

TABLE 7 Regression coefficient (r^2) and t value between weight loss (g) and Nitrogen (N), Phosphorus (P), and Potassium (K) concentration (%).

Nutrients	Components	Intercept (a)	Slope (b)	r^2	SEM	t ($p < 0.01$)
N	Leaves	3.21	−0.05	−0.72	1.50	1.17**
	Reproductive parts	3.26	−0.12	−0.98	1.32	1.38**
	Twigs < 5 mm	2.05	−0.15	−0.68	0.60	5.75**
	Twigs > 5 mm	1.99	−0.15	−0.87	0.49	10.56**
	Bark	1.47	−0.11	−0.97	0.47	11.98**
	Lateral roots	2.38	−0.13	−0.96	0.52	10.91**
	Fine roots	2.39	−0.11	−0.85	0.64	8.21**
P	Leaves	0.07	0.00	−0.75	1.41	3.27**
	Reproductive parts	0.10	−0.01	−0.89	1.18	3.77**
	Twigs < 5 mm	0.12	−0.01	−0.92	0.53	8.95**
	Twigs > 5 mm	0.11	−0.01	−0.89	0.43	14.39**
	Bark	0.09	−0.01	−0.95	0.42	14.92**
	Lateral roots	0.02	0.00	−0.83	0.46	15.10**
	Fine roots	0.04	0.00	−0.93	0.58	11.90**
K	Leaves	0.69	−0.02	0.63	1.45	2.85**
	Reproductive parts	0.26	0.03	0.95	1.14	3.64**
	Twigs < 5 mm	0.08	0.02	0.90	0.51	9.03**
	Twigs > 5 mm	−0.10	0.03	0.91	0.41	14.89**
	Bark	−0.01	0.03	0.95	0.41	15.1394**
	Lateral roots	0.02	0.03	0.97	0.45	15.10**
	Fine roots	0.04	0.03	0.70	0.55	11.90**

Where, SEM = standard error of means, t = value for paired sample "t" test, **Significant at $p < 0.01$.

slow decomposing litter. However, high N concentration and slow decomposition rate recorded for components like fine and lateral roots suggested that higher N concentration is not the only criteria that determine the rate of decomposition (Tu et al., 2014; Zhu et al., 2016; Zhang et al., 2021). Other decomposition studies (Silveira et al., 2011) also indicated that the decomposition of plant litter was related more to initial C quality, such as lignin concentration and acid-soluble carbohydrates than to the relative availability of N.

Significant ($p < 0.01$) inverse linear relationship between N and P concentration in residual material and percent weight remaining for all components was observed (**Table 7**). Galloway et al. (2008) and Allison et al. (2009) have stated that this relationship to be inversely linear in case where physical removal of material from bag is minimized which was also observed in our study.

Conclusion

Litter decomposition is a critically fundamental process that determines the potential return of organic matter and nutrients to the soil. Different litter components of *C. nepalensis* recorded 57–100% mass loss during 1 year period suggesting that organic matter and nutrients provided by decomposing litter can improve soil conditions in degraded hills. Low soil availability of N and P seems to be the major constraints in reclamation of degraded hills. Through litter decomposition and consequent nutrient release *C. nepalensis* can ameliorate soil conditions. In addition, the ability of *C. nepalensis* to form symbiotic association with nitrogen-fixing actinomycetes *Frankia* and arbuscular mycorhizal fungi makes it suitable for the management of fragile hills specially in regeneration and conservation of plant biodiversity in Kumaun Himalaya, India. Climate change could have positive or negative impact on litter decomposition or mass loss of litter depending on the species composition as well as environmental variables. Optimum conditions are needed for quick or healthy decomposition but conditions like prolong drought or global warming can reduce the litter decomposition because these conditions are not suitable for decomposers to grow in ample amount. In long run, the climate change could also influence the growth and chemical properties of the plant which also ultimately influence the decomposition rate of the plant.

Data availability statement

The original contributions presented in this study are included in the article/supplementary material, further inquiries can be directed to the corresponding author/s.

Author contributions

PA collected the data and prepared the first draft. KK helped in manuscript preparation and analysis. KB and SB guided the research, reviewed, and modified the manuscript. All authors contributed to the article and approved the submitted version.

Acknowledgments

The authors are thankful to the Head, Department of Botany, D.S.B. Campus, Kumaun University, Nainital, Uttarakhand for providing all sorts of facilities. Haripriya Pathak (Associate Professor-English, Kumaun University, Nainital, Uttarakhand, India) is highly acknowledged for the language correction. The authors are also thankful to the editor and the reviewers for their constructive comments which improved the quality of our manuscript.

Conflict of interest

The authors declare that the research was conducted in the absence of any commercial or financial relationships that could be construed as a potential conflict of interest.

Publisher's note

References

Akoto, D. S., Partey, S. T., Abugre, S., Akoto, S., Denich, M., Borgemeister, C., et al. (2022). Comparative analysis of leaf litter decomposition and nutrient release patterns of bamboo and traditional species in agroforestry system in Ghana. *Clean. Mater.* 4:100068. doi: 10.1016/j.clema.2022.100068

Allison, S. D., LeBauer, D. S., Ofrecio, M. R., Reyes, R., Ta, A. M., and Tran, T. M. (2009). Low levels of nitrogen addition stimulate decomposition by boreal forest fungi. *Soil Biol. Biochem.* 41, 293–302. doi: 10.1016/j.soilbio.2008.10.032

Awasthi, P., Bargali, K., and Bargali, S. S. (2022a). Relative performance of woody vegetation in response to facilitation by *Coriaria nepalensis* in Central Himalaya, India. *Russ. J. Ecol.* 53, 191–203. doi: 10.1134/S1067413622030031

Awasthi, P., Bargali, K., Bargali, S. S., and Jhariya, M. K. (2022b). Structure and functioning of *Coriaria nepalensis* dominated shrublands in degraded hills of Kumaun Himalaya. I. Dry matter dynamics. *Land Degrad. Dev.* 33, 1474–1494. doi: 10.1002/ldr.4235

Awasthi, P., Bargali, K., Bargali, S. S., Khatri, K., and Jhariya, M. K. (2022c). Nutrient partitioning and dynamics in *Coriaria nepalensis* Wall dominated shrublands of degraded hills of Kumaun Himalaya. *Front. For. Glob. Change* 5:913127. doi: 10.3389/ffgc.2022.913127

Banerjee, P., and Prasad, B. (2020). Determination of concentration of total sodium and potassium in surface and ground water using a flame photometer. *Appl. Water Sci.* 10:113. doi: 10.1007/s13201-020-01188-1

Bargali, K., Maurya, N. R., and Bargali, S. S. (2015a). Effect of a nitrogen-fixing actinorhizal shrub on herbaceous vegetation in a mixed conifer forest of Central Himalaya. *Curr. World Environ.* 10, 957–966. doi: 10.12944/CWE.10.3.27

Bargali, K., Manral, V., and Bargali, S. S. (2015b). Weight loss pattern in decomposing litter of *Coriaria nepalensis*, an actinorhizal shrub from degraded land. *Indian J. Agric. Sci.* 85, 270–273.

Bargali, S. S., Shukla, K., Singh, L., and Ghosh, L. (2015). Leaf litter decomposition and nutrient dynamics in four tree species of dry deciduous forest. *Trop. Ecol.* 56, 57–66.

Bargali, S. S. (1996). Weight loss and nitrogen release in decomposing wood litter in an age series of eucalypt plantation. *Soil Biol. Biochem.* 28, 699–702.

Berg, B., and McClaugherty, C. (2014). *Plant Litter: Decomposition, Humus Formation, Carbon Sequestration*. Berlin: Springer-Verlag, doi: 10.1007/978-3-662-05349-2

Black, C. A. (1965). *Methods Of Soil Analysis Part I*. Madison: American Society of Agronomy, Inc.

Bohara, M., Yadav, R. K. P., Dong, W., Cao, J., and Hu, C. (2019). Nutrient and isotopic dynamics of litter decomposition from different land uses in naturally restoring Taihang Mountain, North China. *Sustainability* 11:1752. doi: 10.3390/su11061752

Bradford, M. A., Berg, B., Maynard, D. S., Wieder, W. R., and Wood, S. A. (2016). Understanding the dominant controls on litter decomposition. *J. Ecol.* 104, 229–238. doi: 10.1111/1365-2745.12507

Bradford, M. A., Veen, G. F., Bonis, A., Bradford, E. M., Classen, A. T., Cornelissen, J. H. C., et al. (2017). A test of the hierarchical model of litter decomposition. *Nat. Ecol. Evol.* 1, 1836–1845. doi: 10.1038/s41559-017-0367-4

Caliman, J. P., Godinho, T. O., Caldeira, M. V. W., Rocha, J. H. T., Drury, M. L., and Castro, K. C. (2020). Seasonal pattern of nutrient cycling in the Atlantic Forest across a topographic gradient. *Sci. For.* 48:e3200. doi: 10.18671/scifor.v48n125.23

Farooq, T. H., Li, Z., Yan, W., Shakoor, A., Kumar, U., Shabbir, R., et al. (2022). Variations in litter fall dynamics, C:N:P stoichiometry and associated nutrient return in pure and mixed stands of camphor tree and masson pine forests. *Front. Environ. Sci.* 10:903039. doi: 10.3389/fenvs.2022.903039

Gaisie, E., Saddick, A., Agyeman, K., Adjei-Gyapong, T., and Quansah, G. (2016). Leaf decomposition and the nutrients release from multipurpose tree for crop production. *Int. J. Sci. Res. Sci. Eng. Technol.* 2, 345–352.

Galloway, J. N., Townsend, A. R., Erisman, J. W., Bekunda, M., Cai, Z., Freney, J. R., et al. (2008). Transformation of the nitrogen cycle: Recent trends, questions, and potential solutions. *Science* 320, 889–892. doi: 10.1126/science.1136674

Guo, C., Cornelissen, J. H. C., Zhang, Q. Q., and Yan, E. R. (2019). Functional evenness of N-to-P ratios of evergreen-deciduous mixtures predicts positive non-additive effect on leaf litter decomposition. *Plant Soil* 436, 299–309. doi: 10.1007/s11104-018-03925-7

Hobbie, S. E., Eddy, W. C., Buyarski, C. R., Adair, E. C., Ogdahl, M. L., and Weisenhorn, P. (2012). Response of decomposing litter and its microbial community to multiple forms of nitrogen enrichment. *Ecol. Monogr.* 82, 389–405. doi: 10.1890/11-1600.1

Huang, Y., Michel, K., An, S. Z., and echmeister-Boltenstern, S. (2011). Changes in microbial-community structure with depth and time in a chronosequence of restored grassland soils on the Loess Plateau in northwest China. *J. Plant Nutr. Soil Sci.* 174, 765–774. doi: 10.1002/jpln.201000397

Jackson, M. L. (1958). *SoilChemical Analysis*. Hoboken: Prentice Hall, Inc.

Joshi, R. K., and Garkoti, S. C. (2020). Litter dynamics, leaf area index and forest floor respiration as indicators for understanding the role of Nepalese alder in white oak forests in central Himalaya, India. *Ecol. Indic.* 111:106065. doi: 10.1016/j.ecolind.2020.106065

Karki, H., Bargali, K., and Bargali, S. S. (2022). Dynamics of fine root and soil nitrogen in *Mangifera indica* based agroforestry systems in Central Himalaya, India. *Land Degrad. Dev.* 1–16. doi: 10.1002/ldr.4406

Krishna, M. P., and Mohan, M. (2017). Litter decomposition in forest ecosystems: A review. *Energy Ecol. Environ.* 2, 236–249. doi: 10.1007/s40974-017-0064-9

Kumar, M., Kumar, M., Pandey, R., Zhi-Guo, Y., and Cabral-Pinto, M. (2021). Forest soil nutrient stocks along altitudinal range of Uttarakhand Himalayas: An aid to nature based climate solutions. *Catena* 207:105667. doi: 10.1016/j.catena.2021.105667

Kumar, M., Kumar, A., Thakur, T. K., Sahoo, U. K., Kumar, R., Konsam, B., et al. (2022). Soil organic carbon estimation along an altitudinal gradient of chir-pine forests of Garhwal Himalaya, India: A field inventory to remote sensing approach. *Land Degrad. Dev* 1–14. doi: 10.1002/ldr.4393

Lanuza, O., Casanoves, F., Delgado, D., and Van den Meersche, K. (2019). Leaf litter stoichiometry affects decomposition rates and nutrient dynamics in tropical forests under restoration in Costa Rica. *Restor. Ecol.* 27, 549–558. doi: 10.1111/rec.12893

Li, H. T., Yu, G. R., Li, J. Y., Liang, T., and Chen, Y. R. (2007). Dynamics of litter decomposition and phosphorus and potassium release in Jinggang Mountain region of Jiangxi Province, China. *Ying Yong Sheng Tai Xue Bao* 18, 233–240.

Li, R., Yang, Q., Guan, X., Chen, L., Wang, Q., Wang, S., et al. (2022). High quality litters with faster initial decomposition produce more stable residue remaining in a subtropical forest ecosystem. *Catena* 213:106134. doi: 10.1016/j.catena.2022.106134

Liu, S., Yang, R., Peng, X., Hou, C., Ma, J., and Guo, J. (2022). Contributions of plant litter decomposition to soil nutrients in ecological tea gardens. *Agriculture* 12:957. doi: 10.3390/agriculture12070957

Lv, Y., Wang, C., Wang, F., Zhao, G., Pu, G., Ma, X., et al. (2013). Effects of nitrogen addition on litter decomposition, soil microbial biomass, and enzyme activities between leguminous and non-leguminous forests. *Ecol. Res.* 28, 793–800. doi: 10.1007/s11284-013-1060-y

Majila, B. S., Joshi, G. C., and Kala, C. P. (2005). Patterns in litter fall and litter decomposition along an altitudinal gradient in the Binsar Wildlife Sanctuary, Central Himalaya. *Int. J. Sustain. Dev. World Ecol.* 12, 205–212. doi: 10.1080/13504500509469631

Makkonen, M., Berg, M. P., Handa, I. T., Hattenschwiler, S., van Ruijven, J., van Bodegom, P. M., et al. (2012). Highly consistent effects of plant litter identity and functional traits on decomposition across a latitudinal gradient. *Ecol. Lett.* 15, 1033–1041. doi: 10.1111/j.1461-0248.2012.01826.x

Manral, V., Bargali, K., Bargali, S. S., Jhariya, M. K., and Padalia, K. (2022). Relationships between soil and microbial biomass properties and annual flux of nutrients in Central Himalayan forests, India. *Land Degrad. Dev.* 33, 2014–2025. doi: 10.1002/ldr.4283

Manral, V., Bargali, K., Bargali, S. S., and Shahi, C. (2020). Changes in soil biochemical properties following replacement of Banj oak forest with Chir pine in Central Himalaya, India. *Ecol. Process.* 9:30. doi: 10.1186/s13717-020-00235-8

Marchante, E., Marchante, H., Freitas, H., Kjoller, A., and Struwe, S. (2019). Decomposition of an N-fixing invasive plant compared with a native species: Consequences for ecosystem. *Appl. Soil Ecol.* 138, 19–31. doi: 10.1016/j.apsoil.2019.02.016

Monroy, S., Larranaga, A., Martinez, A., Perez, J., Molinero, J., Basaguren, A., et al. (2022). Temperature sensitivity of microbial litter decomposition in freshwaters: Role of leaf litter quality and environmental characteristics. *Microb. Ecol.* [Epub ahead of print]. doi: 10.1007/s00248-022-02041-5

Mourya, N. R., Bargali, K., and Bargali, S. S. (2019). Impacts of *Coriaria nepalensis* colonization on vegetation structure and regeneration dynamics in a mixed conifer forest of Indian Central Himalaya. *J. For. Res.* 30, 305–317. doi: 10.1007/s11676-018-0613-x

Ndagurwa, H. G., Dube, J. S., and Mlambo, D. (2015). Decomposition and nutrient release patterns of mistletoe litters in a semi-arid savanna, southwest Z imbabwe. *Aust. Ecol.* 40, 178–185. doi: 10.1111/aec.12191

Olsen, S. R., Cole, C. V., Watanabe, F. S., and Dean, L. A. (1954). *Estimation Of Available Phaosphorus In Soils By Extraction With Sodium Bicarbonate*. Washington, DC: Department of Agriculture Circular, US, 939.

Olson, J. S. (1963). Energy storage and balance of producers and decomposers in ecological systems. *Ecology* 14, 322–331.

Petersen, R. C., and Cummins, K. W. (1974). Leaf processing in a woodland stream. *Freshw. Biol.* 4, 343–368.

Rai, I. D. (2012). *Ecological Attributes Of Timberline Vegetation With Special Reference To Climatic Variability In Kedarnath Wildlife Sanctuary*, Ph.D. thesis, Nainital: Kumaun University.

Rawat, N., Nautiyal, B. P., and Nautiyal, M. C. (2010). Litter decomposition rate and nutrient release from different litter forms in a Himalayan alpine ecosystem. *Environmentalist* 30, 279–288. doi: 10.1007/s10669-010-9275-8

Robertson, G. P., and Paul, E. A. (1999). "Decomposition and soil organic matter dynamics," in *Methods Of Ecosystem Science*, eds O. E. Sala, R. B. Jackson, H. A. Mooney, and R. W. Howarth (Berlin: Springer Verlag), 104–116.

Sanderman, J., and Amundson, R. (2005). "Biogeochemistry of decomposition and detrital processing," in *Treatise on Geochemistry*, eds H. D. Holland, W. H. Schlesinger, and K. K. Turekian (Amsterdam: Elsevier), 217–272. doi: 10.1016/B978-0-08-095975-7.00807-X

Santi, C., Bogusz, D., and Franche, C. (2013). Biological nitrogen fixation in non-legume plants. *Ann. Bot.* 111, 743–767. doi: 10.1093/aob/mct048

Santonja, M., Fernandez, C., Gauquelin, T., and Baldy, V. (2015). Climate change effects on litter decomposition: Intensive drought leads to a strong decrease of litter mixture interactions. *Plant Soil* 393, 69–82. doi: 10.1007/s11104-015-2471-z

Silveira, M. L., Reddy, K. R., and Comerford, N. B. (2011). Litter decomposition and soluble, carbon, nitrogen, and phosphorus release in a forest ecosystem. *Open J. Soil Sci.* 1, 86–96.

Singh, J. S., and Singh, S. P. (1992). *Forests of Himalaya: Structure, Functioning and Impact of Man.* Nainital: Gyanodaya Prakashan.

Siqueira, D. P., de Carvalho, G. C. M. W., de Souza Silva, J. G., Caldeira, M. V. W., and Barroso, D. G. (2022). Litter decomposition and nutrient release for two tropical N-fixing species in Rio de Janeiro, Brazil. *J. For. Res.* 33, 487–496. doi: 10.1007/s11676-021-01383-z

Smeti, E., von Schiller, D., Karaouzas, I., Laschou, S., Vardakas, L., Sabater, S., et al. (2019). Multiple stressor effects on biodiversity and ecosystem functioning in a Mediterranean temporary river. *Sci. Total Environ*. 647, 1179–1187. doi: 10.1016/j.scitotenv.2018.08.105

Steffen, W., Richardson, K., Rockstrom, J., Cornell, S. E., Fetzer, I., Bennett, E. M., et al. (2015). Planetary boundaries: Guiding human development on a changing planet. *Science* 347:1259855 . doi: 10.1126/science.1259855

Steidinger, B. S., Crowther, T. W., Liang, J., Van Nuland, M. E., Werner, G. D., Reich, P. B., et al. (2019). Climatic controls of decomposition drive the global biogeography of forest-tree symbioses. *Nature* 569, 404–408. doi: 10.1038/s41586-019-1128-0

Su, Y., Ma, X., Gong, Y., Ahmed, Z., Han, W., Li, K., et al. (2022). Global patterns and drivers of litter decomposition under nitrogen enrichment: A meta-analysis. *Front. For. Glob. Change* 5:895774. doi: 10.3389/ffgc.2022.895774

Tamura, M., Suseela, V., Simpson, M., Powell, B., and Tharayil, N. (2017). Plant litter chemistry alters the content and composition of organic carbon associated with soil mineral and aggregate fractions in invaded ecosystems. *Glob. Change Biol.* 23, 4002–4018. doi: 10.1111/gcb.13751

Tan, B., Yin, R., Zhang, J., Xu, Z., Liu, Y., He, S., et al. (2021). Temperature and moisture modulate the contribution of soil fauna to litter decomposition via different pathways. *Ecosystems* 24, 1142–1156. doi: 10.1007/s10021-020-00573-w

Tu, L. H., Hu, H. L., Chen, G., Peng, Y., Xiao, Y. L., Hu, T. X., et al. (2014). Nitrogen addition significantly affects forest litter decomposition under high levels of ambient nitrogen deposition. *PLoS One* 9:e88752. doi: 10.1371/journal.pone.0088752

Turmel, M. S., Speratti, A., Baudron, F., Verhulst, N., and Govaerts, B. (2015). Crop residue management and soil health: A systems analysis. *Agric. Syst.* 134, 6–16. doi: 10.1016/j.agsy.2014.05.009

Wang, Y., Chang, S. X., Fang, S., and Tian, Y. (2014). Contrasting decomposition rates and nutrient release patterns in mixed vs singular species litter in agroforestry systems. *J. Soils Sediments* 14, 1071–1081. doi: 10.1007/s11368-014-0853-0

Wieczorek, D., Zyszka-Haberecht, B., Kafka, A., and Lipok, J. (2022). Determination of phosphorus compounds in plant tissues: From colourimetry to advanced instrumental analytical chemistry. *Plant Methods* 18:22. doi: 10.1186/s13007-022-00854-6

Yang, K., Zhu, J., Zhang, W., Zhang, Q., Lu, D., Zhang, Y., et al. (2022). Litter decomposition and nutrient release from monospecific and mixed litters: Comparisons of litter quality, fauna and decomposition site effects. *J. Ecol.* 110, 1673–1686. doi: 10.1111/1365-2745.13902

Yang, R., Dong, J., Li, C., Wang, L., Quan, Q., and Liu, J. (2021). The decomposition process and nutrient release of invasive plant litter regulated by nutrient enrichment and water level change. *PLoS One* 16:e0250880. doi: 10.1371/journal.pone.0250880

Zhang, J., Li, H., Zhang, H., Zhang, H., and Tang, Z. (2021). Responses of litter decomposition and nutrient dynamics to nitrogen addition in temperate shrublands of North China. *Front. Plant Sci.* 11:618675. doi: 10.3389/fpls.2020.618675

Zhu, X., Chen, H., Zhang, W., Huang, J., Fu, S., Liu, Z., et al. (2016). Effects of nitrogen addition on litter decomposition and nutrient release in two tropical plantations with N_2-fixing vs. non-N_2-fixing tree species. *Plant Soil* 399, 61–74. doi: 10.1007/s11104-015-2676-1

frontiers | Frontiers in Forests and Global Change

TYPE Original Research
PUBLISHED 09 January 2023
DOI 10.3389/ffgc.2022.1064502

Check for updates

OPEN ACCESS

EDITED BY
Chonggang Xu,
Los Alamos National Laboratory (DOE),
United States

REVIEWED BY
Manoj Kumar Jhariya,
Sant Gahira Guru Vishwavidyalaya,
India
Dessie Assefa,
Bahir Dar University, Ethiopia
Purabi Saikia,
Central University of Jharkhand, India

*CORRESPONDENCE
Surendra Singh Bargali
✉ surendrakiran@rediffmail.com

SPECIALTY SECTION
This article was submitted to
Forest Disturbance,
a section of the journal
Frontiers in Forests and Global Change

RECEIVED 08 October 2022
ACCEPTED 19 December 2022
PUBLISHED 09 January 2023

CITATION
Pandey R, Bargali SS, Bargali K,
Karki H, Kumar M and Sahoo UK
(2023) Fine root dynamics
and associated nutrient flux in Sal
dominated forest ecosystems
of Central Himalaya, India.
Front. For. Glob. Change 5:1064502.
doi: 10.3389/ffgc.2022.1064502

Fine root dynamics and associated nutrient flux in Sal dominated forest ecosystems of Central Himalaya, India

Rachita Pandey [1], Surendra Singh Bargali [1]*,
Kiran Bargali [1], Himani Karki [1], Munesh Kumar [2] and
U. K. Sahoo [3]

[1]Department of Botany, Kumaun University, Nainital, Uttarakhand, India, [2]Department of Forestry and Natural Resources, HNB Garhwal University, Srinagar, Uttarakhand, India, [3]Department of Forestry, Mizoram University, Aizwal, Mizoram

The belowground systems of trees have a major role in forest functioning through absorption of water and nutrient cycling. This study deals with the fine root dynamics including fine root biomass, necromass, production, turnover, and nutrient return in transitional Sal (*Shorea robusta* Gaertn. f.) dominated sub-tropical forest ecosystems of Central Himalaya, India. Four sites namely, Site-1 (Kaladhungi), Site-2 (Fatehpur), Site-3 (Ranibagh), Site-4 (Amritpur) were selected in Sal forest within an elevational range between 405 and 580 m above sea level. The dominant and associated co-dominant species were selected from each site for the estimation of fine root dynamics by using sequential core and ingrowth core methods. The results revealed that the fine root biomass, necromass, and production were significantly ($p < 0.05$) affected by location, seasons, and soil properties. The fine root biomass and production decreased with increasing soil depth and also influenced by stand characteristics including tree density and basal area. The rainy season was most productive with maximum fine root biomass (507.37 kg ha^{-1}) as well as fine root production (600.26 kg ha^{-1} season^{-1}) in the dominant tree species *S. robusta*. Among the associated co-dominant tree species highest fine root biomass (330.48 kg ha^{-1}) and fine root production (410.04 kg ha^{-1} season^{-1}) was reported for *Tectona grandis* L. during the rainy season, while lowest fine root biomass (126.72 kg ha^{-1}) and fine root production (195.59 kg ha^{-1} season^{-1}) in the *Glochidion velutinum* Wight tree species during the winter season. Annual fine root production ranged from 460.26 to 1583.55 kg ha^{-1} yr $^{-1}$, while turnover rate varied from 1.37 to 4.45 yr^{-1} across all the studied sites. The fine roots added carbon input of 154.38 to 564.20 kg ha^{-1} yr^{-1} and nitrogen input of 6.58 to 24.34 kg ha^{-1} yr^{-1} to the soil through annual flux. The study improves our understanding on fine root parameters under the influence of sites, soils and seasonal and spatial variation. The return of nutrients to the soil through fluxes from the roots illustrates the role of fine roots in carbon and nitrogen cycling of the forests and this potential can be harnessed to assess the long-term carbon and nitrogen pool estimations in forests and to plan and manage the forest ecosystems.

KEYWORDS

fine root dynamics, Central Himalaya, ingrowth core, turnover rate, carbon flux, forest ecosystems

Introduction

The forest ecosystems have four major sources that are responsible for the flux of nutrients within the ecosystem namely aboveground, belowground components, litter, and soil (Persch et al., 2015). Among these, the belowground parts have a pivotal role in the functioning of a forest ecosystem and contribute more than 30% of net primary productivity of the terrestrial ecosystems but majority of the studies mainly focus on the contribution of aboveground parts (Mikieleko et al., 2021). Fine roots have a diameter of ≤2 mm are involved in the nutrient acquisition, organic matter accumulation, and elemental flow within the forest ecosystems (Wang et al., 2016) and are mainly concentrated in the soil surface due to the higher concentrations of soil organic matter and rapid microbial activities in the upper horizon of soil (Bargali et al., 2019; Manral et al., 2022). Fine roots have a key role in soil carbon cycling through rapid turnover and root exudates (Pausch and Kuzyakov, 2018; Keller et al., 2021). These fine roots thorough carbon and nitrogen fluxes also helps for the natural regeneration of forests which ultimately conserve the biodiversity, mitigating the atmospheric carbon, and provide multiple ecosystem goods, and services (Chazdon et al., 2020). Efforts to restore the degraded and lost ecosystems are the need of today (Chazdon and Brancalion, 2019). Natural regeneration of forests is an intersection point for conservation and restoration goals (Chazdon, 2019).

Vegetation, soil characteristics and availability of resources determines the development, distribution and proliferation of root system in trees (Weemstra et al., 2020; Awasthi et al., 2022a). Distinct seasonality in the sub-tropical regions alters the resource availability in different seasons resulting in temporal and spatial variability in fine roots (Cusack et al., 2021; Karki et al., 2022). Fine roots have a crucial role in fluxes of carbon and nitrogen in forest ecosystems (Malhi et al., 2017). The fine root biomass and production constitutes a small fraction of tree biomass but the carbon inputs to the soil from fine roots are 1.4 times higher than the inputs from the aboveground components due to the rapid turnover rate of fine roots in most of the terrestrial ecosystems (Ding et al., 2019).

The Bhabhar region which is an alluvial belt with permeable sediments composed of sub-tropical Sal forests that mark a transitional zone between hills and terai; thus have a peculiar topography and vegetation composition. This region also having several ecologically and economically important species that contributes to the nutrient accumulation and nutrient cycling, cardinally and is under immense anthropogenic pressures. The aboveground components of the species have been explored and well documented, while the belowground systems still remain unfathomed (Persch et al., 2015). Fine roots are immensely important component of the forest ecosystems yet the detailed information on fine root dynamics in the Himalayan terrain is limited to some regions only (Usman et al., 2000; Garkoti, 2012; Karki et al., 2021a; Verma et al., 2021). The objectives of the present study were to study the fine root dynamics in Sal dominated forest ecosystem and to assess their role in organic matter and nitrogen accumulation and turnover in soil.

Materials and methods

Study sites and climate

The study was carried out in the Bhabhar region of Nainital district in Central Himalaya, India. An area of 1 ha was established in *Shorea robusta* Gaertn. f. dominated forests at four sites viz. Site-1 (Kaladhungi), Site-2 (Fatehpur), Site-3 (Ranibagh), and Site-4 (Amritpur) varying in topography and soil characteristics and located between 405 and 580 m asl (**Figure 1**). The characteristics of the sites are given in **Table 1**. The study was conducted during August 2017–2019. The study area comes under sub-tropical zone with peculiar climatic regimes with three distinct seasons namely, rainy (July–October), winter (November–February), and summer (March–June). During the 1st year the mean temperature ranged between 9 (January) and 38°C (June) and annual rainfall varied from 0 (October) to 577.6 mm (July), while during the 2nd year the mean temperature ranged from 5 (December) to 40°C (June) and annual rainfall ranged from 5 (January) to 558 mm (July). The climatic specifics are mentioned in **Figures 2**, **3**.

Vegetation and soil sampling

The vegetation was sampled by placing 10 (10 m × 10 m) quadrats for tree species and the density and basal area were determined by following Misra (1968). Soil samples were collected from the three depths (0–20, 20–40, and 40–60 cm) by using a soil corer in random manner in each season and the soil samples were collected in replicates of three, brought to the laboratory and air-dried. Soil texture that indicates the relative content of particles of various sizes, such as sand, silt, and clay in the soil was determined by passing the soil through a series of sieves having different mesh sizes (Indian Standard, 1965). Soil pH was determined by mixing 20 g of soil sample with 40 ml of distilled water in a ratio of 1:2 and by stirring the suspension thoroughly using the glass rod. The mixture was then kept as such for 1 h. The combined electrode was inserted into supernatant and pH was recorded and before taking each new reading the electrode was washed and cleaned using distilled water following Jackson (1958). Bulk density refers to weight of dry soil per unit of volume typically expressed in gm cm^{-3}. To determine the bulk density, a steel augur of known volume was used to collect soil samples from different soil depths, which were brought to the laboratory and oven dried at 60°C till constant weight and bulk density was determined by dividing oven-dried weight of soil by volume ($\pi r^2 h$), following Black (1965). Water holding capacity refers to the ability of a certain soil texture to physically hold water against the force of gravity and was determined by using nickel sieves with water saturated soil in filter papers following Piper (1950). Soil moisture content was determined by collecting 50 g of fresh

TABLE 1 Site descriptions and soil characteristics of sub- tropical Sal forest.

	Site-1 (Kaladhungi)	Site-2 (Fatehpur)	Site-3 (Rani Bagh)	Site-4 (Amritpur)
Dominant tree species	***Shorea robusta*** Roxb. ex Gaertner f.,	***Shorea robusta***	***Shorea robusta***	***Shorea robusta***
Associated tree species	***Mallotus philippensis*** (Lam.) Muell-Arg, *Cassia fistula* L., *Holoptelea integrifolia* (Roxb.) Planch., *Grewia optiva* Drumm. ex Burret, *Aegle marmelos* (L.) Correa, *Holarrhena pubescens* Wall. ex G.Don, *Syzygium cumini* (L.) Skeels, *Bauhinia variegate* L.	***Glochidion velutinum*** Wight, *Mallotus philippensis* (Lam.) Muell-Arg, *Dalbergia sissoo* Roxb., *Syzygium cumini* (L.) Skeels, *Toona ciliata* Roem., *Grewia asiatica* L.	***Holarrhena pubescens*** Wall. ex G.Don, *Mallotus philippensis* (Lam.) Muell-Arg, *Syzygium cumini* (L.) Skeels, *Grewia optiva* Drumm. ex Burret, *Careya arborea* Roxb, *Randia dumetorum* (Retz.) Poir., *Phyllanthus emblica* L., *Terminalia chebula* Retz., *Cassia fistula* L., *Malva parviflora* L., *Ficus hispida* L., *Lannea coromandelica* (Houtt.) Merr.	***Tectona grandis*** L. F., *Mallotus philippensis* (Lam.) Muell -Arg, *Holarrhena pubescens* Wall. ex G.Don, *Butea monosperma* (Lam.) Taub., *Schleichera oleosa* (Lour.), *Haldina cordifolia* (Roxb.) Ridsdale, *Terminalia chebula* Retz., *Ehretia laevis* Roxb., *Terminalia alata* (Gaertner) Roxb., *Syzygium cumini* (L.) Skeels
Latitude (N)	29°17′07.35″	29°19′23.69″	29°17′10.03″	29°17′54.32″
Longitude (E)	79°20′52.67″	79°18′05.34″	79°32′49.19″	79°32′44.11″
Elevation (m a.s.l.)	405	430	580	575
Total density (ind. ha^{-1})	630	620	810	800
Total basal area (m^2 ha^{-1})	28.80	25.51	25.63	29.52
Sand (%)	36.37 ± 2.63	35.79 ± 1.77	32.13 ± 1.27	39.18 ± 1.32
Clay (%)	23.20 ± 1.34	38.21 ± 2.28	36.06 ± 0.75	25.48 ± 1.52
Silt (%)	40.43 ± 1.89	26.01 ± 1.17	31.80 ± 0.71	35.35 ± 0.65
Soil moisture content (%)	13.56 ± 2.04	9.95 ± 1.40	10.86 ± 1.40	13.15 ± 1.37
Water holding capacity (%)	57.10 ± 1.06	44.91 ± 1.75	46.11 ± 1.25	43.27 ± 1.73
Bulk density (g cm^{-3})	1.30 ± 0.03	1.33 ± 0.03	1.32 ± 0.02	1.25 ± 0.03
Porosity (%)	50.08 ± 1.05	48.80 ± 0.02	49.02 ± 0.90	50.08 ± 1.22
pH	5.78 ± 0.08	7.05 ± 0.09	7.49 ± 0.06	5.41 ± 0.07
Soil organic carbon (SOC) (%)	1.29 ± 0.04	1.74 ± 0.03	1.48 ± 0.03	2.74 ± 0.05
Total nitrogen (%)	0.17 ± 0.003	0.21 ± 0.004	0.19 ± 0.003	0.25 ± 0.009

The dominant and codominant tree species mentioned in bold letters were selected for fine root dynamics.

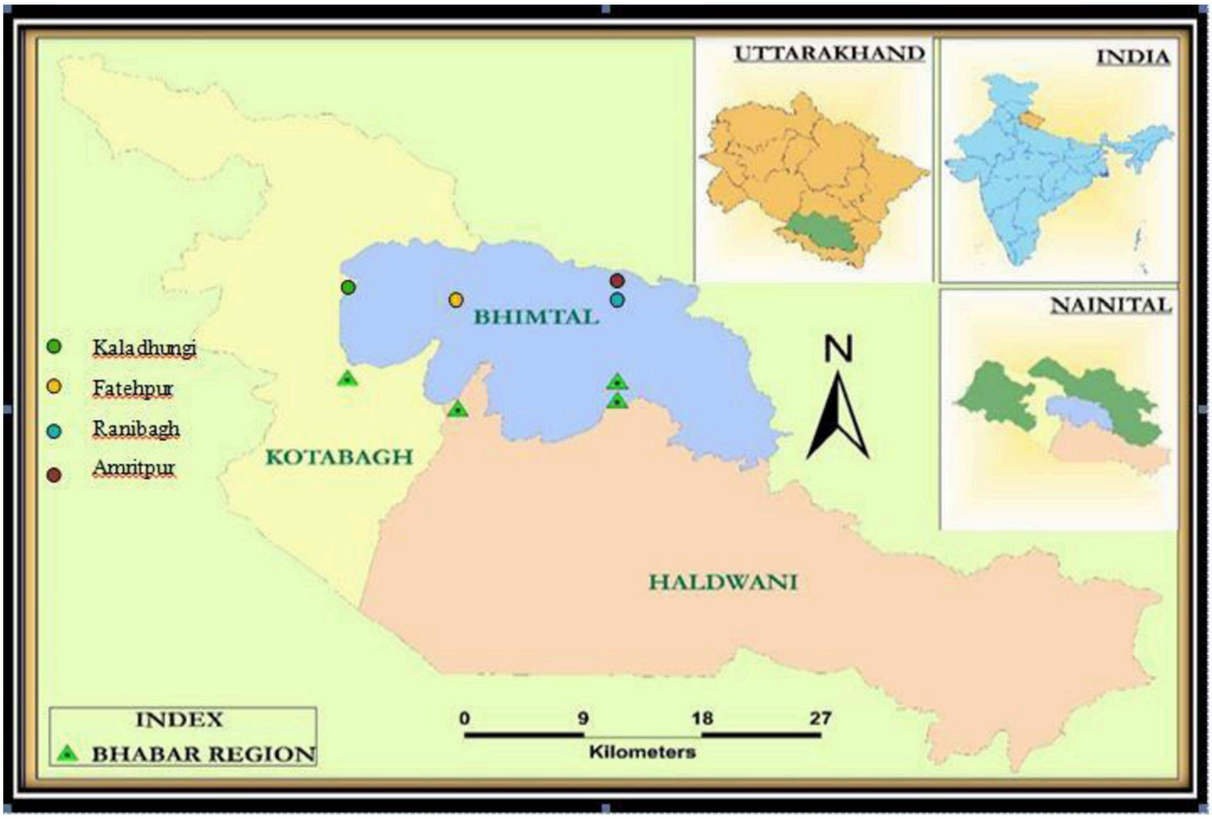

FIGURE 1
Map of the study area.

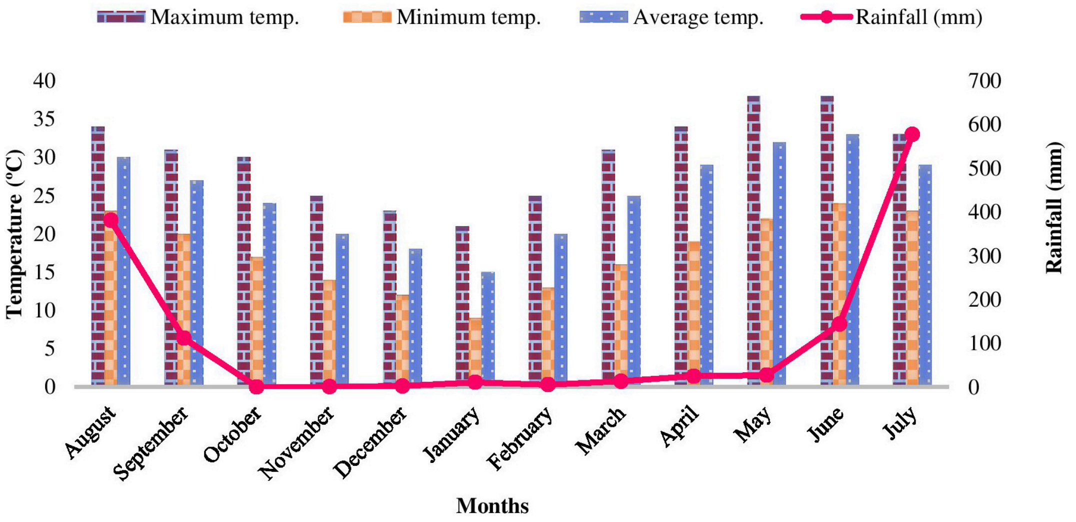

FIGURE 2
Climatic data during August 2017–July 2018.

soil samples (in triplicates), which were oven dried, weighed, and moisture content was calculated on the basis of dry weight following Jackson (1958). Soil porosity that represents void or empty pore spaces in the soil which is of crucial importance for conduction of water, air, and nutrients into the soil was determined by substracting, dividing bulk density values by a

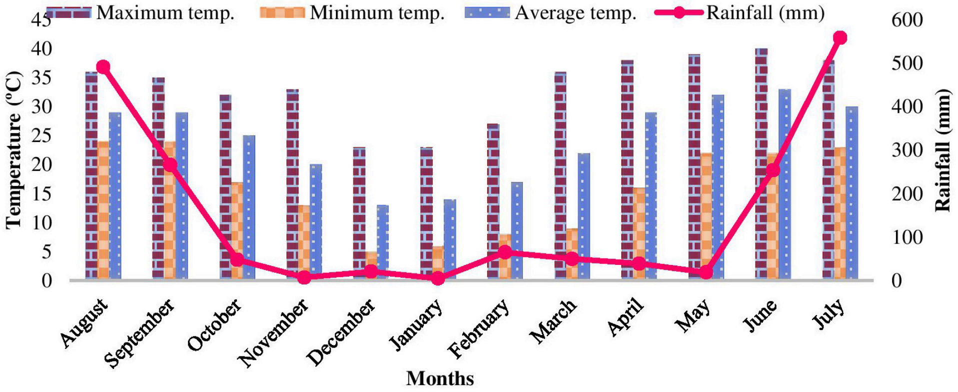

FIGURE 3
Climatic data during August 2018–July 2019.

factor of 2.6 and multiplying with 100 following Kumar (2000). Soil organic carbon was estimated by using Walkley and Black (1934) procedure based on rapid dichromate oxidation. Soil nitrogen was determined by using Kjeldhal digestion method following defined standard ecological protocols (Subbiah and Asija, 1956).

Sampling of fine roots

For fine root estimation, at each location fine roots of dominant and co-dominant tree species were collected at 1 and 1.5 m distance from tree bole at 3 depths (0–20, 20–40, and 40–60 cm) through stratified random sampling. The fine root biomass (FRB) was estimated through sequential soil core method which is a direct method that equates root biomass using a steel auger having an internal diameter of 7.5 cm and a length of 60 cm. This method is simple in operational principle and provides highly accurate details of spatial and temporal variability of fine roots. The fine roots were extracted seasonally (rainy, winter, summer) up to the depth of 60 cm (0–20, 20–40, and 40–60 cm soil depth) using the steel auger. Roots were extracted from soil core and the hole was refilled with root-free soil. Depth wise root samples were collected from different directions and were pooled. Individual cores were placed in separate bags and taken to the laboratory to separate the fine roots. Organic material was separated from the roots by passing the individual soil cores through a sequence of sieves. The living and dead roots were hand sorted from the residues remaining in each sieve on the basis of color and texture and fine root biomass and necromass were determined. Fine root production (FRP) was estimated through ingrowth core method (Lukac and Godbold, 2010; Karki et al., 2022). The ingrowth core method is also a direct method which is based on the assumption that the disturbances to the roots and soil do not affect the root in growth and is highly economical and efficient. In this method, first time sampling of roots was done by using soil corer. Roots were collected and ingrowth cores (nylon net with mesh size of 2 mm and mesh openings) were installed vertically in holes of 60 cm depth where the soil had been removed with a corer, and the ingrowth cores were filled with root-free soil from the same stand and left in the field for about four months' time interval which is optimal duration for assessing the ingrowth of fine roots. Thus, root-free cores were installed three times in each year during the study for the estimation of seasonal FRP. The cylindrical ingrowth core with mesh openings allows only the entry of fine roots, soil microorganisms into it due to its defined mesh size. The subsequent growth of roots in this nylon net was measured and used to estimate fine root production in the field. The collected roots from the respective depths and distances in each site were brought to the laboratory, pooled depth wise and were separated from debris and other organic material, cleaned and divided into live and dead roots on the basis of keen visual inspection and ultimately oven dried at 60°C for 48 h. The oven dried root samples were weighed, grinded, and kept in sealed plastic bags for carbon (Jackson, 1958) and nitrogen (micro-Kjeldhal method) analysis. At each location 3 individuals of each tree species were selected, marked and fine roots were collected seasonally, resulting in a total of 432 fine root samples each year $\{3_{\text{(Trees)}} \times 2_{\text{(species)}} \times 4_{\text{(sites)}} \times 3_{\text{(depths)}} \times 2_{\text{(distances)}} \times 3_{\text{(seasons)}}\}$. Three individuals of each tree species were selected to unify the sampling procedure and to reduce the chances of biasness and errors in the study. The field sampling procedures were designed in such a manner that the clumping or overlapping of sampling locations and fine roots of different trees can be avoided. As the samples for each tree species were collected from a region where mostly the individuals of the same tree species were present within the study area to avoid any confusion in fine root collection and to capture the spatial heterogeneity of root distribution in the studied sites. Annual fine root production was calculated by summing the seasonal fine root production (Lopez et al., 2001). Fine root turnover was determined by dividing the annual fine root ingrowth by maximum fine root biomass depth wise and distance wise (Dahlmand and Kucera, 1965; Karki et al., 2021b). Mean fine root biomass and production and turnover values were determined depth wise seasonally and fine root datasets were prepared site wise for 2 years.

The annual carbon and nitrogen flux from the fine roots were calculated by multiplying the annual fine root production (kg ha^{-1} yr^{-1}) with the carbon and nitrogen concentrations (%) in the fine roots following Xia et al. (2015) that yields the annual carbon and nitrogen input into the soil through fine roots.

Statistical analysis

SPSS 25 was used to establish relationship between vegetational attributes and fine root dynamics among the experimental sites, across the seasons and year. PAST3 (Paleontological Statistics Software for Education and Data Analysis) statistical package was used to determine the impact of soil properties on fine root dynamics.

Results

Vegetation and soil characteristics

The vegetational analysis revealed the dominance of *S. robusta* in all the sites and presence of co-dominant species like *Mallotus philippensis* (Lam.) Muell.-Arg at Kaladhungi, *Glochidion velutinum* Wight at Fatehpur, *Holarrhena pubescens* Wall. ex G.Don at Ranibagh and *Tectona grandis* L. at Amritpur. Across the locations total tree density ranged between 620 (Fatehpur) and 810 ind ha^{-1} (Ranibagh). Highest total basal area was reported in Amritpur (29.52 m^2 ha^{-1}) and lowest in Fatehpur (25.51 m^2 ha^{-1}). The soil was deep, well drained, neutral to slightly alkaline, coarse-loamy/fine loam, mainly composed of poorly sorted unconsolidated sediments like pebbles, gravels, sand, and silt with intervening clay layers which makes it highly porous. The percent sand content in the soil ranged from 32.13 (Ranibagh) to 39.18% (Amritpur), clay content varied from 23.20 (Kaladhungi) to 38.21% (Fatehpur) and silt content ranged between 26.01 (Fatehpur) and 40.43% (Kaladhungi). Soil moisture content was recorded lowest at Fatehpur (9.95%) and highest at Kaladhungi (13.56%). The maximum water holding capacity was recorded at Kaladhungi (57.10%), while, minimum at Amritpur (43.27%). Bulk density was highest at Fatehpur (1.33 g cm^{-3}) and lowest at Amritpur (1.25 g cm^{-3}). Porosity was highest at Kaladhungi and Amritpur (50.08%), while lowest at Fatehpur (48.80%). Soil pH ranged from slightly acidic (5.41) in Amritpur to slightly basic (7.49) in Ranibagh. The soil organic carbon content varied from 1.29 (Kaladhungi) to 2.74% (Amritpur), while total nitrogen content of the soil was reported to be maximum at Amritpur (0.25%) and minimum (0.17%) at Kaladhungi (**Table 1**).

Distribution pattern of fine roots

All the locations showed similar pattern of fine root distribution. Vertically, highest fine root dispersal was recorded in the uppermost layer (262.16–362.03 kg ha^{-1}) which decreased with increasing soil depth during both the experimental years in all the species (**Figures 4A–D**). Horizontally, fine roots were more concentrated at 1 m distance (124.52–356.62 kg ha^{-1}) from tree bole as compared to 1.5 m distance (110.75–313.75 kg ha^{-1}) though the differences were statistically not significant (**Figures 4A–D**).

Fine root biomass

During the 1st year, at 1 m distance from the tree base FRB of *S. robusta* was maximum at Amritpur (362.03 kg ha^{-1}) and minimum at Ranibagh (179.65 kg ha^{-1}), while at 1.5 m distance from the tree base, highest value of FRB was reported at Kaladhungi (431.91 kg ha^{-1}) and lowest FRB was reported at Ranibagh (158.52 kg ha^{-1}). During the 2nd year, at 1 m distance from the tree base, the highest FRB was recorded at Fatehpur (377.90 kg ha^{-1}), and lowest FRB was reported at Ranibagh (225.64 kg ha^{-1}). The value of FRB at 1.5 m distances from the tree base was recorded to be maximum at Kaladhungi (451.83 kg ha^{-1}) whereas, minimum FRB was reported at Ranibagh (181.50 kg ha^{-1}). For the co-dominant species at Kaladhungi, the highest values of FRB (338.97 and 298.66 kg ha^{-1}) were reported for *M. philippensis* at 1 and 1.5 m distance from the tree base, respectively, while lowest FRB was observed at Fatehpur for *G. velutinum,* (107.16 kg ha^{-1} at 1 m distance and 102.19 kg ha^{-1} at 1.5 m distance from tree base), during the 1st year. During the 2nd year, maximum FRB was reported for *M. philippensis* at Kaladhungi while, lowest for *G. velutinum* at Fatehpur at both the distances from the tree base (**Figures 4C, D**).

Fine root necromass

Across the sites, the fine root necromass (FRN) of *S. robusta* was highest (109.05 kg ha^{-1}) at Amritpur and lowest (52.31 kg ha^{-1}) at Kaladhungi at the distance of 1 m from the tree base during the 1st year. At 1.5 m distance from the tree base, maximum FRN was reported at Amritpur (113.08 kg ha^{-1}) and minimum (51.32 kg ha^{-1}) at Kaladhungi. During the 2nd year, the maximum (114.46 kg ha^{-1} at 1 m distance and 114.83 kg ha^{-1} at 1.5 m distance) and minimum (57.48 kg ha^{-1} at 1 m distance and 58.86 kg ha^{-1} at 1.5 m distance)

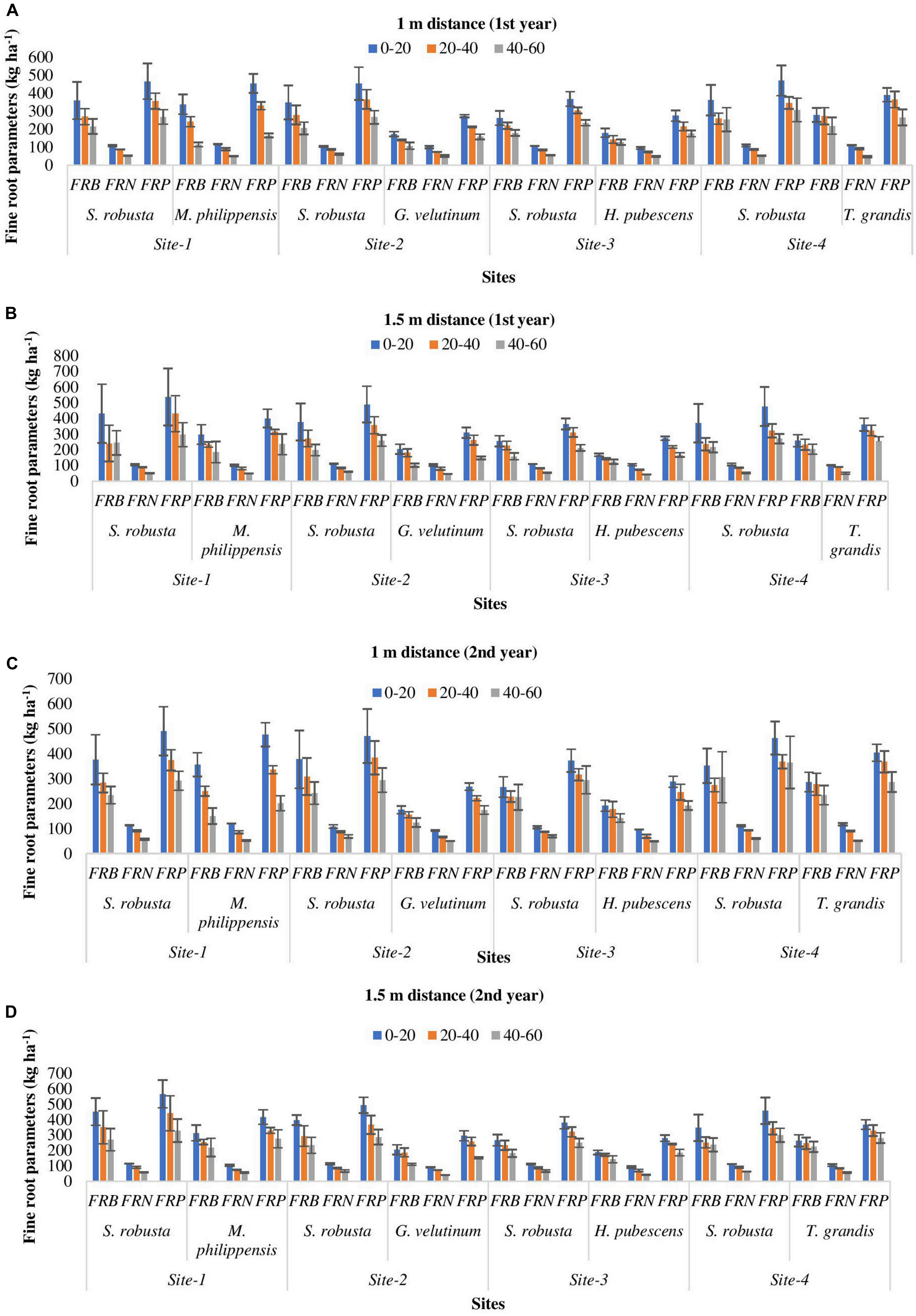

FIGURE 4

Spatial variability **(A–D)** in fine roots parameters (kg ha^{-1}) of trees in Sal forest sites. FRB, fine root biomass; FRN, fine root necromass; FRP, fine root production.

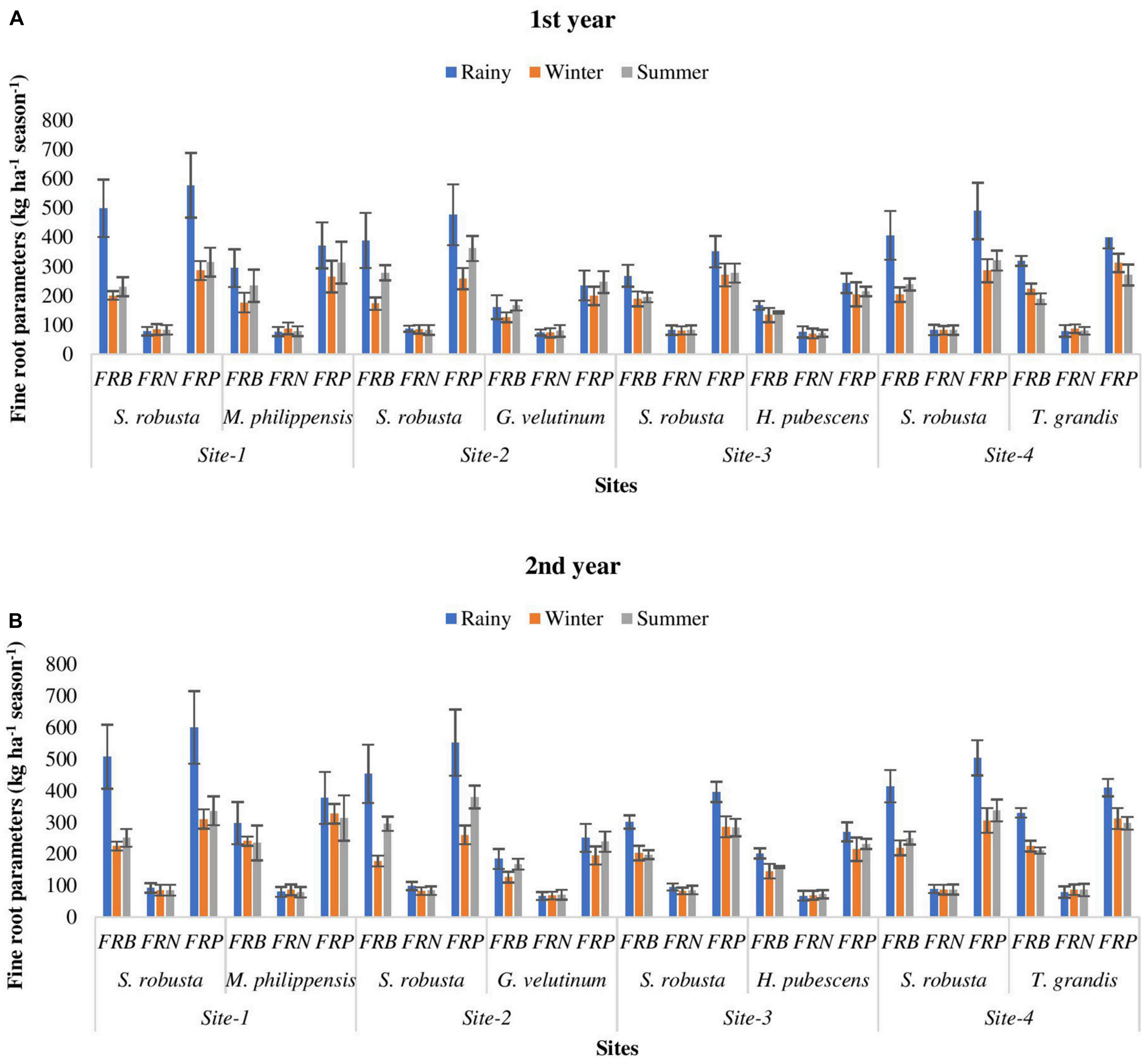

FIGURE 5
Temporal variability in fine root parameters (kg ha^{-1} season^{-1}) among the experimental sites during 1st **(A)** and 2nd **(B)** year. FRB, fine root biomass; FRN, fine root necromass; FRP, fine root production.

FRN was recorded at Kaladhungi. For the co-dominant species, during the 1st year at 1 m distance from the tree base, the maximum FRN was recorded at Kaladhungi for *M. philippensis* (116.34 kg ha^{-1}) and minimum FRN was recorded at Amritpur for *T. grandis* (47.17 kg ha^{-1}) while at 1.5 m distance, the highest (105.65 kg ha^{-1}) and lowest FRN (44.02 kg ha^{-1}) was recorded for *H. pubescens* at Ranibagh. During the 2nd year, at 1 m distance from the tree base, the highest FRN (120.12 kg ha^{-1}) was recorded for *M. philippensis* at Kaladhungi while, lowest value of FRN (49.68 kg ha^{-1}) was recorded for *H. pubescens* at Ranibagh. At 1.5 m distance from the tree base, the maximum FRN (105.02 kg ha^{-1}) was recorded for *T. grandis* of Amritpur and minimum (40.88 kg ha^{-1}) for *G. velutinum* at Fatehpur (**Figures 4C, D**).

Seasonal fine root production

During the 1st year, the fine root production of *S. robusta* across the locations at 1 m distance from the tree base was maximum (471.08 kg ha^{-1} season^{-1}) at Amritpur and minimum (235.49 kg ha^{-1} season^{-1}) at Ranibagh, while at 1.5 m distance from the tree base highest fine root production was reported at Kaladhungi (538.82 kg ha^{-1} season^{-1}) and lowest (212.98 kg ha^{-1} season^{-1}) at Ranibagh. During the 2nd year, at 1 m distance from the tree base, the highest (491.22 kg ha^{-1} season^{-1}) and lowest (291.86 kg ha^{-1} season^{-1}) FRP were recorded at Kaladhungi. The maximum value of FRP at 1.5 m distance from the tree base was recorded at Kaladhungi (566.67 kg ha^{-1} season^{-1}) and minimum at

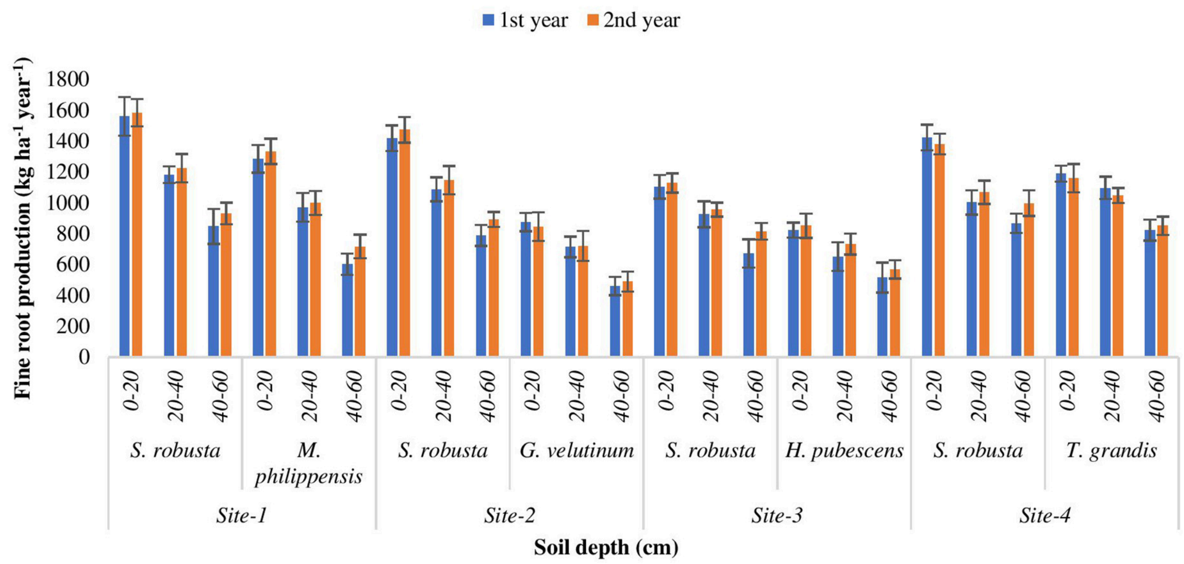

FIGURE 6
Variability in annual fine root production (AFRP) among the experimental sites (kg ha^{-1} year^{-1}).

Ranibagh (249.04 kg ha^{-1} season^{-1}). Among the co-dominant tree species highest FRP was estimated for *M. philippensis* at Kaladhungi while, lowest FRP was recorded for *G. velutinum* at Fatehpur during both the studied years as well as at both the distances. At 1 m distance from the tree base, the maximum FRP was 455.32 kg ha^{-1} season^{-1} and minimum FRP was 158.10 kg ha^{-1} season^{-1}, while at 1.5 m distance, the highest recorded FRP was 401.80 kg ha^{-1} season^{-1} and lowest FRP was 148.73 kg ha^{-1} season^{-1}, during the 1st year. During the 2nd year, at 1 m distance from the tree base, the highest FRP was 476.74 kg ha^{-1} season^{-1} and lowest FRP was 174.83 kg ha^{-1} season^{-1}. At 1.5 m distance from the tree base, the maximum FRP was 416.89 kg ha^{-1} season^{-1} and minimum FRP was 151.62 kg ha^{-1} season^{-1} (**Figures 4C, D**).

Seasonal variation in fine roots

Fine root biomass, production and turnover of dominant and associated species also varied significantly ($p < 0.05$) across the seasons and years ($p < 0.05$).

Fine root biomass

During both the year, FRB of *S. robusta,* was maximum during the rainy season at Kaladhungi, while minimum during the winter season at Fatehpur. Among the co-dominant tree species, the highest FRB during 1st year was reported during rainy season for *T. grandis* (319.64 kg ha^{-1}) at Amritpur, while lowest FRB was recorded during winter season for *G. velutinum* (126.72 kg ha^{-1}). During 2nd year, the maximum FRB was observed for *T. grandis* (330.48 kg ha^{-1}) at Amritpur and minimum FRB was reported for *G. velutinum* (126.72 kg ha^{-1}) at Fatehpur (**Figures 5A, B**).

Fine root necromass

During both the years, for *S. robusta,* the FRN was highest at Fatehpur during the rainy season and minimum at Ranibagh during the winter season. For the co-dominant tree species, during 1st year, the FRN was maximum during rainy season for *T. grandis* (79.87 kg ha^{-1}) at Amritpur, and minimum during winter season for *H. pubescens* (71.06 kg ha^{-1}) at Ranibagh. The FRN was highest at Kaladhungi for *M. philippensis* (80.18 kg ha^{-1}) and lowest for *G. velutinum* (68.87 kg ha^{-1}) at Fatehpur, during the 2nd year (**Figures 5A, B**).

Fine root production

During both the years, the FRP of *S. robusta* was maximum during rainy season at Kaladhungi, and minimum during winter season at Fatehpur. Across the years, during 1st year maximum FRP was 578.39 kg ha^{-1} season^{-1}, while during 2nd year it was 600.26 kg ha^{-1} season^{-1}. The minimum values of FRP were 258.91 and 260.54 kg ha^{-1} season^{-1} during 1st year and 2nd year, respectively. Among the co-dominant tree species, during 1st year, the FRP was maximum during rainy for *T. grandis* (399.50 kg ha^{-1} season^{-1}) at Amritpur, and minimum during winter season for *G. velutinum* (200.30 kg

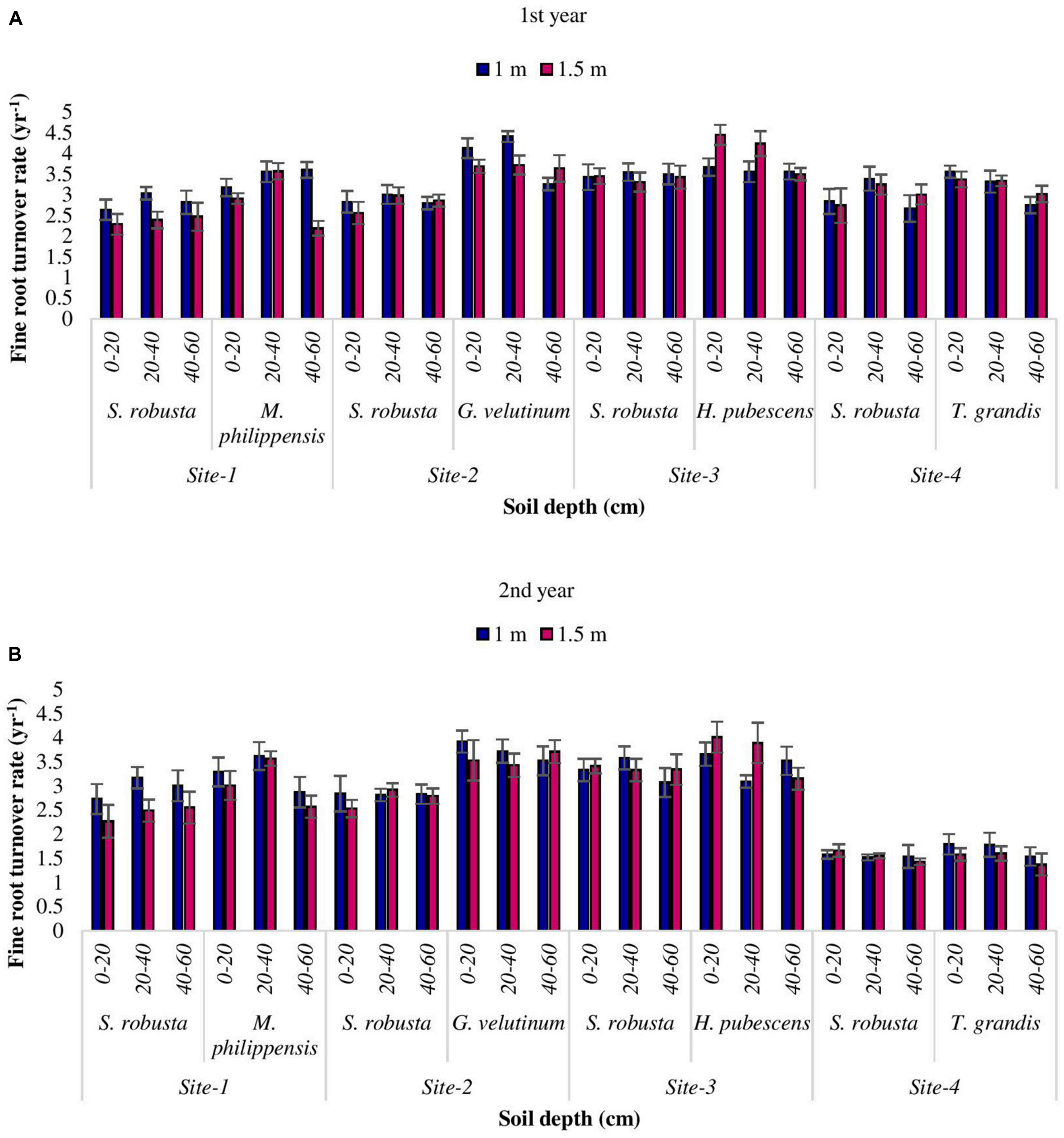

FIGURE 7
Variability in turnover rate (yr^{-1}) among the studied Sal forest sites during 1st **(A)** and 2nd year **(B)**.

ha^{-1} season^{-1}) at Fatehpur. The highest FRP was observed at Amritpur for *T. grandis* (410.04 kg ha^{-1} season^{-1}) and lowest FRP was reported for *G. velutinum* (195.59 kg ha^{-1} season^{-1}) at Fatehpur, during 2nd year (Figures 5A, B).

Annual fine root production

In the present study, AFRP showed a decreasing trend with increasing soil depth. During the 1st year, annual fine root production of *S. robusta* ranged from 672.709 (Ranibagh) in deepest (40–60 cm) soil depth to 1559.935 kg ha^{-1} yr^{-1} (Kaladhungi) in uppermost (0–20 cm) soil depth. During the 2nd year, the AFRP for *S. robusta* varied from 816.547 (Ranibagh) to 1583.554 kg ha^{-1} yr^{-1} (Kaladhungi). During the 1st year, for the co-dominant tree species, the highest annual fine root production (1285.67 kg ha^{-1} yr^{-1}) was recorded for *M. philippensis* (Kaladhungi) in 0–20 cm soil depth, while lowest AFRP (460.255 kg ha^{-1} yr^{-1}) was observed for *G. velutinum* (Fatehpur) in 40–60 cm soil depth. During the 2nd year, AFRP ranged between 489.685 kg ha^{-1} yr^{-1} for *G. velutinum* (Fatehpur) in 40–60 cm soil depth to 1333.78 kg ha^{-1} yr^{-1} for *M. philippensis* (Kaladhungi) in 0–20 cm soil depth (**Figure 6**).

Turnover rate (yr^{-1})

The rate of fine root turnover was observed highest at upper most soil layer while, least at deeper soil depth in the present study. Fine root turnover rate of *S. robusta* ranged between 2.67 (Amritpur) and 3.43 yr^{-1} (Ranibagh) at 1 m distance from the tree base while, at 1.5 m distance from the tree base, the maximum turnover rate was reported at Ranibagh (3.45 yr^{-1}) and minimum at Kaladhungi (2.47 yr^{-1}) during the 1st year. During the 2nd year, at 1 m distance the turnover rate for *S. robusta* varied from 1.54 (Amritpur) to 3.33 yr^{-1} (Ranibagh), while at 1.5 cm distance from the tree base, the highest turnover rate was observed at Ranibagh (3.41 yr^{-1}) and least at Amritpur (1.43 yr^{-1}). Among the co-dominant tree species, during the 1st year at 1 m distance from the tree base turnover rate varied from 2.75 (for *T. grandis* at Amritpur) to 4.13 yr^{-1} (for *G. velutinum*) at Fatehpur, whereas at 1.5 m distance, the highest turnover rate (4.45 yr^{-1}) was reported for *H. pubescens* at Ranibagh and lowest turnover rate (2.19 yr^{-1}) was observed for *M. philippensis* at Kaladhungi. During the 2nd year, the turnover rate ranged from 1.54 (for *T. grandis*) at Amritpur to 3.92 yr^{-1} (for *G. velutinum*) in Fatehpur at 1 m distance whereas, at 1.5 m distance from the tree base the highest turnover rate (4.01 yr^{-1}) was observed for *H. pubescens* at (Ranibagh) and lowest turnover rate (1.37 yr^{-1}) was reported for *T. grandis* at Amritpur (**Figures 7A, B**).

TABLE 2 Carbon concentration (%) in fine roots of trees under selected sub- tropical Sal forests.

Tree species	1st year			2nd year		
Soil depths (cm)						
	0–20	20–40	40–60	0–20	20–40	40–60
Site-1						
S. robusta	35.93	36.03	35.83	35.79	35.59	35.46
M. philippensis	33.23	33.26	33.63	32.90	33.34	32.89
Site-2						
S. robusta	37.05	36.32	36.31	36.97	36.22	35.92
G. velutinum	33.33	33.22	33.54	32.82	32.99	32.86
Site-3						
S. robusta	37.65	37.55	37.87	37.56	37.64	37.61
H. pubescens	32.20	32.21	32.46	31.92	32.42	32.51
Site-4						
S. robusta	39.64	39.97	40.36	39.71	39.97	40.53
T. grandis	34.24	34.15	34.19	33.80	33.98	33.98

TABLE 3 Nitrogen concentration (%) in fine roots of trees under selected sub- tropical Sal forests.

Tree species	1st year			2nd year		
Soil depths (cm)						
	0–20	20–40	40–60	0–20	20–40	40–60
Site-1						
S. robusta	1.44	1.32	1.29	1.44	1.32	1.29
M. philippensis	1.14	1.13	1.14	1.10	1.15	1.16
Site-2						
S. robusta	1.56	1.48	1.42	1.53	1.49	1.45
G. velutinum	1.50	1.43	1.43	1.48	1.43	1.42
Site-3						
S. robusta	1.69	1.64	1.56	1.64	1.59	1.53
H. pubescens	1.40	1.36	1.32	1.41	1.35	1.33
Site-4						
S. robusta	1.71	1.58	1.47	1.65	1.55	1.47
T. grandis	1.38	1.28	1.25	1.35	1.31	1.28

Nutrient return

Fine roots are an important source and sink for nutrients in terrestrial ecosystems. There were important differences in the nutrient concentrations (carbon and nitrogen) of roots as a function of soil depth with significant declines in concentration with depth (**Tables 2**, **3**). The highest annual carbon flux (564.20 kg ha^{-1} yr^{-1}) was recorded for *S. robusta* in 0–20 cm soil depth at Amritpur during 1st year as well as at Kaladhungi during the 2nd year. The lowest carbon flux was observed in 40–60 cm soil depth at site-3 (254.76 kg ha^{-1} yr^{-1}) during 1st and 2nd year (307.10 kg ha^{-1} yr^{-1}). Among the associated tree species, maximum carbon flux was reported for *M. philippensis* in 0–20 cm soil depth during 1st (427.16 kg ha^{-1} yr^{-1}) as well as 2nd year (438.86 kg ha^{-1} yr^{-1}) at Kaladhungi, while minimum flux was reported for *G. velutinum* in 40–60 cm soil depth during 1st year (154.38 kg ha^{-1} yr^{-1}) and 2nd year (160.93 kg ha^{-1} yr^{-1}) at Fatehpur (**Figure 8**).

The maximum annual nitrogen flux was observed for *S. robusta* at in 0–20 cm soil depth at Amritpur (24.34 kg ha^{-1} yr^{-1}) during the 1st year and at Kaladhungi (22.80 kg ha^{-1} yr^{-1}) during the 2nd year. The lowest carbon flux was observed in 40–60 cm soil depth at Ranibagh during the 1st year (10.49 kg ha^{-1} yr^{-1}) and at Kaladhungi during the 2nd year (12.01 kg ha^{-1} yr^{-1}). Among the associated tree species highest annual nitrogen flux was reported for *T. grandis* during 1st (16.41 kg ha^{-1} yr^{-1}) as well as 2nd year (15.65 kg ha^{-1} yr^{-1}) at Amritpur, while minimum flux was reported for *G. velutinum* during 1st year (6.58 kg ha^{-1} yr^{-1}) and 2nd year (6.97 kg ha^{-1} yr^{-1}) at Fatehpur (**Figure 9**).

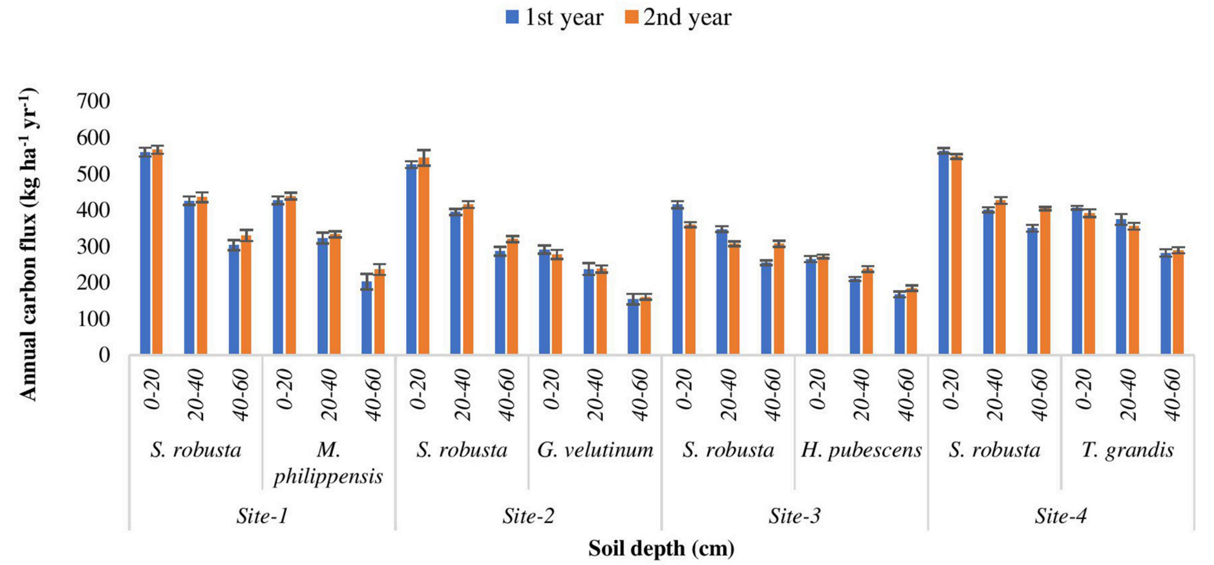

FIGURE 8
Annual carbon flux (kg ha^{-1} yr^{-1}) into the soil *via* fine roots in sub- tropical Sal forest.

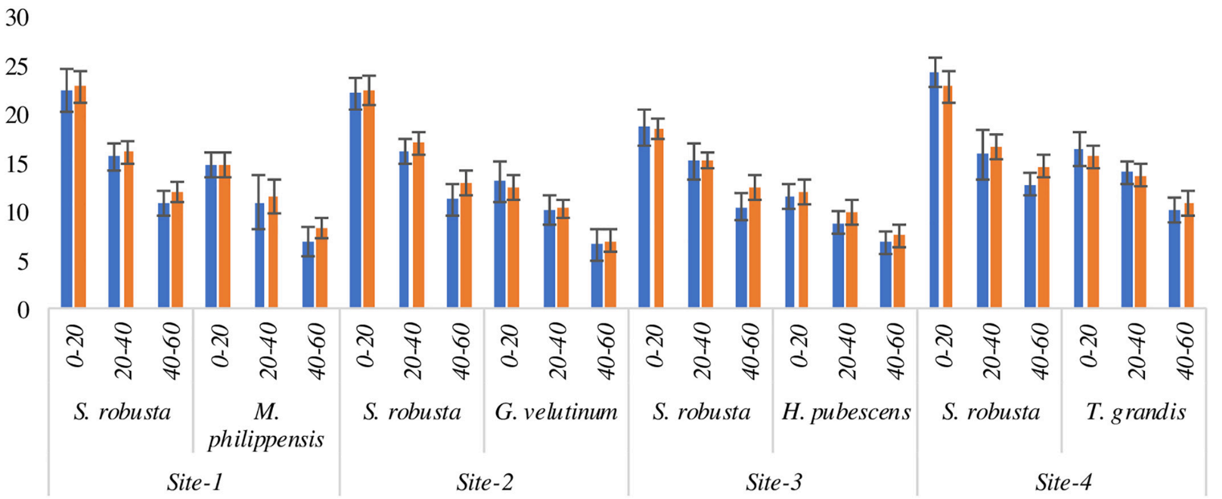

FIGURE 9
Annual nitrogen flux (kg ha^{-1} yr^{-1}) into the soil *via* fine roots in sub- tropical Sal forest.

Discussion

The vertical gradient of fine root distribution revealed a distinct pattern with higher biomass, necromass and production in the superficial horizon of soil (0–20 cm) which declined subsequently in the deeper soil depths (20–40 and 40–60 cm). This pattern was observed probably because the top layer of soil (0–20 cm) is enriched with nutrient contents, organic matter which provides favorable microclimatic conditions for the expansion of root system. The different soil layers differ in their nutrient and water contents and thus have disparity in the distribution of fine roots (Sahu et al., 2013; Wang et al., 2016). The nutrient concentration of the surface layer is also supplemented by litter decomposition (Rosado et al., 2011; Oraon et al., 2018). Similar patterns of fine root distribution were also reported by Mikieleko et al. (2021) in semi-deciduous forest of Republic of Congo and Katayama et al. (2019) in tropical rainforest of Joshi and Garkoti (2021) in white oak forests of the Indian Central Himalayan region.

The present study revealed that spatial distribution of fine root biomass exhibited a peculiar pattern with highest fine root

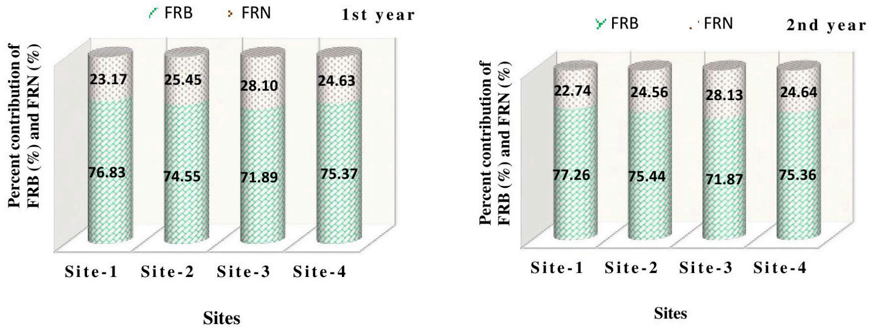

FIGURE 10
Percent contribution of fine root biomass (FRB) and fine root necromass (FRN) to fine root production among the study sites during the study period.

biomass (507.37 kg ha^{-1}) and fine root production (600.26 kg ha^{-1} season^{-1}) during the rainy season followed by summer and winter seasons, respectively. These seasonal variations in fine root biomass and production may be ascribed to the suitable moisture and temperature regimes as also supported by the climatic data obtained during the study periods. As the rainy season coincides with active growth period of many Himalayan tree species and during this season, the nutrients get dissolved in soil solution and percolate into deeper soil, thus to meet the demand of metabolic activities and growing vegetative structures, the root system elaborates resulting in higher fine root production. The temperature and moisture conditions are pertinent with respect to fine root growth as they are accountable for the carbon and nutrient allocation within terrestrial tropical and sub-tropical ecosystems. The significant relationship between fine root parameters and rainfall patterns in tropical forests of Ghana and chir-pine mixed banj-oak forests of Central Himalaya were also reported by Ibrahim et al. (2020) and Verma et al. (2021). Significant effect of temperature on fine root dynamics in sub-tropical forests was observed by Fu et al. (2015). The annual fine root production was higher for the dominant tree species *S. robusta* (672.71–1583.55 kg ha^{-1} yr^{-1}) as compared to the associated co-dominant species (460.26–1333.78 kg ha^{-1} yr^{-1}).

Across the sites, maximum fine root biomass was recorded at Kaladhungi (76.83–77.26%), while maximum FRN (28.10–28.13%) was recorded at Ranibagh during 1st as well as 2nd year (**Figure 10**). The FRB values obtained in the present study are comparable with the studies conducted in forests around the globe. Fine root biomass within a range of 1.1–5.8 t ha^{-1} in sub-tropical forests of China was observed by Yang et al. (2002) and Pei et al. (2018). The values of fine root biomass were reported from 174.3 to 516.6 g m^{-2} in protected natural forests of, in tropical Central Amazonian forest of Brazil by Singha et al. (2020), the FRB values ranged between 1.9 and 13.1 Mg ha^{-1} (Cordeiro et al., 2020) and in Central Himalayan chir-pine and banj-oak forests the FRB values were 24 to 972 kg ha^{-1} (Usman et al., 1997). Similar findings were also reported for fine root production from the deciduous forest of Central Himalaya (2.94–6.34 Mg ha ha^{-1} yr^{-1}) by Garkoti (2011) and the agro-ecosystems of Central Himalaya (232.2–1905.9 kg ha^{-1} yr^{-1}) by Karki et al. (2021c, 2022).

Turnover rate (yr^{-1}) refers to the growth and dieback of fine roots and plays a crucial role in forest ecosystems as it provides carbon and nutrient inputs into the soil (Lukac, 2012). The water and nutrient accessibility to the growing vegetation in the forest ecosystems regulates the fine root turnover rates (Lima et al., 2010). The results showed no definite trend across the sites as well as depth the possibly due to the specific habitat conditions and climatic attributes as these variations are very evident in the Himalayan regions (Bargali et al., 2018). Similar findings from the global as comparison of turnover rates in boreal, temperate and tropical forests also reported by Finer et al. (2011). The values (1.37–4.45 yr^{-1}) are comparable with the values (2.3–3.1 yr^{-1}) reported by Ibrahim et al. (2020) and were comparatively higher than the values reported by Usman et al. (2000) and Verma et al. (2021) for chir- pine and banj-oak forests (0.67–0.84 yr^{-1}) and Karki et al. (2021a) for agroforestry systems (1.38–2.67 yr^{-1}) of Central Himalaya. The sub-tropical and tropical forests have higher fine root production and rapid turnover rates in comparison to the boreal and temperate forests (Wang et al., 2019).

Fine roots significantly contribute to the carbon and nitrogen inputs of the soil through fluxes, decomposition and mortality (Gautam and Mandal, 2018; Bibi et al., 2022). About 70% of soil organic carbon is sequestered by roots and is returned back to the soil on mortality (Finer et al., 2019). In the present study, the carbon fluxes from tree fine roots ranged between 154.38 and 564.20 kg ha^{-1} yr^{-1}, while nitrogen fluxes varied from 6.58 to 24.34 kg ha^{-1} yr^{-1}, during the study period. Similar findings were observed by Cornejo et al. (2021) for the carbon flux (171.26–211.72 g m^{-2} yr^{-1}), nitrogen flux (2.83–7.67 g m^{-2} yr^{-1}) and by Hertel et al. (2009) for carbon flux (127.2–232.8 g m^{-2} yr^{-1}) in tropical forest stands varying

TABLE 4 Pearson's correlation matrix of soil and fine root parameters ($n = 1800$).

	Y	SI	SE	SD	Sand	Silt	Clay	bD	Po	SMC	WHC	SOC	SN	C: N	pH	FRB-Sal	FRN-Sal	FRP-Sal	FRB -AS	FRN-AS	FRP-AS
Y		1^{NS}	1^{NS}	1^{NS}	1^{NS}	1^{NS}	1^{NS}	1^{NS}	1^{NS}	1^{NS}	1^{NS}	0.78^{NS}	0.83^{NS}	0.95^{NS}	0.97^{NS}	0.53^{NS}	0.33^{NS}	0.46^{NS}	0.38^{NS}	0.71^{NS}	0.53^{NS}
SI			1^{NS}	1^{NS}	0.34^{NS}	0.53^{NS}	0.23^{NS}	0.94^{NS}	0.19^{NS}	0.89^{NS}	$9.99 \times 10^{-15*}$	0.11^{NS}	$8.46 \times 10^{-05*}$	0.01^{NS*}	0.48^{NS}	0.22^{NS}	0.96^{NS}	0.26^{NS}	0.86^{NS}	0.86^{NS}	0.85^{NS}
SE				1^{NS}	1^{NS}	1^{NS}	1^{NS}	1^{NS}	1^{NS}	1^{NS}	1^{NS}	0.45^{NS}	0.04^{NS*}	0.35^{NS}	0.75^{NS}	$1.02 \times 10^{-06*}$	0.50^{NS}	$5.14 \times 10^{-06*}$	0.01^{NS*}	0.73^{NS}	0.03^{NS*}
SD					0.81^{NS}	0.03^{NS*}	0.02^{NS*}	$4.13 \times 10^{-16*}$	$3.46 \times 10^{-26*}$	0.08^{NS}	0.17^{NS}	0.06^{NS}	0.42^{NS}	0.28^{NS}	0.74^{NS}	0.01^{NS*}	$2.96 \times 10^{-38*}$	$1.37 \times 10^{-06*}$	$3.40 \times 10^{-05*}$	$4.08 \times 10^{-33*}$	$1.79 \times 10^{-09*}$
Sand						0.03^{NS*}	0.01^{NS*}	0.11^{NS}	0.09^{NS}	0.20^{NS}	0.83^{NS}	0.38^{NS}	0.25^{NS}	0.35^{NS}	0.01^{*}	0.04^{NS*}	0.85^{NS}	0.05^{NS}	0.01^{NS*}	0.37^{NS}	0.01^{NS*}
Silt							$2.01 \times 10^{-16*}$	0.36^{NS}	0.72^{NS}	$6.82 \times 10^{-08*}$	$5.82 \times 10^{-06*}$	0.59^{NS}	0.37^{NS}	0.02^{NS*}	$5.17 \times 10^{-20*}$	0.73^{NS}	0.02^{NS*}	0.95^{NS}	$3.58 \times 10^{-05*}$	0.73^{NS}	0.01^{NS*}
Clay								0.05^{NS}	0.16^{NS}	$5.15 \times 10^{-05*}$	$9.80 \times 10^{-065*}$	0.29^{NS}	0.11^{NS}	0.13^{NS}	$3.13 \times 10^{-06*}$	0.33^{NS}	0.02^{NS*}	0.21^{NS}	0.10^{NS}	0.37^{NS}	0.26^{NS}
bD									$2.94 \times 10^{-32NS*}$	0.33^{NS}	0.64^{NS}	0.10^{NS}	0.39^{NS}	0.15^{NS}	0.34^{NS}	0.01	$2.46 \times 10^{-29*}$	$5.45 \times 10^{-07*}$	$2.67 \times 10^{-07*}$	$7.49 \times 10^{-34*}$	$1.49 \times 10^{-12*}$
Po										0.24^{NS}	0.15^{NS}	0.06^{NS}	0.11^{NS}	0.05^{NS}	0.06^{NS}	0.01^{NS*}	$2.29 \times 10^{-20*}$	$3.35 \times 10^{-06*}$	$5.05 \times 10^{-07*}$	$1.86 \times 10^{-25*}$	$1.34 \times 10^{-11*}$
SMC											0.09^{NS}	0.68^{NS}	0.59^{NS}	0.49^{NS}	$1.15 \times 10^{-06*}$	0.88^{NS}	0.12^{NS}	0.90^{NS}	0.01^{NS*}	0.75^{NS}	0.06^{NS}
WHC												0.01^{NS*}	$5.25 \times 10^{-05*}$	0.28^{NS}	0.02^{NS*}	0.66^{NS}	0.16^{NS}	0.85^{NS}	0.24^{NS}	0.44^{NS}	0.45^{NS}
SOC													0.01^{NS*}	0.05^{NS}	0.43^{NS}	0.05^{NS}	0.03^{NS*}	0.03^{NS*}	0.53^{NS}	0.06^{NS}	0.31^{NS}
SN														0.03^{NS*}	0.47^{NS}	0.81^{NS}	0.49^{NS}	0.91^{NS}	0.72^{NS}	0.32^{NS}	0.97^{NS}
C: N															0.01^{NS*}	0.20^{NS}	0.39^{NS}	0.19^{NS}	0.01^{NS*}	0.04^{NS*}	0.01^{NS*}
pH																0.31^{NS}	0.56^{NS}	0.39^{NS}	$1.04 \times 10^{-06*}$	0.12^{NS*}	$9.80 \times 10^{-06*}$
FRB-Sal																	0.01	$1.26 \times 10^{-60*}$	$3.62 \times 10^{-12*}$	0.01^{*}	$4.78 \times 10^{-11*}$
FRN-Sal																		$2.50 \times 10^{-07*}$	$3.64 \times 10^{-05*}$	$2.50 \times 10^{-28*}$	$3.29 \times 10^{-09*}$
FRP-Sal																			$5.77 \times 10^{-13*}$	$2.95 \times 10^{-05*}$	$5.08 \times 10^{-13*}$
FRB -AS																				$5.91 \times 10^{-07*}$	$2.40 \times 10^{-47*}$
FRN-AS																					$8.54 \times 10^{-13*}$
FRP-AS																					

Correlation is significant at the 0.05 level (2-tailed), where, NS, not significant ($p > 0.05$); NS, significant before but not after the Bonferroni correction is applied ($a < p < 0.05$, where $a = 0.0016$), *significant after the Bonferroni correction is applied. Y, year; SI, sites; SE, seasons; SD, soil depth (cm); bD, bulk density (g cm^{-3}); Po, porosity; SMC, soil moisture content (%); WHC, water holding capacity (%); SOC, soil organic carbon (%); SN, soil nitrogen (%); C: N, carbon: nitrogen ratio); FRB-Sal, fine root biomass of Sal tree (Kg ha^{-1}); FRN-Sal, fine root necromass of Sal tree (Kg ha^{-1}); FRP-Sal, fine root production of Sal tree (Kg ha^{-1} $season^{-1}$); FRB-AS, fine root biomass of associated tree (Kg ha^{-1}); FRN-AS, fine root necromass of associated tree (Kg ha^{-1}); FRP-AS, fine root production of associated tree (Kg ha^{-1} $season^{-1}$).

TABLE 5 Multivariate analysis of variance (MANOVA) table for fine root dynamics with sites, seasons, year and their interactions (Df, degrees of freedom).

	FRB-Sal	FRN-Sal	FRP-Sal	FRT-Sal	FRB-AS	FRN-AS	FRP-AS	FRT-AS
Sites								
Df	3	3	3	3	3	3	3	3
F-value	1.927	0.024	1.617	24.393	14.271	1.228	11.195	26.401
P-value	0.133	0.995	0.193	0.01	0.01	0.306	0.01	0.01
Sum of square	85700.92	35.396	86204.95	12.025	150405.6	2078.01	187620.7	18.627
Mean sum of square	28566.97	11.799	28734.98	4.008	50135.2	692.67	62540.24	6.209
Seasons								
Df	2	2	2	–	2	2	2	–
F-value	101797.2	22.369	20030.46	–	1038.715	11861.18	957.026	–
P-value	0.002	0.148	0.005	–	0.022	0.006	0.023	–
Sum of square	419553.7	171.199	435485.4	–	53146.37	176.317	47247.45	–
Mean sum of square	209776.9	85.599	217742.7	–	26573.18	88.159	23623.72	–
Year								
Df	1	1	1	1	1	1	1	1
F-value	3217.056	120.562	972.843	164.396	10905.86	126.367	1.1	6.14
P-value	0.011	0.058	0.02	0.05	0.006	0.056	0.01	0.01
Sum of square	6629.491	461.345	10575.37	4205.692	81.058	3119.302	2.426	4.64
Mean sum of square	3314.746	230.6725	5287.686	2102.846	40.529	1559.651	1.213	2.32
Sites × seasons								
Df	6	6	6	–	6	6	6	–
F-value	5491.433	9.703	964.452	–	143.704	9830.888	139.781	–
P-value	0.01	0.241	0.025	–	0.064	0.008	0.065	–
Sum of square	67898.24	222.768	62904.92	–	22058.03	438.41	20702.56	–
Mean sum of square	11316.37	37.128	10484.15	–	3676.339	73.068	3450.427	–
Sites × year								
Df	3	3	3	3	3	3	3	3
F-value	152.492	1.076	24.288	8.886	8871.861	15.646	1.01	2.53
P-value	0.059	0.594	0.148	0.241	0.008	0.183	0.01	0.01
Sum of square	942.736	12.353	792.069	681.967	197.821	1158.678	6.651	5.735
Mean sum of square	314.245	4.118	264.023	227.322	65.94	386.226	2.217	1.912
Seasons × year								
Df	2	2	2	–	2	2	2	–
F-value	157.928	42.829	85.256	–	9.756	153.122	9.101	–
P-value	0.056	0.107	0.076	–	0.221	0.057	0.228	–
Sum of square	650.896	327.783	1853.567	–	499.154	2.276	449.31	–
Mean sum of square	325.448	163.891	926.783	–	249.577	1.138	224.655	–
Sites × seasons × year								
Df	6	6	6	–	6	6	6	–
F-value	183.399	3.436	38.74	–	25.373	2179.557	22.322	–
P-value	0.056	0.391	0.122	–	0.151	0.016	0.161	–
Sum of square	2267.613	78.887	2526.773	–	3894.644	97.198	3306.082	–
Mean sum of square	377.936	13.148	421.129	–	649.107	16.2	551.014	–

Significance level ($p < 0.05$). FRB-Sal, fine root biomass of Sal tree (Kg ha^{-1}); FRN-Sal, fine root necromass of Sal tree (Kg ha^{-1}); FRP-Sal, fine root production of Sal tree (Kg ha^{-1} season^{-1}); FRB-AS, fine root biomass of associated tree (Kg ha^{-1}); FRN-AS, fine root necromass of associated tree (Kg ha^{-1}); FRP-AS, fine root production of associated tree (Kg ha^{-1} season^{-1}).

TABLE 6 One-way Analysis of variance (ANOVA) table for fine root dynamics with tree density and total basal area (Df, degrees of freedom).

	FRB-Sal	FRN-Sal	FRP-Sal	FRT-Sal	FRB-AS	FRN-AS	FRP-AS	FRT-AS
Total density (ind. ha^{-1}) and total basal area (m^2 ha^{-1})								
Df	3	3	3	3	3	3	3	3
F-value	1.927	0.024	1.617	14.271	1.228	11.195	24.393	26.401
P-value	0.133	0.995	0.193	0.01	0.306	0.01	0.01	0.01
Sum of square	85700.92	35.396	86204.95	150405.6	2078.01	187620.7	12.025	18.627
Mean sum of square	28566.97	11.799	28734.98	50135.2	692.67	62540.24	4.008	6.209

Significance level ($p < 0.05$). FRB-Sal, fine root biomass of Sal tree (Kg ha^{-1}); FRN-Sal, fine root necromass of Sal tree (Kg ha^{-1}); FRP-Sal, fine root production of Sal tree (Kg ha^{-1} $season^{-1}$); FRB-AS, fine root biomass of associated tree (Kg ha^{-1}); FRN-AS, fine root necromass of associated tree (Kg ha^{-1}); FRP-AS, fine root production of associated tree (Kg ha^{-1} $season^{-1}$).

in elevation and stand characteristics. Wapongnungsang, and Tripathi (2019) also reported that about 18–58% of soil nitrogen is returned to the soil through fine root mortality, turnover and decomposition. The slightly higher amount of carbon and nitrogen fluxes in the present study may be due to the vegetation and climatic conditions that through decomposition and exudates enhanced the soil nutrients and soil biota plays an important role in better growth of fine roots that ultimately resulted in higher fluxes on production and mortality (Keller et al., 2021; Awasthi et al., 2022b,c).

The forest structure including vegetation and floristic diversity (Ma and Chen, 2016), soil characteristics (Frouz et al., 2008) are also the crucial factors influencing fine root dynamics as soil properties can alter the root growth by regulating various physiological and chemical processes occurring within the ecosystem. Fine root dynamics is limited by various soil nutrients in the terrestrial ecosystems (Kochsiek et al., 2013). In the present study, Pearson's correlation matrix with Bonferroni correction unveiled the effect of soil characteristics on fine root dynamics (**Table 4**). Fine root biomass, necromass and production of the dominant (*S. robusta*) and associated tree species showed strong negative correlation with soil depth and bulk density, while strong positive correlation with porosity across all the sites. Higher bulk density results in more compaction of the soil which makes it difficult for the roots to penetrate and expand thus the fine roots generally decline with increasing bulk density. The release of nutrients through litter decomposition and fluxes from the roots, results in higher quantities of the soil micronutrients such as carbon and nitrogen in the surface layer which subsequently decline in the deeper soil depths which may be the reason for declining biomass and production of fine roots (Bibi et al., 2022).

Soil pH also showed negative correlation with sand content, clay content, soil moisture content and fine root biomass and production of associated species. Bulk density and porosity were negatively correlated. Soil moisture content and water holding capacity of the soil showed negative correlation with silt content, while positive with clay content of the soil. The fine root parameters also showed positive correlation with sand content and soil organic matter, while negative correlation with clay content but the relationship was not significant. Sandy soils are considered to be more resource limited in comparison to clay or loam and the nutrient deficient soil promotes the growth and expansion of belowground components resulting in higher fine root biomass and production in sandy soil (Mosquera and Moreno-Hurtado, 2022). The higher organic matter contents in the soil results in improved water holding capacity thus helps in expansion of the root system (Lorenz et al., 2019). The resource availability in the soil regulates the fine root distribution and fine root biomass and it is positively correlated with soil organic carbon and negatively correlated with bulk density of the soil (Chen et al., 2016).

Fine root parameters showed significant ($p < 0.05$) variability among locations, seasons, years and their interactions (**Table 5**). These observations may be due to the changes in soil characteristics, microclimatic conditions, composition of vegetation that influences the temperature, moisture and nutrient availability and results in different fine root concentration and distribution site-wise and season-wise (An and Osawa, 2021). The highest fine root biomass and production observed during the rainy season is attributable to higher precipitation, suitable temperature for microbial activities resulting in ample nutrients through decomposition processes and exudates that supported the growth of fine roots. The low precipitation and temperature during the winter season resulted in low microbial activities; slower decomposition rates that might have subjected the fine roots to drought stress and reduce their growth.

In the present study, fine root parameters were also affected by stand density and basal area. The fine root biomass, necromass, production as well as turnover of the associated tree species significantly ($p < 0.05$) varied with tree density and total basal area, while in *S. robusta* significant variability with respect to density and basal area was only observed for fine root turnover (**Table 6**). The reason may be that the density and basal area of a forest regulate the quality and quantity of litter which in-turn manages the nutrient availability such as carbon and nitrogen inputs for growth of the inhabiting species resulting in expansion of root system (Verma et al., 2021). The above-ground and below-ground partitioning of biomass and resources is dependent on the stand density which regulates the ecosystem functioning and nutrient uptake and higher density results in higher fine root biomass (Ile et al., 2021). Zhou et al. (2018) also reported significant relationships between tree basal area and fine root biomass and considered tree basal area is an efficacious variable to estimate the fine root biomass in forest ecosystems.

Caveat of the study

The study enhanced the understanding on fine root dynamics and spatio-temporal relationship between fine roots and nutrients, but still extensive detailed studies covering wider spectrum, focusing on effect of anthropogenic disturbances, biotic and abiotic variations on fine roots and linking nutrient fluxes to biogeochemical cycling would be beneficial in developing overall ecosystem-scale understanding and management of forest ecosystems.

Conclusion

The study revealed that the fine root distribution in sub-tropical Sal forests was significantly affected by soil physical and chemical characteristics. The fine root dynamics of dominant as well as co-dominant tree species were significantly influenced by the site characteristics, distance, soil depth, seasons and climatic variables. At all the sites, fine root biomass and production was higher in the uppermost (0–20 cm) soil layer, which subsequently declined in the deeper soil depths (20–60 cm). Across the seasons a peak value was recorded in the rainy season due to better microclimatic conditions and nutrient availability. Fine root turnover showed inconsistent patterns across the depths and seasons. Fine roots play a cardinal role in return of nutrients to the soil which enriches the soil quality. The annual flux of carbon and nitrogen recorded in this study verified that the fine roots of the forests have a substantial role in conservation of huge quantities of carbon in the form of biomass, production, thus reducing the atmospheric carbon concentrations and through planning proper forest management regimes this potential can be harvested to mitigate atmospheric carbon contents.

Data availability statement

The original contributions presented in this study are included in this article/supplementary material, further inquiries can be directed to the corresponding author.

Author contributions

RP collected the data and prepared the manuscript. SB guided the research and edited the manuscript. KB reviewed, modified, and improved the manuscript. HK revised and edited the manuscript. MK and US helped in editing the manuscript. All authors contributed to the article and approved the submitted version.

Acknowledgments

We are grateful to the Head, Department of Botany for providing lab facilities and Uttarakhand Tea Development Board Bhowali, Nainital for analysis of soil samples.

Conflict of interest

The authors declare that the research was conducted in the absence of any commercial or financial relationships that could be construed as a potential conflict of interest.

Publisher's note

References

An, J. Y., and Osawa, A. (2021). Seasonal patterns of fine root dynamics and their contribution to net primary production in Hinoki cypress (*Chamaecyparis obtusa*) and Konara oak *(Quercus serrata)* forests. *Trees* 35, 255–271. doi: 10.1007/s00468-020-02030-6

Awasthi, P., Bargali, K., Bargali, S. S., and Jhariya, M. K. (2022a). Structure and functioning of Coriaria nepalensis dominated shrublands in degraded hills of Kumaun Himalaya. I. Dry matter dynamics. *Land Degrad. Dev.* 33, 1474–1494. doi: 10.1002/ldr.4235

Awasthi, P., Bargali, K., Bargali, S. S., and Khatri, K. (2022c). Nutrient return through decomposing Coriaria nepalensis litter in degraded hills of Kumaun Himalaya. India. *Front. For. Glob. Change* 5:1008939. doi: 10.3389/ffgc.2022.1008939

Awasthi, P., Bargali, K., Bargali, S. S., Khatri, K., and Jhariya, M. K. (2022b). Nutrient partitioning and dynamics in *Coriaria nepalensis* Wall dominated shrublands of degraded hills of Kumaun Himalaya. *Front. For. Glob. Change* 5:913127. doi: 10.3389/ffgc.2022.913127

Bargali, K., Manral, V., Padalia, K., Bargali, S. S., and Upadhyay, V. P. (2018). Effect of vegetation type and season on microbial biomass carbon in Central Himalayan forest soils. India. *CATENA* 171, 125–135. doi: 10.1016/j.catena.2018.07.001

Bargali, S. S., Padalia, K., and Bargali, K. (2019). Effects of tree fostering on soil health and microbial biomass under different land use systems in Central Himalaya. *Land Degrad. Dev.* 30, 1984–1998. doi: 10.1002/ldr.3394

Bibi, F., Tomlinson, K. W., Liu, C., Liu, C., Jin, Y., and Tang, J. (2022). Fine root production and soil available nutrients in Rubber monoculture versus Rubber–Flemingia macrophylla agroforestry. *Forests* 13:830. doi: 10.3390/f13060830

Black, C. A. (1965). *Methods of soil analysis*. New York: Academic press Inc, 369.

Chazdon, R. L. (2019). Towards more effective integration of tropical forest restoration and conservation. *Biotropica* 51, 463–472.

Chazdon, R. L., Lindenmayer, D., Manuel, R., Guariguata, M. R., Crouzeilles, R., Benayas, J. M. R., et al. (2020). Corrigendum: Fostering natural forest regeneration on former agricultural land through economic and policy interventions. *Environ. Res. Lett.* 15:099501. doi: 10.1088/1748-9326/ab97cc

Chazdon, R., and Brancalion, P. (2019). Restoring forests as a means to many ends. *Science* 365, 24–25.

Chen, L., Mu, X., Yuan, Z., Deng, Q., Chen, Y., Yuan, L. Y., et al. (2016). Soil nutrients and water affect the age-related fine root biomass but not production in two plantation forests on the Loess Plateau. China. *J. Arid. Environ.* 135, 173–180. doi: 10.1016/j.jaridenv.2016.09.003

Cordeiro, A. L., Norby, R. J., Andersen, K. M., Valverde-Barrantes, O., Fuchslueger, L., Oblitas, E., et al. (2020). Fine-root dynamics vary with soil depth and precipitation in a low-nutrient tropical forest in the Central Amazonia. *Plant Environ. Int.* 1, 1–14. doi: 10.1002/pei3.10010

Cornejo, N. S., Leuschner, C., Becker, J. N., Andreas, H., Costa, D. S., and Hertel, D. (2021). Climate implications on forest above- and belowground carbon allocation patterns along a tropical elevation gradient on Mt. Kilimanjaro (Tanzania). *Oecologia* 195, 797–812. doi: 10.1007/s00442-021-04860-8

Cusack, D. F., Addo-Danso, S. D., Agee, E. A., Andersen, K. M., Arnaud, M., Batterman, S. A., et al. (2021). Tradeoffs and synergies in tropical forest root traits and dynamics for nutrient and water acquisition: Field and modeling advances. *Front. For. Glob. Change* 4:704469. doi: 10.3389/ffgc.2021.704469

Dahlmand, R. C., and Kucera, C. L. (1965). Root productivity and turnover in native Prairie. *Ecology* 46, 84–89. doi: 10.2307/1935260

Ding, Y., Leppalammi-Kujansuu, J., and Helmisaari, H. S. (2019). Fine root longevity and below-and aboveground litter production in a boreal Betula pendula forest. *For. Ecol. Manag.* 431, 17–25. doi: 10.1016/j.foreco.2018.02.039

Finer, L., Ohashi, M., Noguchi, K., and Hirano, Y. (2011). Fine root production and turnover in forest ecosystems in relation to stand and environmental characteristics. *For. Ecol. Manag.* 262, 2008–2023. doi: 10.1016/j.foreco.2011.08.042

Finer, L., Zverev, V., Palviainen, M., Romanis, T., and Kozlov, M. V. (2019). Variation in fine root biomass along a 1000 km long latitudinal climatic gradient in mixed boreal forests of North-East Europe. *For. Ecol. Manag.* 432, 649–655. doi: 10.1016/j.foreco.2018.09.060

Frouz, J., Prach, K., Pizl, V., Hanel, L., Stary, J., Tajovsky, K., et al. (2008). Interactions between soil development, vegetation and soil fauna during spontaneous succession in post mining sites. *Eur. J. Soil Biol.* 44, 109–121. doi: 10.1016/j.ejsobi.2007.09.002

Fu, X., Wang, J., Di, Y., and Wang, H. (2015). Differences in fine-root biomass of trees and understory vegetation among stand types in subtropical forests. *PLoS One* 10:e0128894. doi: 10.1371/journal.pone.0128894

Garkoti, S. C. (2011). Fine root dynamics in three Central Himalayan high elevation forests ranging from closed canopied to open-canopied treeline vegetation. *J. For. Res.* 16, 136–143. doi: 10.1007/s10310-010-0218-5

Garkoti, S. C. (2012). Dynamics of fine root N, P and K in high elevation forests of Central Himalaya. *For. Stud. China* 14, 145–151. doi: 10.1007/s11632-012-0203-5

Gautam, T. P., and Mandal, T. N. (2018). Storage and flux of nutrients in disturbed and undisturbed Tropical moist forest of Eastern Nepal. *Hindawi Int. J. For. Res.* 4, 1–12. doi: 10.1155/2018/8516321

Hertel, D., Harteveld, M., and Leuschner, C. (2009). Conversion of a tropical forest into agroforest alters the fine root-related carbon flux to the soil. *Soil Biol. Biochem.* 41, 481–490. doi: 10.1016/j.soilbio.2008.11.020

Ibrahim, F., Adu-Bredu, S., Addo-Danso, S. D., Duah-Gyamfi, A., Manu, E. A., and Malhi, Y. (2020). Patterns and controls on fine-root dynamics along a rainfall gradient in Ghana. *Trees* 34, 917–929. doi: 10.1007/s00468-020-01970-3

Ile, O. J., Aguilos, M., Morkoc, S., Heitman, J., and King, J. S. (2021). Root biomass distribution and soil physical properties of short-rotation coppice American sycamore (*Platanus occidentalis* L.) Grown at different planting densities. *Forests* 12:1806. doi: 10.3390/f12121806

Indian Standard (1965). *Part IV: Grain size analysis*. New Delhi: Indian Standard Institute, 2720.

Jackson, M. L. (1958). *Soil Chemical Analysis*. Clift, NJ: Prentice Hall, Inc, 39–40.

Joshi, R. K., and Garkoti, S. C. (2021). Influence of Nepalese alder on soil physico-chemical properties and fine root dynamics in white oak forests in the Central Himalaya. India. *Catena* 200:105140. doi: 10.1016/j.catena.2020.105140

Karki, H., Bargali, K., and Bargali, S. S. (2021a). Nitrogen mineralization patterns in Populus deltoides and Tectona grandis based agrisilvicultural practices in Central Himalaya, India. *Vegetos* 34, 86–93. doi: 10.1007/s42535-021-00195-0

Karki, H., Bargali, K., and Bargali, S. S. (2021b). Spatial and seasonal pattern of fine root biomass and turnover rate in different land use systems in Central Himalaya. India. *Russ. J. Ecol.* 52, 36–48. doi: 10.1134/S1067413621010070

Karki, H., Bargali, K., and Bargali, S. S. (2021c). Spatial and temporal trends in soil N-mineralization rates under the agroforestry systems in bhabhar belt of Kumaun Himalaya, India. *Agrofor. Syst.* 95, 1603–1617. 021- 00669-9 doi: 10.1007/s10457-

Karki, H., Bargali, K., and Bargali, S. S. (2022). Dynamics of fine root and soil nitrogen in Mangifera indica based agroforestry systems in Central Himalaya, India. *Land Degrad. Dev.* 33, 3523–3538. doi: 10.1002/ldr.4406

Katayama, A., Kho, L. K., Makita, N., Kume, T., Matsumoto, K., and Ohashi, M. (2019). Estimating fine root production from ingrowth cores and decomposed roots in a Bornean tropical rainforest. *Forests* 10, 1–13. doi: 10.3390/f10010036

Keller, A., Brzostek, E. A., Craig, M. E., Fisher, J. B., and Phillips, R. P. (2021). Root-derived inputs are major contributors to soil carbon in temperate forests, but vary by mycorrhizal type. *Ecol. Lett.* 24, 626–635. doi: 10.1111/ele.13651

Kochsiek, A., Tan, S., and Russo, S. E. (2013). Fine root dynamics in relation to nutrients in oligotrophic Bornean rain forest soils. *Plant Ecol.* 214, 869–882.

Kumar, B. M. (2000). Ailanthus triphysa in the homegardens of Kerala, India: Occurrence, basal area, average standing stock of wood and diameter structure. *Indian J. Agrofor.* 2, 49–52.

Lima, T. T. S., Miranda, I. S., and Vasconcelos, S. S. (2010). Effects of water and nutrient availability on fine root growth in eastern Amazonian forest regrowth. *Brazil. New Phytol.* 187, 622–630. doi: 10.1111/j.1469-8137.2010.03299.x

Lopez, B., Sabate, S., and Gracia, C. A. (2001). Annual and seasonal changes in fine root biomass of Quercus ilex L. *Plant Soil* 230, 125–134. doi: 10.1023/A:1004824719377

Lorenz, K., Lal, R., and Ehlers, K. (2019). Soil organic carbon stock as an indicator for monitoring land and soil degradation in relation to United Nations'. Sustainable Development Goals. *Land Degrad. Dev.* 30, 824–838. doi: 10.1002/ldr.3270

Lukac, M. (2012). "Fine root turnover," in *Measuring roots*, ed. S. Mancuso (Berlin: Springer), 363–373. doi: 10.1007/978-3-642-22067-818

Lukac, M., and Godbold, D. L. (2010). Fine root biomass and turnover in southern taiga estimated by root inclusion nets. *Plant Soil* 331, 505–513. doi: 10.1007/s11104-009-0271-z

Ma, Z., and Chen, H. Y. H. (2016). Effects of species diversity on fine root productivity in diverse ecosystems: A global meta-analysis. *Global Ecol. Biogeogr.* 25, 1387–1396. doi: 10.1111/geb.12488

Malhi, Y., Girardin, C. A., Goldsmith, G. R., Doughty, C. E., Salinas, N., Metcalfe, D. B., et al. (2017). The variation of productivity and its allocation along a tropical elevation gradient: A whole carbon budget perspective. *New Phytol* 214, 1019–1032. doi: 10.1111/nph.14189

Manral, V., Bargali, K., Bargali, S. S., Jhariya, M. K., and Padalia, K. (2022). Relationships between soil and microbial biomass properties and annual fluxof nutrients in Central Himalayan forests, India. *Land Degrad. Dev.* 33, 2014–2025. doi: 10.1002/ldr.4283

Mikieleko, E. F. K., Bocko, Y. E., Loubota-Panzou, G. J., and Loumeto, J. J. (2021). Fine roots dynamics in two forest strata of a semi-deciduous forest in Northern Republic of Congo. *Open J. For.* 11, 192–205. doi: 10.4236/ojf.2021.113013

Misra, R. (1968). *Ecology work book*. Calcutta: Oxford & IBH Publishing Company.

Mosquera, H. Q., and Moreno-Hurtado, F. H. (2022). Effects of nutrient (N, P, K) fertilization on the dynamics of fine roots in tropical rain forests with different soil texture in the Colombian Pacific region. *Rev. Biol. Trop.* 70, 482–494. doi: 10.15517/rev.biol.trop.2022.47351

Oraon, P. R., Singh, L., and Jhariya, M. K. (2018). Forest floor biomass, litterfall and physico-chemical properties of soil along the anthropogenic disturbance regimes in tropics of Chhattisgarh. *India. J. For. Environ. Sci.* 34, 359–375. doi: 10.7747/JFES.2018.34.5.359

Pausch, J., and Kuzyakov, Y. (2018). Carbon input by roots into the soil: Quantification of rhizodeposition from root to ecosystem scale. *Glob. Change Biol.* 24, 1–12. doi: 10.1111/gcb.13850

Pei, Y., Lei, P., Xiang, W., Ouyang, S., and Xu, Y. (2018). Effect of stand age on fine root biomass, production and morphology in Chinese fir plantations in subtropical China. *Sustainability* 10:2280. doi: 10.3390/su10072280

Persch, S., Clendenning, J., Dawson, L., and Jourdan, C. (2015). *Fine root dynamics within land-use change from tropical forests to agriculture: A systematic review protocol. Working Paper No. 200*. Bogor: Center for International Forestry Research (CIFOR), 18. doi: 10.17528/cifor/005912

Piper, C. S. (1950). *Soil and plant analysis.the university of adelaide*. New York: Academic press.

Rosado, B. H. P., Martins, A. C., Colomeu, T. C., Oliveira, R. S., Joly, C. A., and Aidar, M. P. M. (2011). Fine root biomass and root length density in a lowland and a montane tropical rain forest, SP, Brazil. *Biota Neotr.* 11, 203–209. doi: 10.1590/S1676-06032011000300018

Sahu, K. P., Singh, L., and Jhariya, M. K. (2013). Fine root biomass, forest floor and nutrient status of soil in an age series of teak plantation in dry tropics. *The Bioscan* 8, 1149–1152.

Singha, D., Brearley, F. Q., and Tripathi, S. K. (2020). Fine root and soil nitrogen dynamics during stand development following shifting agriculture in Northeast India. *Forests* 11:1236. doi: 10.3390/f11121236

Subbiah, B. V., and Asija, G. L. (1956). A rapid procedure for the determination of available nitrogen in soil. *Curr. Sci.* 25, 259–260.

Usman, S., Rawat, Y. S., Singh, S. P., and Garkoti, S. C. (1997). Fine root biomass production and turnover in evergreen forests of Central Himalaya. India. *Oecol. Mont.* 6, 4–8.

Usman, S., Singh, S. P., Rawat, Y. S., and Bargali, S. S. (2000). Fine root decomposition and nitrogen mineralisation patterns in Quercus leucotrichophora and Pinus roxburghii forests in Central Himalaya. *For. Ecol. Manag.* 131, 191–199. . doi: 10.1016/S0378-1127(99)00213-3

Verma, A., Garkoti, S., Singh, S., Pal, S., and Kumar, M. (2021). Fine root production and nutrient dynamics in relation to stand characteristics of chir pine mixed banj oak forests in central Himalaya. *Flora* 279:151808. doi: 10.1016/j.flora.2021.151808

Walkley, A., and Black, I. A. (1934). An examination of Degtjareff method for determining soil organic matter and the proposed modification of the chromic acid titration method. *Soil Sci.* 37, 29–38. doi: 10.1097/00010694-193401000-00003

Wang, W., Mo, Q., Han, X., Hui, D., and Shen, W. (2019). Fine root dynamics responses to nitrogen addition depend on root order, soil layer, and experimental duration in a subtropical forest. *Biol. Fert. Soils* 55, 723–736. doi: 10.1007/s00374-019-01386-3

Wang, W., Wu, X. G., Hu, K., Liu, J. C., and Tao, J. P. (2016). Understorey fine root mass and morphology in the litter and upper soil layers of three Chinese subtropical forests. *Plant Soil* 406, 219–230. doi: 10.1007/s11104-016-2878-1

Wapongnungsang, and Tripathi, S. K. (2019). Fine root growth and soil nutrient dynamics during shifting cultivation in tropical semi-evergreen forests of northeast India. *J. Environ. Biol.* 40, 45–52. doi: 10.22438/jeb/40/1/MRN-813

Weemstra, M., Kiorapostolou, N., Ruijven, J., Mommer, L., Vries, J., and Sterck, F. (2020). The role of fine-rootmass, specific root length and life span in tree performance: A whole-tree exploration. *Funct. Ecol.* 34, 575–585. doi: 10.1111/1365-2435.13520

Xia, M., Talhelm, A. F., and Pregitzer, K. S. (2015). Fine roots are the dominant source of recalcitrant plant litter in sugar maple-dominated northern hardwood forests. *New Phytol.* 208, 715–726. doi: 10.1111/nph.13494

Yang, Y. S., Chen, G. S., He, Z. M., Chen, Y. X., and Guo, J. F. (2002). Production, distribution and nutrient return of fine roots in a mixed and a pure forest in subtropical China. *Chinese J. Appl. Environ. Biol.* 8, 223–233.

Zhou, G., Shengwang, M., Jian, Y., Hua, Z., and Qi-jing, L. (2018). Quantitative relationships between fine roots and stand characteristics. *Eur. J. For. Res.* 137, 385–399. doi: 10.1007/s10342-018-1112-5

frontiers | Frontiers in Forests and Global Change

TYPE Original Research
PUBLISHED 11 January 2023
DOI 10.3389/ffgc.2022.1088291

OPEN ACCESS

EDITED BY
Uttam Kumar Sahoo,
Mizoram University, India

REVIEWED BY
Qing-Wei Wang,
Institute of Applied Ecology (CAS), China
Bhupendra Singh,
VCSG Uttarakhand University, India

*CORRESPONDENCE
Wenjie Yang
✉ yangwenjie@mail.hzau.edu.cn
Shuqing An
✉ anshq@nju.edu.cn

SPECIALTY SECTION
This article was submitted to
Forest Disturbance,
a section of the journal
Frontiers in Forests and Global Change

RECEIVED 03 November 2022
ACCEPTED 30 December 2022
PUBLISHED 11 January 2023

CITATION
Zhou L, Thakur MP, Jia Z, Hong Y, Yang W, An S and Zhou X (2023) Light effects on seedling growth in simulated forest canopy gaps vary across species from different successional stages.
Front. For. Glob. Change 5:1088291.
doi: 10.3389/ffgc.2022.1088291

Light effects on seedling growth in simulated forest canopy gaps vary across species from different successional stages

Lingyan Zhou[1,2], Madhav P. Thakur[3], Zhen Jia[1], Yu Hong[1], Wenjie Yang[2,4]*, Shuqing An[2]* and Xuhui Zhou[1,5]

[1]Zhejiang Tiantong Forest Ecosystem National Observation and Research Station, School of Ecological and Environmental Sciences, East China Normal University, Shanghai, China, [2]Laboratory of Forest Ecology, School of Life Sciences, Nanjing University, Nanjing, China, [3]Institute of Ecology and Evolution and Oeschger Centre for Climate Change Research, University of Bern, Bern, Switzerland, [4]College of Horticulture and Forestry Science, Huazhong Agricultural University, Wuhan, China, [5]Key Laboratory of Sustainable Forest Ecosystem Management-Ministry of Education, Center for Ecological Research, School of Forestry, Northeast Forestry University, Harbin, China

Tropical forests continue to suffer from various kinds of disturbances in the Anthropocene. An immediate impact of disturbances on forest ecosystems is the creation of numerous large and small canopy gaps, which dramatically affect forest structure and function. Yet, we know little about the effect of canopy gaps on forest successional trajectory. More specifically, the responses of seedlings from different successional stages to increased light intensity under large and small canopy gaps in understory remain unclear. In this study, dominant tree seedlings from early-, mid-, and late-successional stages were selected, respectively from a tropical montane forest in Hainan Island, China to study their growth rate, biomass and traits. Our results showed that the light condition under small canopy gaps (SG, 10–15% of full sunlight) and large canopy gaps (LG, 40–50% of full sunlight) induced greater increment of relative growth rates for seedlings from early- and mid-successional stages relative to that in late-successional stage. Both SG and LG also significantly increased photosynthesis rate, leaf area (LA), light saturation point (LSP), root mass ratio (RMR) and root: shoot ratio, but decreased specific leaf area (SLA) of seedlings across successional stages. Tree seedlings from the early-successional stage displayed the greatest decrease in leaf mass ratio, increase in LA, LSP, and RMR, in comparison to those from mid- and late- successional stages. Light condition and SLA were the most important factors for seedlings' relative growth rate across successional stages. SLA connected the interaction between the light condition and successional stage on seedlings' growth, thereby jointly explaining the 93% variation of seedlings' growth, combining with area-based light saturated rate of CO_2 assimilation. Our study highlights the distinct effect of disturbance-induced canopy gaps on seedling regeneration in the understory in tropical forest due to the variation of light intensity. We suspect that the seedlings from late-successional stage will recover relatively slow after disturbances causing canopy losses, which can have detrimental impacts on structure feature and successional trajectory in tropical forest, as well as forest-based ecosystem services.

KEYWORDS

light condition, successional stage, seedling growth, photosynthetic properties, biomass allocation

Introduction

Tropical forests harbor over one half of global biodiversity on land, and play a crucial role in terrestrial carbon cycle (Malhi and Marthews, 2013; Behera et al., 2022). It is crucial to understand the sustainability of functions and services in tropical forest for ecosystem management in context of global change (Lohbeck et al., 2015). In the Anthropocene, deforestation and climate changes continue to exert tremendous stress on ecosystems (Broadbent et al., 2008; Thakur et al., 2022), inducing detrimental consequences for tropical forest diversity and associated ecosystem functions (Emanuel, 2005; Miller et al., 2011; Olivero-Lora et al., 2022). Several such disturbances, like drought, heat waves, disease outbreaks, and extreme weather events (e.g., typhoon) induce tree mortality and heavy defoliation, causing canopy senescence and resulting in numerous canopy gaps (Corona-Lozada et al., 2019; Thakur et al., 2022). As a double-edged sword, disturbance-induced formation of canopy gaps cause more opportunity for germination from the soil seed bank, as well as huge loss of tree biomass (Barlow and Peres, 2004). With the formation of canopy gaps, the environment at forest understory correspondingly shifts, e.g., the enhanced available light and nutrient release from decomposition of dead trees, affecting the seedlings' growth and the process of forest regeneration and succession after these disturbances are over (Prescott, 2002; Lin et al., 2003). Understanding the growth and survival of tree seedlings under canopy gaps at the understory is key for predicting forest resilience and also to help shed insights on the ongoing debate about the role of canopy gaps for maintaining forest's diversity and function (Muscolo et al., 2014; Wang and Lin, 2019; Xi et al., 2019).

In the understory, the nursery for young seedlings in tropical forests, the availability of light and nutrient determine seedlings' growth, survivorship and competition, driving forest regeneration and succession (Trauernicht et al., 2006; Mazzochini and Camargo, 2020). The formation of canopy gaps are generally considered to have positive effect on seedlings' growth, due to the alleviated limitation of light availability (Alvarez-Clare and Avalos, 2007; Westerband and Horvitz, 2015). However, what species of tree are recruited and be more stimulated by increased light, becomes a critical determinant for the forest recovery and subsequent trajectory of natural regeneration after disturbance, in the understory of tropical forest (Matsuo et al., 2021; Tourville et al., 2022; Wang et al., 2022).

For example, tree seedlings of species from different successional stages (e.g., early-, mid-, and late- stage) exhibit distinct survival, growth rates, and susceptibility to photoinhibition in understory habitats, due to their respective physiological and growth traits (Kitao et al., 2000; Martinez-Garza et al., 2005). In general, germination of early-successional tree species occur in tree-fall gaps, characterized by a high mortality rates and high inherent growth rates (Souza and Válio, 2003). Conversely, species germinated from the later successional stages (e.g., mid- and late-successional species) or shade-tolerant species germinated in relative deep shade, exhibit high survival and lower relative growth rates to adapt the potential nutrient limitation (Kneeshaw and Bergeron, 1998; Kitao et al., 2000). The distinct optimal illumination condition among species from different successional stages is one of the main factors that determines demography of the understory seedlings' community (Pollastrini et al., 2022). Thus, in facing with suddenly enhanced light intensity under canopy gaps after disturbance, seedlings of species from different successional stages might exhibit diverse response in growth (Hogan et al., 2022).

Besides of inherent difference in characteristics of germination and growth, species from different successional stages also represent differences in leaf traits (e.g., specific leaf area, SLA) and resource allocation strategies (e.g., pattern of biomass partitioning), which in turn regulate their ability to obtain above–(e.g., light and CO_2) and below-ground resources (e.g., nutrients and water) (Davidson et al., 2002; Toledo-Aceves and Swaine, 2008). Relative to the seedlings from the late-successional stage, that from early-successional stage generally have shorter leaf life-span, higher SLA, lesser investments to defense compounds and structures, and smaller root: shoot ratio (Reich et al., 1992; Antos and Halpern, 1997; Batuwatta and Singhakumara, 2014). These different traits among species from diverse successional stage control their growth rates in forest, regulating species' competitiveness and understory biodiversity together with forest succession (Hu et al., 2018; Tsai et al., 2018). Whether the seedlings from different successional stages, display diverse response in leaf-scale photosynthetic and/or individual morphological traits, to enhanced light intensity or not, become a crucial issue (Kitajima, 1994; Wang et al., 2022). Especially in the context of more frequent natural or anthropogenic disturbance in tropical forest, the formation of canopy gaps would affect future forest succession due to the distinct growth responses among different seedlings (Zong et al., 2018; Li et al., 2021).

In this study, we selected the dominant species from early-, mid-, and late-successional stages at the understory layer from a tropical forest in Hainan Island, which lies on the northern edge of Asian tropical rain forest as an important biodiversity hotspot in China (Li, 2002). The frequency and intensity of natural or anthropogenic disturbances, e.g., typhoon and selective logging, have increased tremendously in this district, resulting in a higher frequency of canopy gaps in tropical forest (Ding et al., 2017; Yang et al., 2017). The effects of canopy gap-induced increasing light intensity on seedlings' growth were hypothesized to be different among species from early-, mid-, and late-successional stages, consequently regulating the future recovery and successional trajectory for tropical forest after disturbances (Olivero-Lora et al., 2022). Thus, the relative growth rates of seedlings under manipulated three light conditions, i.e., light intensity in ambient understory of tropical forest (Control, 0–5% of full light), that in small (SG, 10–15% of full sunlight, to simulate the canopy opening caused by snapped branches and defoliation) and large canopy gap (LG, 40–50% of full sunlight, to simulate the canopy opening caused by tree fall and selective logging) (Valladares et al., 2000; Yang et al., 2017), were investigated together with their photosynthetic properties (e.g., light-saturated rate of CO_2 assimilation and apparent quantum efficiency) and resource allocation strategy (e.g., root: shoot ratio and leaf area ratio). Here, we seek to answer the following questions: (1) how does the increased light intensity due to canopy gaps, respectively affect relative growth rate of seedlings for tree species from early-, mid-, and late-successional stages of tropical forests; (2) what are the key properties of tree seedlings regulating their growth responses to enhanced light conditions?

Materials and methods

Experimental design

In order to probe the effects of light condition altered by canopy gaps on the growth of understory tree seedlings in tropical forest, six native tree species from early- [*Dolichandrone cauda-felina* (Hance) Benth. et Hook. F. and *Radermachera hainanensis* Merr.], mid- [*Syzygium cumini* (L.) Skeels and *Sterculia lanceolata* Cav.], and late- successional stages (*Dillenia turbinate* Finet et Gagnep. and *Cryptocarya chinensis* Hance) were selected from Jianfengling tropical montane rainforest (E 108°46′–109°45′, N 18°23′–18°50′, Hainan, China) (Li, 2002; Fang et al., 2004; Sheng et al., 2012). The seeds for each species were collected from the understory layer under five parent trees during seed dispersal stage in Jianfengling natural reserve and germinated in shallow trays filled with forest topsoil (Yang et al., 2011). The parent trees were selected in habitat without canopy opening to avoid the effect of disturbance on selected seeds. After growing in a nursery with 5% full sunlight, 1 month-old tree seedlings for each species with 20 replicates were removed to three shade-houses from June. The three shade–houses were covered with plastic shade nets of different thicknesses to achieve 0–5% (as control, i.e., the light condition in tropical forest understory without disturbance) (Capers and Chazdon, 2004), 10–15% (SG, as light condition under small canopy gaps caused by heavy defoliation or broken branches) and 40–50% of full sunlight (LG, as light condition under large canopy gaps caused by fallen tree) (Clark et al., 1996; Tobita et al., 2010; Yang et al., 2017), respectively. All the seedlings were received natural rainfall, and sprayed monthly with 100 ml solution of NPK (ammonium, phosphate, and potassium) compound fertilizer (2 g l^{-1}) and a fungicide solution (50% Carbendazim, Pesticide Technology Development Co., Ltd., Wuhan Scarlett, China) twice during the experiment in order to control fungal infections. In order to calculate the seedlings' relative growth rates for each species under Control, SG and LG treatments, the averaged initial biomass parameters (e.g., stem height, dry mass in leaves, stem and root) of each species were measured based ten additional replicates.

Measurements of photosynthetic, morphological properties, and relative growth rate

From July to October, the photosynthetic properties of five seedlings per species under three light treatments were measured from 09:00 to 11:30 a.m. under clear skies, by taking on five fully expanded leaves per plant. Light response curves were generated with a Li-6400 portable photosynthesis system (Li-Cor Inc., Lincoln, NE, USA) using the "Light Curve" automatic program (Yang et al., 2008). Leaves were allowed 10 min to acclimate to light intensity changes before measurements at light levels of 2,000, 1,500, 1,000, 500, 200, 100, 50, 20, 10, and 0 μmol $m^{-2} \cdot s^{-1}$. Ambient temperature ranged from 24 to 28°C, and leaf chamber temperature was about 25°C. The leaf chamber environment was maintained at 370 mmol m^{-2} s^{-1} CO_2, 28 ± 2°C leaf temperature and 65 ± 5% relative air humidity in the measuring chamber, respectively. Light response curves (A/PAR) were fit using non-rectangular hyperbola least square curve fitting procedure (Equation 1, Eq. 1; Lambers et al., 1998):

$$Pn = \frac{AQE \times PAR + Pmax - \sqrt{\begin{array}{l}(AQE \times PAR + Pmax) \times (AQE \times PAR + Pmax)\\ -4 \times AQE \times PAR \times k \times Pmax\end{array}}}{2 \times k} \quad (1)$$

where AQE is the apparent quantum efficiency; PAR is photosynthetic available radiation; P_{max} (μmol CO_2 m^{-2} s^{-1}) is the light-saturated rate of CO_2 assimilation; R_d (μmol CO_2 m^{-2} s^{-1}) is the dark respiration rate; and k is the convexity or curvature factor. The light compensation point (LCP) was determined to be the light intensity on the light curve where the rate of photosynthesis exactly matches the rate of cellular respiration. The light saturation point (LSP) was calculated by the same equation, considering that LSP is the value when net photosynthetic rate (P_n) reaches 90% of P_{max} (Quero et al., 2006).

After 12 months of experimental duration in shade houses to create canopy conditions caused by disturbances, 10 seedlings per species from three treatments of light conditions (i.e., Control, SG, and LG) were harvested for relative growth rate in mass (RGR_m, Eq. 2). Before being dried at 72°C in a forced air oven for 48 h for dry mass measurement, seedlings were separated into roots, stems and leaves, and washed for morphological characteristics determination, including specific leaf area (SLA, Eq. 3), leaf mass ratio (LMR, Eq. 4), stem mass ratio (SMR, Eq. 5), root mass ratio (RMR, Eq. 6), and leaf area ratio (LAR, Eq. 7).

$$\text{Relative growth rate in mass } (RGR_m, \text{mg } g^{-1}d^{-1}) = (\ln W_2 - \ln W_1)/(T_2 - T_1) \quad (2)$$

where W_2 and W_1 are the final and initial total dry weights per plant; and T_2–T_1 is the growth time interval (i.e., 12 months, Yang et al., 2011).

$$\text{Specific leaf area } (SLA, cm^2\, g^{-1}) = \text{leaf area/leaf mass} \quad (3)$$

$$\text{Leaf mass ratio } (LMR, g\, g^{-1}) = \text{leaf mass/total plant mass} \quad (4)$$

$$\text{Stem mass ratio } (SMR, g\, g^{-1}) = (\text{stem} + \text{petiole mass})/\text{total plant mass} \quad (5)$$

$$\text{Root mass ratio } (RMR, gg^{-1}) = \text{root mass/total plant mass} \quad (6)$$

$$\text{Leaf area ratio } (LAR, cm^2\, g^{-1}) = \text{total leaf area/total plant mass} \quad (7)$$

where leaf total area of each seedling was measured using a Li-3000 leaf area meter (Li-Cor Inc., Lincoln, NE, USA, An et al., 2010).

Data analysis

The mean effect size of light condition changed by SG and LG on morphological and photosynthetic properties on tree seedlings from early-, mid-, and late-successional stages were calculated as Eq. 8–12 (Hedges et al., 1999):

$$\text{Mean effect size} = \frac{\sum_{i=1}^{2} W_i \times E_i}{\sum_{i=1}^{2} w_i} \tag{8}$$

$$E = ln\left(\frac{\overline{X_{SG\ or\ LG}}}{\overline{X_{CK}}}\right) = ln\left(\overline{X_{SG\ or\ LG}}\right) - ln(\overline{X_{CK}}) \tag{9}$$

$$w_i = \frac{1}{\mathbf{V}_i},\ v = \frac{S_{SG\ or\ LG}{}^2}{n_{SG\ or\ LG}\overline{X_{SG\ or\ LG}}^2} + \frac{S_{CK}{}^2}{n_{CK}\overline{X_{CK}}^2} \tag{10}$$

where, i is the number of species of tree seedlings from early-, mid-, and late-successional stages; $\overline{X_{SG\ or\ LG}}$ and $\overline{X_{CK}}$, $n_{SG\ or\ LG}$, and n_{CK}, $S_{SG\ or\ LG}$ and S_{CK} are the mean value, number of replication and standard deviation of morphological and photosynthetic properties for tree seedlings in SG or LG, and control treatment, respectively. A significant mean effect size of light condition changed by SG and LG on morphological and photosynthetic properties was considered only when the 95% confidence interval (CI) did not overlap with zero (Zhou et al., 2014).

The importance of morphological and photosynthetic properties on seedlings' RGR_m was expressed as %IncMSE (percent increase in mean squared error) using the package "RandomForest" (version 4.6-12, Liaw and Wiener, 2002) in R (R Core Team, 2015). The relationships among predictors with RGR_m were analyzed by Pearson correlation analysis. The effect of light conditions (Control, SG, and LG) and successional stage (early-, mid-, and late-) on the variables were examined by analysis of variance (ANOVA). The path analysis was performed using the "lavaan" package (version 0.6-12, Rosseel, 2010) in R to examine the effect of light conditions and successional stages on RGR_m through morphological and photosynthetic properties.

Results

Response of seedlings' relative growth rates to increased light intensity

In the control groups with ambient light intensity, seedlings from different successional stages exhibited significant differences in the relative growth rate (RGR_m, $p < 0.0001$), with the lowest values of –8.61 (± 0.41 standard error, s.e.) mg $g^{-1}d^{-1}$ at early-successional stage and the highest value of 5.61 (± 0.80 s.e.) mg $g^{-1}d^{-1}$ at late-successional stage (**Supplementary Table 1** and **Figures 1A–D**). Relative to control, both SG and LG induced significant increment of RGR_m for seedlings ($P < 0.05$, **Supplementary Table 1** and **Figure 1E**). Improved light condition caused greater enhancement of growth for seedlings from both early- and mid-successional stage than that from the late-one, that SG and LG increased RGR_m of seedlings from both early- and mid-successional stage significantly, but not always of the seedling RGR_m of late- successional tree species (**Figures 1A–C**). Canopy gaps could affect the structure of understory community due to these distinct positive effects of increased light intensity on relative growth rates among seedlings from different successional stages (**Figure 1**).

Response of seedlings' photosynthetic and morphological properties to increased light intensity

Improved light intensity (i.e., in SG and LG) caused higher photosynthesis rates (P_n) relative to that in control, inducing 24.6–212.1, 35.0–107.8, and 17.8–50.2% increase of mass- and area-based light-saturated rate of CO_2 assimilation (A_{mass} and A_{area}) for species at early-, mid-, and late-successional stage, respectively ($P < 0.05$, **Figures 2A–F**). Leaf area (LA) and light saturation point (LSP) in both SG and LG were greater than that in control ($P < 0.05$, **Supplementary Tables 1**, **2**), while the pattern of specific leaf area (SLA) was contrary (**Figures 2G–I** and **Supplementary Table 2**). Increased light intensity induced larger positive effects on both LA and LSP for seedlings from early-successional stage than that from mid- and late-ones (**Figure 2**). Relative to SG, LG induced greater effect on seedlings' photosynthetic properties, especially for species from early-successional stage (**Figure 2** and **Supplementary Table 1**). Both dark respiration (R_d) and light compensation point (LCP) displayed positive response to LG ($P < 0.05$) but not to SG ($P > 0.05$, **Figures 2G–I**, and **Supplementary Table 2**).

Both SG and LG caused positive effect on root: shoot ratio (R/S) and root mass ratio (RMR) for seedlings from all three successional stages, while only LG significantly decreased seedlings' leaf area ratio (LAR) due to the dependence on both light condition and successional stages ($P < 0.05$, **Figures 2D–F** and **Supplementary Tables 1**, **3**). Species at early-successional stage displayed the greatest decrease of leaf mass ratio (LMR) and increase of RMR in comparison with that at mid- and late-successional stage, especially for those at late- stage, seedlings displayed no significant decrease of LMR under both SG and LG ($P < 0.05$, **Figure 2F** and **Supplementary Figure 1**). Seedlings from early-stage displayed greater positive responses of both photosynthetic and morphological properties to enhanced light intensity, suggesting a larger advantage in growth in early-stage tree species over mid- and late-successional tree species (**Figures 2**, **3**).

Regulation of successional stage on RGR_m's response to increased light condition

Among the predictor variables, we confirmed that light condition was the most important factor for seedlings' RGR_m, followed by SLA, LA, LAR, successional stage, and LSP (**Figure 1F**). Light condition increased LA, RMR, R/S, R_d, LCP, LSP and A_{area}, but decreased SLA (**Figures 2**, **3**, **5**), and displayed significant interactions with successional stage on SLA, R_d, LCP and A_{area} (P = 0.021, 0.014, 0.012 and 0.048, **Supplementary Table 1**). RGR_m displayed positive correlations with A_{area}, LA, LSP and R/S (R^2 = 0.51, 0.39, 0.46, and 0.24, respectively, $P < 0.05$, **Figures 4A–C, F**), while exhibited negative relationship with SLA and LAR (R^2 = 0.52 and 0.45, $P < 0.01$, **Figures 4D, E**). The positive effects of improved light condition on RGR_m included direct and indirect pathways (through SLA and A_{area}, **Figure 5**). The regulation of species' successional stage on RGR_m was through the path of SLA. Light condition, A_{area} and SLA all had direct path to affect RGR_m, and jointly explained 93% of seedlings' RGR_m in total (P = 0.319, **Figure 5**). As one of crucial traits of plants, SLA represented the important regulation of successional

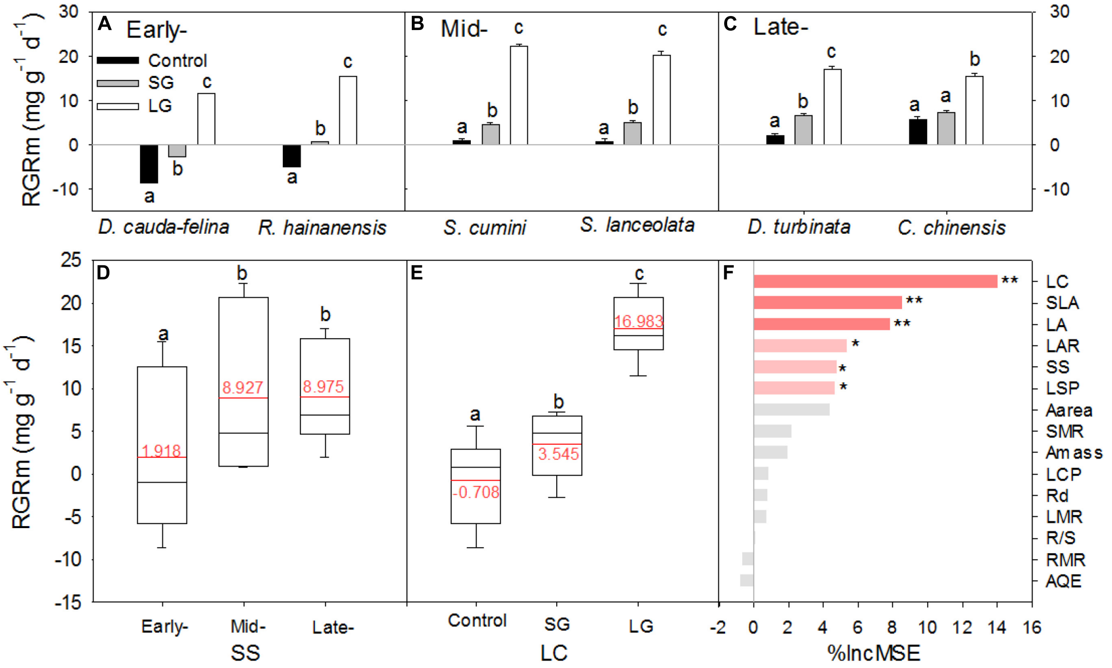

FIGURE 1

Relative mass growth rate [RGR$_m$, **(A–D)**] for tree seedlings at early– **(A,D)**, mid- **(B,D)** and late-successional stage **(C,D)**, and in light conditions of Control, SG and LG **(E)**, and the importance of predictor variables for RGR$_m$ in random forest modelling **(F)**. Control, 0–5% of full sunlight; SG: small canopy gaps, 10–15% of full sunlight; LG: large canopy gaps, 40–50% of full sunlight. The red lines and figures in plots **(D,E)** are the mean value of RGR$_m$ in each group. LC, SLA, LA, LAR, SS, LSP, LCP, A$_{area}$, A$_{mass}$, SMR, R$_d$, LMR, R/S, RMR, and AQE in panel **(F)** were abbreviations of light condition, specific leaf area, leaf area, leaf area ratio, successional stage, light saturation and compensation point, area- and mass- based light saturated rate of CO$_2$ assimilation, stem mass ratio, dark respiration, leaf mass ratio, root: shoot ratio, root mass ratio, and apparent quantum efficiency, respectively. In random forest modeling, "1," "2," and "3" were assigned to treatments of Control, SG and LG; and species at early-, mid-, and late-successional stage, respectively. %IncMSE is the per cent increase in mean squared error. Error bars and the different letters in plots **(A–E)** are standard error (n = 25) and significant difference at P < 0.05, respectively. Symbols ** and * in plot **(F)** indicates statistical significance at P < 0.01 and 0.05, respectively.

stages on seedlings' RGR$_m$ in responding to enhanced light intensity after disturbance-induced canopy gaps (**Figures 1F**, **5**).

Discussion

Changes in the canopy structure and resource availability due to various anthropogenic activities continue to alter forest regeneration and ecosystem functioning. Here, we tested whether the increased light availability (and intensity) due to various size of canopy gaps created from anthropogenic activities differentially affect the growth rates of tree seedlings from different successional stages, which are crucial for predicting future forest recovery and successional trajectory. The results agreed with our hypothesis that the light condition under small canopy gaps (SG, 10–15% of full sunlight) and large canopy gaps (LG, 40–50% of full sunlight) induced greater increment of relative growth rates for seedlings from early- and mid-successional stages relative to that in late- successional stage.

Effect of light condition under canopy gap on growth of seedlings at different successional stages

Canopy opening readily alleviate the light limitation for understory plants in a forest (Lin et al., 2003; Lee et al., 2017). In our study, seedlings grown with light intensity to mimic small (SG) and large canopy gap (LG) displayed significantly higher RGR$_m$ than that with ambient light intensity (Control, P < 0.05, **Figure 1** and **Supplementary Table 1**). Moreover, we found that the development of leaf area (LA, **Figures 2**, **4**) was one of the most important mechanisms to improve photosynthetic assimilation for plant individuals at enhanced light availability (Evans and Poorter, 2001; Tang et al., 2021). The formation of canopy gaps was verified to be beneficial for the understory regeneration in Jianfengling tropical montane rainforest (Feldmann et al., 2020), without considering the impacts on the direction of forest succession.

Exposed to increased light intensity, seedlings at early successional stage with a negative RGR$_m$ in ambient light condition, exhibited the greatest improvement in their RGR$_m$ (**Figure 1**), altering the survival rate, competition and dynamics of seedling community in the tropical forest understory subsequently (Valladares et al., 2000). In contrast, relative to seedlings from early- and mid- successional stage, those from the late-successional stage displayed a lower increment in RGR$_m$ at increased light intensity (**Figure 1**), potentially confirming to the narrow niche breadth of species from the late-successional stage (Parrish and Bazzaz, 1982; Carscadden et al., 2020). Therefore, the canopy gaps due to defoliation (with the equivalent light intensity in SG) and tree fall (with the equivalent light intensity in LG) would trigger the changes of understory productivity, biodiversity and successional trajectory in disturbed patches, altering the structural heterogeneity in tropical forest (Takafumi et al., 2010; Lee et al., 2017).

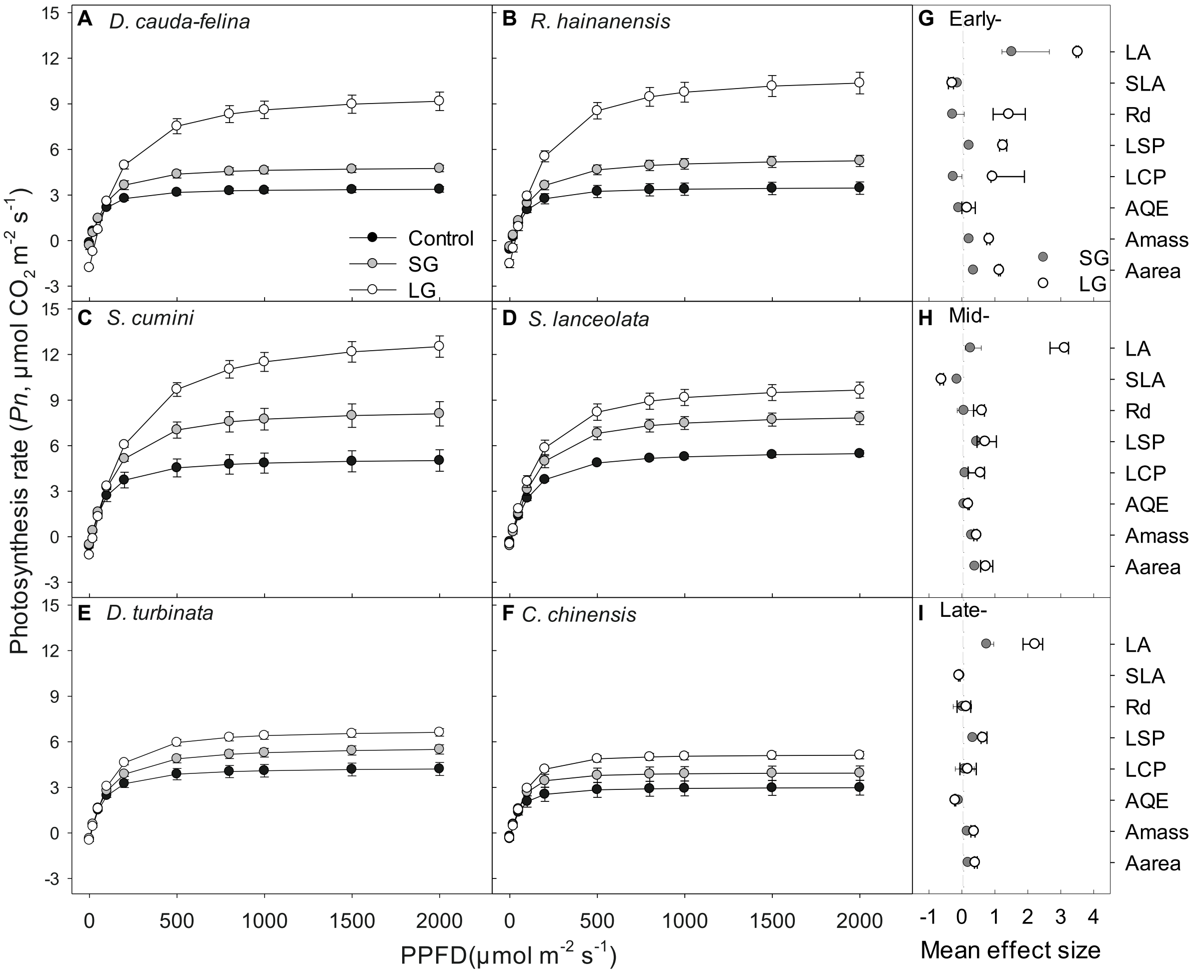

FIGURE 2

Photosynthetic light response curves **(A–F)** for seedlings grown in light conditions under Control, SG and LG, and the mean effect size **(G–I)** of SG and LG on leaf area (LA), specific leaf area (SLA), dark respiration (R_d), light saturation point (LSP), light compensation point (LCP), apparent quantum efficiency (AQE), mass-, and area- based light saturated rate of CO_2 assimilation (A_{mass} and A_{area}) for seedlings at early- **(G)**, mid- **(H)** and late-successional stage **(I)**. Control: 0–5% of full sunlight; SG: small canopy gaps, 10–15% of full sunlight; LG: large canopy gaps, 40–50% of full sunlight. Light curves were fitted by non-linear regression using non-rectangular hyperbola least square curve fitting procedure (Lambers et al., 1998). Data points in plots **(A–F)** and **(G–I)** represent mean ± s.e. [standard error, n = 25 (5 plants × 5 leaves)] and mean ± CI (the 95% confidence interval), respectively. If the CI in plots **(G–I)** did not overlap with zero (the gray dotted line), a significant mean effect of SG and/or LG was considered ($P < 0.05$).

Effect of light condition under canopy gap on photosynthetic properties of seedling at different successional stages

The different response of RGR_m among seedlings from three successional stages could be firstly reflected by corresponding changes in leaf-scale photosynthetic properties (**Figures 1**, **2**, **4**), which is the foundation for regulating plant carbon assimilation to take the advantage from enhanced light due to temporary canopy gaps (Kneeshaw and Bergeron, 1998; Yao et al., 2015). Especially for the greatest improvement of RGR_m for seedlings at early successional stage could be ascribed to their changes in photosynthetic properties, e.g., a significant enhancement of light saturated point (LSP, **Figures 2**, **4**). We suspect that greater LSP may have benefited the seedlings to achieve a higher saturated photosynthetic rate, such as the light–demanding species from the early stage of succession (Ackerly, 1996; Qi et al., 2004). Especially for light condition in LG, seedlings from early-successional stage displayed the largest improvement in both mass- and area-based light-saturated rate of CO_2 assimilation (A_{mass} and A_{area}, **Figure 2**), thus the more light penetrated into forest understory the more advantage would be found for seedlings from early-successional stage (Baul et al., 2022). Beside changes in LSP, light compensation point (LCP) and dark respiration (R_d) in seedlings from early successional stages may also have enhanced due to increased growth respiration driven by accelerated development of leaf and total biomass (**Figures 1**, **2**; Marcelis et al., 1998; Inoue et al., 2022). Furthermore, seedlings from early- and mid-successional stages declined their specific leaf area (SLA, **Figure 2**) as a response to improved light conditions, especially in LG treatment, while that from the late- with an original successional stage lower SLA had no significant changes in SLA (**Figure 2** and **Supplementary Table 3**), displaying the evolutionary conservatism in this functional trait among these plant species (Schweizer et al., 2013; Letcher et al., 2015). The intensity and range of disturbance would be crucial for species composition and successional process in understory patches in tropical forest, the larger canopy gap might brought

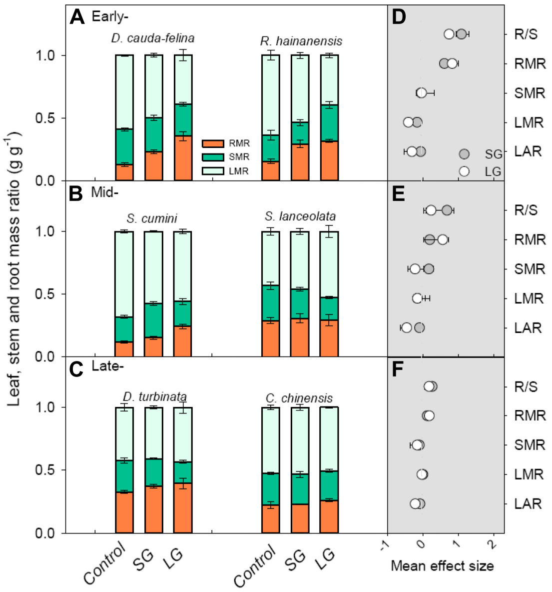

FIGURE 3

Leaf, stem and root mass ratio [LMR, SMR, and RMR, **(A–C)**] of seedlings in Control, SG, and LG, and the mean effect size **(D–F)** of SG and LG on root: shoot ratio (R/S), root, stem, and leaf mass ratio (RMR, SMR, and LMR), and leaf area ratio (LAR) for tree seedlings at early- **(D)**, mid- **(E)**, late-successional stage **(F)**. Control, 0–5% of full sunlight; SG: small canopy gaps, 10–15% of full sunlight; LG: large canopy gaps, 40–50% of full sunlight. The bars in plots **(A–C)** and **(D–F)** represent standard error (n = 5 plants) and 95% confidence interval (CI), respectively. If the CI in plots **(D–F)** did not overlap with zero (the gray dotted line), a significant mean effect of SG and/or LG was considered (P < 0.05).

more advantage for seedlings from early- and mid-successional stages (Yamashita et al., 2000; Liu B. et al., 2012).

Different from other photosynthetic properties with positive or negative responses, the apparent quantum yields (AQE) didn't change even for the seedlings from the early-successional stage (**Figure 2** and **Supplementary Table 1**), which agreed with the correlated results in comparing AQE between shade-tolerant species (i.e., from the late-successional stage) and pioneer species (i.e., from the early-successional stage) previous studies (e.g., Ramos and Grace, 1990; Marenco et al., 2001; Tsvuura et al., 2010).

Effect of light condition under canopy gap on morphological properties in seedlings at different successional stages

Apart from the regulation in leaf-scale photosynthesis properties, seedlings would also alter allocation strategy of photosynthates to the organs acquiring the resource that strongly limits seedling growth (McCarthy and Enquist, 2007; Zhou et al., 2020). In this study, the sensitivity of root mass ratio was greater than that of leaf and stem mass ratio under improved light intensity (**Figure 3**; Poorter and Nagel, 2000). The adequate root development was considered to be crucial for improving seedlings' survival in forest understory, since more belowground sources, e.g., nutrients and water, could support seedlings with an accelerated growth and a greater competitiveness in understory community (Landhausser and Lieffers, 2001; Myers and Kitajima, 2007). Correspondingly, the vertical biomass allocations between below- and above- ground biomass, reflected in root: shoot ratio (R/S) in these seedlings were altered by improved light availability (**Figure 3**; Poorter and Nagel, 2000). However, the significant positive response of R/S to both SG and LG exhibiting an increasing trend from late- to early-successional stage (**Figure 3**), that the seedlings from early- and mid- successional stages displayed a greater morphological plasticity than that from late- stage (Yan et al., 2006). The greater increment of R/S for seedlings from early- and mid- successional stages would be more beneficial for root nutrient absorption, particularly for phosphorus capture, in tropical montane forests, such as our study site (Liu et al., 2010, Liu F. et al., 2012). Thus, seedlings from early- and mid- could successional stages take advantage of the transitory opportunity of improved light condition caused by anthropogenic disturbances, regulating seedlings' niche-partitioning and successional process in the understory of tropical forest (Dupuy and Chazdon, 2006; Yang et al., 2011).

In contrast to the positive correlation between R/S and RGR$_m$, leaf area ratio (LAR) exhibited a negative relationship with RGR$_m$ (**Figure 4**). Under higher light intensity, per unit leaf area or shoot mass could provide greater productivity for plant individual than ambient light condition in understory (Kong et al., 2016), that seedlings with lower LAR and higher R/S potentially had a sufficient functions of above-ground organs, e.g., adequate photosynthetic capacity under increased light intensity (Shafiq et al., 2021). Therefore, canopy gap-induced greater light intensity could drive the trade-off between above- and below-ground biomass allocation, regulating morphological properties of seedlings for better resource acquisition and growing (Freschet et al., 2013; Baez and Homeier, 2018).

The dependence of seedlings' RGR$_m$ on successional stage in responding to increased light condition under canopy gap

Our results show that the seedlings in the understory from different successional stages are characterized by diverse strategies in responding to improved light condition caused by canopy gap after disturbance (**Figures 1–3**). In ambient light condition of understory, seedlings from the late-successional stage had a higher RGR$_m$, ensuring a greater competitiveness relative to seedlings from early- and mid-successional stages in the understory tree community (**Figure 2**; Gao et al., 2016). However, greater light availability due to canopy gaps provided a potential opportunity for the seedlings from early- or mid- successional stages to offset the competitive advantage of late-successional plants (Abbas et al., 2020).

Seedlings' RGR$_m$ in the understory of tropical forest performed a dependence on the light condition, while the successional stage of species displayed a significant regulation on changes of RGR$_m$ through effects on A_{mass}, LAR and SLA (**Figure 5**). Thereinto, SLA was a critical traits connected the effects of light condition and successional stage on seedlings' growth, and playing the most important role for RGR$_m$ after light condition (**Figures 1F**, **5**; Baez and Homeier, 2018). For different seedlings, interspecific functional trait differentiation had been indicated to mainly associate with SLA, that at early-successional stage are generally characterized by a higher SLA relative to that at mid- and late- stages (**Supplementary Table 3**; Wang et al., 2012). Light condition and successional stage

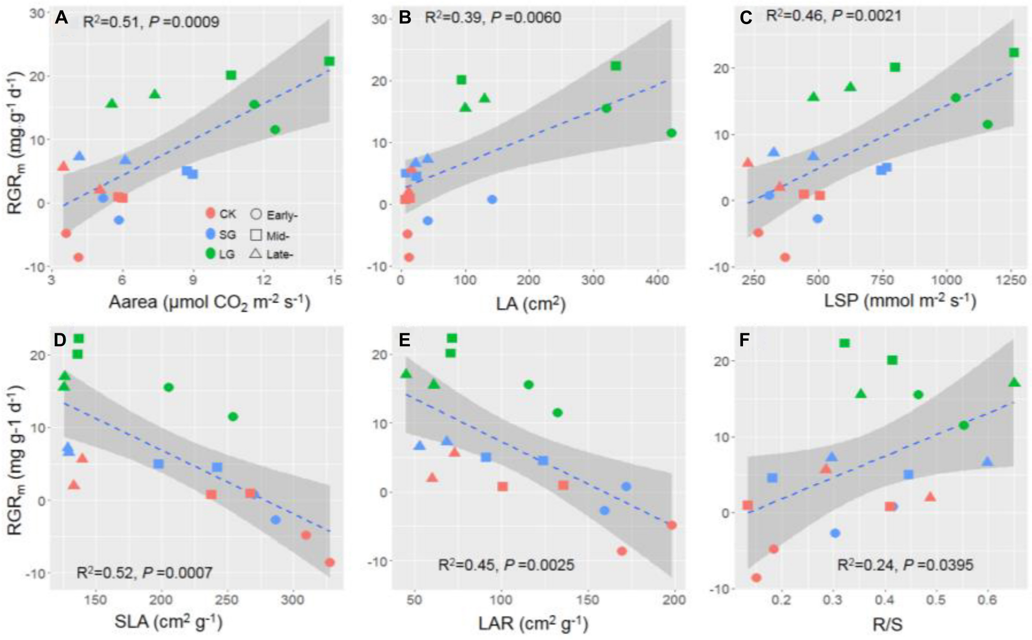

FIGURE 4
The relationship between relative mass growth rate (RGR$_m$) with area- based light saturated rate of CO$_2$ assimilation [A$_{area}$, **(A)**], leaf area [LA, **(B)**], light saturation point [LSP, **(C)**], specific leaf area [SLA, **(D)**], leaf area ratio [LAR, **(E)**], and root: shoot ratio [R/S, **(F)**]. The gray shadow represents the 95% confidence interval for the estimates.

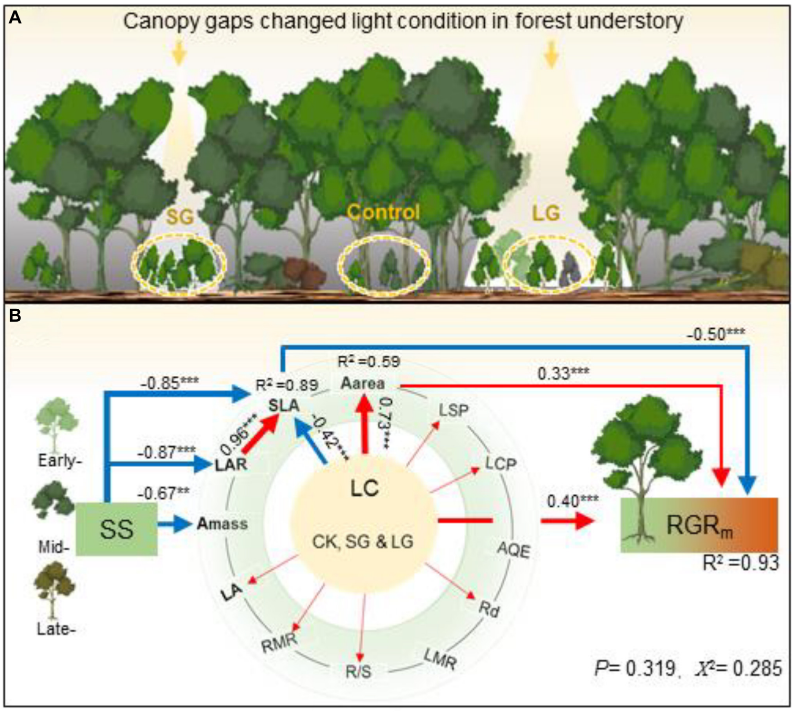

FIGURE 5
Illustration of disturbance-caused canopy gaps' impact on light condition (LC, i.e., Control, SG, and LG) in forest understory **(A)**, and their effects on seedlings' relative mass growth rate [RGR$_m$, **(B)**] for tree species at different successional stage (SS, i.e., early-, mid-, and late- successional stage) based on the path analysis. Control, 0–5% of full sunlight; SG: small canopy gaps, 10–15% of full sunlight; LG: large canopy gaps, 40–50% of full sunlight. In path analysis, "1," "2", and "3" were assigned to treatments of Control, SG and LG; and species at early-, mid-, and late-successional stage, respectively. The red and blue arrows indicate significantly positive and negative effects of light condition (LC), successional stage (SS), leaf area (LA), specific leaf area (SLA), dark respiration (R$_d$), light saturation point (LSP), light compensation point (LCP), apparent quantum efficiency (AQE), mass-, and area- based light saturated rate of CO$_2$ assimilation (A$_{mass}$ and A$_{area}$), leaf mass ratio (LMR), root mass ratio (RMR) and root: shoot ratio (R/S) on RGR$_m$ ($P < 0.05$), respectively. Symbols **, *** indicate statistical significance at $P < 0.01$ and 0.001. In Chi-square test for the path model, the P-value (0.319, >0.05) calculated from one-tailed test indicated that model fit had been established.

displayed a significant interaction on seedlings' SLA, jointly affected seedlings' RGR_m in the understory of tropical forest (**Supplementary Table 1** and **Figure 5**; Kitao et al., 2000). Under the more frequency and intensity disturbances, the advantage of seedlings from late-successional stage would be weaken much more than that from early- and mid-successional stages, slowing down the process of forest forward succession.

Conclusion

Natural and anthropogenic disturbance induced canopy gaps affecting the forest structure and function. Increased light intensity under canopy gaps were verified to accelerate the relative growth rate (RGR_m) of seedlings, improving the understory productivity in Jianfengling tropical rainforest. Relative to the seedlings from late- successional stages, early- and mid-successional stage seedlings displayed stronger positive response of RGR_m due to the higher improvement of leaf area, light saturation point, mass- or area-based light saturated rates of CO_2 assimilation, root mass ratio and root: shoot ratio, as well as the decrement of specific leaf area and leaf area ratio. Light condition and SLA were the most important factors for seedlings' relative growth rate across successional stages. The formation of canopy gaps would open up opportunities for the seedlings of tree species from the early- and mid-successional stages, being beneficial for species diversity and habitat heterogeneity, while go against the forward successional process due to the depressed advantage of species from late-successional stage in tropical forest. Especially, in the context of global climate change, facing higher frequency and intensity of natural disturbance (i.e., typhoon and forest fire), whether the succession of tropical forest would be redirected by too many big scale canopy gaps should depend on both disturbance *per se* and forest stability.

Data availability statement

The original contributions presented in this study are included in the article/**Supplementary material**, further inquiries can be directed to the corresponding authors.

Author contributions

LZ completed the experiment and analyzed the data with substantial contributions from MT, WY, and SA. LZ, WY, and SA conceived, designed, and oversaw the study. LZ wrote the manuscript with substantial contribution from MT. ZJ and YH did the statistical analysis with suggestions from LZ. MT, SA, and XZ commented on the manuscript. All authors contributed to the article and approved the submitted version.

Funding

This research was funded by the National Natural Science Foundation of China (Grant Nos. 32071593, 31600352, and 31930072), Shanghai Key Lab for Urban Ecological Processes and Eco-Restoration (SHUES2021B01), and the Fundamental Research Funds for the Central Universities. MT acknowledges the support from the Swiss State Secretariat for Education, Research and lnnovation (SERI) under contract number M822.00029.

Acknowledgments

We acknowledge the staff of the Jianfengling Experimental Station (Research Institute of Tropical Forestry, Chinese Academy of Forestry) for their field assistance.

Conflict of interest

The authors declare that the research was conducted in the absence of any commercial or financial relationships that could be construed as a potential conflict of interest.

Publisher's note

Supplementary material

The Supplementary Material for this article can be found online at: https://www.frontiersin.org/articles/10.3389/ffgc.2022.1088291/full#supplementary-material

References

Abbas, S., Nichol, J. E., Fischer, G. A., Wong, M. S., and Irteza, S. M. (2020). Impact assessment of a super-typhoon on Hong Kong's secondary vegetation and recommendations for restoration of resilience in the forest succession. *Agric. For. Meteorol.* 280:107784. doi: 10.1016/j.agrformet.2019.107784

Ackerly, D. D. (1996). "Canopy structure and dynamics: Integration of growth processes in tropical pioneer trees," in *Tropical forest plant ecophysiology*, eds S. Strauss-Debenedetti, F. A. Bazzaz, S. S. Mulkey, R. L. Chazdon, and A. P. Smith (New York, NY: Springer), 619–658. doi: 10.1007/978-1-4613-1163-8_21

Alvarez-Clare, S., and Avalos, G. (2007). Light interception efficiency of the understory palm *Calyptrogyne ghiesbreghtiana* under deep shade conditions. *Ecotropica* 13, 57–65.

An, D., Li, M., and Zhang, L. (2010). Measurement of tomato leaf area using computer image processing technology. *Sens. Lett.* 8, 56–60. doi: 10.1166/sl.2010.1201

Antos, J. A., and Halpern, C. B. (1997). Root system differences among species: Implications for early successional changes in forests of Western Oregon. *Am. Midl. Nat.* 138, 97–108. doi: 10.2307/2426658

Baez, S., and Homeier, J. (2018). Functional traits determine tree growth and ecosystem productivity of a tropical montane forest: Insights from a long-term nutrient manipulation experiment. *Glob. Change Biol.* 24, 399–409. doi: 10.1111/gcb.13905

Barlow, J., and Peres, C. A. (2004). Ecological responses to El Nino-induced surface fires in central Brazilian Amazonia: Management implications for flammable tropical forests. *Philos. Trans. R. Soc. B Biol. Sci.* 359, 367–380. doi: 10.1098/rstb.2003.1423

Batuwatta, S., and Singhakumara, B. (2014). "Sun-shade plasticity in leaf traits of early and late-successional tree species in a low land rain forest South West Sri Lanka," in *Proceedings of the 2014 international forestry and environment symposium*, Sigiriya. doi: 10.31357/fesympo.v18i0.1864

Baul, T. K., Chowdhury, A. I., Uddin, M., Hasan, M. K., Nandi, R., Nath, T. K., et al. (2022). Evaluating gap characteristics and their effects on regeneration in Sitapahar forest reserve, Bangladesh. *Eur. J. For. Res.* doi: 10.1007/s10342-022-01502-3

Behera, S. K., Mishra, S., Sahu, N., Manika, N., Singh, S. N., Anto, S., et al. (2022). Assessment of carbon sequestration potential of tropical tree species for urban forestry in India. *Ecol. Eng.* 181:106692. doi: 10.1016/j.ecoleng.2022.106692

Broadbent, E. N., Asner, G. P., Keller, M., Knapp, D. E., Oliveira, P. J. C., and Silva, J. N. (2008). Forest fragmentation and edge effects from deforestation and selective logging in the Brazilian Amazon. *Biol. Conserv.* 141, 1745–1757. doi: 10.1016/j.biocon.2008.04.024

Capers, R. S., and Chazdon, R. L. (2004). Rapid assessment of understory light availability in a wet tropical forest. *Agric. For. Meteorol.* 123, 177–185. doi: 10.1016/j.agrformet.2003.12.009

Carscadden, K. A., Emery, N. C., Arnillas, C. A., Cadotte, M. W., Afkhami, M. E., Gravel, D., et al. (2020). Niche breadth: Causes and consequences for ecology, evolution, and conservation. *Q. Rev. Biol.* 95, 179–214. doi: 10.1086/710388

Clark, D. B., Clark, D. A., Rich, P. M., Weiss, S., and Oberbauer, S. F. (1996). Landscape scale evaluation of understory light and canopy structure: Methods and application in a neotropical lowland rain forest. *Can. J. For. Res.* 26, 747–757. doi: 10.1139/x26-084

Corona-Lozada, M. C., Morin, S., and Choler, P. (2019). Drought offsets the positive effect of summer heat waves on the canopy greenness of mountain grasslands. *Agric. For. Meteorol.* 276-277:107617. doi: 10.1016/j.agrformet.2019.107617

Davidson, R., Mauffette, Y., and Gagnon, D. (2002). Light requirements of seedlings: A method for selecting tropical trees for plantation forestry. *Basic Appl. Ecol.* 3, 209–220. doi: 10.1078/1439-1791-00098

Ding, Y., Zang, R., Lu, X., and Huang, J. (2017). The impacts of selective logging and clear-cutting on woody plant diversity after 40years of natural recovery in a tropical montane rain forest, south China. *Sci. Total Environ.* 579, 1683–1691. doi: 10.1016/j.scitotenv.2016.11.185

Dupuy, J. M., and Chazdon, R. L. (2006). Effects of vegetation cover on seedling and sapling dynamics in secondary tropical wet forests in Costa Rica. *J. Trop. Ecol.* 22, 65–76. doi: 10.1017/S0266467405002890

Emanuel, K. (2005). Increasing destructiveness of tropical cyclones over the past 30 years. *Nature* 436, 686–688. doi: 10.1038/nature03906

Evans, J. R., and Poorter, H. (2001). Photosynthetic acclimation of plants to growth irradiance: The relative importance of specific leaf area and nitrogen partitioning in maximizing carbon gain. *Plant Cell Environ.* 24, 755–767. doi: 10.1046/j.1365-3040.2001.00724.x

Fang, J., Li, Y., Zhu, B., Liu, G., and Zhou, G. (2004). Community structures and species richness in the montane rain forest of Jianfengling,Hainan Island, China. *Chin. Biodivers.* 12, 29–43.

Feldmann, E., Glatthorn, J., Ammer, C., and Leuschner, C. (2020). Regeneration dynamics following the formation of understory gaps in a Slovakian beech virgin forest. *Forests* 11:585. doi: 10.3390/f11050585

Freschet, G. T., Bellingham, P. J., Lyver, P. O. B., Bonner, K. I., and Wardle, D. A. (2013). Plasticity in above- and belowground resource acquisition traits in response to single and multiple environmental factors in three tree species. *Ecol. Evol.* 3, 1065–1078. doi: 10.1002/ece3.520

Gao, Y., Du, F., Wang, Y., Wang, Y., Li, W., and Shi, H. (2016). Interspecific competition of six succession series species with different soil moisture treatments in loess hilly region. *Res. Soil Water Conserv.* 23, 192–197.

Hedges, L. V., Gurevitch, J., and Curtis, P. S. (1999). The meta-analysis of response ratios in experimental ecology. *Ecology* 80, 1150–1156. doi: 10.1890/0012-9658(1999)080[1150:TMAORR]2.0.CO;2

Hogan, J. A., Sharpe, J. M., Van Beusekom, A., Stankavich, S., Carmona, S. M., Bithorn, J. E., et al. (2022). Solar radiation and soil moisture drive tropical forest understory responses to experimental and natural hurricanes. *Ecosphere* 13:11543. doi: 10.1002/ecs2.4150

Hu, M., Liu, Y., Sun, Z., Zhang, K., Liu, Y., Miao, R., et al. (2018). Fire rather than nitrogen addition affects understory plant communities in the short term in a coniferous-broadleaf mixed forest. *Ecol. Evol.* 8, 8135–8148. doi: 10.1002/ece3.4263

Inoue, T., Akaji, Y., and Noguchi, K. (2022). Distinct responses of growth and respiration to growth temperatures in two mangrove species. *Ann. Bot.* 129, 15–28. doi: 10.1093/aob/mcab117

Kitajima, K. (1994). Relative importance of photosynthetic traits and allocation patterns as correlates of seedling shade tolerance of 13 tropical trees. *Oecologia* 98, 419–428. doi: 10.1007/BF00324232

Kitao, M., Lei, T. T., Koike, T., Tobita, H., and Maruyama, Y. (2000). Susceptibility to photoinhibition of three deciduous broadleaf tree species with different successional traits raised under various light regimes. *Plant Cell Environ.* 23, 81–89. doi: 10.1046/j.1365-3040.2000.00528.x

Kneeshaw, D. D., and Bergeron, Y. (1998). Canopy gap characteristics and tree replacement in the southeastern boreal forest. *Ecology* 79, 783–794. doi: 10.1890/0012-9658(1998)079[0783:CGCATR]2.0.CO;2

Kong, D.-X., Li, Y.-Q., Wang, M.-L., Bai, M., Zou, R., Tang, H., et al. (2016). Effects of light intensity on leaf photosynthetic characteristics, chloroplast structure, and alkaloid content of *Mahonia bodinieri* (Gagnep.) Laferr. *Acta Physiol. Plant.* 38:120. doi: 10.1007/s11738-016-2147-1

Lambers, H., Chapin, F. S., and Pons, T. L. (1998). *Plant physiological ecology*. New York, NY: Springer-Verlag. doi: 10.1007/978-1-4757-2855-2

Landhausser, S. M., and Lieffers, V. J. (2001). Photosynthesis and carbon allocation of six boreal tree species grown in understory and open conditions. *Tree Physiol.* 21, 243–250. doi: 10.1093/treephys/21.4.243

Lee, C. M., Kwon, T.-S., and Cheon, K. (2017). Response of ground beetles (Coleoptera: Carabidae) to forest gaps formed by a typhoon in a red pine forest at Gwangneung Forest, Republic of Korea. *J. Forestry Res.* 28, 173–181. doi: 10.1007/s11676-016-0291-5

Letcher, S. G., Lasky, J. R., Chazdon, R. L., Norden, N., Joseph Wright, S., Meave, J. A., et al. (2015). Environmental gradients and the evolution of successional habitat specialization: A test case with 14 Neotropical forest sites. *J. Ecol.* 103, 1276–1290. doi: 10.1111/1365-2745.12435

Li, Y. (2002). "Tropical forests and biodiversity of Jianfengling region," in *Research and conservation of tropical forest and the biodiversity. A special reference to Jianfengling, Hainan Island*, eds Y. Li, B. Chen, and G. Zhou (Beijing: China Forestry Publishing House), 44–133.

Li, Y., Mwangi, B., Zhou, S., Liu, S., Zhang, Q., Liu, J., et al. (2021). Effects of typhoon Mangkhut on a monsoon evergreen broad-leaved forest community in Dinghushan nature reserve, lower subtropical China. *Front. Ecol. Evol.* 9:692155. doi: 10.3389/fevo.2021.692155

Liaw, A., and Wiener, M. (2002). Classification and regression by random forest. *R News* 2, 18–22. Available online at: https://cogns.northwestern.edu/cbmg/LiawAndWiener2002.pdf

Lin, T.-C., Hamburg, S. P., Hsia, Y.-J., Lin, T.-T., King, H.-B., Wang, L.-J., et al. (2003). Influence of typhoon disturbances on the understory light regime and stand dynamics of a subtropical rain forest in northeastern Taiwan. *J. For. Res.* 8, 139–145. doi: 10.1007/s10310-002-0019-6

Liu, B., Pan, L., and Xue, L. (2012). A review of the effect of typhoon on forests. *Acta Ecol. Sin.* 32, 1596–1605. doi: 10.5846/stxb201012231832

Liu, F., Zhang, M., Yang, W., Liu, Y., Wang, W., Zheng, J., et al. (2012). Leaf functional traits and trait relationships of tropical woody vegetation in relation to successional stage: Shifts in understory and canopy layers. *Ecoscience* 19, 198–208. doi: 10.2980/19-3-3499

Liu, F., Yang, W., Zhang, M., Liu, Y., Zheng, J., Wang, W., et al. (2010). Does strategy of resource acquisition in tropical woody species vary with life form, leaf texture, and canopy gradient? *Eur. J. For. Res.* 129, 1093–1108. doi: 10.1007/s10342-010-0394-z

Lohbeck, M., Poorter, L., Martinez-Ramos, M., and Bongers, F. (2015). Biomass is the main driver of changes in ecosystem process rates during tropical forest succession. *Ecology* 96, 1242–1252. doi: 10.1890/14-0472.1

Malhi, Y., and Marthews, T. R. (2013). "Tropical forests:: Carbon, climate and biodiversity," in *Law, tropical forests and carbon: The Case of REDD+*, eds C. MacKenzie, C. McDermott, and R. Lyster (Cambridge: Cambridge University Press), 26–43. doi: 10.1017/CBO9781139236904.004

Marcelis, L. F. M., Heuvelink, E., and Goudriaan, J. (1998). Modelling biomass production and yield of horticultural crops: A review. *Sci. Hortic.* 74, 83–111. doi: 10.1016/S0304-4238(98)00083-1

Marenco, R. A., Gonçalves, J. F. D. C., and Vieira, G. (2001). Leaf gas exchange and carbohydrates in tropical trees differing in successional status in two light environments in central Amazonia. *Tree Physiol.* 21, 1311–1318. doi: 10.1093/treephys/21.18.1311

Martinez-Garza, C., Pena, V., Ricker, M., Campos, A., and Howe, H. F. (2005). Restoring tropical biodiversity: Leaf traits predict growth and survival of late-successional trees in early-successional environments. *For. Ecol. Manage.* 217, 365–379. doi: 10.1016/j.foreco.2005.07.001

Matsuo, T., Martinez-Ramos, M., Bongers, F., van der Sande, M. T., and Poorter, L. (2021). Forest structure drives changes in light heterogeneity during tropical secondary forest succession. *J. Ecol.* 109, 2871–2884. doi: 10.1111/1365-2745.13680

Mazzochini, G. G., and Camargo, J. L. C. (2020). Understory plant interactions along a successional gradient in Central Amazon. *Plant Soil* 450, 81–92. doi: 10.1007/s11104-019-04100-2

McCarthy, M. C., and Enquist, B. J. (2007). Consistency between an allometric approach and optimal partitioning theory in global patterns of plant biomass allocation. *Funct. Ecol.* 21, 713–720. doi: 10.1111/j.1365-2435.2007.01276.x

Miller, A. D., Roxburgh, S. H., and Shea, K. (2011). How frequency and intensity shape diversity-disturbance relationships. *Proc. Natl. Acad. Sci. U.S.A.* 108, 5643–5648. doi: 10.1073/pnas.1018594108

Muscolo, A., Bagnato, S., Sidari, M., and Mercurio, R. (2014). A review of the roles of forest canopy gaps. *J. Forestry Res.* 25, 725–736. doi: 10.1007/s11676-014-0521-7

Myers, J. A., and Kitajima, K. (2007). Carbohydrate storage enhances seedling shade and stress tolerance in a neotropical forest. *J. Ecol.* 95, 383–395. doi: 10.1111/j.1365-2745.2006.01207.x

Olivero-Lora, S., Rojas-Sandoval, J., Melendez-Ackerman, E. J., and Orengo-Rolon, J. L. (2022). Hurricane driven changes in vegetation structure and ecosystem services in tropical urban yards: A study case in San Juan, Puerto Rico. *Urban Ecosyst.* 25, 1431–1444. doi: 10.1007/s11252-022-01236-5

Parrish, J. A. D., and Bazzaz, F. A. (1982). Niche responses of early and late successional tree seedlings on three resource gradients. *Bull. Torrey Bot. Club* 109, 451–456. doi: 10.2307/2996486

Pollastrini, M., Brüggeman, W., Fotelli, M., and Bussotti, F. (2022). Downregulation of PSI regulates photosynthesis in early successional tree species. Evidence from a field survey across European forests. *J. Photochem. Photobiol.* 12:100145. doi: 10.1016/j.jpap.2022.100145

Poorter, H., and Nagel, O. (2000). The role of biomass allocation in the growth response of plants to different levels of light, CO2, nutrients and water: A quantitative review. *Aust. J. Plant Physiol.* 27, 595–607. doi: 10.1071/PP99173

Prescott, C. E. (2002). The influence of the forest canopy on nutrient cycling. *Tree Physiol.* 22, 1193–1200. doi: 10.1093/treephys/22.15-16.1193

Qi, X., Cao, K.-F., and Feng, Y.-L. (2004). Photosynthetic acclimation to different growth light environments in seedlings of three tropical rainforest Syzygium species. *Zhiwu Shengtai Xuebao* 28, 31–38. doi: 10.17521/cjpe.2004.0005

Quero, J. L., Villar, R., Marañón, T., and Zamora, R. (2006). Interactions of drought and shade effects on seedlings of four *Quercus* species: Physiological and structural leaf responses. *New Phytol.* 170, 819–834. doi: 10.1111/j.1469-8137.2006.01713.x

R Core Team (2015). *R: A language and environment for statistical computing.* Vienna: R Foundation for Statistical Computing.

Ramos, G., and Grace, J. (1990). The effects of shade on the gas exchange of seedlings of four tropical trees from Mexico. *Funct. Ecol.* 4, 667–677. doi: 10.2307/2389735

Reich, P. B., Walters, M. B., and Ellsworth, D. S. (1992). Leaf life-span in relation to leaf, plant, and stand characteristics among diverse ecosystems. *Ecol. Monogr.* 62, 365–392. doi: 10.2307/2937116

Rosseel, Y. (2010). *lavaan: An R package for structural equation modeling and more Version 0.5-10 (BETA).* Ghent: Ghent University.

Schweizer, D., Gilbert, G. S., and Holl, K. D. (2013). Phylogenetic ecology applied to enrichment planting of tropical native tree species. *For. Ecol. Manage.* 297, 57–66. doi: 10.1016/j.foreco.2013.02.012

Shafiq, I., Hussain, S., Raza, M. A., Iqbal, N., Ahsan Asghar, M., Raza, A., et al. (2021). Crop photosynthetic response to light quality and light intensity. *J. Integr. Agric.* 20, 4–23. doi: 10.1016/S2095-3119(20)63227-0

Sheng, D.-Y., Zhuang, X.-Y., Xu, H., Li, Y.-D., Hu, Y.-H., Shi, L.-L., et al. (2012). Community structure of endemic woody plants in tropical montane rainforest of Jianfengling, Hainan Island, China. *Chin. J. Plant Ecol.* 36, 935–947. doi: 10.3724/SP.J.1258.2012.00935

Souza, R. P., and Válio, I. F. (2003). Seedling growth of fifteen Brazilian tropical tree species differing in successional status. *Braz. J. Bot.* 26, 35–47. doi: 10.1590/S0100-84042003000100005

Takafumi, H., Kawase, S., Nakamura, M., and Hiura, T. (2010). Herbivory in canopy gaps created by a typhoon varies by understory plant leaf phenology. *Ecol. Entomol.* 35, 576–585. doi: 10.1111/j.1365-2311.2010.01216.x

Tang, J., Sun, B., Cheng, R., Shi, Z., Luo, D., Liu, S., et al. (2021). The effect of low irradiance on leaf nitrogen allocation and mesophyll conductance to CO_2 in seedlings of four tree species in subtropical China. *Plants* 10:2213. doi: 10.3390/plants10102213

Thakur, M. P., Risch, A. C., and van der Putten, W. H. (2022). Biotic responses to climate extremes in terrestrial ecosystems. *iScience* 25:104559. doi: 10.1016/j.isci.2022.104559

Tobita, H., Utsugi, H., Kitao, M., Kayama, M., Uemura, A., Kitaoka, S., et al. (2010). Variation in photoinhibition among Sasa senanensis, Quercus mongolica, and Acer mono in the understory of a deciduous broad-leaved forest exposed to canopy gaps caused by typhoons. *Trees* 24, 307–319. doi: 10.1007/s00468-009-0400-6

Toledo-Aceves, T., and Swaine, M. D. (2008). Biomass allocation and photosynthetic responses of lianas and pioneer tree seedlings to light. *Acta Oecol.* 34, 38–49. doi: 10.1016/j.actao.2008.03.003

Tourville, J. C., Wason, J. W., and Dovciak, M. (2022). Canopy gaps facilitate upslope shifts in montane conifers but not in temperate deciduous trees in the Northeastern United States. *J. Ecol.* 110, 2870–2882. doi: 10.1111/1365-2745.13993

Trauernicht, C., Ticktin, T., and Herrera, G. L. (2006). Cultivation of non-timber forest products alters understory light availability in a humid tropical forest in Mexico. *Biotropica* 38, 428–436. doi: 10.1111/j.1744-7429.2006.00143.x

Tsai, H.-C., Chiang, J.-M., McEwan, R. W., and Lin, T.-C. (2018). Decadal effects of thinning on understory light environments and plant community structure in a subtropical forest. *Ecosphere* 9:e02464. doi: 10.1002/ecs2.2464

Tsvuura, Z., Griffiths, M. E., Gunton, R. M., Franks, P. J., and Lawes, M. J. (2010). Ecological filtering by a dominant herb selects for shade tolerance in the tree seedling community of coastal dune forest. *Oecologia* 164, 861–870. doi: 10.1007/s00442-010-1711-4

Valladares, F., Wright, S. J., Lasso, E., Kitajima, K., and Pearcy, R. W. (2000). Plastic phenotypic response to light of 16 congeneric shrubs from a Panamanian rainforest. *Ecology* 81, 1925–1936. doi: 10.1890/0012-9658(2000)081[1925:PPRTLO]2.0.CO;2

Wang, L., and Lin, T.-C. (2019). Forests affected by frequent and intense typhoons challenge the intermediate disturbance hypothesis. *Biotropica* 51, 797–801. doi: 10.1111/btp.12711

Wang, Y., Tao, J., Liu, J., and He, Z. (2012). Response of leaf functional traits to different light regimes in an evergreen broad-leaved forest in the Jinyun Mountain. *Sci. Silvae Sin.* 48, 23–29.

Wang, Z., Jiang, L., Gao, J., Qing, S., Pan, C., Wu, Y., et al. (2022). The influence of microhabitat factors on the regeneration and species composition of understory woody plants in *Pinus tabuliformis* plantations on the Loess Plateau. *For. Ecol. Manage.* 509:120080. doi: 10.1016/j.foreco.2022.120080

Westerband, A. C., and Horvitz, C. C. (2015). Interactions between plant size and canopy openness influence vital rates and life-history tradeoffs in two neotropical understory herbs. *Am. J. Bot.* 102, 1290–1299. doi: 10.3732/ajb.1500041

Xi, W., Peet, R. K., Lee, M. T., and Urban, D. L. (2019). Hurricane disturbances, tree diversity, and succession in North Carolina Piedmont forests, USA. *J. Forestry Res.* 30, 219–231. doi: 10.1007/s11676-018-0813-4

Yamashita, N., Ishida, A., Kushima, H., and Tanaka, N. (2000). Acclimation to sudden increase in light favoring an invasive over native trees in subtropical islands, Japan. *Oecologia* 125, 412–419. doi: 10.1007/s004420000475

Yan, E.-R., Wang, X.-H., and Huang, J.-J. (2006). Shifts in plant nutrient use strategies under secondary forest succession. *Plant Soil* 289, 187–197. doi: 10.1007/s11104-006-9128-x

Yang, H., Liu, S., Cao, K., Wang, J., Li, Y., and Xu, H. (2017). Characteristics of typhoon disturbed gaps in an old-growth tropical montane rainforest in Hainan Island, China. *J. Forestry Res.* 28, 1231–1239. doi: 10.1007/s11676-017-0402-y

Yang, H. B., An, S. Q., Sung, O. J., Shi, Z. M., She, X. S., Sun, Q. Y., et al. (2008). Seasonal variation and correlation with environmental factors of photosynthesis and water use efficiency of Juglans regia and Ziziphus jujuba. *J. Integr. Plant Biol.* 50, 210–220. doi: 10.1111/j.1744-7909.2007.00391.x

Yang, W., Liu, F., Zhou, L., Zhang, S., and An, S. (2011). Trade-offs between growth and survival of non-pioneer light-demanding tree seedlings in tropical forest of Hainan Island, China. *J. Trop. Ecol.* 27, 611–620. doi: 10.1017/S0266467411000435

Yao, A.-W., Chiang, J.-M., McEwan, R., and Lin, T.-C. (2015). The effect of typhoon-related defoliation on the ecology of gap dynamics in a subtropical rain forest of Taiwan. *J. Veg. Sci.* 26, 145–154. doi: 10.1111/jvs.12217

Zhou, L., Hong, Y., Li, C., Lu, C., He, Y., Shao, J., et al. (2020). Responses of biomass allocation to multi-factor global change: A global synthesis. *Agric. Ecosyst. Environ.* 304:107115. doi: 10.1016/j.agee.2020.107115

Zhou, L., Zhou, X., Zhang, B., Lu, M., Luo, Y., Liu, L., et al. (2014). Different responses of soil respiration and its components to nitrogen addition among biomes: A meta-analysis. *Glob. Change Biol.* 20, 2332–2343. doi: 10.1111/gcb.12490

Zong, S., He, H., Liu, K., Du, H., Wu, Z., Zhao, Y., et al. (2018). Typhoon diverged forest succession from natural trajectory in the treeline ecotone of the Changbai Mountains, Northeast China. *For. Ecol. Manage.* 407, 75–83. doi: 10.1016/j.foreco.2017.09.051

frontiers | Frontiers in Forests and Global Change

TYPE Original Research
PUBLISHED 17 July 2023
DOI 10.3389/ffgc.2023.1198626

OPEN ACCESS

EDITED BY
Uttam Kumar Sahoo,
Mizoram University, India

REVIEWED BY
Rajiv Pandey,
Indian Council of Forestry Research and Education (ICFRE), India
Bhupendra Singh,
VCSG Uttarakhand University, Ranichauri, India

*CORRESPONDENCE
Waseem Razzaq Khan
✉ khanwaseem@upm.edu.my

RECEIVED 01 April 2023
ACCEPTED 17 May 2023
PUBLISHED 17 July 2023

CITATION
Yaseen M, Khan WR, Bahadur S, Batool F, Khalid F, Ahmed U and Ashraf M (2023) Intra- and inter-specific responses of plant functional traits to environmental variables: implications for community ecology in the tropical monsoonal dwarf forest on Hainan Island. *Front. For. Glob. Change* 6:1198626. doi: 10.3389/ffgc.2023.1198626

Intra- and inter-specific responses of plant functional traits to environmental variables: implications for community ecology in the tropical monsoonal dwarf forest on Hainan Island

Muhammad Yaseen[1,2], Waseem Razzaq Khan[3]*, Saraj Bahadur[1,2], Farwa Batool[1,2], Farhan Khalid[4], Umair Ahmed[5] and Maria Ashraf[6,7]

[1]Wuzhishan National Long-Term Forest Ecosystem Monitoring Research Station, College of Forestry, Hainan University, Haikou, China, [2]Hainan Key Laboratory for Sustainable Utilization of Tropical Bioresource, College of Forestry, Hainan University, Haikou, China, [3]Department of Forestry Science, Faculty of Agricultural and Forestry Sciences, Universiti Putra Malaysia Kampus Bintulu Sarawak Jalan Nyabau, Bintulu, Sarawak, Malaysia, [4]Faculty of Agriculture and Environment, The Islamia University of Bahawalpur, Bahawalpur, Pakistan, [5]College of Horticulture and Forestry Sciences, Huazhong Agriculture University, Wuhan, China, [6]Key Laboratory of Agroforestry Environmental Process and Ecological Regulation of Hainan Province, Hainan University, Haikou, China, [7]College of Ecology and Environment, Hainan University, Haikou, China

In the context of tropical monsoonal dwarf forest restoration, it is well known that the interaction between soil properties and plant functional traits influences the dynamics and forest composition of plant communities. The main aim of this study was to determine the relationships and variations between the plant functional traits and environmental variables in tropical coastal secondary forests. However, it is undisputed whether trait variation is coordinated and whether there is a relationship between the community-weighted mean (CWM) traits and soil variables. TNNR conducted a ground survey to collect actual ground data on the biophysical characteristics of individual trees and shrubs, along with soil sample data. All soil samples and plant materials were collected at the end of June, in the 2020 growing season (July and August), in each quadrat with a 400-m^2 area. To gain insight into these questions, a total of 4 plant functional traits of 167 species and 5 soil nutrients from 128 soil samples were analyzed from 128 plots in a tropical evergreen monsoon forest on Hainan Island. Using SMA (standardized major axis), wood density (WD), and leaf thickness (LT), as well as specific leaf area (SLA) and relative leaf water content (RLWC), were significantly positively correlated. Using Pearson correlation analysis, leaf thickness (LT) was significantly positively correlated with soil organic matter (OM). Using principal component analysis (PCA), we also found that soil TN and OM were the strongest predictors for functional traits, i.e., WD and LT. Moreover, using path analysis, OM and TN have a major impact on plant CWM traits, e.g., SLA and RLWC. Our results show a significant relationship between functional traits and soil pH and soil nutrients in tropical coastal secondary forests. Our results highlight that plant traits can be used to predict specific soil nutrients and ecosystem functioning in tropical secondary forests, but we are concerned about how variation in the physical structure of plant affect ecosystem function in forest communities. This research can help us to better understand the restoration of habitats and green infrastructure design, suggesting that selecting different species across multiple trait axes can help ensure functionality at the maximum level.

KEYWORDS

regression analyses, principal component analysis, tropical coastal secondary forest, community-weighted mean, soil nutrients

Introduction

Analysis of plant functional traits is becoming a more and more useful ecological approach for understanding plant community assembly (Funk et al., 2017). Plant functional traits are increasingly recognized as a powerful framework for understanding shifts in species distribution and responses to environmental change (Funk et al., 2017; Costa et al., 2018; Griffin-Nolan et al., 2018), and this could provide a powerful framework to generate insights into how simultaneous changes in drought and nutrient availability differentially impact coexisting dryland species. For example, a rapid or slow strategy needs the same sets of leaf, root, and stem features regardless of whether the main limiting factor is light, N, P, water, or temperature due to the small number of coupled resources in plant economics (Reich, 2014). Rather, certain species have characteristics that relate to their ability to store resources in protected tissues, which is referred to as a conservation strategy (Reich, 2014). It is demonstrated in the experimental data that abiotic stress factors, i.e., due to less availability of nutrients and light (Lohbeck et al., 2015), the plant functional traits and plant species composition can change, leading to changes from an acquisitive strategy to a conservative strategy (Raevel et al., 2012). In this way, changes in leaf functional traits (LFTs) may reflect changes in the environment, such as light and soil property variations (Reich, 2014). Hodgson et al. (2011) revealed that specific leaf area (SLA), a key component of the worldwide leaf economic spectrum, is the preferred soft (morphological) plant trait for assessing soil fertility. At present, the intraspecific variation at a community level has been consistently reported, but its consequences have not been completely explored (Siefert, 2014).

Recently, empirical studies have quantified the relative amount of intraspecific trait variation (ITV) compared to interspecific variation for various plant functional traits and communities (e.g., Messier et al., 2010; Auger and Shipley, 2013). Therefore, quantifying intraspecific trait variability as well as interspecific variability is important for understanding niche segregation and species distribution at the regional level.

Differences in forest composition, i.e., age, size, and spatial arrangement within a forest stand, have been influenced by the distribution of environmental factors such as soil nutrients and soil pH (Spence et al., 2008). Plant functional traits (PFTs) aggregate features of individual plants with similar activities in an ecosystem and similar responses to external factors such as water and nutrient availability based on a finite number of static parameters (Kattge et al., 2011). The relationships among traits, resources, and biodiversity are supported by parallel gradients in species abundances and traits (i.e., fast–slow variation) with respect to soil nutrients, e.g., phosphorus (P) gradients. For example, with limited resources of soil P in Western Australia, plants with slow functional traits compete a little with each other, resulting in high diversity (Lambers et al., 2013), like the less availability of soil nitrogen (N) in temperate grasslands (Clark and Tilman, 2008). Increased plant diversity due to reduced soil fertility most likely reflects global patterns (Laliberté et al., 2013). For example, several long-term soil chrono sequences around the world have shown that local plant species richness increases with soil age. This is associated with low P in older soils (Laliberté et al., 2013). These patterns raise the possibility that P limitation itself promotes plant species coexistence (Olde Venterink, 2011). This may be related to the fact that soil phosphorus exists in many chemical forms and several different phosphorus uptake strategies can target specific forms (Lambers et al., 2006, 2008). Soil P gradients related to soil substrate type or age are important with respect to economic plant attributes, whether the gradients are landscape or regional (Lambers et al., 2013). Despite these identified patterns, very little research has been done about the relationship between plant functional traits and soil properties under specific climatic conditions.

Aboveground and belowground feature variability can be incorporated into dynamic global vegetation models (DGVMs) in several ways. One approach is to vary parameters within the PFT as a function of environment variables. One such approach has the rationale that community mean trait values (or PFTs) are selected by environmental conditions, thereby triggering trait convergence. This environmental selection may influence functional leaf traits by climate (Wright et al., 2005), soil fertility (Ordoñez et al., 2009), or a combination thereof (e.g., van Ommen Kloeke et al., 2012). The incorporation of empirical feature–environment relationships into the JSBACH DGVM, part of the Max Planck Institute Earth System Model (MPI-ESM), suggests a large impact of feature variability on vegetation and carbon dynamics in the present climate (Verheijen et al., 2013). The second approach is to use trait variability to predict survival of the fittest trait combinations for a range of environmental variables using tradeoffs between traits and evolutionary rules (Langan et al., 2017). It is documented in a few studies about how plant functional traits respond to environmental variables, e.g., soil pH, and nutrients, such as N and P in soil, play an important role, all of which influence plant functional traits (Pan et al., 2018). On the other hand, the leaf morphological properties, i.e., leaf thickness (LT), leaf area (LA), specific leaf area (SLA), and leaf dry matter content (LDMC) are functional traits that can be easily measured to designate the resource strategies and adaptive traits of a plant in relation to its environment (Vendramini et al., 2002). It is therefore important to realize how functional traits express plant strategies when changes occur in plant functional traits due to the effect of soil nutrients. To identify factors related to alterations in community functional traits, it is also necessary to determine the relationship between the functional traits of plants and surrounding environmental conditions (Reich et al., 2003).

Therefore, experimental projects that aim to better understand the relationships between plant functional traits and soil properties in natural forest communities are needed (Wardle, 2016). These linkages may support identifying the factors that influence changes in plant functional traits and the composition of tropical forest communities. The significant intraspecific variation at the local level and environmental variation at the larger level have been consistently reported; nonetheless, their significance is still under investigation (Siefert et al., 2015).

A comparative study of plant functional trait (PFTs) dynamics in species provides one basis for the identification of life history strategies (Adler et al., 2014) and parameterization of dynamic vegetation models (Atkin et al., 2015). Some leaves, trees, and seed characteristics are thought to indicate that the plant receives resources, reproduces, and competes with other plants (Westoby et al., 2002). While there is a wide variety of variables that determine fundamental strategies worldwide, recent research has shown that at the local scale, this relationship will be weak (Messier et al., 2017), and the intraspecific relationship differing between sites characterized by different species and/or growing conditions (Lira-Martins et al., 2019) or within the species (Anderegg et al., 2018). This means that a general equation for estimating one of the other parameters will not affect multiple measurements. The change in productivity may be related to the type of harvest as well as the environmental conditions in which individuals grow (Garnier et al., 2016). Geographic gradients, where a group of species is repeatedly found in different conditions, provide a natural laboratory for investigating the relative impact of taxonomic and environmental plasticity on differences (Turnbull et al., 2016). Hence, to fill this gap, the main objective of our study was to examine the linkages and changes between selected functional traits and soil abiotic properties in tropical coastal secondary forests. Hainan Island, off the northeastern coast of China, is known for its tropical coastline forests. The changes in leaf functional traits (LFTs) may reflect environmental variations such as light and soil property variations (Reich, 2014). One of the characteristics of tropical monsoonal cloud forest (TMCF) is the persistent existence of haze or low clouds, resulting in waterlogging on plants (Bruijnzeel and Veneklaas, 1998), less solar radiation, and lower soil temperatures compared to tropical rain forests (Vitousek and Sanford, 1986). However, the tropical monsoonal dwarf forests of TNNR have been severely affected by human disturbances, i.e., shifting cultivation and slash and burn, and natural catastrophe such as typhoons (Long et al., 2018). Tongguling National Nature Reserve (TNNR) in Wenchang County, Hainan Province, is surrounded on three sides by the sea (Si tu, 1987). It has lateritic soil (Long et al., 2012). Only a few similar ecosystems exist in the TNNR monsoonal evergreen forest, which is the natural forest vegetation in southern China (Wu, 1995). Therefore, the most important issues in this county are natural environmental monitoring, biodiversity conservation, and typhoon mitigation (Long et al., 2018). At present, the tropical secondary forests have been restored. Therefore, our research was on productive or rich species in tropical coastal secondary forests in a TNNR region with an attempt to answer the following questions: (a) Are plant functional traits linked to soil nutrients, and which nutrients contribute most to community assembly? (b) Are variations in plant functional traits distinctly affected by soil properties in the forest community? We predicted that plant morphological traits related to soil nutrients would show consistent relationships in tropical forest community. Second, we expected that plant functional traits and soil properties (i.e., using community-weighted mean (CWM) trait values) would predict ecosystem processes.

Materials and methods

Study site

The current survey was conducted in 2020 in TNNR, located in the northeastern part of Hainan Island in southern China (19°36′19°41′ N 110°58′111°03′ E). TNNR is a 44-square-kilometer nature reserve with an elevation of 338 m.a.s.l. above sea level. It has a tropical monsoon climate. From May until October is the wet season and from November until April is the dry season. The average annual temperature is 23.9°C and the precipitation is 1,721.6 mm. The tropical evergreen monsoonal forest possesses a lateritic soil type (Long et al., 2012). The predominant forest type in TNNR is tropical evergreen monsoonal forest, which covers the total area. Before the year 1980, all these forests had been logged and altered into shrublands, grassland, or second-growth forests. Deforestation was restricted once the TNNR was established in 1983, and forests have been well-recovered (Long et al., 2018).

Plant sampling

In the area of TNNR, tropical evergreen monsoonal forest, we randomly established nine 50 × 50 m (2,500 m^2) plots. To precisely measure tree coordinates, 128 plots were divided into 20 × 20-m quadrates and any two plots were always separated by more than 50 m. TNNR conducted a ground survey to collect actual ground data on the biophysical characteristics of individual trees and shrubs, along with soil sample data. The Flora of the Republic of China helped identify the species (Editorial Committee of Flora of China) (Wu, 1995). We collected all soil samples and plant material at the end of June, in the 2020 growing season (July and August), in each quadrat with a 400-m^2 area.

However, we conducted our study at the plot level in a vegetation community with the same type of topography and climatic condition, i.e., the inclination of gradient, parental substances, and aspects.

Soil sampling and analysis

During the rainy season in July 2020, soil samples were collected from the top 0–20 cm of the mineral soil in the center of each quadrat in a total of 128 20 × 20 m (400 m^2) plots. The nutrients and transformation fluxes were calculated using a compound sample made up of these samples (described in a later section). During the growing season (July and August), a total of 128 soil samples were taken in TNNR.

Soil pH, organic matter (OM), total nitrogen (TN), total phosphorus (TP), and soil water content (SWC) were all tested during the wet season. Five soil profiles were randomly selected from each 20 × 20-m (400 m^2) plot, and samples were taken from each plot. Then, for each profile, the grass layer above the soil was removed, and a sample from the soil surface specimen (0–20 cm) was collected (Jobbagy and Jackson, 2001). The soil sample was mixed well, air-dried, and then milled into a fine powder. The samples were then manually screened and examined (Anderson and Ingram, 1989).

For the analysis of the concentration of OM (g. kg-1), 5 mL of 1N potassium dichromate ($K_2Cr_2O_7$) solution and 5 mL of 98% sulfuric acid (H_2SO_4) solution were mixed with 0.5 g of soil and kept at room temperature for 30 min. After adding deionized water, the color changes from blue to green, add concentrated phosphoric acid (H_3PO_4), and then added 0.5 M iron ammonium sulfate (NH_4) 2Fe (SO_4)2.6H_2O titrate the mercury solution. Finally, the titration was repeated till the color changed from violet-blue to green.

For pH analysis, 25 g of soil was carefully mixed with deionized water and stirred. The pH of the suspension was then determined using a pH electrode at a temperature in the range of 20°C to 25°C (Phoenix Electrode Company, Houston, TX, USA).

To measure the concentration of TN (g. kg^{-1}), 1.0 g of soil was digested with potassium sulfate, copper sulfate (K_2SO_4-$CuSO_4$ × 5), and hydroxy selenide (H_2O–Se) in 98% sulfuric acid (H_2SO_4). After that, ammonium nitrogen was extracted from the digest using steam and a pH increase of 0.1 M sodium hydroxide (NaOH). Third, the distillate was obtained in 2% H^3BO^3 and titrated with 0.05 H_2SO_4 to give a pH of 5.0. Finally, the TN concentration was computed based on the volume change of a 0.05 M sulfuric acid (H_2SO_4) solution.

To determine the TP concentration (g. kg^{-1}), 0.25 g of soil was carefully mixed with a 60% $HClO_4$ solution. The mixture was then diluted with standard and sample vanadium-molybdate reagents at a wavelength of 700 nm. Finally, TP was calculated using the calibration curve.

For soil water content (SWC) calculation, the Gravimetric method was used in the laboratory. A detailed amount of soil was placed in a container that is heated to 105°C and dried until all moisture has evaporated (Liu et al., 2016). The gravimetric method, also known as the drying method, is a direct way of assessing the moisture content of a soil sample by drying it and calculating the difference in weight between the wet and dry samples. The soil water content was calculated as the following: water content (%) = fresh weight-dry weight divided by dry weight multiplied by 100.

Trait collection and measurements

Plant functional traits (PFTs) were measured using a standardized protocol on sun-exposed leaves from the tops of crowns (Cornelissen et al., 2003). In many cases, a 3–4-m long pruning pole was used for smaller trees. When necessary, we used climbing tools and a pruning pole to reach the high tops of larger tree crowns. We collected trait data of species present during surveys using standard methods (Libalah et al., 2017). Using a clinometer, the height of all individual trees in each plot was investigated with a dbh ≤ 5 (diameter at breast height). To investigate the functional properties of the plants, 2–3 freshly emerged sun-exposed leaves on the current-year shoots were taken from each plant and measured on 3 standard trees of each species. Leaf thickness was measured using a digital reading caliper (SF2000, Guilin, China; Long et al., 2022; Yaseen et al., 2022). In addition, leaf area was measured using a leaf area meter (LI-COR 3100C Area Meter, LI-COR, Lincoln, NE, USA). The leaves were first dried at 70°C for at least 72 h to constant weight, weighed on a digital balance (Ohaus Adventurer AR2140 Analytical Balance, Hayward, CA, USA), and leaf area and dry matter were used to calculate the specific leaf area (SLA) (mm^2 mg−1) for each tree. We focused on four plant functional traits: wood density (WD-g.cm^{-3}), leaf thickness (LT-mm), specific leaf area (SLA-mm^2.g^{-1}), and relative leaf water content (RLWC %) across the 167 species in our dataset. Within 6 to 24 h, the fresh weight of the leaves was measured immediately with a SE202F electronic balance (Ohaus Corp., Parsippany, NJ, US), then stored in damp paper towels and placed in the refrigerator. The average area of the three leaves (LA) per tree was calculated, and the ratio between LA and SLA (cm^2g^{-1}) (the average mass of the three leaves) was calculated (Pérez-Harguindeguy et al., 2016). SLA is also associated with competitive ability, as species with low SLA compete better for scarce resources such as nitrogen (Weiher et al., 1999). Similarly, SLA is linked to growth rate and stress tolerance, with higher SLA associated with species that develop faster and are less stress-tolerant (Wright et al., 2004). Before measuring the mass and area of the fresh leaves, the leaf samples were stored in a wet bag below 4°C for up to 72 h. A leaf area meter was used to measure the size of the leaves (LI-COR 3100C Area Meter, LICOR), while the dry leaf mass was calculated after drying in the oven at 70°C for 72 h. After drying for at least 72 h at 70°C and weighing to the nearest 0.01 g, leaf mass per unit area (mg.mm^2) was calculated for each tree based on leaf area and dry mass. We collected three twigs (width 1–2 cm) from each representative individual collected for leaf attributes to describe the species (WD, g.cm^3) (501 twigs in total). We removed the pith, phloem, and bark from the branch after at least 3 days at 70°C, measured fresh volume with water displacement on the rest of the branch, and calculated dry mass (Cornwell et al., 2006). Branch density is strongly associated with core wood density for mature trees in TNNR by dividing the dry mass of the rest of the branch (excluding the pith, phloem, and bark) by its volume (Bu et al., 2014). The relative leaf water content (RLWC) was calculated as the following: water content (%) = fresh weight-dry weight divided by fresh weight multiplied by 100 (Jin et al., 2017). Each sample was measured in biological triplicate. Thus, the leaf thickness was calculated by a digital vernier caliper (Long et al., 2022; Yaseen et al., 2022).

Statistical analysis

Before the analysis, a principal component analysis (PCA) was used to explain the multivariate variations in soil variables and CWM functional traits of each species (Libalah et al., 2017), with data Box–Cox transformations (Box and Cox 1964). After that, to conduct mean standardized major axis analysis (Figure 1),

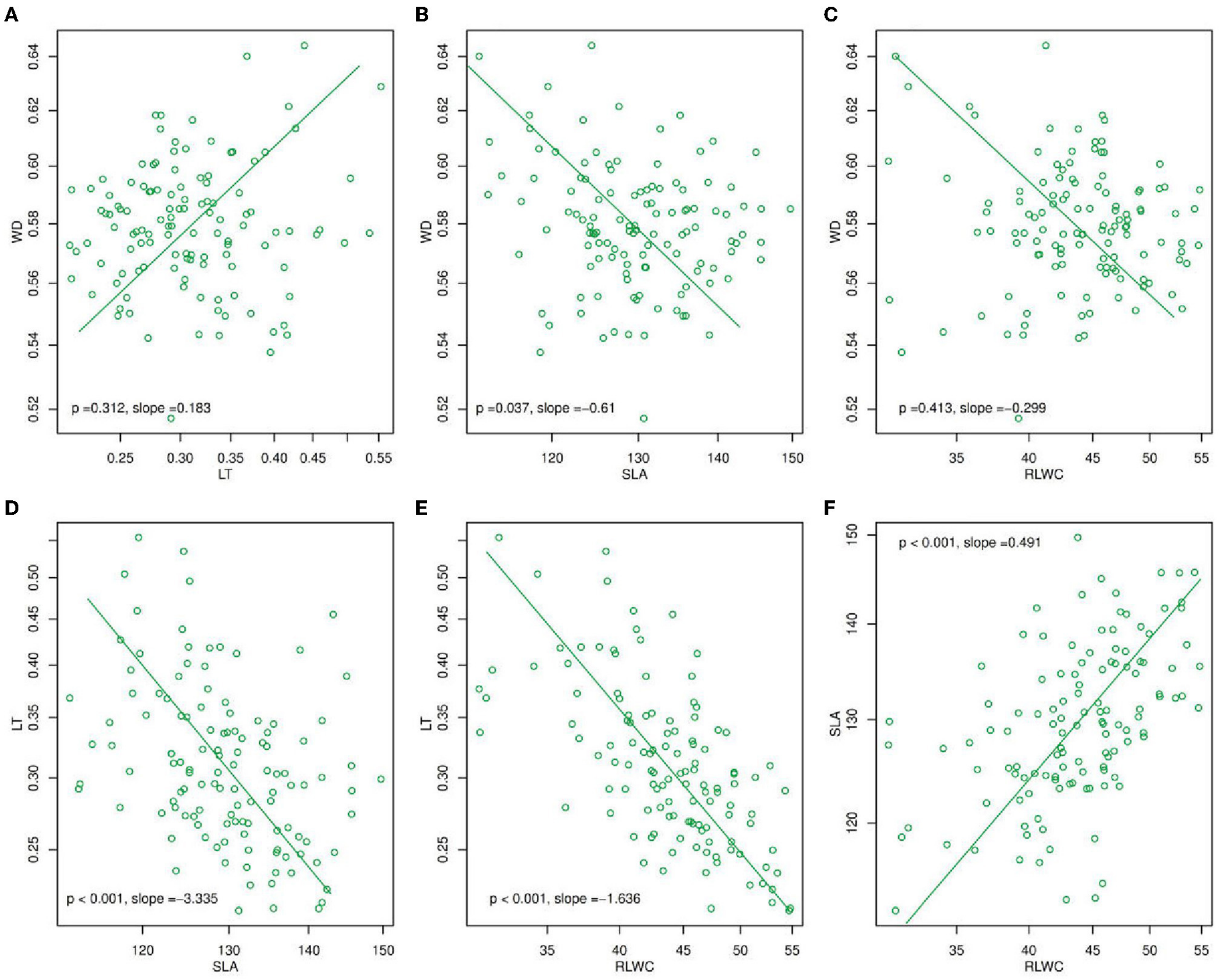

FIGURE 1
Mean standardized major axis (SMA) slopes for **(A)** WD and LT, **(B)** WD and SLA, **(C)** WD and RLWC, **(D)** LT and SLA, **(E)** LT and RLWC, and **(F)** SLA and RLWC. The slope values in **(A–F)** were calculated as the mean value for each trait pair across all species at the within-species level, and the *p*-value ($p \leq 0.05$) was derived from a Student's *t*-test which determines whether slopes differed significantly from zero. LT, leaf thickness; WD, wood density; SLA, specific leaf area; RLWC, relative leaf water content.

the scatter plots with trend lines were created using the *"smatr"* package while graphs were created using the plot function from the *"base"* package. For bar graph implementation to see the variation in CWM values of plant functional traits across dominant species (Figure 2), the "ggplot2" package was applied. For Pearson correlation analysis (Figure 3), the *"lm"* function is to build the model using the *"ggmisc"* package along with the *"ggplot2"* package for visualization. The R-value indicated Pearson correlation and a probability value lower than 0.05 indicated that there is a significant association between the variables. In addition, a biplot was created (Figure 4) to see the relationship between CWM plant functional traits and soil abiotic properties using *"factoextra"* package. Finally, to conduct path analysis graphical representation (Figure 5), the library *"lavann"*, *"semPlot"*, *"OpenMx"*, *"tidyverse"*, *"knitr"*, *"kableExtra"*, and *"GGally"* packages were used. All analyses were performed in R software 4.0.2 (R Core Development Team, 2016).

Regression and path analysis

A path analysis or non-causal effect model was developed to further understand the relationship between the plant functional traits and environmental variables patterns (Figure 5). This model was also used in previous studies to measure the relationships among plant leaf traits (Scheiner et al., 2000). Path analysis is a relationship model that reveals complicated interactions such as non-existent realistic ties, gradual loops, and self-feedback. A straight path is shown by the arrow to the other component (Aamir et al., 2021). Path analysis differs from multiple regression in that the former assumes a specific causal structure among the variables, whereas the latter assumes that all attributes directly affect fitness. A path diagram includes estimates of the strength of relationships called path coefficients (p). In the context of the other independent variables, a path coefficient is the standardized slope of the regression of the

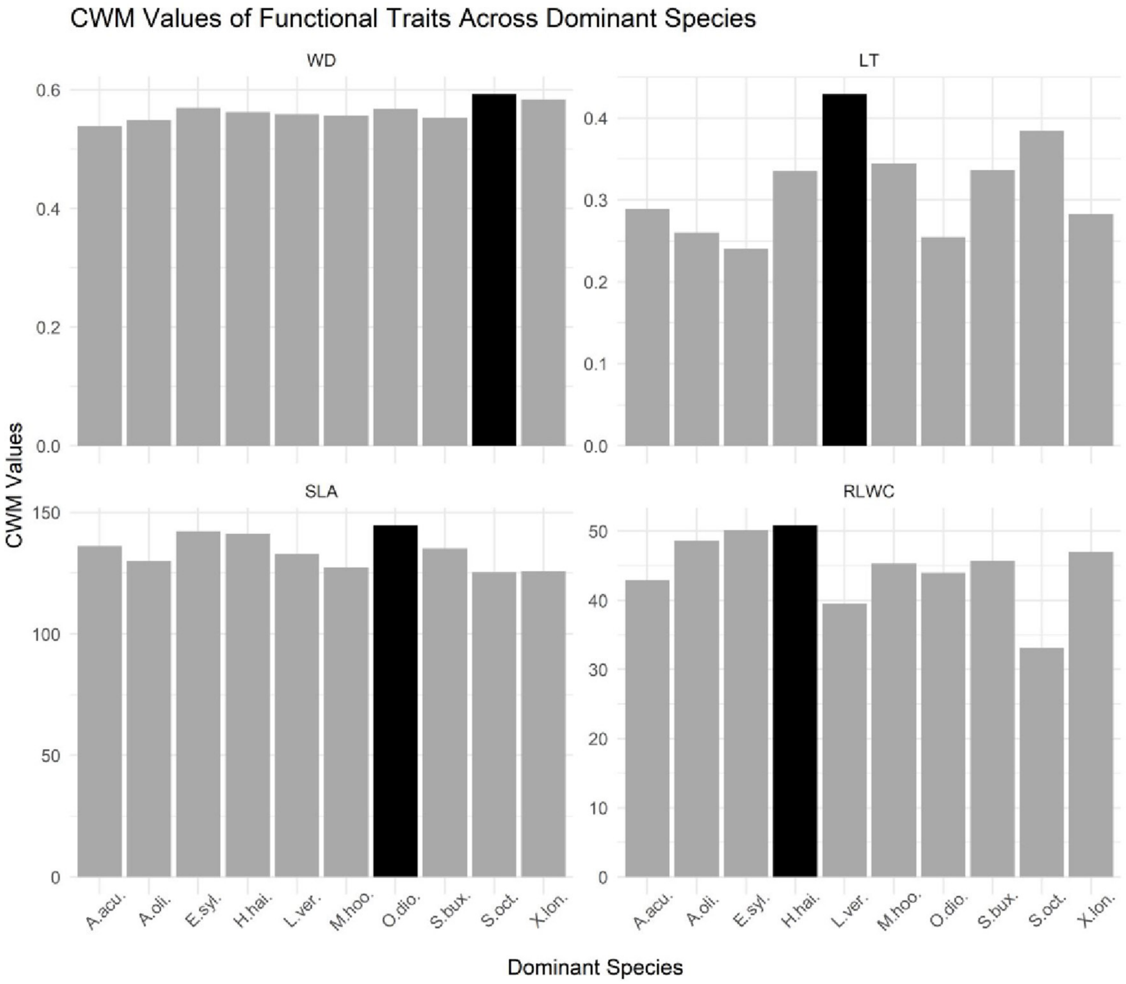

FIGURE 2

Bar graph of CWM values of functional traits across dominant species in a tropical evergreen monsoonal forest. LT, leaf thickness; WD, stem density; SLA, specific leaf area; RLWC, relative leaf water content. The black bar in each facet represents the maximum value for this variable across all dominant species, while the dark gray bars represent the values for a single species.

dependent variable on the independent variable (Scheiner et al., 2000).

A path analysis (Figure 5) was used to observe the direct or indirect effect between soil variables and CWM traits while regression analysis (Supplementary Table S1) was used to detect the interspecific relationships. These two methods are important to discuss the impact of soil properties on plant functional traits. This aim was to analyze the changes in CWM traits due to environmental variables in TNNR in the year 2020. In contrast, it also provides a reference and ideas that how CWM traits differ due to soil properties in tropical monsoonal forest. As well as it suggests many ways to improve the tropical vegetation community and its control measures.

Multiple linear regression was applied to determine the association between the plant functional traits and environmental variables. Before regression analysis, the values of plant functional traits for each species were used to calculate the CWM. To do this, we calculated a mean value for each trait at each site by multiplying the trait value of each species by its total abundance at each site. For each PFTs, the CWM was determined separately. The calculation was as follows:

$$\mathrm{CWM} = \sum\nolimits_{\mathrm{i=1}}^{\mathrm{n}} (\mathrm{xi}^{*}\mathrm{wi}) / \sum\nolimits_{\mathrm{i=1}}^{\mathrm{n}} \mathrm{wi}$$

Where n represents the total number of species and the relative abundance (density) of each species is represented by Wi, while the value of PFT in the *i*th species is denoted by Xi. Before being used to calculate the CWM, the PFTs data were log-transformed and then normalized according to the formula, Zi = $(Xi - X_{mean})/SD$, where Zi signifies the standardized value for a specific species *I;* Xi denotes the trait value of each individual of species attribute *i*; and the standard deviation of the value of each specie's feature is also referred to as SD. CWM trait values were calculated by using the *package "dplyr"* in *R v.3.0.2*.

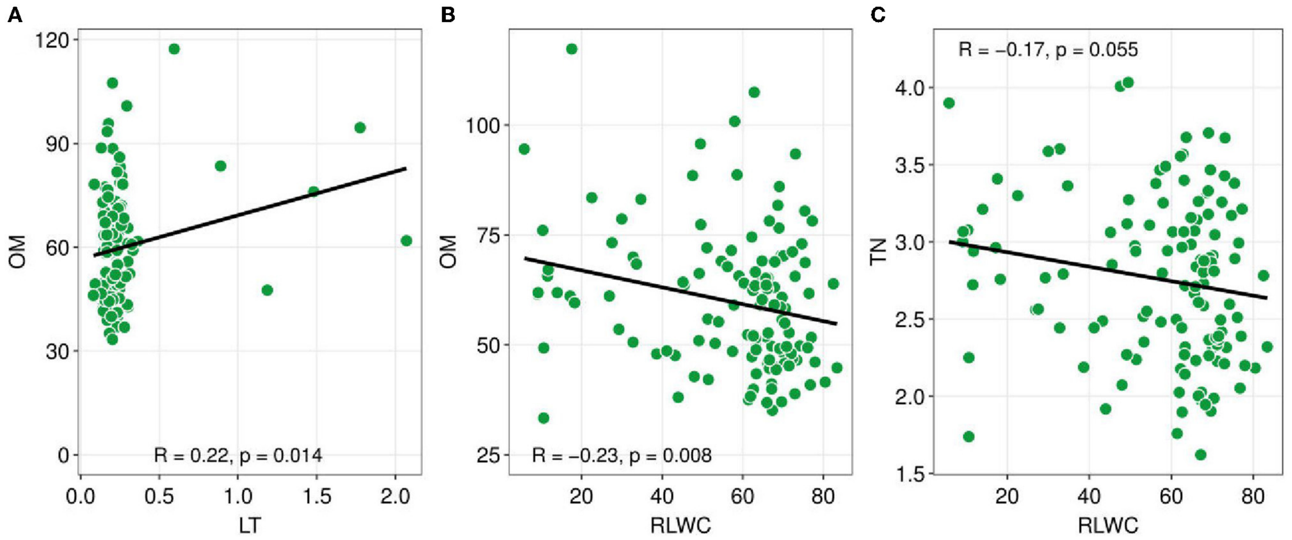

FIGURE 3
Pearson correlation coefficients between soil nutrients and plant functional traits. Soil nutrients such as TN (total nitrogen), OM (organic matter), versus plant functional traits e.g., LT (leaf thickness), and RLWC (relative leaf water content). Green dots show the sites. The black line is a trend line, and the grey-shaded area represents the SE (standard error). The R-value indicated Pearson correlation and a probability value lower than 0.05 indicates there is a significant association between the variables.

Results

Bivariate relationships among functional traits

Using a standardized major axis (SMA) (Figure 1), there were found many changes in plant functional traits e.g., LT, WD, SLA, and RLWC during the year of 2020. In these, WD and LT ($p = 0.312$, slope = 0.183, Figure 1A) were positively correlated while SLA and RLWC ($p < 0.001$, slope = 0.491, Figure 1F) had a significantly positive association. On the other hand, LT with SLA and RLWC ($p < 0.001$, slope = −3.335, Figure 1D; $p < 0.001$, slope = −1.66, Figure 1E) were significantly negatively correlated. But, WD with SLA and RLWC ($p = 0.037$, slope = −0.61, Figure 1B; $p = 0.413$, slope = −0.299, Figure 1C) were negatively correlated.

Variations in community-weighted mean values of functional traits across dominant species

A bar graph was used to compare the different CWMs traits across dominant species in the tropical evergreen forest (Figure 2). The purpose of the bar graph is to quickly convey relational information between traits and dominant species visually. Based on the bar chart and the accompanying data, it appears that the species *Olea dioica* has the highest value for the variable SLA, which represents a specific leaf area. This means that *Olea dioica* has relatively thin leaves compared to the other species in the dataset. In contrast, *Hydnocarpus hainanensis* has the highest value for the variable RLWC, which represents relative water content, indicating that it has a relatively high water content compared to the other species. Moreover, the species *Schefflera octophylla* has the highest value for the WD which signifies the wood density and the species *Litsea verticillata* has the highest value for the variable LT which signifies leaf thickness, indicating high leaf thickness than other species in the dataset. Furthermore, the black bar in each facet represents the maximum value for that variable across all the species, while the dark gray bars represent the values for the individual species. Hence, the dominant species were *Acronychia oligophlebia, Syzygium buxifolium, Elaeocarpus sylvestris, Acmena acuminatissima, Xantolis longispinosa, Olea dioica, Hydnocarpus hainanensis, Mallotus hookerianus, Schefflera octophylla,* and *Litsea verticillata* (Supplementary Table S2).

Dominant species based on their basal area

We conducted our study at the community and plot level in a vegetation community with the same type of topography and climatic condition, i.e., the inclination of gradient, parental substances, and aspects. Hence, the dominant species were *Acronychia oligophlebia, Syzygium buxifolium, Elaeocarpus sylvestris, Acmena acuminatissima, Xantolis longispinosa, Olea dioica, Hydnocarpus hainanensis, Mallotus hookerianus, Schefflera octophylla,* and *Litsea verticillata* (Supplementary Table S2).

Relationships between functional traits and soil conditions

The Pearson correlation analysis showed the changes in the CWM-PFTs and the soil abiotic properties (Figure 3). The CWM-LT has a significant positive relationship with soil OM (R = 0.22,

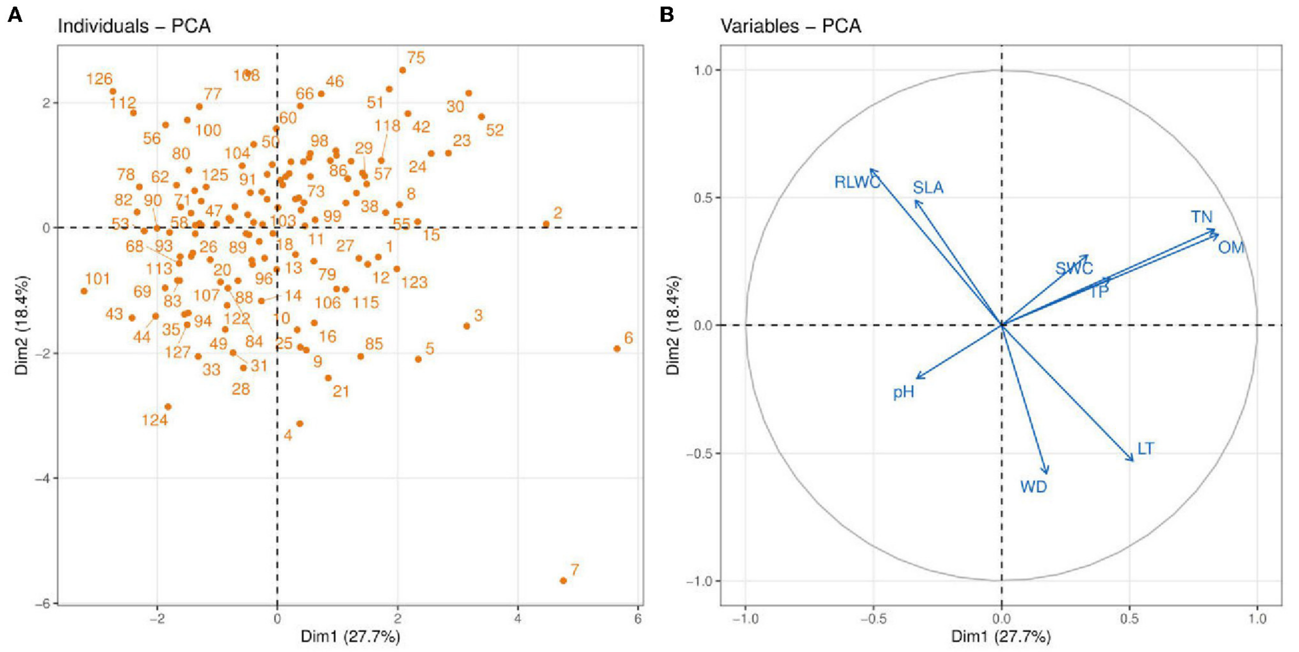

FIGURE 4
Principle component analysis (PCA) between soil abiotic properties such as soil pH; TN, total nitrogen; TP, total phosphorus; OM, organic matter; SWC, soil water content and plant functional traits e.g., LT, leaf thickness; WD, wood density; SLA, leaf-specific area; RLWC, relative leaf water content. Blue vectors show the soil abiotic properties and plant functional traits, and orange dots show the vegetation sites.

p = 0.014). On the other hand, CWM-RLWC had a negative significant association with OM and TN (R = −0.23, p = 0.008; R = −0.17, p = 0.055).

We performed PCA analysis of 4 plant functional traits and 5 soil properties to assess multivariate relationships and reveal the dimension of variation in traits and soil variables (Figure 4). In this figure, circular symbols were representing vegetation sites. The soil variables and functional traits of the plants are represented as vectors. The first PC accounts for a higher variance (27.7%) compared to the second PC (18.4%). The variables TN and OM have a strong positive association with PC2 while WD, SLA, and RLWC contributed more toward PC1. Among the soil variables, TN and OM showed a strong positive association indicating that with an increase in soil OM, there is an increase in soil TN. Soil OM and TN also have a strong positive association with CWM traits such as LT and WD. The increase in SWC is highly dependent on soil OM and SWC has a weak positive connection with TP. A similar association was also recorded between RLWC and SLA indicating an increase in plant SLA with an increase in RLWC. Another interesting aspect is that there is a strong negative association of soil pH with TP, TN, OM, and SWC while no or very slight influence on all of the plant functional traits.

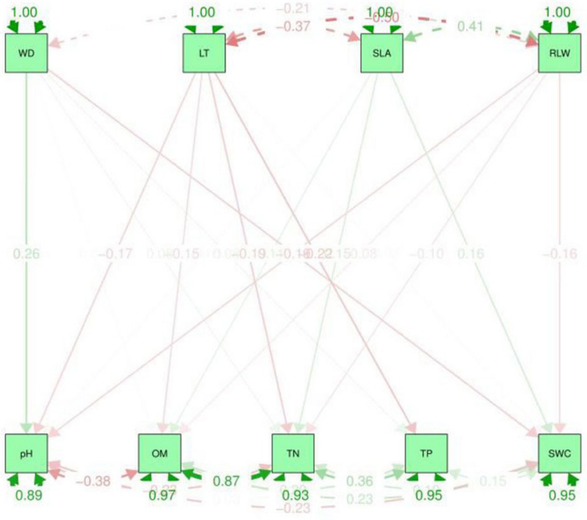

FIGURE 5
Path analysis graphical representation between soil properties and CWM traits. The upper dotted lines represent the indirect effect and the values in the graph are standard deviations. LT, leaf thickness; WD, wood density; SLA, specific leaf area; RLWC, relative leaf water content; TN, total nitrogen; TP, total phosphorus; OM, organic matter; SWC, soil water content.

Path analyses were used to find the direct and indirect relationship between CWM traits (dependent variables) and soil variables (independent variables). β is the correlation coefficient range from 0 to 1. The higher the value of beta, the stronger the association between the variables. It can be observed that the greater value of CWM plant functional traits e.g., SLA β coefficient, was 4.988 with the soil properties such as TN. Whereas, LT −0.00 and −0.013 with OM and TN have a lower value (Supplementary Table S1). The TN was positively correlated to CWM traits, i.e., SLA. On the other hand, based on the multiple R2 values, the soil pH was 0.120 and was positively significantly

TABLE 1 Mean and standard error values of environmental variables, as well as the minimum and maximum.

Soil variables	Mean ± SE	Min	Max
Soil variables and soil pH			
pH	4.85 ± 0.14	4.10	5.88
OM	**60.06 ± 7.19**	**33.35**	**117.33**
TN	2.76 ± 0.23	1.62	4.03
TP	0.3 ± 0.03	0.12	0.55
SWC	**49.64 ± 3.84**	**24.77**	**71.86**

The properties highlighted in bold show higher values. TN, total nitrogen; TP, total phosphorus; OM, organic matter; SWC, soil water content. Mean, SE, standard error; Min, Minimum; Max, Maximum.

TABLE 2 Relationship between soil properties and the two axes resulting from PCA.

Soil variables	PC1 (41.5%)	PC2 (25.6%)
pH	−0.176	−0.104
OM	**0.390**	−0.025
TN	**0.349**	−0.144
TP	0.045	−0.438
SWC	0.056	**0.172**

Values in bold indicate the higher values of soil variables. PCA, principal component analysis. TN, total nitrogen; TP, total phosphorus; OM, organic matter; SWC, soil water content.

correlated to CWM traits such as WD and SLA while TP has a lower value and is negatively correlated to LT and SLA (Supplementary Table S1). Therefore, the results from the path analysis showed a strong positive relationship between soil variables such as OM and cwm traits, i.e., RLWC as well as TN and SLA. Hence, soil variables such as OM and TN have a major impact on plant CWM traits, e.g., SLA and RLWC (Figure 5).

According to regression analysis, five soil properties changed significantly in the year 2020. Soil organic matter (OM) and soil water content (SWC) showed the highest values than that of soil pH, soil TN, and TP in the tropical evergreen monsoonal forest (Table 1).

The principal component analysis shows that soil OM (0.390) and TN (0.349) were strongly positively related to the first axis while negatively related to the second axis (−0.025 and −0.144). The SWC had a positive relationship on both axes (PC1 = 0.056, PC2 = 0.172). On the other hand, soil pH was negatively related on both axes (PC1 = −0.176, PC2 = −0.104). The soil TP was positively related to PC1 (0.045) and negatively related to PC2 (−0.438) (Table 2).

Table 2 shows the results of the eigenvectors of two components. These two components were selected to identify the most influencing variable. The variable which has a higher value contributes more to the variation.

Discussion

Our study quantifies to examine the dynamic patterns of soil variables and plant functional traits, as well as their relationship. According to assumptions, we observed the differences in soil nutrients and plant functional traits in tropical evergreen monsoonal forests.

Differences between plant functional traits in bivariate trait relationships

The relationships among CWM traits are useful for classifying functional tradeoffs and plant strategies, and they are often used in dynamic vegetation models to conclude one functional trait from another (Sakschewski et al., 2015). Rather than relying on average species or average PFT values, the next generation of dynamic vegetation models will use universal scaling relationships to reflect functional diversity within trait spectra (Fyllas et al., 2014). As a result, this common scaling relationship is relatively useful (Anderegg et al., 2018). Furthermore, Fyllas et al. (2020) showed the correlation between the PFTs in Mountainous Mediterranean Forests (MMF), LMA and LT, and LDMC and LMA, were significantly positively correlated while LT and LDMC were significantly negatively associated. A similar negative trend was found in LT and RLWC (Figure 1E) and a positive trend was found in RLWC and SLA (Figure 1F) in our study Moreover, SLA and LT had a significantly negative correlation (Figure 1D). The backbone of the leaf economics spectrum is leaf mass per unit area (LMA), which incorporates numerous features of leaf construction such as LDMC, tissue density, and LT (Garnier et al., 2001). Wood density is a well-researched stem feature (Zanne et al., 2010) because it is a simple way to quantify resource allocation to structural support. Moreover, it is proved that the correlation between functional traits such as LMA vs. WD was significantly positively related (Long et al., 2020). Nonetheless, we found contradictory results that SLA vs. WD had a significantly negative relationship (Figure 1B).

Some functional traits such as WD and SLA are globally considered to be fundamental functional traits that explain plant growth rates (Kunstler et al., 2016). A high WD is related to a slow potential growth rate, indicating a high level of competitive tolerance and a strong competitive effect. Whereas LT of plant species (Kunstler et al., 2016) is due to the limited resources of soil nutrients (Ordoñez et al., 2009). Generally, CWM traits to measure community dynamics and ecosystem attributes have been demonstrated (Garnier et al., 2007).

Variation in community-weighted mean values of plant functional traits across dominant species

Functional leaf traits like specific leaf area (SLA) and relative leaf water content (RLWC) have frequently been examined and they show directional changes during forest recovery. The occurrence of trait alterations in the process of succession has been well described. It was reported in recent studies that some traits are important in the dynamic of litter decomposability in the multiple regression analysis, such as LDMC, which did not change significantly during the forest recovery process (Eichenberg et al., 2015). Our observations demonstrated that SLA and RLWC were greater than WD and LT (Figure 2). Similarly, a previous study found that CWM for WD was not decreased on the windward side while it is slightly decreased on the leeward side (Marod et al., 2020). Most studies have used cover to estimate abundance and have focused on identifying CWM responses to environmental change, for instance, natural and anthropogenic disturbances (Lavorel et al., 2008). In contrast, of the four plant morphology traits, the CWMs were not significantly different (Figure 2).

According to recent studies, changes in dominant species composition are found in severely damaged and undamaged forests due to some environmental factors, for instance, light density, nutrient availability, and soil processes (Prach and Walker, 2011). Moreover, most of the studies proved that the most common or dominant species in forests in the primary successional stage have a higher SLA than species in forests in the climax successional stage (Chai et al., 2015). Xiao et al. (2018) found the highest value for the variable SLA for *Ardisia quinquegona*. Furthermore, high WD enhances the stiffness and strength of wood, thus protecting trees against biophysical hazards and enhancing plant survival (Van Gelder et al., 2006). Our results also clearly show the higher values of SLA for *Olia dioca* and WD for *Schefflera octophylla* (Figure 2). Leaf traits of the most dominant species should have the highest influence on ecosystem processes such as decomposition (Garnier et al., 2004).

The pattern of a few predominant species and many rarer species is a defining feature of communities on a large scale. These abundant species are commonly referred to as dominant species. At present, the phrase dominant species is poorly defined, and different authors use it to convey different information (Avolio et al., 2019).

In addition, the important value index (IVI) of the most common or dominant species was found (Supplementary Table S2) in recent studies, which proved that each species plays an important role in maintaining ecosystem equilibrium (Chala et al., 2016). During the year 2020, the important values (IV) were used to describe the most important species of vegetation sites. The decline in the dominant species altered and species with higher decline ratios were possibly removed for forest conservation in the following years. Furthermore, species with lower decline ratios have been suggested to conserve for longer periods (Lu et al., 2018). However, at the secondary stage of succession, these species may be creating enough space for the most prevalent species.

Association between community-weighted mean traits and soil conditions

It is demonstrated that in the tropical region, only two traits, for example, SLA and LT, describe soil properties strongly linked with the axis (Marod et al., 2020). Wood density (WD) and SLA are two functional traits that are thought to be important in understanding plant growth rates worldwide (Kunstler et al., 2016). According to Marod et al. (2020), the first PC (PC1) was strongly correlated with CWM-SLA, whereas the second axis of PCA contributed most to CWM-LDMC, CWM-WD, and CWM-LA. Moreover, they reported that only two CWM traits such as SLA and LT were significantly related to soil properties and the PC (Dim1) axis separated most of the CWM attributes and soil variables (Marod et al., 2020). Ordoñez et al. (2009) proved that it is a common strategy in linking community-level trait responses to the environment. A negative association was found in RDA (redundancy analysis) between CWM for SLA and LT (Marod et al., 2020; Figure 4). On the other hand, Chai et al. (2019) demonstrated that soil water content (SWC) was more contributed to the primary axis of CCA while soil pH contributed more to the second axis of CCA2. Zirbel et al. (2017) found that the first PC axis was positively related to soil organic matter (OM). Hence, our findings show that the first axes of PC most contributed to SWC and OM, whereas soil pH had little influence on both axes. However, Nielsen et al. (2019) described the soil's total phosphorus and total nitrogen as more contributed to secondary axes of PC. Our evidence also showed that TP and TN most contributed to the second axes (Figure 4). On the contrary, Chen et al. (2021) found that the primary axis of PCA was strongly positively related to soil nutrients, i.e., TN (Figure 4).

CWM attribute values are particularly useful for describing soil properties because CWMs of leaf attributes indicate nutrient cycling via decomposing plant material available for soil resources (Eichenberg et al., 2015). In general, CWM for SLA has historically been shown to be associated with nutrient cycling and dynamics (Garnier et al., 2004; Eichenberg et al., 2015). CWM for SLA is related to nutritional dynamics (Kleyer et al., 2012). The changes in LMA are controlled by various environmental factors and should be considered part of an integrated trait complex (Poorter et al., 2009, 2014). We found a negative association between soil TP and CWM for SLA (Figure 4). Furthermore, a significant positive connection was found between OM and LT (Figure 3A) and a significant negative relationship was found between RLWC and OM (Figure 3B). Hence, Marod et al. (2020) found a similar and dissimilar finding, a positive relationship between available phosphorus (AP) and CWM for SLA. Whereas, a negative relationship was found between leaf dry matter content (LDMC) and soil OM and found a positive relationship between available phosphorus (AP) and CWM for SLA.

Soil nutrients are one of the most important limiting variables for tropical forest structure and primary productivity, as well as for other biological processes such as plant root distribution, development, and litter formation (Zhang et al., 2015). Moreover, TMCF soil is characterized by low pH, which could lead to limited nutrient availability (Bruijnzeel and Veneklaas, 1998). Our results also show a low mean value of soil pH than that of OM and SWC (Table 1). The accumulation of soil OM, which stimulates the generation of organic acids, could be the reason for increasing soil acidity during forest community restoration (Roman et al., 2011). The SWC controls erosion, river discharge, and groundwater recharge by determining the separation of precipitation into surface runoff and infiltration. SWC is a major influence on plant development and crop quality at the field scale (McBratney et al., 2016) (Table 1). Furthermore, Libalah et al. (2017) found that the summary statistics of the soil and topography variables, such as soil TN, TP, OM, and moisture content, had positive values. Our findings also identified the almost same values of soil variables, e.g., TN, OM, and SWC (Table 1).

Two PCA axes were selected using Guttman's Kaiser criterion to summarize the most important gradients of the soil variables and to select the most important PCA axes that can be interpreted. Unlike other selection methods that rely on visual evaluation of PCA axes, this method calculates the mean of all eigenvalues and saves only those axes with eigenvalues greater than the mean, i.e., eigenvalues ≥ 1 for standardized PCA (Borcard et al., 2011). Zirbel et al. (2017) found that soil OM was positively correlated to the first axis of PCA. Our results support the above findings that soil OM was positively related to the primary axis of PCA; whereas, we also found controversial results that soil pH was negatively correlated to PC1 (Table 2). It is also described that soil P could be critical in defining plant community structure (Mason et al., 2012). Whereas, Hernández-Vargas et al. (2019) found the total P and total N contributed positively to the PC (Dim1) as compared to other minerals (Table 2). Conversely, Libalah et al. (2017) demonstrated that the same soil variables were positively correlated to the primary axis of PC while moisture content (MOC) was positively related to the second axes of PC. Our results also show that the soil TN, TP, and OM had a positive association with the primary axes while SWC was positively correlated to both axes (Table 2). Similarly, Trujillo et al. (2021) found a negative correlation between soil pH on the first axis of PCA. Meanwhile, our observations also showed a negative association of soil pH on primary axes (PC1) PCs (Table 2).

Conclusion

By using the data of the four most prevalent PFTs, five soil properties in TNNR were established for differences and relationships in important functional traits and environmental variables. We report a key set of morphological traits that are important for understanding the community assembly patterns in a tropical evergreen monsoonal forest. We found in interspecific correlation that soil OM and TN are strongly positively related to CWM-LT and CWM-WD. Furthermore, evidence showed that CWM-WD with CWM-LT and CWM-SLA with CWM-RLWC had a significant positive relationship. The overall inter- and intra-specific relationship in these forests suggests that they are mostly specialists in the local environment for limiting resources such as nutrients and moisture, and survival during wind disturbance may be more important than competition for resources at the regional scale. Moreover, this suggests that resource allocation patterns for these important functional traits, which describe important plant strategies, are driven by a combination of extreme conditions linked to solar radiation and soil nutrient content.

Suggestions and future prospects

Plant functional traits can be used to predict soil nutrients and ecosystem functioning in tropical secondary forests. The coexistence of species and community assembly can increase our knowledge of the tropical coastal secondary forests. This study will help to better understand the restoration of habitats and green infrastructure design, suggesting that selecting different species across multiple trait axes will ensure functionality at the maximum level. However, further studies are needed to explore the soil properties and their association with plant functional features and their role in ecosystem functioning.

Data availability statement

The original contributions presented in the study are included in the article/Supplementary material, further inquiries can be directed to the corresponding author.

Author contributions

MY, FK, and UA designed the methodology, contributed to conceptual development and critically to the drafts, abstract writing, introduction, research questions and hypothesis making, and analyzed the data. WRK, SB, FB, and MA helped in cross-checking the citations with references, and arranging the manuscript as per guidelines of the journal and gave final approval for publication. All authors contributed to the article and approved the submitted version.

Funding

This research was funded by the Universiti Putra Malaysia Kampus Bintulu Sarawak (63008).

Acknowledgments

We are obliged to our lab fellows for their generous cooperation and especially to Rana Ahmer Javaid (The Islamia University of Bahawalpur, Punjab, Pakistan) who supported us throughout this project.

Conflict of interest

The authors declare that the research was conducted in the absence of any commercial or financial relationships that could be construed as a potential conflict of interest.

Publisher's note

Supplementary material

The Supplementary Material for this article can be found online at: https://www.frontiersin.org/articles/10.3389/ffgc.2023.1198626/full#supplementary-material

References

Aamir, M., Li, Z., Bazai, S., Wagan, R. A., Bhatti, U. A., Nizamani, M. M., et al. (2021). Spatiotemporal change of air-quality patterns in Hubei Province—a pre- to post-COVID-19 analysis using path analysis and regression. *Atmosphere (Basel).* 12, 1338. doi: 10.3390/atmos12101338

Adler, P. B., Salguero-Gomez, R., Compagnoni, A., Hsu, J., Ray-Mjkherjee, J., Mbeau-Ache, C., et al. (2014). "Functional traits explain variation in plant life history strategies," in *Proceedings of the National Academy of Sciences of the United States of America.* doi: 10.1073/pnas.1315179111

Anderegg, L. D. L., Berner, L. T., Badgley, G., Sethi, M. L., Law, B. E., and HilleRisLambers, J. (2018). Within-species patterns challenge our understanding of the leaf economics spectrum. *Ecol. Lett.* 21, 734–744. doi: 10.1111/ele.12945

Anderson, J. M., and Ingram, J. S. I. (1989). *Tropical Soil Biology and Fertility: A Handbook of Methods.* Aberystwyth, UK: C.A.B. International 265. doi: 10.1097/00010694-199404000-00012

Atkin, O. K., Bloomfield, K. J., Reich, P. B., Tjoelker, M. G., Asner, G. P., Bonal, D., et al. (2015). Global variability in leaf respiration in relation to climate, plant functional types and leaf traits. *New Phytol.* 206, 614–636. doi: 10.1111/nph.13253

Auger, S., and Shipley, B. (2013). Inter-specific and intra-specific trait variation along short environmental gradients in an old-growth temperate forest. *J. Veget. Sci.* 24, 419–428. doi: 10.1111/j.1654-1103.2012.01473.x

Avolio, M. L., Forrestel, E. J., Chang, C. C., La Pierre, K. J., Burghardt, K. T., and Smith, M.D. (2019). Demystifying dominant species. *New Phytol.* 223, 1106–1126. doi: 10.1111/nph.15789

Borcard, D., Gillet, F., and Legendre, P. (2011). *Numerical Ecology with R.* New York: Springer. doi: 10.1007/978-1-4419-7976-6

Bruijnzeel, L. A., and Veneklaas, E. J. (1998). Climatic conditions and tropical montane forest productivity: The fog has not lifted yet. *Ecology* 79, 3–9. doi: 10.1890/0012-9658(1998)079[0003:CCATMF]2.0.CO;2

Bu, W., Zang, R., and Ding, Y. (2014). Field observed relationships between biodiversity and ecosystem functioning during secondary succession in a tropical lowland rainforest. *Acta Oecol.* 55, 1–7. doi: 10.1016/j.actao.2013.10.002

Chai, Y., Dang, H., Yue, M., Xu, J., Zhang, L., Quan, J., et al. (2019). The role of intraspecific trait variability and soil properties in community assembly during forest secondary succession. *Ecosphere* 10, e02940. doi: 10.1002/ecs2.2940

Chai, Y., Liu, X., Yue, M., Guo, J., Wang, M., Wan, P., et al. (2015). Leaf traits in dominant species from different secondary successional stages of deciduous forest on the Loess Plateau of northern China. *Appl. Veg. Sci.* 18, 50–63. doi: 10.1111/avsc.12123

Chala, D., Brochmann, C., Psomas, A., Ehrich, D., Gizaw, A., Masao, C. A., et al. (2016). Good-bye to tropical alpine plant giants under warmer climates? Loss of range and genetic diversity in Lobelia rhynchopetalum. *Ecol. Evol.* 6, 8931–8941. doi: 10.1002/ece3.2603

Chen, J., Qu, M., Zhang, J., Xie, E., Huang, B., and Zhao, Y. (2021). Soil fertility quality assessment based on geographically weighted principal component analysis (GWPCA) in large-scale areas. *CATENA* 201, 105197. doi: 10.1016/j.catena.2021.105197

Clark, C. M., and Tilman, D. (2008). Loss of plant species after chronic low-level nitrogen deposition to prairie grasslands. *Nature* 451, 712–715. doi: 10.1038/nature06503

Cornelissen, J. H. C., Lavorel, S., Garnier, E., Díaz, S., Buchmann, N., Gurvich, D. E., et al. (2003). A handbook of protocols for standardised and easy measurement of plant functional traits worldwide. *Aust. J. Bot.* 51, 335. doi: 10.1071/BT02124

Cornwell, W. K., Schwilk, D. W., and Ackerly, D. D. (2006). A trait-based test for habitat filtering: convex hull volume. *Ecology* 87, 1465–1471. doi: 10.1890/0012-9658(2006)87[1465:ATTFHF]2.0.CO;2

Costa, D. S., Gerschlauer, F., Kiese, R., Fischer, M., Kleyer, M., and Hemp, A. (2018). Plant niche breadths along environmental gradients and their relationship to plant functional traits. *Divers. Distrib.* 24, 1869–1882. doi: 10.1111/ddi.12815

Eichenberg, D., Trogisch, S., Huang, Y., He, J. S., and Bruelheide, H. (2015). Shifts in community leaf functional traits are related to litter decomposition along a secondary forest succession series in subtropical China. *J. Plant Ecol.* 8, 401–410. doi: 10.1093/jpe/rtu021

Funk, J. L., Larson, J. E., Ames, G. M., Butterfield, B. J., Cavender-Bares, J., Firn, J., et al. (2017). Revisiting the Holy Grail: Using plant functional traits to understand ecological processes. *Biol. Rev.* 92, 1156–1173. doi: 10.1111/brv.12275

Fyllas, N. M., Gloor, E., Mercado, L. M., Sitch, S., Quesada, C. A., Domingues, T. F., et al. (2014). Analysing Amazonian forest productivity using a new individual and trait-based model (TFS v.1). *Geosci. Model Dev.* 7, 1251–1269. doi: 10.5194/gmd-7-1251-2014

Fyllas, N. M., Michelaki, C., Galanidis, A., Evangelou, E., Zaragoza-Castells, J., Dimitrakopoulos, P. G., et al. (2020). Functional trait variation among and within species and plant functional types in mountainous mediterranean forests. *Front. Plant Sci.* 11, 212. doi: 10.3389/fpls.2020.00212

Garnier, E., Cortez, J., Billès, G., Navas, M. L., Roumet, C., Debussche, M., et al. (2004). Plant functional markers capture ecosystem properties during secondary succession. *Ecology* 85, 2630–2637. doi: 10.1890/03-0799

Garnier, E., Lavorel, S., Ansquer, P., Castro, H., Cruz, P., Dolezal, J., et al. (2007). Assessing the effects of land-use change on plant traits, communities and ecosystem functioning in grasslands: a standardized methodology and lessons from an application to 11 European Sites. *Ann. Bot.* 99, 967–985. doi: 10.1093/aob/mcl215

Garnier, E., Navas, M.-L., and Grigulis, K. (2016). *Plant Functional Diversity: Organism Traits, Community Structure, and Ecosystem Properties*. Oxford: Oxford University Press. doi: 10.1093/acprof:oso/9780198757368.001.0001

Garnier, E., Shipley, B., Roumet, C., and Laurent, G. (2001). A standardized protocol for the determination of specific leaf area and leaf dry matter content. *Funct. Ecol.* 15, 688–695. doi: 10.1046/j.0269-8463.2001.00563.x

Griffin-Nolan, R. J., Bushey, J. A., Carroll, C. J. W., Challis, A., Chieppa, J., Garbowski, M., et al. (2018). Trait selection and community weighting are key to understanding ecosystem responses to changing precipitation regimes. *Funct. Ecol.* 32, 1746–1756. doi: 10.1111/1365-2435.13135

Hernández-Vargas, G., Sánchez-Velásquez, L. R., López-Acosta, J. C., Noa-Carrazana, J. C., and Perroni, Y. (2019). Relationship between soil properties and leaf functional traits in early secondary succession of tropical montane cloud forest. *Ecol. Res.* 34, 213–224. doi: 10.1111/1440-1703.1267

Hodgson, J. G., Montserrat-Mart,i, G., Charles, M., Jones, G., Wilson, P., and Shipley, B., et al. (2011). Is leaf dry matter content a better predictor of soil fertility than specific leaf area? *Ann. Botany* 108, 1337–1345. doi: 10.1093/aob/mcr225

Jin, X., Shi, C., Yu, C. Y., Yamada, T., and Sacks, E. J. (2017). Determination of leaf water content by visible and near-infrared spectrometry and multivariate calibration in miscanthus. *Front. Plant Sci.* 8, 721. doi: 10.3389/fpls.2017.00721

Jobbagy, E. G., and Jackson, R. B. (2001). The distribution of soil nutrients with depth: Global patterns and the imprint of plants. *Biogeochemistry* 53, 51–77. doi: 10.1023/A:1010760720215

Kattge, J., Diaz, S., Lavorel, S., Prentice, I. C., Leadley, P., Bonisch, G., et al. (2011). TRY - a global database of plant traits. *Glob. Chang. Biol.* 17, 2905–2935. doi: 10.1111/j.1365-2486.2011.02451.x

Kleyer, M., Dray, S., Bello, F., Lep,š, J., Pakeman, R. J., Strauss, B., et al. (2012). Assessing species and community functional responses to environmental gradients: which multivariate methods? *J. Veg. Sci.* 23, 805–821. doi: 10.1111/j.1654-1103.2012.01402.x

Kunstler, G., Falster, D., Coomes, D. A., Hui, F., Kooyman, R. M., and Laughlin, D. C., et al. (2016). Plant functional traits have globally consistent effects on competition. *Nature* 529, 204–207. doi: 10.1038/nature16476

Laliberté, E., Grace, J. B., Huston, M. A., Lambers, H., Teste, F. P., Turner, B. L., et al. (2013). How does pedogenesis drive plant diversity? *Trends Ecol. Evol.* 28, 331–340. doi: 10.1016/j.tree.2013.02.008

Lambers, H., Ahmedi, I., Berkowitz, O., Dunne, C., and Finnegan, P. M., et al. (2013). Phosphorus nutrition of phosphorus-sensitive Australian native plants: threats to plant communities in a global biodiversity hotspot. *Conserv. Physiol.* 1, cot010. doi: 10.1093/conphys/cot010

Lambers, H., Raven, J. A., Shaver, G. R, and Smith, S. E. (2008). Plant nutrient-acquisition strategies change with soil age. *Trends Ecol. Evol.* 23, 95–103. doi: 10.1016/j.tree.2007.10.008

Lambers, H., Shane, M. W., Cramer, M. D., Pearse, S. J., and Veneklaas, E. J. (2006). Root structure and functioning for efficient acquisition of phosphorus: matching morphological and physiological traits. *Ann. Botany* 98, 693–713. doi: 10.1093/aob/mcl114

Langan, L., Higgins, S. I., and Scheiter, S. (2017). Climate-biomes, pedo-biomes or pyro-biomes: which world view explains the tropical forest-savanna boundary in South America? *J. Biogeogr.* 44, 2319–2330. doi: 10.1111/jbi.13018

Lavorel, S., Grigulis, K., McIntyre, S., Williams, N. S. G., Garden, D., Dorrough, J., et al. (2008). Assessing functional diversity in the field – methodology matters! *Funct. Ecol.* 22, 134–137. doi: 10.1111/j.1365-2435.2007.01339.x

Libalah, M. B., Droissart, V., Sonké, B., Hardy, O. J., Drouet, T., Pescador, D. S., et al. (2017). Couteron, P. Shift in functional traits along soil fertility gradient reflects non-random community assembly in a tropical African rainforest. *Plant Ecol. Evol.* 150, 265–278. doi: 10.5091/plecevo.2017.1318

Lira-Martins, D., Humphreys-Williams, E., Strekopytov, S., Ishida, F. Y., Quesada, C. A., and Lloyd, J. (2019). Tropical tree branch-leaf nutrient scaling relationships vary with sampling location. *Front. Plant Sci.* 10, 877. doi: 10.3389/fpls.2019.00877

Liu, Y., Li, S., Sun, X., and Yu, X. (2016). Variations of forest soil organic carbon and its influencing factors in east China. *Ann. For. Sci.* 73, 501–511. doi: 10.1007/s13595-016-0543-8

Lohbeck, M., Lebrija-Trejos, E., Martínez-Ramos, M., Meave, J. A., Poorter, L., and Bongers, F. (2015). Functional trait strategies of trees in dry and wet tropical forests are similar but differ in their consequences for succession. *PLoS ONE* 10. e0123741. doi: 10.1371/journal.pone.0123741

Long, C., Yang, X., Long, W., Li, D., Zhou, W., and Zhang, H. (2018). Soil nutrients influence plant community assembly in two tropical coastal secondary forests. *Trop. Conserv. Sci.* 11, 194008291881795. doi: 10.1177/1940082918817956

Long, W., Yang, X., and Li, D. (2012). Patterns of species diversity and soil nutrients along a chrono sequence of vegetation recovery in Hainan Island, South China. *Ecol. Res.* 27, 561–568. doi: 10.1007/s11284-011-0923-3

Long, W., Zang, R., Wang, X., and Bahadur, S. (2022). Environmental characteristics in tropical cloud forests. In *Tropical cloud forest ecology in Hainan Island* (Singapore: Springer Nature Singapore), (pp. 3–12).

Long, W., Zhou, Y., Schamp, B. S., Zang, R., Yang, X., Poorter, L., et al. (2020). Scaling relationships among functional traits are similar across individuals, species, and communities. *J. Veg. Sci.* 31, 571–580. doi: 10.1111/jvs.12893

Lu, X., Zang, R., Ding, Y., and Huang, J. (2018). Partitioning the functional variation of tree seedlings during secondary succession in a tropical lowland rainforest. *Ecosphere* 9, e02305. doi: 10.1002/ecs2.2305

Marod, D., Sungkaew, S., Mizunaga, H., and Thongsawi, J. (2020). Association of community-level traits with soil properties in a tropical coastal sand dune. *Environ. Nat. Resour. J.* 18, 101–109. doi: 10.32526/ennrj.18.1.2020.10

Mason, N. W. H., Richardson, S. J., Peltzer, D. A., de Bello, F., Wardle, D. A., et al. (2012). Changes in coexistence mechanisms along a long-term soil chronosequence revealed by functional trait diversity. *J. Ecol.* 100, 678–689. doi: 10.1111/j.1365-2745.2012.01965.x

McBratney, A., Minasny, B., Padarian Campusano, J., and Amelung, W. (2016). Modeling soil processes: review, key challenges, and new perspectives. *Soil Sci. Soc. Am.* 15, 131. doi: 10.2136/vzj2015.09.0131

Messier, J., Lechowicz, M. J., McGill, B. J., Violle, C., and Enquist, B. J. (2017). Interspecific integration of trait dimensions at local scales: the plant phenotype as an integrated network. *J. Ecol.* 105, 1775–1790. doi: 10.1111/1365-2745.12755

Messier, J., McGill, B. J., and Lechowicz, M. J. (2010). How do traits vary across ecological scales? A case for trait-based ecology. *Ecol. Lett.* 13, 838–848. doi: 10.1111/j.1461-0248.2010.01476.x

Nielsen, R. L., James, J. J., and Drenovsky, R. E. (2019). Functional traits explain variation in chaparral shrub sensitivity to altered water and nutrient availability. *Front. Plant Sci.* 10, 505. doi: 10.3389/fpls.2019.00505

Olde Venterink, H. (2011). Does phosphorus limitation promote species-rich plant communities? *Plant Soil* 345, 1–9. doi: 10.1007/s11104-011-0796-9

Ordoñez, J. C., van Bodegom, P. M., Witte, J. P. M., Wright, I. J., Reich, P. B., and Aerts, R. (2009). A global study of relationships between leaf traits, climate and soil measures of nutrient fertility. *Glob. Ecol. Biogeogr.* 18, 137–149. doi: 10.1111/j.1466-8238.2008.00441.x

Pan, F., Liang, Y., Wang, K., and Zhang, W. (2018). Responses of fine root functional traits to soil nutrient limitations in a karst ecosystem of southwest China. *Forests* 9, 743. doi: 10.3390/f9120743

Pérez-Harguindeguy, N., Díaz, S., Garnier, E., Lavorel, S., Poorter, H., Jaureguiberry, P., et al. (2016). Corrigendum to: New handbook for standardized measurement of plant functional traits worldwide. *Aust. J. Bot.* 64, 715. doi: 10.1071/BT12225_CO

Poorter, H., Lambers, H., and Evans, J.R. (2014). Trait correlation networks: a whole-plant perspective on the recently criticized leaf economic spectrum. *New Phytol.* 201, 378–382. doi: 10.1111/nph.12547

Poorter, H., Niinemets, Ü., Poorter, L., Wright, I. J., and Villar, R. (2009). Causes and consequences of variation in leaf mass per area (LMA): a meta-analysis. *New Phytol.* 182, 565–588. doi: 10.1111/j.1469-8137.2009.02830.x

Prach, K., and Walker, L. R. (2011). Four opportunities for studies of ecological succession. *Trends Ecol. Evol.* 26, 119–123. doi: 10.1016/j.tree.2010.12.007

R Core Development Team (2016). *A Language and Environment for Statistical Computing.* Vienna, Austria: R Foundation for Statistical Computing. Available online at: www.R-project.org/ (accessed June 16, 2023).

Raevel, V., Violle, C., and Munoz, F. (2012). Mechanisms of ecological succession: insights from plant funcional strategies. *Oikos* 121, 1761–1770. doi: 10.1111/j.1600-0706.2012.20261.x

Reich, P. B. (2014). The world-wide 'fast-slow' plant economics spectrum: a traits manifesto. *J. Ecol.* 102, 275–301. doi: 10.1111/1365-2745.12211

Reich, P. B., Wright, I. J., Cavender-Bares, J., Craine, J. M., Oleksyn, J., Westoby, M., et al. (2003). The evolution of plant functional variation: traits, spectra, and strategies. *Int. J. Plant Sci.* 164, S143–S164. doi: 10.1086/374368

Roman, L., Scatena, F. N., and Bruijnzeel, L. A., Scatena, F. N., and Hamilton, L. S. (2011). "Global and local variations in tropical montane cloud forest soils," in *Tropical montane cloud forest,* eds. L. S., Hamilton, J. O., Juvik, and F. N. Scatena (Cambridge: Cambridge University Press) 77–89. doi: 10.1017/CBO9780511778384.008

Sakschewski, B., von Bloh, W., Boit, A., Rammig, A., Kattge, J., Poorter, L., et al. (2015). Leaf and stem economics spectra drive diversity of functional plant traits in a dynamic global vegetation model. *Glob. Chang. Biol.* 21, 2711–2725. doi: 10.1111/gcb.12870

Scheiner, S. M., Mitchell, R. J., and Callahan, H. S. (2000). Using path analysis to measure natural selection. *J. Evol. Biol.* 13, 423–433. doi: 10.1046/j.1420-9101.2000.00191.x

Si tu, S. J. (1987). *Study on the Historical Land Exploitation of Hainan Island*. Haikou: Hainan Press.

Siefert, A. (2014). *Intraspecific trait variation and community assembly in Oldfield grasslands*. PhD Thesis, Syracuse University, Syracuse, NY.

Siefert, A., Violle, C., Chalmandrier, L., Albert, C. H., Taudiere, A., Fajardo, A., et al. (2015). A global meta-analysis of the relative extent of intraspecific trait variation in plant communities. *Ecol. Lett.* 18, 1406–1419. doi: 10.1111/ele.12508

Spence, J. R., Langor, D. W., Jacobs, J. M., Work, T. T., and Volney, W. J. A. (2008). Conservation of forest-dwelling arthropod species: simultaneous management of many small and heterogeneous risks. *Can. Entomol.* 140, 510–525. doi: 10.4039/n07-LS05

Trujillo, W., Rivera-Rondón, C. A., and Balslev, H. (2021). Palm functional traits, soil fertility and hydrology relationships in western amazonia. *Front. For. Glob. Chang.* 4, 723553. doi: 10.3389/ffgc.2021.723553

Turnbull, M. H., Griffin, K. L., Fyllas, N. M., Lloyd, J., Meir, P., and Atkin, O. K. (2016). Separating species and environmental determinants of leaf functional traits in temperate rainforest plants along a soil development chrono sequence. *Funct. Plant Biol.* 43, 751–765. doi: 10.1071/FP16035

Van Gelder, H. A., Poorter, L., and Sterck, F. J. (2006). Wood mechanics, allometry, and life-history variation in a tropical rain forest tree community. *New Phytol.* 171, 367–378. doi: 10.1111/j.1469-8137.2006.01757.x

van Ommen Kloeke, A. E. E., Douma, J. C., Ordonez, J. C., Reich, P. B., and Van Bodegom, P. M. (2012). Global quantification of contrasting leaf life span strategies for deciduous and evergreen species in response to environmental conditions. *Global Ecol. Biogeogr.* 21, 224–235. doi: 10.1111/j.1466-8238.2011.00667.x

Vendramini, F., Diaz, S., Gurvich, D. E., et al. (2002). Leaf traits as indicators of resource-use strategy in floras with succulent species. *New Phytol.* 154, 147–157. doi: 10.1046/j.1469-8137.2002.00357.x

Verheijen, L. M., Brovkin, V., Aerts, R., Bönisch, G., Cornelissen, J. H. C., Kattge, J., et al. (2013). Impacts of trait variation through observed trait–climate relationships on performance of an Earth system model: a conceptual analysis. *Biogeosciences* 10, 5497–5515. doi: 10.5194/bg-10-5497-2013

Vitousek, P., and Sanford, R. L. (1986). Nutrient cycling in moist tropical forest. *Ann. Rev. Ecol. System.* 17, 137–167. doi: 10.1146/annurev.es.17.110186.001033

Wardle, D. A. (2016). Do experiments exploring plant diversity-ecosystem functioning relationships inform how biodiversity loss impacts natural ecosystems? *J. Veg. Sci.* 27, 646–653. doi: 10.1111/jvs.12399

Weiher, E., Werf, A., Thompson, K., Roderick, M., Garnier, E., and Eriksson, O. (1999). Challenging Theophrastus: A common core list of plant traits for functional ecology. *J. Veg. Sci.* 10, 609–620. doi: 10.2307/3237076

Westoby, M., Falster, D. S., Moles, A. T., Vesk, P. A., and Wright, I. J. (2002). Plant ecological strategies: some leading dimensions of variation between species. *Annu. Rev. Ecol. Syst.* 33, 125–159. doi: 10.1146/annurev.ecolsys.33.010802.150452

Wright, I. J., Reich, P. B., Cornelissen, J. H. C., Falster, D. S., Groom, P. K., Hikosaka, K., et al. (2005). Modulation of leaf economic traits and trait relationships by climate. *Glob. Ecol. Biogeogr.* 14, 411–421. doi: 10.1111/j.1466-822x.2005.00172.x

Wright, I. J., Reich, P. B., Westoby, M., Ackerly, D. D., Baruch, Z., Bongers, F., et al. (2004). The worldwide leaf economics spectrum. *Nature* 428, 821–827. doi: 10.1038/nature02403

Wu, Z. Y. (1995). *Vegetation in China*. Beijing, China: Science Press.

Xiao, Y., Liu, S., Tong, F., Chen, B., and Kuang, Y. (2018). Dominant species in subtropical forests could decrease photosynthetic n allocation to carboxylation and bioenergetics and enhance leaf construction costs during forest succession. *Front. Plant Sci.* 9, 117. doi: 10.3389/fpls.2018.00117

Yaseen, M., Long, W., Khalid, F., Bahadur, S., and Noushahi, H. A. (2022). Shifts in community vegetative organs and their dissimilar trade-off patterns in a tropical coastal secondary forest, Hainan Island, Southern China. *Diversity*, 14, 823.

Zanne, A. E., Westoby, M., Falster, D. S., Ackerly, D. D., and Loarie, S. R., et al. (2010). Angiosperm wood structure: global patterns in vessel anatomy and their relation to wood density and potential conductivity. *Am. J. Botany* 97, 207–215. doi: 10.3732/ajb.0900178

Zhang, W., Zhao, J., Pan, F., Li, D., Chen, H., and Wang, K. (2015). Changes in nitrogen and phosphorus limitation during secondary succession in a karst region in southwest China. *Plant Soil* 391, 77–91. doi: 10.1007/s11104-015-2406-8

Zirbel, C. R., Bassett, T., Grman, E., and Brudvig., L. A. (2017). Plant functional traits and environmental conditions shape community assembly and ecosystem functioning during restoration. *J. Appl. Ecol.* 54, 1070–1079. doi: 10.1111/1365-2664.12885

frontiers | Frontiers in Forests and Global Change

TYPE Original Research
PUBLISHED 04 August 2023
DOI 10.3389/ffgc.2023.1193792

OPEN ACCESS

EDITED BY
Mehebub Sahana,
The University of Manchester, United Kingdom

REVIEWED BY
Amit Kumar,
Nanjing University of Information Science and Technology, China
Pravin Rawat,
ICFRE-Himalayan Forest Research Institute, Shimla, India
Shashi Sekhar,
Banaras Hindu University, India

*CORRESPONDENCE
Vinod Prasad Khanduri
✉ khandurivp@yahoo.com
Deepa Rawat
✉ rawatdeepa291@gmail.com
Bhupendra Singh
✉ butola_bs@yahoo.co.in

RECEIVED 25 March 2023
ACCEPTED 14 July 2023
PUBLISHED 04 August 2023

CITATION
Tiwari A, Khanduri VP, Rawat D, Singh B, Riyal MK, Mishra G and Kumar M (2023) Vegetation composition, soil properties, and carbon stock of montane forests along a disturbance in the Garhwal Himalaya, India. *Front. For. Glob. Change* 6:1193792.
doi: 10.3389/ffgc.2023.1193792

Vegetation composition, soil properties, and carbon stock of montane forests along a disturbance in the Garhwal Himalaya, India

Avadhesh Tiwari[1], Vinod Prasad Khanduri[1]*, Deepa Rawat[1]*, Bhupendra Singh[1]*, Manoj Kumar Riyal[1], Gaurav Mishra[2] and Munesh Kumar[3]

[1]College of Forestry, VCSG Uttarakhand University of Horticulture and Forestry, Ranichauri, New Tehri, Uttarakhand, India, [2]Centre of Excellence on Sustainable Land Management, Indian Council of Forestry Research and Education, Dehradun, Uttarakhand, India, [3]Department of Forestry and Natural Resources, HNB Garhwal University, Srinagar, Uttarakhand, India

The management of forests is essential for the conservation of biodiversity and climate change. Studies on the variation in forest tree diversity and carbon sequestration by the forests along altitudinal gradients are limited for most parts of the Garhwal Himalaya. The present study was carried out in montane forests in a part of district Tehri of the Garhwal Himalaya, India at four different sites between altitudinal ranges of 850 to 2,200 masl (i.e., 850–1,500 masl under sub-tropical region and 1,800–2,200 masl under temperate region) for vegetation, soil, and carbon stock analysis using different parameters including the existing pressure on the sites for fuel, fodder, timber, grazing, and browsing. All the standard methods were used for vegetation and soil analysis. The highest value of tree diversity (H = 0.48) and concentration of dominance (CD = 0.95) was recorded at 850–1,100 masl altitude under sub-tropical forests. The aboveground biomass density (AGBD) and belowground biomass density (BGBD) ranged from 271 to 703.20 and 83.21 to 163.92 Mg ha^{-1}, respectively. The pH value ranged from 5.63 to 6.86 (0–15 cm) and 6.17 to 7.21 (15–30 cm). Similarly, soil organic carbon (SOC) was reported to range from 1.86 to 2.57% and 1.78 to 2.44% at 0–15 cm and 15–30 cm depths, respectively. Available nitrogen (N) under temperate forests was reported to be significantly higher than at other altitudes. Among the studied parameters, a significant positive correlation was reported between the pH of the soil and the Shannon–Wiener and Margalef diversity indices. The study revealed that the sub-tropical region was more diversified in terms of tree species whereas soil properties were reported to be better in the temperate region. Among the species in the study region, *Pinus roxburghii*, *Boswellia serrata*, *Quercus leucotrichophora*, and *Cedrus deodara* have shown good potential for carbon storage. Thus, based on the dominant and associated species present in the area, forest management activities may be followed for the survival and regeneration of species with the potential of being the next dominant species in the future.

KEYWORDS

montane sub-tropical, montane temperate, carbon stock, tree diversity, SOC range, Garhwal Himalayas

Introduction

The Garhwal Himalaya is a hot spot of biodiversity, located in the western part of Central Himalaya. Forests in the Himalayas have been under various kinds of pressure in the past decades because of changes in socioeconomic status, exponential population growth, and infrastructure development (Singh et al., 2009). The variation in physiography, soil types, and climatic conditions in the Garhwal Himalaya has changed the community structure and its dynamics which has attracted researchers to conduct comprehensive studies in tropical and sub-tropical montane forests to study species richness, biomass, and productivity (Tripathi and Khongjee, 2010). In Uttarakhand, *Quercus leucotrichophora* forest covers 5.24% of the area (i.e., 1,284 km^2) from 1,000 to 2,500 masl, whereas, between 1,000 and 1,500 m, patches with other forests are observed (Singh et al., 2016). The pine-oak forest is believed to be between 1,500 and 1,800 m in altitude, whereas, *Pinus roxburghii* is widespread from 900 to 1,500 m in altitude (Chaturvedi and Singh, 1987), and sometimes reaches the higher elevations. However, recent alterations as a consequence of climatic and anthropogenic disturbances have also resulted in huge canopy gaps and interference in forest soils. The change in forest species composition is usually expected to affect the properties of soil because soil and vegetation have a complex interrelation. Similarly, the changes also influence carbon accumulation in the forest. Further, soil properties and soil fertility differ significantly based on the tree species grown in it (Augusto et al., 2002).

The disturbance processes in the ecosystems usually increase greenhouse gas emissions (GHGs) and affect the atmospheric gas concentration (Kumar et al., 2019, 2021b). The level of greenhouse gas emissions, especially from rapid anthropogenic disturbances, leads to further disturbances in the carbon cycle (Anderegg et al., 2015; Waltham et al., 2020; Kumar et al., 2021b; Rawat et al., 2021). In the central part of India, disturbances associated with mining have augmented the fragmentation of natural forests and a reduction in the density and diversity of vegetation has been documented. This loss of biomass has reportedly resulted in a net loss of 1.08 Tg C in the past two decades (Mishra et al., 2022). Dong et al. (2022) reported the changes in soil carbon decomposition due to the priming effect caused by an accumulation of more plant-derived substrate on the surface soil as being affected by climate change.

In the western Himalayas, the trees in temperate forests are *P. roxburghii, Quercus* spp. *Rhododendron arboreum*, *Lyonia ovalifolia*, *Myrica esculenta*, *Cedrus deodara*, and *Pinus wallichiana* (Luna, 2005) and are used for quality fodder, fuel, charcoal making, and agricultural implements apart from providing other ecosystem services (Rawat D. et al., 2022). But owing to the increasing human interferences in forests and rapid urbanization in the nascent Himalayan region, the extent of deforestation, loss of biodiversity, and forest degradation is growing rapidly along with crucial alterations in land use patterns. These changes in the terrestrial landscapes are also affecting the tree composition and nutrient dynamics of the system (Mishra et al., 2017a; Kumar et al., 2021c; Rawat S. et al., 2022; Tariyal et al., 2022; Sharma et al., 2023).

Usually, 43–50% of the dry biomass of trees consists of carbon (Malhi et al., 2002; Negi et al., 2003; Rawat S. et al., 2022) and soil carbon plays an important role in the global carbon cycle (Gupta and Sharma, 2011). Also, biogeochemical nutrient cycling is important for the quality of a site. However, the vegetation of the area influences the physicochemical characteristics of soil and these soil characteristics change due to various biotic and abiotic factors. The stoichiometric ratios of nutrients such as carbon, nitrogen, and phosphorus within a forest ecosystem can alter the status of soil nutrients and the future sink of carbon (Kumar et al., 2021a). Further, forest soils impact forest composition, growth rate, regeneration, etc (Sheikh and Kumar, 2010; Rawat S. et al., 2022). Altitude plays an important role in that it changes both climatic and site conditions and has a significant influence on the plant communities (Kharkwal et al., 2005; Gauthier et al., 2011). Moreover, altitude plays an important role in species distribution which also sustains other associated flora and fauna. Various studies on tree diversity and carbon stocks (Gairola et al., 2011a; Sharma et al., 2011), the physical properties of the soil (Sharma et al., 2010a), and the structure and composition of forests (Gairola et al., 2011b) have also been carried out previously. Verma and Garkoti (2019) studied the species composition, soil properties, and carbon stock of the regenerated *Q. leucotrichophora* forests in the Kumaon region of the Himalaya. Meena et al. (2021) documented the significant influence of the topographical position factor on the concentration of soil organic carbon and carbon management value in the Indian Himalayan ecosystem. However, the investigations that bring together the cumulative information about vegetation composition, tree diversity, soil properties, and carbon density of forests of Garhwal Himalaya are meager. Therefore, this study was conducted with the following objectives: (i) to understand how vegetation composition, structure, and carbon storage are influenced by altitude, (ii) to understand the variation in physicochemical characteristics of soil among different forests and altitudes, and (iii) to assess the influence of various anthropogenic disturbances on vegetation patterns at different altitudes.

TABLE 1 Geographical description of the study area.

Region/forest type	Location	Altitude (masl)	Latitude (N)	Longitude (E)
Sub-tropical 9/C 1B upper or Himalayan chir pine	Khadi	850–1,100	30°15′0″–30°16′34″N	78°23′35″–78°22′13″E
	Gaja	1,300–1,500	30°14′48″–30°15′51″N	78°23′49″–78°24′51″E
Temperate (12/C 1C moist Deodar forest)	Kanatal	1,800–2,000	30°23′32″–30°24′59″N	78°21′26″–78°22′50″E
	Dhanolti	2,000–2,200	30°24′37″–30°26′32″N	78°20′32″–78°26′13″E

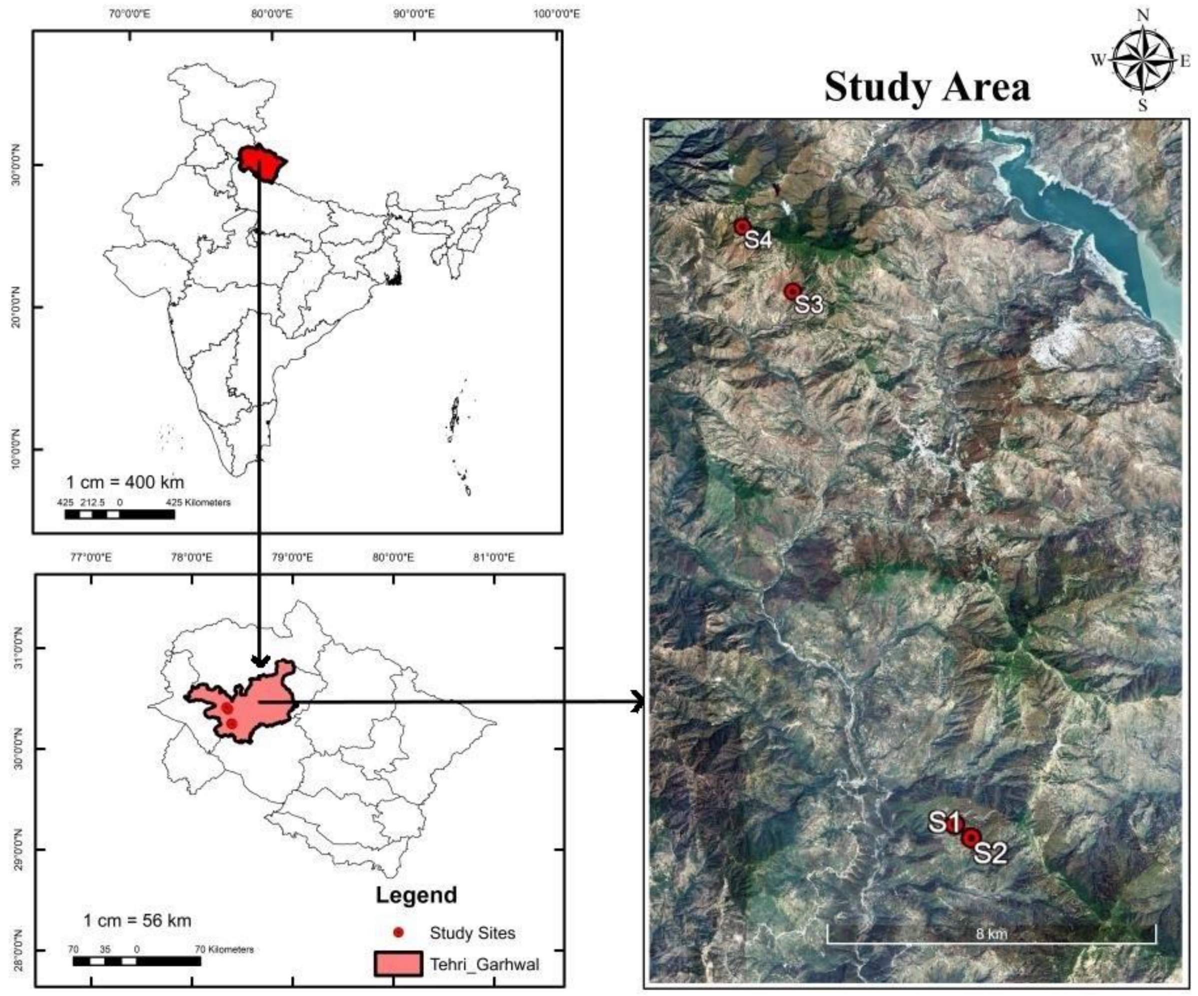

FIGURE 1
Map of the study area. S1 = Khadi, S2 = Gaja, S3 = Kanatal, S4 = Dhanolti.

Materials and methods

This study was conducted in the district of Tehri in the Garhwal Himalaya. Four different sites at different altitudinal ranges were selected for the study (Table 1). The vegetation of the area and soil properties were studied at two sites of sub-tropical montane forests, i.e., Khadi (850–1,100 masl) and Gaja (1,300–1,500 masl), as well as two sites of temperate montane forests, i.e., Kanatal (1,800–2,000 masl) and Dhanolti (2,000–2,200 masl) (Figure 1). The climate of the study area falls under sub-tropical to temperate regions. The soil of the region is developed from granite-ferrous biotite, granite, gneiss, and phyllites. Usually, the soil color in this region ranges from brown to dark grayish and the soils are slightly acidic in reaction. The texture of the soil at Khadi was sandy loam, at Gaja, sandy clay loam, and at Kanatal and Dhanolti, it was loam.

Vegetation analysis

For vegetation analysis, a total of 50 quadrats (10 m^2 × 10 m^2 size) were laid out randomly in each forest site to study the structure, composition, and biomass carbon. The study area plants were identified by their local names and unidentified species specimens were brought to the laboratory and identified with the help of the Flora of District Garhwal, North West Himalaya (Gaur, 1999). The vegetation data were analyzed for density, frequency, and abundance (Curtis and McIntosh, 1950) and the importance value index (IVI) of species was calculated using the method of Phillips (1959). The Simpson's index (Cd-concentration of dominance) calculated by Simpson (1949), Shannon–Wiener index (h) calculated by Shannon and Weaver (1963), and Margalef's index (Margalef, 1968) were assessed using standard methods and the following formulae;

$$D = \sum_{i=0}^{n} (Pi)1 \qquad (1)$$

$$H' = -\sum_{i=0}^{n} Pi_{I_n} Pi \qquad (2)$$

$$D_{mg} = (S - 1)/I_n N \qquad (3)$$

Where D is the Simpson's index of dominance, P_i is the proportion of importance value of the ith species. P_i is the proportion of importance value of the ith species. P_i was calculated by dividing the importance value index (IVI) of the ith species (n_i) by the IVI of all the species. H′ is the Shannon–Weiner index of diversity. The D_{mg} is Margalef's index of richness, S is the total number of species, and N is the total number of individuals.

The impact of various anthropogenic pressure on forests and further on local people were assessed, i.e., fuel, fodder, timber, fruit, grazing, browsing, etc. This information was collected from the villagers during the field survey and based on other available information about the study area.

General volume equations were used to estimate standing tree volume for each species (FSI, 1996). Growing stock density (GSD) was estimated for an individual tree within a sample plot. The total volume was multiplied by the digit 100 for converting the growing stock volume density (GSVD) into $m^3\ ha^{-1}$.

$$GSVD = \Sigma\ Volume$$

Some of the species with no volume equations were calculated based on the volume tables/equations of similar species representing similar height, form, taper, and growth rate. Further, the calculated GSVD was converted into aboveground biomass density (AGBD), which was calculated by multiplying it with the appropriate biomass expansion factor (BEF) (Brown and Schroeder, 1999). The BEFs for hardwood, spruce-fir, and pine were estimated by using the following equations:

> Hardwood: BEF = exp [1.91–0.34 × In (GSVD)] for GSVD $\leq$ 200 $m^3\ ha^{-1}$, BEF = 1.0 for GSVD > 200 $m^3\ ha^{-1}$;
> Spruce-fir: BEF = exp [1.77–0.34 × In (GSVD)] for GSVD $\leq$ 160 $m^3\ ha^{-1}$, BEF = 1.0 for GSVD 160 $m^3\ ha^{-1}$;
> Pine: BEF = 1.68 Mg m for GSVD < 10 $m^3\ ha^{-1}$. BEF = 0.95 for GSVD = 10–100 $m^3\ ha^{-1}$. BEF = 0.81 (for GSVD > 10 $m^3\ ha^{-1}$).

The equation of spruce-fir was used for other conifer species by using the regression equation (Brown and Schroeder, 1999). Using the regression equation (Cairns et al., 1997), the belowground biomass density (BGBD; fine and coarse roots) was also estimated for each forest type using the following equation:

$$BGBD = exp\{-1.059 + 0.884 \times In(AGBD) + 0.284\}$$

Total biomass density (TBD) was calculated by adding the AGBD and BGBD. For estimating the total carbon density (TCD), the total biomass values were converted to carbon stock (C) by using a default value of 0.50 C fractions (IPCC, 2003).

Soil sampling and analysis

For the determination of soil properties, samples were collected from two different depths i.e., 0–15 cm and 15–30 cm from ten quadrats (10 m^2 × 10 m^2 size) laid in each site in both the sub-tropical (Khadi, Gaja) and temperate (Kanatal, Dhanolti) regions. The collected soil samples were air-dried, grounded, and sieved using a 2 mm sieve and further analysis was conducted in the Soil Science Laboratory, College of Forestry, Ranichauri, Tehri Garhwal, Uttarakhand. The bulk density (BD) of the soil was calculated using the core tube method. In order to take samples from the surface soil, the ground surface was cleared carefully to remove the entire residue followed by the collection of soil samples by inserting a core tube into the soil. The topsoil was excavated in rectangular volumes using a grub knife to reach the 15 cm and 30 cm soil layers and the sample was collected from the lower depths. The soil bulk density was calculated with the help of the following formula and expressed in g cm^{-3} (Duan et al., 2019).

$$BD = \frac{\text{Weight of oven dry soil collected in core tube}}{\text{Volume of core tube}}$$

The soil moisture content (gravimetric) was measured as the difference between the moist soil and the soil dried at 105°C in an oven, known as the oven-dry weight (Voroney, 2019). The percentage of soil moisture content was calculated as follows:

$$\text{Soil moisture \%} = \frac{\text{Weight of moist soil (g)} - \text{weight of oven dried soil (g)}}{\text{Weight of oven dried soil}} \times 100$$

The particle density (PD) of the soil was determined by pycnometer methods as described by Heiskanen (1992).

The soil pH was determined with a dynamic digital pH meter using 1:2 soil water suspensions. SOC was estimated using Walkley and Black's (1934) rapid titration method. SOC (%) was converted into soil organic matter (%) by multiplying by a factor of 1.724, i.e., SOC × 1.724. Olsen et al.'s (1954) method was used to determine the available phosphorus (P) in the soil. Available nitrogen (N) in soil was determined by using the Kjeldahl procedure (Subbiah and Asija, 1956). Available sulfur was determined using the 0.15% calcium chloride extraction method (Williams and Steinberg, 1959).

Statistical analysis

One-way analysis of variation (ANOVA) was performed for the analysis of soil data and the mean values were compared by

TABLE 2 Dominant and associated vegetation species at different altitudes and forests.

Forest type	Site	Altitude range	Tree	Shrub	Herb	Use of forest	Pressure on forest
Sub-tropical forest	Khadi	850–1,100 (masl)	*Quercus leucotrichophora* A. Camus, *Syzygium cumini* (L.), Skeels, *Boswellia serrata* Roxb. ex Colebr., *Holoptelea integrifolia* (Roxb.) *Planchon*., *Populus ciliata* Wallichex Royle, *Pinus roxburghii* Sargent, *Melia azedarach* L., *Mallotus philippensis* (Lam.) Muell.-Arg., *Alnus nepalensis* D.Don., *Bauhinia racemosa* Lam.	Actinidiacallosa Lindley, Carissa opaca L, Flemingia macrophylla (Willd.) Prain ex Merrill, Lantana camara L, Murraya koenigii (L.) Sprengel, Phlogacanthus thyrsiformis (Hardwicke) Mabberley, Phoenix acaulis Roxb., Ricinus communis L., Vitex negundo L., Woodfordia fruticose (L.) Kurz.	*Amaranthus caudatus* L., *Bidens pilosa* L., *Eupatorium adenophorum Sprengel*, *Fragaria nubicola* Lindley ex Lacaita. *Mentha arvensis* L., *Mukiamadera spatana* (L.) M. *Roemer*. *Rumex hastatus* D.Don., *Rumex nepalensis Sprengel.*	Fuel, fodder, minor timber, grazing, etc.	High
	Gaja	1,300–1,500 (masl)	*P. roxburghii* Sargent, *Q. leucotrichophora* A. Camus	*Inula cuspidata* (DC.) C. B. Clarke, *Lantana camara* L., *Murraya koenigii* (L.) *Sprengel*., *Maoutiapuya* (Hook.) Wedd., *Rhus parviflora* Roxb., *Rubus ellipticus* Smith., *Zanthoxylum armatum* DC., *Woodfordia fruticosa* (L.) Kurz.	*Dioscorea belophylla* (Prain) J.O. Voigt ex Haines. *Diplazium esculentum*, *Eupatorium adenophorum Sprengel*., *Galinsoga parviflora* Cav. *Micromeria biflora* (Buch.–Ham.ex D. Don) Benth. *Parthenium hysterophorus* L., *Paspalidium flavidum* (Retz.) A. Camus., *Vernonia cinerea* (L.) Lessing., *Saccharum bengalensis* Retz.	Fuel, fodder minor timber, fruits, browsing	Medium
Temperate forest	Kanatal	1,800–2,000 (masl)	*Q. leucotrichophora* A. Camus, *Cedrus deodara* (Roxb. Ex, D.Don) G. Don. *Rhododendron arboreum*, *P. roxburghii* Sargent, *Cornus capitata* Wall. Ex Roxb, *Lyonia ovalifolia* (Wallich) Drude.	*Berberis chitria Edwards*., *Berberis asiatica* Roxb. ex DC., *Sarcococca saligna* (D.Don) Muell.– Arg., *Leycesteria formosa* Wallich., *Lonicera quinquelocularis* Hardwicke., *Viburnum cotinifolium* D.Don., *Coriaria nepalensis* Wallich.	*Anaphalis margaritacea* (L.) Benth., *Anemone vitifolia* Buch.–Ham. ex DC., *Artemisia nilagirica* (C.B. Clarke), *Artemisia roxburghiana* Wallich., *Aster peduncularis* Wallich ex Nees. *Aster thomsonii* C.B. Clarke., *Bergenia ciliata* (Haworth) Sternberg., *Cyathula tomentose* (Roth) Moq., *Elsholtziaflava* (Benth.) Benth., *Geranium wallichianum* D.Don.	Fuel, fodder minor timber, fruits, herbal medicine	Very low
	Dhanolti	2,000–2,200 (masl)	*C. deodara* Roxb. ex. D.Don, *P. roxburghii* Sargent, *Ilex dipyrena Wallich*, *Myrica esculenta Buch*.- Ham. ex. D.Don.	*Euonymus echinatus* Wallich., *Indigofera heterantha* Wallich ex Brandis, *Deutzia staminea* R. Br. ex Wallich., *Hypericum oblongifolium* Choisy *Jasminumhumile* L., *Cotoneaster bacillaris* Wallich ex Lindley., *Cotoneaster microphyllus* Wallich ex Lindley *Rubusellipticus* Smith.	*Micromaria biflora* Benth., *Origanum vulgare* L., *Parnessia amibicola* Wall ex Royle, *Pesicaria amplexicaulis* D.Don *Pimpinella diversifolia* DC., *Plantago major* L., *Rumex hastatus* D.Don. Prodr., *Rumex nepalensis Sprengel. Satyrium nepalensis* D.Don., *Sedum adenotrichum* Wall. ex Edgew.	Fuel, fodder minor timber, fruits	Very low

TABLE 3 Shannon–Wiener diversity, Simpson's diversity, and Margalef diversity indices at different altitudes of sub-tropical and temperate forests.

Forest	Altitude (masl)	Shannon–Wiener diversity index (H)	Simpson's dominanc index (CD)	Margalef's index (Dmg)
Sub-tropical forest	850–1,100	0.48	0.95	2.51
	1,300–1,500	0.13	0.18	0.52
Temperate forest	1,800–2,000	0.44	0.49	2.68
	2,000–2,200	0.09	0.09	1.62

Duncan's multiple range test at $p < 0.05$ level of significance using SPSS 16.0 statistical software. The Pearson correlation coefficient was calculated among the different physical and chemical parameters of the soil and various vegetation parameters using SPSS-16 software.

Results

In this study, a total of 79 species belonging to different types of vegetation, i.e., trees, shrubs, and herbs, were found. At different altitudinal ranges, out of 79 species, 16 trees (belong to 16 genera and 14 families), 30 shrubs (belong to 28 genera and 26 families), and 33 herbs (belong to 30 genera and 18 families). The survey of the study area revealed that at sub-tropical forest sites (850–1,100 masl and 1,300–1,500 masl) trees are specifically being used for fuel, fodder, and minor timber, and forests also serve as grazing sites close to the villages. Thus in the sub-tropical forests, these services imparted a high pressure at 850–1,100 masl and medium pressure at 1,300–1,500 masl. On the other hand, the temperate forests (1,800–2,000 and 2,000–2,200 masl) were used for the collection of herbal medicines and wild fruits including fuel, fodder, and minor timbers (Table 2). However, the disturbance caused by grazing was reported as low pressure on the forests.

In the sub-tropical region, species diversity (H) parameters indicated that the maximum value of tree diversity, $H' = 0.48$, was recorded at 850–1,100 masl, followed by $H' = 0.27$ at 1,100–1,300 masl and the minimum value, $H' = 0.13$, was recorded at 1,300–1,500 masl. In the temperate region, the highest tree diversity ($H' = 0.44$) was at 1,800–2,000 masl, and the lowest was at 2,000–2,200 masl ($H' = 0.09$). For the Simpson's dominance index of the tree, the maximum (0.95) value was observed at 850–1,100 masl, and the minimum (0.18) at 1,300–1,500 masl in the sub-tropical region. For Margalef's index of richness, the maximum (2.68) value was at 1,800–2,000 masl and the minimum (0.52) was noted at 1,300–1,500 masl in the sub-tropical montane forest (Table 3).

At lower altitudes (850 and 1,100 masl), 10 trees were recorded with the dominance of *P. roxburghii* with maximum density and IVI. At the altitudinal range of 1,300–1,500 masl, the trees reported were *P. roxburghii* and *Q. leucotrichophora*, where *P. roxburghii* was dominant with the highest density (730 ind./ha) and IVI (265.56). At the altitude of 1,800–2,000 masl, a total of six trees were recorded and *Q. leucotrichophora* was dominant with the highest density (520 ind./ha) and IVI (172.31). At the altitudinal range of 2,000–2,200 masl, only four trees were recorded and *C. deodara* was dominant (IVI-272.54) with a density value of 690 ind./ha (Table 4).

At the different altitudinal ranges for sub-tropical forests, overall, the highest AGBD (596.31 Mg/ha), BGBD (133.46 Mg/ha), TBD (729.78 Mg/ha), and TCD (364.89 Mg/ha) were recorded at 1,300–1,500 masl where *P. roxburghii* was reported to be the dominant and *Q. leucotrichophora* the co-dominant tree species. However, the lowest values for AGBD, BGBD, TBD, and TCD were 270.94, 83.17, 354.18, and 177.06 Mg/ha, respectively, at 850–1,100 masl. In the temperate region, the highest values for AGBD, TBD, and TCD were reported as 338.25, 421.53, and 210.76 Mg/ha, respectively, at 2,000–2,200 masl, which was dominated by *C. deodara* while the maximum BGBD (89.18 Mg/ha) was recorded at 1,800–2,200 masl (Table 4).

Amongst the soil properties, a significant difference was recorded in soil BD at the 15–30 cm depth while a statistically non-significant difference was observed at the 0–15 cm depth. The difference in the values of PD of various sites and depths was also statistically non-significant. For the 0–15 cm depth, the moisture percentage of soil at 2,000–2,200 masl was reported as 14.83% which was significantly higher than the soil moisture at 850–1,100 masl (8.10%), 1,300–1,500 masl (8.24%), and 1,800–2,000 masl (10.62 %). Similarly, the soil pH in both depths varied significantly. The maximum value of pH in both the soil depths, i.e., 6.97 (0–15 cm) and 7.28 (15–30 cm) was observed at the lower altitudinal range of 850–1,100 masl. Significant variations in soil organic carbon and soil organic matter at both the soil depths were also observed and the higher values were recorded at higher altitudes ranging between 2,000 and 2,200 masl. The value of available N was recorded to be maximum at the altitude of 2,000–2,200 masl at both the soil depths and was significantly higher compared to the available N at other altitudes considered in the present study. The available P at 850–1,100 masl was significantly higher than the P at 1,800–2,000 masl and 2,000–2,200 masl. The values of available S also varied significantly ($p < 0.05$) among the different altitudes of the study sites. The maximum (29.88 mg/kg) value of available S was recorded at 850–1,100 masl and the lowest at 1,800–2,000 masl at the 0–15 cm soil depth (Table 5).

At the depth of 0–15 cm, a significant negative correlation was observed between BD and PD. A significant negative correlation was observed between SOC/Soil organic matter (SOM) with Moisture %. Both SOC and SOM were positively correlated with available S. A significant negative correlation between available P and PD was also observed. On the other hand, a significant positive correlation was recorded between TBD and AGBD, TBD and BGBD, and AGBD and BGBD (Table 6). At the 15–30 cm depth, BD showed a significant positive correlation with TBD, AGBD, and BGBD. The SOC had a significant positive correlation with SOM and N % and SOM with N %. A significant positive correlation was also recorded between TBD and AGBD, TBD and BGBD, and AGBD and BGBD (Table 7).

Discussion

Time plays an important role in the plant community to occupy an area of a region among many other factors such as

TABLE 4 AGBD, BGBD, TBD, and TCD of sub-tropical and temperate forests.

Forest type	Altitude (masl)	Tree species	AGBD (Mg/ha)	BGBD (Mg/ha)	TBD (Mg/ha)	TCD (Mg/ha)	Density (ha^{-1})	IVI
Sub-tropical forest	850–1,100	*Syzygium cumini*	27.01	8.49	35.51	17.75	30	31.65
		Bosswellia Serrata	56.47	16.29	72.77	36.38	30	25.11
		Holoptelea integrifolia	19.04	6.23	25.27	12.63	60	41.35
		Populus ciliate	18.77	6.15	24.92	12.46	30	22.38
		Pinus roxburghii	73.23	20.5	93.74	46.87	90	66.48
		Melia azedarach	14.33	4.84	19.18	9.59	80	73.08
		Mallotus philippensis	16.08	5.36	21.45	10.72	10	10.04
		Alnus nepalensis	19.55	6.38	25.94	12.97	10	10.41
		Bauhinia racemosa	19.25	6.29	25.55	12.77	10	10.41
		Quercus leucotrichophora	7.21	2.64	9.85	4.92	10	9.05
	Total		270.94	83.17	354.18	177.06		
	1,300–1,500	*P. roxburghii*	577.04	127.15	704.21	352.11	730	265.56
		Q. leucotrichophora	19.27	6.31	25.57	12.78	80	34.43
	Total		596.31	133.46	729.78	364.89		
Temperate forest	1,800–2,000	*Q. leucotrichophora*	110.73	29.55	140.29	70.14	520	172.31
		Cedrus deodara	9.65	3.42	13.08	6.54	10	9.92
		Rhododendron arboretum	28.29	8.84	37.13	18.56	20	8.53
		P. roxburghii	125.67	33.04	158.72	79.36	70	29.51
		Cornus capitata	21.75	7.01	28.76	14.38	70	48.86
		Lyonia ovalifolia	22.56	7.24	29.8	14.9	50	30.84
	Total		318.65	89.1	407.78	203.88		
	2,000–2,200	*C. deodara*	309.49	73.3	382.8	191.4	690	272.54
		P. roxburghii	6.63	2.45	9.09	4.54	10	9.17
		Ilex dipyrena	3.47	1.38	4.86	2.43	10	9.14
		Myrica esculenta	18.66	6.12	24.78	12.39	10	9.13
	Total		338.25	83.25	421.53	210.76		

altitude, aspect, slope, latitude, rainfall, and humidity which help the vegetation to grow and develop (Kharkwal et al., 2005). A total of 79 species of trees, shrubs, and herbs were recorded in different altitudes. The different species grow together in a community because they require similar environmental conditions for survival (Ter Braak, 1987). *Q. leucotrichophora* was the dominant tree at 1,800–2,000 masl and was also found co-dominant at 1,300–1,500 masl after *P. roxburghii* which suggests its ability to tolerate biotic pressures and wider ecological amplitude (Rawat S. et al., 2022).

The Shannon–Wiener index measures the scarcity and frequency of species in a habitat and usually varies from 1.5 to 3.5, not exceeding 4.5 (Kent and Coker, 1992), and the value observed is usually less in temperate forests. The maximum value for tree diversity ($H' = 0.48$) at 850–1,100 masl was reported in the sub-tropical region, which could be because of human interference in these low-elevation forest areas which assisted the plantation and survival of exotic species (Rawal and Pangtey, 1994). A higher number of species was reported at lower elevations compared to higher elevations. These observations recorded in our study were in conformity with the findings of Wani et al. (2022). In the present investigation, the richness of non-native species such as *Alnus nepalensis*, *Melia azedarach*, and *Mallotus philippensis*, was more widespread in early succession/pioneer communities. In the temperate region, the highest value for tree diversity ($H' = 0.44$) was recorded at 1,800–2,000 masl and a similar trend was also described by Kumar and Ram (2005). Further, the higher availability of nutrients in the soil at higher elevations favored the growth of most trees. Pausas and Austin (2001) suggested that the distribution of species richness in any large region is likely to be governed by two or more environmental factors.

The Simpson's index exhibited the "concentration" of dominance and a higher value shows the dominance of one or a few species. The concentration of dominance (CD) for different life forms ranges between 0.12 and 0.80 for Himalayan regions (Tiwari and Tiwari, 2012). The CD of trees in the recent study ranged from 0.18 to 0.95 in sub-tropical regions at different altitudes. While in the temperate region, it ranged from 0.09 to 0.49. The higher reported CD values of trees in the sub-tropical region make it clear that the forest has less diversity and is mostly dominated by single species of *P. roxburghii*. The maximum value of CD of trees (0.49) was reported at 2,000–2,000 masl in the temperate region. Higher community stability indicates higher species richness which means greater species diversity (Swamy et al., 2000). The tree species richness was the highest at 1,800–2,000 masl and the least (1.62) was recorded at 2,000–2,200 masl in the temperate region. Dangwal et al. (2012) showed an increasing trend in the diversity of herbs and shrubs with increasing altitudes, whereas the diversity of tree species declined with increasing altitude in the western Himalayan region. Similar outcomes for species richness were reported in an elevation gradient study conducted by Sharma et al. (2017). The total species richness was found to be higher in warmer sites (lower elevation) as compared to the cooler sites (higher elevation).

The AGBD and BGBD ranged from 270.94 to 596.31 Mg/ha and 83.17 to 133.456 Mg/ha, respectively, while TBD ranged from 354.21 to 729.78 Mg/ha. The variation in the amount of biomass might be due to the differences in species composition at different altitudes. In this study, the average value of TBD was reported to be 541.98 Mg/ha in sub-tropical forests and

TABLE 5 Soil properties at a different altitudinal range of the study area (mean ± SD).

Elevation (masl)	Bulk density (g/cm^3)		Particle density (g/cm^3)		Moisture %		pH		Soil organic carbon (%)		Soil organic matter (%)		Available nitrogen (Kg ha^{-1})		Available phosphorus (Kg ha^{-1})		Available sulfur (mg/kg soil)	
	Depth (cm)		Depth (cm)		Depth (cm)		Depth (cm)		Depth (cm)		Depth (cm)		Depth (cm)		Depth (cm)		Depth (cm)	
	0–15	16–30	0–15	16–30	0–15	16–30	0–15	16–30	0–15	16–30	0–15	16–30	0–15	16–30	0–15	16–30	0–15	16–30
850–1,100	1.04^{ns} ± 0.06	1.00^{b} ± 0.02	2.04^{ns} ± 0.35	2.05^{ns} ± 0.08	8.10^{b} ± 1.47	10.11^{ns} ± 3.18	6.97^{a} ± 0.16	7.28^{a} ± 0.26	2.35^{b} ± 0.48	2.37^{ab} ± 0.88	4.05^{b} ± 0.83	4.08^{ab} ± 1.52	250.71^{b} ± 31.34	239.47^{b} ± 76.46	31.23^{a} ± 6.51	26.49^{ns} ± 5.97	29.88^{a} ± 2.83	16.40^{ns} ± 3.12
1,300–1,500	1.03^{ns} ± 0.03	1.45^{a} ± 0.06	2.06^{ns} ± 0.10	2.05^{ns} ± 0.06	8.24^{b} ± 1.30	8.57^{ns} ± 1.22	5.59^{b} ± 0.28	6.18^{b} ± 0.07	2.37^{b} ± 0.23	1.93^{b} ± 0.15	4.08^{b} ± 0.39	3.32^{b} ± 0.27	322.93^{b} ± 96.99	203.09^{b} ± 20.71	29.16^{ab} ± 3.55	18.87^{ns} ± 1.49	21.76^{b} ± 2.95	17.81^{ns} ± 3.91
1,800–2,000	1.03^{ns} ± 0.05	1.03^{b} ± 0.03	2.07^{ns} ± 0.07	2.12^{ns} ± 0.13	10.62^{b} ± 1.80	9.57^{ns} ± 2.01	5.67^{b} ± 0.16	6.36^{b} ± 0.85	2.17^{b} ± 0.36	2.00^{b} ± 0.30	3.60^{b} ± 0.43	3.46^{b} ± 0.51	239.62^{b} ± 52.48	213.19^{b} ± 21.09	16.85^{b} ± 4.54	15.46^{ns} ± 5.06	15.97^{c} ± 1.38	12.59^{ns} ± 1.27
2,000–2,200	1.07^{ns} ± 0.01	1.02^{b} ± 0.04	2.09^{ns} ± 0.11	2.01^{ns} ± 0.04	14.83^{a} ± 3.36	10.57^{ns} ± 4.73	5.94^{b} ± 0.07	6.27^{b} ± 0.08	3.21^{a} ± 0.28	3.19^{a} ± 0.33	5.522^{a} ± 1.47	5.49^{a} ± 0.47	517.93^{a} ± 124.87	466.65^{a} ± 38.53	12.29^{b} ± 2.60	21.54^{ns} ± 3.01	23.04^{b} ± 1.38	14.27^{ns} ± 1.95

Mean followed by the same alphabet in each column indicates the non-significant variation.

TABLE 6 Pearson correlation coefficient between different vegetation and soil parameters of the sub-tropical and temperate forest at 0–15 cm soil depth.

	BD (g/cm^3)	pH	SOC %	SOM %	Moisture %	PD (g/cm^3)	Avl. N (Kg/ha)	Avl. S (ppm)	Avl. P (Kg/ha)	H′	CD	D_{mg}	TCD	TBD	AGBD
BD (g/cm^3)	1.000														
pH	0.999**	1.000													
SOC %	0.515	0.472	1.000												
SOM %	0.540	0.497	1.000**	1.000											
Moisture %	−0.610	−0.570	−0.993**	−0.996**	1.000										
PD (g/cm^3)	−0.943	−0.925	−0.771	−0.789	0.839	1.000									
Avl. N (Kg/ha)	−0.821	−0.849	0.066	0.037	0.048	0.584	1.000								
Avl. S (ppm)	0.663	0.625	0.983*	0.988*	−0.998**	−0.875	−0.117	1.000							
Avl. P (Kg/ha)	0.910	0.888	0.824	0.840	−0.884	−0.996**	−0.511	0.914	1.000						
H′	0.639	0.654	0.061	0.081	−0.142	−0.498	−0.703	0.189	0.452	1.000					
CD	0.897	0.903	0.348	0.372	−0.441	−0.801	−0.813	0.495	0.761	0.911	1.000				
D_{mg}	0.456	0.494	−0.430	−0.407	0.337	−0.171	−0.817	−0.278	0.093	0.841	0.696	1.000			
TCD (Mg/ha)	−0.696	−0.722	0.099	0.074	0.001	0.478	0.876	−0.062	−0.412	0.274	−0.494	−0.521	1.000		
TBD	−0.506	−0.549	0.478	0.452	−0.374	0.190	0.908	0.310	−0.103	0.616	−0.583	−0.913	0.797	1.000	
AGBD	−0.502	−0.544	0.481	0.456	−0.378	0.185	0.905	0.314	−0.099	0.629	−0.589	−0.922	0.784	1.000**	1.000
BGBD	−0.386	−0.431	0.587	0.564	−0.491	0.058	0.841	0.431	0.029	0.465	−0.428	−0.844	0.805	0.983*	0.980*

**Correlation is significant at the 0.01 level.

*Correlation is significant at the 0.05 level.

TABLE 7 Pearson correlation coefficient between different vegetation and soil parameters of the sub-tropical and temperate forest at 15–30 cm soil depth.

	BD (g/cm^3)	pH	SOC %	SOM %	Moisture %	PD (g/cm^3)	Avl. N (Kg/ha)	Avl. S (ppm)	Avl. P (Kg/ha)	H′	CD	D_{mg}	TCD	TBD	AGBD
BD (g/cm^3)	1.000														
pH	−0.474	1.000													
SOC %	−0.520	0.023	1.000												
SOM %	−0.521	0.024	1.000**	1.000											
Moisture %	−0.889	0.380	0.846	0.847	1.000										
PD (g/cm^3)	−0.082	−0.062	−0.736	−0.735	−0.373	1.000									
Avl. N (Kg/ha)	−0.405	−0.197	0.976*	0.976*	0.746	−0.709	1.000								
Avl. S (ppm)	0.696	0.227	−0.244	−0.245	−0.493	−0.467	−0.288	1.000							
Avl. P (Kg/ha)	−0.300	0.820	0.421	0.421	0.488	−0.622	0.233	0.469	1.000						
H′	−0.521	0.689	−0.420	−0.419	0.124	0.668	−0.563	−0.280	0.154	1.000					
CD	−0.460	0.919	−0.284	−0.283	0.192	0.336	−0.480	0.049	0.529	0.911	1.000				
D_{mg}	−0.883	0.545	0.057	0.058	0.573	0.499	−0.064	−0.676	0.123	0.841	0.696	1.000			
TCD (Mg/ha)	0.769	−0.730	−0.690	−0.691	−0.885	0.465	−0.517	0.107	−0.824	−0.274	−0.494	−0.521	1.000		
TBD	0.989*	−0.591	−0.442	−0.443	−0.852	−0.110	−0.303	0.616	−0.378	−0.616	−0.583	−0.913	0.797	1.000	
AGBD	0.989*	−0.587	−0.425	−0.426	−0.841	−0.132	−0.287	0.626	−0.363	−0.629	−0.589	−0.922	0.784	1.000**	1.000
BGBD	0.997**	−0.473	−0.583	−0.584	−0.922	−0.003	−0.467	0.666	−0.344	−0.465	−0.428	−0.844	0.805	0.983*	0.980*

**Correlation is significant at the 0.01 level.

*Correlation is significant at the 0.05 level.

414.66 Mg/ha in temperate forests. These values were higher than the values reported by Gairola et al. (2011a) for similar forests in the Uttarakhand region. The average AGBD (381.04 Mg/ha) and BGBD (97.25 Mg/ha) in the present study were on par with the values given for different forests of the Garhwal Himalaya (Sharma et al., 2010). On average, the TCD value was 270.98 Mg/ha in the sub-tropical forests and 207.32 Mg/ha in the temperate forests, which falls within the range (92–640 Mg/ha) reported by Singh et al. (1994). The cites with minimum human or natural disturbance have optimum to higher values of biomass/carbon stock (Lugo and Brown, 1992). Higher capacity to produce high levels of biomass as reported in the mixed stands was generally due to the varying carbon fixing rates of different species as the majority of forest trees have a huge potential for short-term and long-term carbon storage (Houghton, 2005). In any forest's ecosystems, large storage of carbon is recognized in big, long-lived tree species with dense wood (Bunker et al., 2005). The results of the present study also highlighted the disproportionate contribution of a small number of species viz., *Cornus capitata*, *Ilex dipyrone*, *Myrica esculenta*, and *Lyonia ovalifolia* to carbon stock as these areas contained a great amount of biomass and carbon storage. These species are slow-growing and survive under trees in these forests.

The soil moisture content in the present study sites was comparable to the reported values for the Himalayan region (Khera et al., 2001; Nazir, 2009). However, variation in moisture content might be because of altitude, rainfall, forest cover, types of vegetation, aspect, slope, water holding capacity, etc., and higher water absorbing characteristics of some trees (i.e., *Q. leucotrichophora*, *Q. floribunda*, and *Q. semecarpifolia*). The soil moisture content was reported higher with increasing altitude. Singh and Singh (1986) have also reported that the soil of oak forests was comparatively rich in moisture. In the present study, the maximum moisture content was reported at 2,000–2,200 masl in the Dhanolti region which was associated with lower temperatures, leading to low evaporation rate and soil moisture loss.

Soil acidity and alkalinity indicate the soil pH. Leskiw (1998) reported that forest soils require slightly acidic pH values for nutrient supply. The pH values of the present study varied from 6.86 to 7.21 at 850–1,500 masl (sub-tropical forests) and 5.63 to 6.24 at 1,800–2,200 masl (temperate forests). All the sites of the temperate region had pH levels below 6.0, at 0–15 cm depth, owing to an uninterrupted layer of high organic matter content. The higher assemblage of SOC and release of weak organic acids due to the slow decomposition rate usually lowers the soil pH (De Hann, 1977; Robertson and Vitousek, 1981; Adams and Sidle, 1987; Mishra et al., 2017a). However, higher pH values than the present study were found in the Kumaun region (Khera et al., 2001). The highest soil organic carbon percentage was found in Dhanolti (2,000–2,200 masl) in temperate forests and the lowest in Khadi in sub-tropical forests (850–1,100 masl). The SOM-enriched soil of the higher altitude zone of the Dhanolti site has been ascribed to low temperature and slower decomposition rate (Dimri et al., 1997). The lower SOM content in the Khadi has been attributed to the meager status of understory vegetation in the region. Furthermore, lesser understory vegetation facilitates the loss of topsoil and SOM sediments through erosion (Li et al., 2015; Song et al., 2020). Among the essential nutrients for plants, N is an essential primary nutrient that is responsible for the vegetative growth of plants (Rawat D. et al., 2022). The deficiency of N in plants may be seen as the yellowing of leaves and stunted growth. The values of N at the present study sites were comparable to the values observed in various previous works (Khera et al., 2001, Srivastava et al., 2005; Semwal, 2006; Sharma et al., 2010b) in the Uttarakhand Himalaya. The maximum value of soil N in the study sites was in the upper layers because of the large amount of litter and humus in the upper layer and possible leaching of N in lower altitudes due to the presence of a coarser fraction in the soil (Saha et al., 2018). The available P in the soil was recorded to be significantly higher at 850–1,100 masl compared to the temperate areas at both depths. Similar findings were recorded by Rawat et al. (2020) in the montane forests of the Garhwal Himalaya. This trend could be associated with the pH of the soil which is near neutral in case of 850–1,100 m because P remains in plant-available forms in neutral pH whereas low pH leads to its fixation in insoluble forms in the soil (Murphy, 1958; Mishra et al., 2017b). The available S decreased with an increase in soil depths due to greater inputs of organic matter on the surface soil (Amanuel et al., 2018).

The present study area has shown that pressure from the local people on the forests existed. Singh et al. (2022) observed that, on average, 15.01% of the forests in the Garhwal Himalaya were disturbed annually from 2005 to 2018. However, the pressure is based on the requirements of the local people and the availability of resources in the different altitudinal ranges. It has been noticed that lower altitudes are rich in species used by the local villagers and thus anthropogenic activities are reported dominant. Similar findings were documented by Singh et al. (2018) as the unmanaged extraction of trees through the collection of fuel, fodder, and overgrazing was found to be the major factor of forest disturbance along an altitudinal range of < 1,700 to > 1,900 masl in the Garhwal Himalaya. The field surveys in our investigation also confirmed the fact that at lower altitudes, the villagers were residing closer to the forest environment, and the dependence on a thick population has increased the level of pressure on forest resources as compared to the temperate region. The resources availed of by the villagers in the study area were fuel, fodder, fiber, timber, fruits, etc., along with other associated requirements such as grazing and browsing. Anthropogenic activities such as tree cutting and lopping were also seen prominently at lower altitudes of temperate forests in the Tehri and Uttarkashi districts of the Garhwal Himalaya (Tewari and Sharma, 2023). Overall, this study presented an insight into the condition of the sub-tropical forests in the study area which are under high pressure due to the large-level needs of the surrounding population as compared to the forests at high altitudinal ranges.

Conclusion

The intervention of human activities in the lower altitude forests of the sub-tropical region with the introduction of non-native tree species and the probable climatic gradient developed in the altitude ranges of temperate forests accounted for the diversity of tree species in these forests. Amongst the species, *P. roxburghii* dominated the altitudinal ranges of 1,100–1,300 masl and 1,300–1,500 masl in sub-tropical forests, with higher values of AGBD, BGBD, TBD, and total carbon stock signifying its superior carbon sequestration potential. The contribution of species such as

Q. leucotrichophora, *Q. floribunda*, *R. arboreum*, and *C. deodara*, improved the soil moisture, SOC, and available N in the soil in the temperate forests. However, the lower availability of P and S was influenced by the low pH of the soil. The present study indicated that coniferous species such as *P. roxburghii*, in the sub-tropical forests and *Q. leucotrichophora*, *C. deodara* in the temperate forests of the Garhwal Himalaya have high carbon storage potential and require conservation and carbon management attention through plantation and natural regeneration because regular pressure on the forests for various purposes and resources by the villagers may affect the species survival and further carbon sequestration potential. Although, this study was limited to four sites in the Garhwal Himalaya, the findings contribute to an important understanding of species distribution and soil health in sub-tropical and temperate montane forests which may further be helpful for long-term monitoring of and assessment studies on ongoing anthropogenic disturbances. The framework of management activities focusing on forest conservation may also be developed with the help of information gathered from this investigation.

Data availability statement

The raw data supporting the conclusions of this article will be made available by the authors, without undue reservation.

Author contributions

AT experimented, data collection, and prepared the first draft. DR and BS helped in the analysis of data and preparation of the first manuscript. VK and DR designed the research and supervised the research. VK, DR, GM, and MK reviewed and modified the manuscript. MR analyzed the data and software. All authors contributed to the manuscript writing, revised and approved the submitted version.

Acknowledgments

We are thankful to the College of Forestry, VCSG Uttarakhand University of Horticulture and Forestry, Ranichauri, Tehri Garhwal, Uttarakhand for providing all the facilities.

Conflict of interest

The authors declare that the research was conducted in the absence of any commercial or financial relationships that could be construed as a potential conflict of interest.

Publisher's note

References

Adams, P. W., and Sidle, R. C. (1987). Soil conditions in three recent landslides in southeast Alaska. *For. Ecol. Manag.* 18, 93–102. doi: 10.1016/0378-1127(87)90136-8

Amanuel, W., Yimer, F., and Karltun, E. (2018). Soil organic carbon variation in relation to land use changes: The case of birr watershed, upper Blue Nile River Basin, Ethiopia. *J. Ecol. Environ.* 42:16. doi: 10.1186/s41610-018-0076-1

Anderegg, W. R., Schwalm, C., Biondi, F., Camarero, J. J., Koch, G., Litvak, M., et al. (2015). Pervasive drought legacies in forest ecosystems and their implications for carbon cycle models. *Science* 349, 528–532.

Augusto, L., Ranger, J., Binkley, D., and Rothe, A. (2002). Impact of several common tree species of European temperate forests on soil fertility. *Ann. Sci.* 59, 233–253. doi: 10.1051/forest:2002020

Brown, S., and Schroeder, P. E. (1999). Spatial patterns of aboveground production and mortality of woody biomass for eastern US forests. *Ecol. Applic.* 9, 968–980. doi: 10.2307/2641343

Bunker, D. E., DeClerck, F., Bradford, J. C., Colwell, R. K., Perfecto, I., Phillips, O. L., et al. (2005). Species loss and aboveground carbon storage in a tropical forest. *Science* 310, 1029–1031. doi: 10.1126/science.1117682

Cairns, M. A., Brown, S., Helmer, E. N., and Baumgardener, G. A. (1997). Root biomass allocation in the world's upland forests. *Oecologia* 111, 1–11. doi: 10.1007/s004420050201

Chaturvedi, O. P., and Singh, J. S. (1987). The structure and function of pine forest in Central Himalaya. I. dry matter dynamics. *Ann. Bot.* 60, 237–252. doi: 10.1093/aob/mcf004

Curtis, J. T., and McIntosh, R. (1950). The interrelations of certain analytic and synthetic phytosociological characters. *Ecology* 31, 434–455. doi: 10.2307/1931497

Dangwal, L. R., Singh, T., Singh, A., and Sharma, A. (2012). Plant diversity assessment in relation to disturbances in subtropical chir pine forest of the Western Himalaya of district Rajouri. J and K, India. *Int. J. Plant Anim. Environ. Sci.* 2, 206–213.

De Hann, S. (1977). *Humus, its formation, its relation with the mineral part of the soil and its significance for soil productivity*. Vienna: International Atomic Energy Agency.

Dimri, B. M., Jha, M. N., and Gupta, M. K. (1997). Status of soil nitrogen at different altitudes in Garhwal Himalaya. *Van Vigyan* 359, 77–84.

Dong, H., Lin, J., Lu, J., Li, L., Yu, Z., Kumar, A., et al. (2022). Priming effects of surface soil organic carbon decreased with warming: A global meta-analysis. *Plant Soil* doi: 10.1007/s11104-022-05851-1 [Epub ahead of print].

Duan, A., Lei, J., Hu, X., Zhang, J., Du, H., Zhang, X., et al. (2019). Effects of planting density on soil bulk density, pH and nutrients of un-thinned Chinese fir mature stands in south subtropical region of China. *Forests* 10:351. doi: 10.3390/f10040351

FSI (1996). *Volume equations for forests of India, Nepal and Bhutan*. Dehradun: Forest Survey of India.

Gairola, S., Sharma, C. M., Ghildiyal, S. K., and Suyal, S. (2011a). Live tree biomass and carbon variation along an altitudinal gradient in moist temperate valley slopes of the Garhwal Himalaya (India). *Curr. Sci.* 100, 1862–1870.

Gairola, S., Sharma, C. M., Ghildiyal, S. K., and Suyal, S. (2011b). Tree species composition and diversity along an altitudinal gradient in moist tropical montane valley slopes of the Garhwal Himalaya, India. *For. Sci. Technol.* 7, 91–102. doi: 10.1080/21580103.2011.597109

Gaur, R. D. (1999). *Flora of the District Garhwal North West Himalaya (with ethnobotanical notes)*. Srinagar: Transmedia Publication.

Gauthier, G., Berteaux, D., Bêty, J., Tarroux, A., Therrien, J. F., McKinnon, L., et al. (2011). The tundra food web of Bylot Island in a changing climate and the role of exchanges between ecosystems. *Ecoscience* 18, 223–235.

Gupta, M. K., and Sharma, S. D. (2011). Sequestrated carbon: Organic carbon pool in the soils under different forest covers and land uses in Garhwal Himalayan region of India. *Int. J. Agric. For.* 1, 14–20.

Heiskanen, J. (1992). Comparison of three methods for determining the particle density of soil with liquid pycnometers. *Soil Sci. Plant Anal.* 23, 841–846. doi: 10.1080/00103629209368633

Houghton, R. A. (2005). Aboveground forest biomass and the global carbon balance. *Glob. Change Biol.* 11, 945–958. doi: 10.1111/j.1365-2486.2005.00955.x

IPCC (2003). *Good practice guidance for land use, land-use change, and forestry*. Hayama: IPCC National Greenhouse Gas Inventories Programme.

Kent, M., and Coker, P. (1992). *Vegetation description and analysis a practical approach*. Boca Raton, FL: CRC Press, 363.

Kharkwal, G., Mehrotra, P., Rawat, Y. S., and Pangtey, Y. P. S. (2005). Phytodiversity and growth form in relation to altitudinal gradient in the Central Himalayan (Kumaun) region of India. *Curr. Sci.* 89, 873–878.

Khera, A. N., Kumar, A., and Ram, J. (2001). Plant biodiversity assessment in relation to disturbances in mid-elevation forest of Central Himalaya, India. *Trop. Ecol.* 42, 83–95.

Kumar, A., Yu, Z., Klemeš, J. J., and Bokhari, A. (2021b). A state-of-the-art review of greenhouse gas emissions from Indian hydropower reservoirs. *J. Clean. Prod.* 320:128806. doi: 10.1016/j.jclepro.2021.128806

Kumar, S., Bijalwan, A., Singh, B., Rawat, D., Yewale, A. G., Riyal, M. K., et al. (2021c). Comparison of carbon sequestration potential of *Quercus leucotrichophora*–based agroforestry systems and natural forest in central Himalaya, India. *Water Air Soil Pollut.* 232:350.

Kumar, A., Kumar, M., Pandey, R., ZhiGuo, Y., and Cabra-Pinto, M. (2021a). Forest soil nutrient stocks along altitudinal range of Uttarakhand Himalayas: An aid to nature based climate solutions. *Catena* 207:105667. doi: 10.1016/j.catena.2021.105667

Kumar, A., and Ram, J. (2005). Anthropogenic disturbances and plant biodiversity in forests of Uttaranchal, Central Himalaya. *Biodivers. Conserv*. 14, 309–331.

Kumar, A., Yang, T., and Sharma, M. P. (2019). Long-term prediction of greenhouse gas risk to the Chinese hydropower reservoirs. *Sci. Total Environ.* 646, 300–308. doi: 10.1016/j.scitotenv.2018.07.314

Leskiw, L. A. (1998). *Land capability classification for forest ecosystem in the oil stands region*. Edmonton: Alberia Environmental Protection.

Li, Y., Yu, H. Q., Zhou, N., Tian, G., Poesen, J., and Zhang, Z. D. (2015). Linking fine root and understory vegetation to channel erosion in forested hillslopes of southwestern China. *Plant Soil* 389, 323–334. doi: 10.1007/s11104-014-2362-8

Lugo, A. E., and Brown, S. (1992). Tropical forests as sinks of atmospheric carbon. *For. Ecol. For. Manage.* 54, 239–255.

Luna, R. K. (2005). *Plantation trees*. Dehradun: International book distributors, 826.

Malhi, Y., Meir, P., and Brown, S. (2002). Forests, carbon and global climate. *Philos. Trans. R. Soc. Lond. Ser. A* 360, 1567–1591.

Margalef, R. (1968). *Perspective in ecological theory*. Chicago, IL: University of Chicago Press.

Meena, V. S., Ghosh, B. N., Singh, R. J., Bhattacharyya, R., Sharma, N. K., Alam, N. M., et al. (2021). Land use types and topographic position affect soil aggregation and carbon management in the mountain agroecosystems of the Indian Himalayas. *Land Degrad. Dev.* 32, 3992–4003. doi: 10.1002/ldr.3864

Mishra, A., Swamy, S. L., Thakur, T. K., Kumar, A., and Pandey, M. (2022). Impact of coal mining on land use changes, deforestation, biomass, and C losses in Central India: Implications for offsetting CO_2 emissions. *Land Degrad. Dev*. 33, 3374–3731. doi: 10.1002/ldr.4419

Mishra, G., Das, P. K., Borah, R., and Dutta, A. (2017a). Investigation of phytosociological parameters and physicochemical properties in northern tropical semi-evergreen Forests of Eastern Himalaya. *J. For. Res.* 28, 513–520.

Mishra, G., Debnath, S., and Rawat, D. (2017b). Managing phosphorus in terrestrial ecosystem: A review. *Eur. J. Biol. Res.* 7, 255–270.

Murphy, H. P. (1958). *The fertility status of some soils of Ethiopia*. Alemaya: College of Agriculture and Mechanical Arts.

Nazir, T. (2009). *Estimation of site quality of important temperate forest covers on the basis of soil nutrients and growing stock in Garhwal Himalaya*. Ph.D. thesis. Srinagar: HNB Garhwal University.

Negi, J. D. S., Manhas, R. K., and Chauhan, P. S. (2003). Carbon allocation in different components of some tree species of India: A new approach for carbon estimation. *Curr. Sci.* 85, 1528–1531.

Olsen, S. R., Cole, C. L., Watanabe, F. S., and Dean, D. A. (1954). *Estimation of available phosphorus in soil by extraction with sodium bicarbonate*. Washington, DC: US Government Printing Office.

Pausas, J. G., and Austin, M. P. (2001). Patterns of plant species richness in relation to different environments: An appraisal. *J. Veg. Sci.* 12, 153–166.

Phillips, E. A. (1959). *Methods of vegetation study*. New York, NY: Henry Holt.

Rawal, R. S., and Pangtey, Y. P. S. (1994). High altitude forests in a part of Kumaun, Central Himalaya. *Proc. Ind. Natl. Sci. Acad.* 60, 557–564.

Rawat, D., Mukhopadhyay, D., Mishra, G., and Bijalwan, A. (2022). "Soil nitrogen dynamics and management in agroforestry systems for ecological sustainability," in *Land degradation neutrality: Achieving SDG 15 by forest management*, eds P. Panwar, G. Shukla, J. A. Bhat, and S. Chakravarty (Singapore: Springer), doi: 10.1007/978-981-19-5478-8_20

Rawat, S., Khanduri, V. P., Singh, B., Riyal, M. K., Thakur, T. K., Kumar, M., et al. (2022). Variation in carbon stock and soil properties in different *Quercus leucotrichophora* forests of Garhwal Himalaya. *Catena* 213:106210. doi: 10.1016/j.catena.2022.106210

Rawat, D., Sati, S. P., Khanduri, V. P., Riyal, M., and Mishra, G. (2021). "Carbon sequestration potential of different land use sectors of Western Himalaya," in *Advances in carbon capture and utilization. energy, environment, and sustainability*, eds D. Pant, A. Kumar Nadda, K. K. Pant, and A. K. Agarwal (Singapore: Springer), doi: 10.1007/978-981-16-0638-0_12

Rawat, D. S., Tiwari, P., Das, S. K., and Tiwari, J. K. (2020). Tree species composition and diversity in montane forests of Garhwal Himalaya in relation to environmental and soil properties. *J. Mt. Sci.* 17, 3097–3111. doi: 10.1007/s11629-019-5761-8

Robertson, G. P., and Vitousek, P. M. (1981). Nitrification in primary and secondary succession. *Ecology* 1981, 376–386. doi: 10.1007/BF00396734

Saha, S., Rajwar, G. S., and Kumar, M. (2018). Soil properties along altitudinal gradient in Himalayan temperate forest of Garhwal region. *Acta Ecol. Sin*. 38, 1–8. doi: 10.1016/j.chnaes.2017.02.003

Semwal, S. (2006). *Studies on phytosociology, diversity patterns and competition along an altitudinal gradient in a part of lesser Himalaya in Garhwal, Uttaranchal*. Ph.D. Thesis. Srinagar: HNB Garhwal University.

Shannon, C. E., and Weaver, W. (1963). *The mathematical theory of communication*. Urbana, IL: University of Illinois Press.

Sharma, C. M., Baduni, N. P., Gairola, S., Ghildiyal, S. K., and Suyal, S. (2010a). Tree diversity and carbon stocks of some major forest types of Garhwal Himalaya, India. *For. Ecol. Manage.* 260, 2170–2179.

Sharma, C. M., Gairola, S., Ghildiyal, S. K., and Suyal, S. (2010b). Physical properties of soils in relation to forest composition in moist temperate valley slopes of the Central Western Himalaya. *J. For. Sci*. 26, 117–129.

Sharma, C. M., Gairola, S., Baduni, N. P., Ghildiyal, S. K., and Suyal, S. (2011). Variation in carbon stocks on different slope aspects in seven major forest types of temperate region of Garhwal Himalaya, India. *J Biosci.* 36, 701–708. doi: 10.1007/s12038-011-9103-4

Sharma, C. M., Mishra, A. K., Tiwari, O. P., Krishan, R., and Rana, Y. S. (2017). Effect of altitudinal gradients on forest structure and composition on ridge tops in Garhwal Himalaya. *Energ. Ecol. Environ.* 2, 404–417. doi: 10.1007/s40974-017-0067-6

Sharma, H., Pant, K. S., Bishist, R., Gautam, L., Ludarmani, D. R., Kumar, M., et al. (2023). Estimation of biomass and carbon storage potential in agroforestry systems of north western Himalayas, India. *Catena* 225:107009. doi: 10.1016/j.catena.2023.107009

Sheikh, M. A., and Kumar, M. (2010). Nutrient status and economic analysis of soils in oak and pine forests in Garhwal Himalaya. *J. Am. Sci.* 6, 117–122.

Simpson, E. H. (1949). Measurement of diversity. *Nature* 163:688.

Singh, G., Padalia, H., Rai, I. D., Bharti, R. R., and Rawat, G. S. (2016). Spatial extent and conservation status of Banj oak (*Quercus leucotrichophora* A. Camus) forests in Uttarakhand, Western Himalaya. *Trop. Ecol.* 57, 255–262.

Singh, H., Kumar, M., and Sheikh, M. A. (2009). Distribution pattern of oak and pine along altitudinal gradients in Garhwal Himalaya. *Nat. Sci.* 7, 81–85.

Singh, J. S., and Singh, S. P. (1986). Structure and function of central Himalaya oak forests. *Proc. Ind. Natl. Acad.* 96, 156–189.

Singh, R., Kumar, P., Pandey, R., and Bala, N. (2022). Forest disturbance detection in Garhwal Himalayas using MODIS NDVI time-series and BFAST model. *Geocarto Int*. 37, 12689–12708. doi: 10.1080/10106049.2022.2071472

Singh, S. P., Adhikari, B. S., and Zobel, D. B. (1994). Biomass productivity, leaf longevity and forest structure in the Central Himalaya. *Ecol. Monogr.* 64, 401–421.

Singh, V., Singh, D. S., and Dasgupta, S. (2018). Effect of stand structure and aspect on the regeneration of banj oak (*Quercus leucotrichophora* A. Camus) forest along disturbance in Garhwal Himalaya, Uttarakhand, India. *For. Stud.* 68, 33–39. doi: 10.2478/fsmu-2018-0003

Song, L., Boithias, L., Sengtaheuanghoung, O., Oeurng, C., Valentin, C., Souksavath, B., et al. (2020). Understory limits surface runoff and soil loss in teak tree plantations of Northern Lao PDR. *Water* 12:2327. doi: 10.3390/w12092327

Srivastava, R. K., Khanduri, V. P., Sharma, C. M., and Kumar, P. (2005). Structure, diversity and regeneration potential of oak-dominant conifer mixed forest along an altitudinal gradient in Garhwal Himalaya. *Indian For.* 131, 1537–1553.

Subbiah, B. V., and Asija, G. L. (1956). A rapid method for estimation of available N in soil. *Curr. Sci.* 25, 259–260.

Swamy, P. S., Sundarapandian, S. M., Chandrasekar, P., and Chandrasekaran, S. (2000). Plant species diversity and tree population structure of a humid tropical forest in Tamil Nadu, India. *Biodivers. Conserv*. 9, 1643–1669.

Tariyal, N., Bijalwan, A., Chaudhary, S., Singh, B., Dhanai, C. S., Tewari, S., et al. (2022). Crop production and carbon sequestration potential of *Grewia oppositifolia*-based traditional agroforestry systems in Indian Himalayan Region. *Land* 11:839.

Ter Braak, C. J. E. (1987). The analysis of vegetation-environment relationships by canonical correspondence analysis. *Vegetatio* 69, 69–77.

Tewari, O. P., and Sharma, C. M. (2023). Anthropogenic disturbance impact on forest composition and dominance-diversity: A case of an ecosensitive region of Garhwal Himalaya, India. *Acta Ecol. Sin.* 43, 662–673. doi: 10.1016/j.chnaes.2022.08.003

Tiwari, P. K., and Tiwari, S. C. (2012). *Environmental regeneration of woody species: A case study of forest ecosystems of submontane and montane zones of Garhwal Himalaya, India*. Saarbrücken: LAP LAMBERT Academic Publishing.

Tripathi, O. P., and Khongjee, R. (2010). Effect of forest fragment size on tree diversity and population structure of humid subtropical forest of Meghalaya. *Biodivers. Sci.* 18, 208–214.

Verma, A. K., and Garkoti, S. K. (2019). Population structure, soil characteristics and carbon stock of the regenerating banj oak forests in Almora, Central Himalaya. *For. Sci. Technol.* 15, 117–127. doi: 10.1080/21580103.2019.1620135

Voroney, P. (2019). "Soils for horse pasture management," in *Horse pasture management*, ed. S. Paul (Cambridge, MA: Academic Press).

Walkley, A., and Black, J. A. (1934). Estimation of soil organic carbon by chromic acid filtration method. *Soil Sci.* 37, 38–39.

Waltham, N. J., Elliott, M., Lee, S. Y., Lovelock, C., Duarte, C. M., Buelow, C., et al. (2020). UN decade on ecosystem restoration 2021–2030—what chance for success in restoring coastal ecosystems? *Front. Mar. Sci.* 7:71. doi: 10.3389/fmars.2020.00071

Wani, Z. A., Khan, S., Bhat, J. A., Malik, A. H., Alyas, T., Pant, S., et al. (2022). Pattern of β-diversity and plant species richness along vertical gradient in Northwest Himalaya, India. *Biology* 11:1064. doi: 10.3390/biology11071064

Williams, C. H., and Steinberg, A. (1959). Soil sulphate fractions as chemical indices of available sulphur in some Australian Soils. *Aust. J. Agric. Res.* 10, 340–352.

frontiers | Frontiers in Forests and Global Change

TYPE Original Research
PUBLISHED 28 September 2023
DOI 10.3389/ffgc.2023.1204596

Isolating the effects of land use and functional variation on Yucatán's forest biomass under global change

Stephanie P. George-Chacon[1], T. Luke Smallman[2], Juan Manuel Dupuy[1], José Luis Hernández-Stefanoni[1], David T. Milodowski[2] and Mathew Williams[2]*

[1]Centro de Investigación Científica de Yucatán, Mérida, Yucatán, Mexico, [2]School of GeoSciences and NCEO, University of Edinburgh, Edinburgh, United Kingdom

OPEN ACCESS

EDITED BY
Donald Mlambo,
National University of Science and Technology, Zimbabwe

REVIEWED BY
Bhupendra Singh,
VCSG Uttarakhand University, India
Kaushal Singh,
Banda University of Agriculture and Technology, India

*CORRESPONDENCE
Mathew Williams
✉ mat.williams@ed.ac.uk

RECEIVED 12 April 2023
ACCEPTED 22 August 2023
PUBLISHED 28 September 2023

CITATION
George-Chacon SP, Smallman TL, Dupuy JM, Hernández-Stefanoni JL, Milodowski DT and Williams M (2023) Isolating the effects of land use and functional variation on Yucatán's forest biomass under global change.
Front. For. Glob. Change 6:1204596.
doi: 10.3389/ffgc.2023.1204596

Tropical forests hold large stocks of carbon in biomass and face pressures from changing climate and anthropogenic disturbance. Forests' capacity to store biomass under future conditions and accumulate biomass during regrowth after clearance are major knowledge gaps. Here we use chronosequence data, satellite observations and a C-cycle model to diagnose woody C dynamics in two dry forest ecotypes (semi-deciduous and semi-evergreen) in Yucatán, Mexico. Woody biomass differences between mature semi-deciduous (90 MgC ha^{-1}) and semi-evergreen (175 MgC ha^{-1}) forest landscapes are mostly explained by differences in climate (c. 60%), particularly temperature, humidity and soil moisture effects on production. Functional variation in foliar phenology, woody allocation, and wood turnover rate explained c. 40% of biomass differences between ecotypes. Modeling experiments explored varied forest clearance and regrowth cycles, under a range of climate and CO_2 change scenarios to 2100. Production and steady state biomass in both ecotypes were reduced by forecast warming and drying (mean biomass 2021–2100 reduced 16–19% compared to 2001–2020), but compensated by fertilisation from rising CO_2. Functional analysis indicates that trait adjustments amplify biomass losses by 70%. Experiments with disturbance and recovery across historically reported levels indicate reductions to mean forest biomass stocks over 2021–2100 similar in magnitude to climate impacts (10–19% reductions for disturbance with recovery). Forest disturbance without regrowth amplifies biomass loss by three- or four-fold. We conclude that vegetation functional differences across the Yucatán climate gradient have developed to limit climate risks. Climate change will therefore lead to functional adjustments for all forest types. These adjustments are likely to magnify biomass reductions caused directly by climate change over the coming century. However, the range of impacts of land use and land use change are as, or more, substantive than the totality of direct and indirect climate impacts. Thus the carbon storage of Yucatan's forests is highly vulnerable both to climate and land use and land use change. Our results here should be used to test and enhance land surface models use for dry forest carbon cycle assessment regionally and globally. A single plant functional type approach for modeling Yucatán's forests is not justified.

KEYWORDS

forest biomass, plant traits, carbon cycle, land surface model, chronosequence, leaf area index

1. Introduction

Tropical forests are major stores of carbon (C) in the biosphere (Mitchard, 2018) and their preservation is a key part of global efforts to avoid dangerous climate change. However, tropical forests may become significant net carbon sources in the future (Chazdon et al., 2016) driven by land use change and by climate change. Each year, large areas of tropical forests are cleared, and either left to regrow or converted to other land uses (Hansen et al., 2013). Increasing temperatures may limit the storage capacity of remaining or regrowing forests (Chazdon et al., 2016; Sullivan et al., 2020). In warmer temperatures carbon storage capacity is hypothesised to reduce with growth rates slowing under rising temperatures and increasing drought (Mitchard, 2018), countering the fertilization effect from increased concentrations of CO_2 in the atmosphere (Chazdon et al., 2016).

Tropical forests are currently estimated to be approximately carbon neutral, due to the uptake of carbon by both intact and recovering or secondary forests being roughly equal to the emissions released to the atmosphere from deforestation and forest degradation (Mitchard, 2018). However there are large uncertainties in current estimates of carbon stored in tropical forests, due to a lack of consistent estimations through time, differing estimation methods and their associated uncertainties (Pan et al., 2011; Baccini et al., 2017; Mitchard, 2018). There is evidence that tree mortality is rising with greater atmospheric water stress linked to climate change (Choat et al., 2012; Bauman et al., 2022). The rate and magnitude of carbon recovery by secondary forests are also affected by climate change and anthropogenic disturbance and remain highly uncertain (Pan et al., 2011; Mitchard, 2018).

Understanding the future of tropical forest biomass depends on identifying the importance of direct environmental controls on processes versus functional characteristics of the community. Recovery rates of forest biomass after disturbance will depend on photosynthetic activity, and the allocation of photosynthate to wood. The steady-state storage of biomass in forests will further depend on the mean residence time of wood biomass. Environmental controls on photosynthesis (temperature, rainfall, length of the dry season) (Hofhansl et al., 2015) and mortality are known to vary among different tropical species and forest types (Malhi et al., 2011; Chen et al., 2013) but are poorly characterised. Species' intrinsic residence times and fractional allocation to wood are also variable, depending on life history strategies linked to plant traits such as root to shoot ratios, wood density and bark thickness (Baker et al., 2004). The diversity of tropical forests and the decadal timescales involved argues for regionally targeted studies linked to local long term data to investigate the determinants of biomass dynamics.

This study focuses on tropical dry forests, ecosystems that develop in tropical environments where potential evapotranspiration commonly exceeds precipitation (Murphy and Lugo, 1986) and production therefore has strong seasonal cycles. Woody plants in these ecosystems tend to have higher wood densities in response to a need for higher hydraulic safety, seasonal leaf loss during dry periods, and investment in deep roots for water access in water-limited environments. Tropical dry forests sit on the moisture gradient between tropical moist forests and tropical savannas, and within dry forests there is diversity of structure and function reflecting the moisture environment. Forests adapted to wetter environments are hypothesised to be more susceptible to changes in water availability linked to climate change (Markesteijn et al., 2011; Lohbeck et al., 2013; Poorter et al., 2016). Tropical dry forests are understudied compared to other forest types, severely threatened by deforestation and degradation (Houghton, 2005) and also at risk from climate change.

The Yucatán Peninsula (YP) hosts the second largest continuous extent of tropical forest in Latin America (Dupuy et al., 2015) following the Amazon rainforest. The YP contains a complex dry tropical forest landscape with a mosaic of land uses and forest cover types. There is a precipitation gradient from the drier north west (mean annual precipitation of 500 mm) and more humid south-east (MAP 1,400 mm). Spatial difference in water availability results in three main dry forest types distinguished by their phenology (deciduous, semi-deciduous, semi-evergreen) distributed along the dry to wet gradient. Deciduous and semi-deciduous forests are found in the drier northwest. Semi-evergreen forests extend through the south-east portion (Ellis et al., 2019). The YP has a long history of forest use, shaping the landscape into a mosaic of forests in different stages of secondary succession.

Yucatán's forests are under severe anthropogenic pressure (Ellis et al., 2017). Global Forest Watch reports that Yucatán state saw disturbance to 17% of its forest cover 2001–2021 (0.85% yr^{-1}). In neighbouring Quintana Roo state 15% of its forest cover was disturbed during the same period (0.75% yr^{-1}). Independent estimates of deforestation and degradation rates across the YP suggest similar values, with a mean value of 0.9%, varying among states from 0.5 to 1.3% (Ellis et al., 2020). Annual rates of deforestation across YP vary spatially depending on land cover, protected area status, and local management practices. The interaction of varying rates of disturbance with biomass recovery under potential climate change has not been investigated nor compared to the extreme case where land use change prevents forest recovery after disturbance. Under future land use pressures, the lower limit of biomass loss would be associated with forest clearance followed by immediate forest regrowth. The upper limit of loss would occur under clearance and immediate land use change to agriculture.

In this work we address the knowledge gaps identified above by answering the following research questions (RQs):

- RQ1 What are the climate and vegetation functional characteristic controls on biomass accumulation rate and steady-state woody biomass for two dry forest ecosystem types in the Yucatán Peninsula?
- RQ2 How are steady-state biomass stocks likely to change under future environmental conditions in the YP?
- RQ3 What are the potential recovery rates and stocks of woody biomass under different frequencies of forest clearance and with immediate or no forest recovery .
- RQ4 What is the relative importance of global factors (climate and atmospheric effects) versus local factors (clearance rate with and without recovery) on the mean biomass stocks of the YP forests over the period 2021–2100?

Flack-Prain et al. (2019) investigated the drivers of variation in GPP across a moisture gradient in the tropical forests of the Amazon basin and found that indirect effects of climate via ecosystem functional characteristics accounted for 54% of variation in GPP. Direct effects of climate accounted for only 16% of observed variance. Assuming that biomass has similar sensitivity, for RQ1 we hypothesise that biomass differences between sites will be controlled primarily by functional trait differences and secondarily by climate differences. Following Flack-Prain et al. (2019), we hypothesise that phenological differences between forest types will be the most important trait controls on biomass through GPP.

For RQ2, we expect that the CO_2 fertilization effect will balance climate-driven reductions at low CO_2 emissions scenarios leading to no change in biomass, but for high CO_2 emissions scenarios we expect climate-driven reductions will be larger than CO_2 fertilisation leading to net reductions in biomass. Following the analyses of Wright et al. (2013) and Flack-Prain et al. (2019) on GPP sensitivity, we hypothesise that biomass stocks will be more sensitive to changes in climate in the more productive (semi-evergreen) forests.

For RQ3 forest mean biomass will be strongly reduced in landscapes where forest regrowth is prevented after clearance compared to landscapes where regrowth is allowed. We hypothesise the lower limit (minimum) of biomass reduction caused by forest clearance and regrowth will be relatively greater in semi-evergreen forests than semi-deciduous, related to the higher biomass in undisturbed semi-evergreen forests.

For RQ4 we hypothesise that climate change will reduce wood C stocks by 5–10% consistent with estimates from inventory data shown for YP in Sullivan et al. (2020). We further hypothesise that reductions in wood C stocks from expected forest disturbance rates (c. 1% per annum) will be of similar magnitude given recovery of biomass, but much larger given no recovery (land-use change). We expect semi-evergreen forest biomass to be more sensitive to both climate and land use than semi-deciduous.

To answer our research questions we produce a probabilistic calibration of an intermediate complexity terrestrial carbon-cycle model, DALEC (Williams et al., 2005; Bloom and Williams, 2015) with multi-decadal chronosequence data on forest age and biomass, multi-annual remote sensing estimates of leaf area index (LAI), and environmental drivers for two YP dry forest ecosystem types. We evaluate calibrated traits and biomass climate sensitivity to understand and partition controls on steady state biomass from functional characteristics and climate. We use model experiments to determine climate and land use sensitivity of biomass. Our approach has similarities to research undertaken in other biomes, for instance in boreal European forests (Smallman et al., 2017; Mäkelä et al., 2020).

The rigour of this study arises from combining multiple independent data sets (forest plot biomass chronosequences, satellite LAI time series) to produce a probabilistic calibration of a process-model for system diagnostics. The analyses for two dominant forest types within YP allows exploration of the key characteristics driving current environmental controls on biomass, providing confidence for model forecasts under environmental change across the YP. The model experiments use well founded global change scenarios for climate and CO_2. The future of land use and land use change (LULUC) in the YP could follow a variety of trajectories. To span these trajectories we explore a range of realistic forest clearance rates, and combine these with scenarios that either allow forest regrowth immediately afterwards, or prevent any regrowth (i.e. land use change). The actual impact of future LULUC will be between these two extremes.

2. Methods

The approach used to address the research questions involves using a process model of forest carbon dynamics with a record of application across many forest types, DALEC (Bloom and Williams, 2015; Smallman et al., 2021). The model is calibrated and validated with local data, and then used to (i) diagnose the C cycle of both forest types, and (ii) quantify biomass sensitivity to external forcing. The model provides a full mass balance for live and dead C pools, major biogenic fluxes and their climate and CO_2 sensitivities. The model is intermediate in complexity, with 25 calibrated parameters and seven initial conditions for state variables. This level of complexity is optimal for robust forecasting (Famiglietti et al., 2021) given available data for calibration. Model calibration is achieved with a Bayesian approach that generates posterior estimates of parameters with uncertainties. Parameter uncertainties can be propagated through model experiments into forecast uncertainties. Explicit treatment of uncertainty supports interpretation of results and robust decision making.

2.1. Study landscapes

We selected two distinct forest landscapes in the YP with chronosequence observations and which span the major YP climate gradient. These forests typically support around 100 tree species per hectare (Hernández-Stefanoni et al., 2006; Gutiérrez-Granados et al., 2011) more than half of which have commercial timber value. The hotter and more arid landscape, at Kaxil Kiuic (KK, mean air temperature 27.3°C, mean annual precipitation 1,080 mm yr^{-1}), is mostly a semi-deciduous forest ecotype, located in central YP. The KK landscape is situated between 19.61° and 20.16° North latitude and 89.27° and 89.84° West longitude. KK is situated in the transition zone between the drier north-west and the wetter south-east, and is dominated by mid-stature (8–12 m) semi-deciduous forest, but with some presence of low deciduous forest and low evergreen forest. There is some slash and burn agriculture in this landscape, but a portion is protected and fire incidence is low. The annual rate of forest cover loss during 1985–2010 was estimated at 0.85% yr^{-1} (Dai et al., 2014).

The other landscape, Felipe Carrillo Puerto (FCP), is a cooler, more humid semi-evergreen forest ecotype located in the south eastern region of the YP (MAT 26.4°C, MAP 1301 mm yr^{-1}). The FCP landscape is situated between 19.98° and 19.53° North latitude and between 88.02° and 88.60° West longitude (Figure 1). FCP is dominated by mid-stature (15–30 m) semi-evergreen forest and some low evergreen forest. The landscape has some low impact selective logging and fire incidence is low.

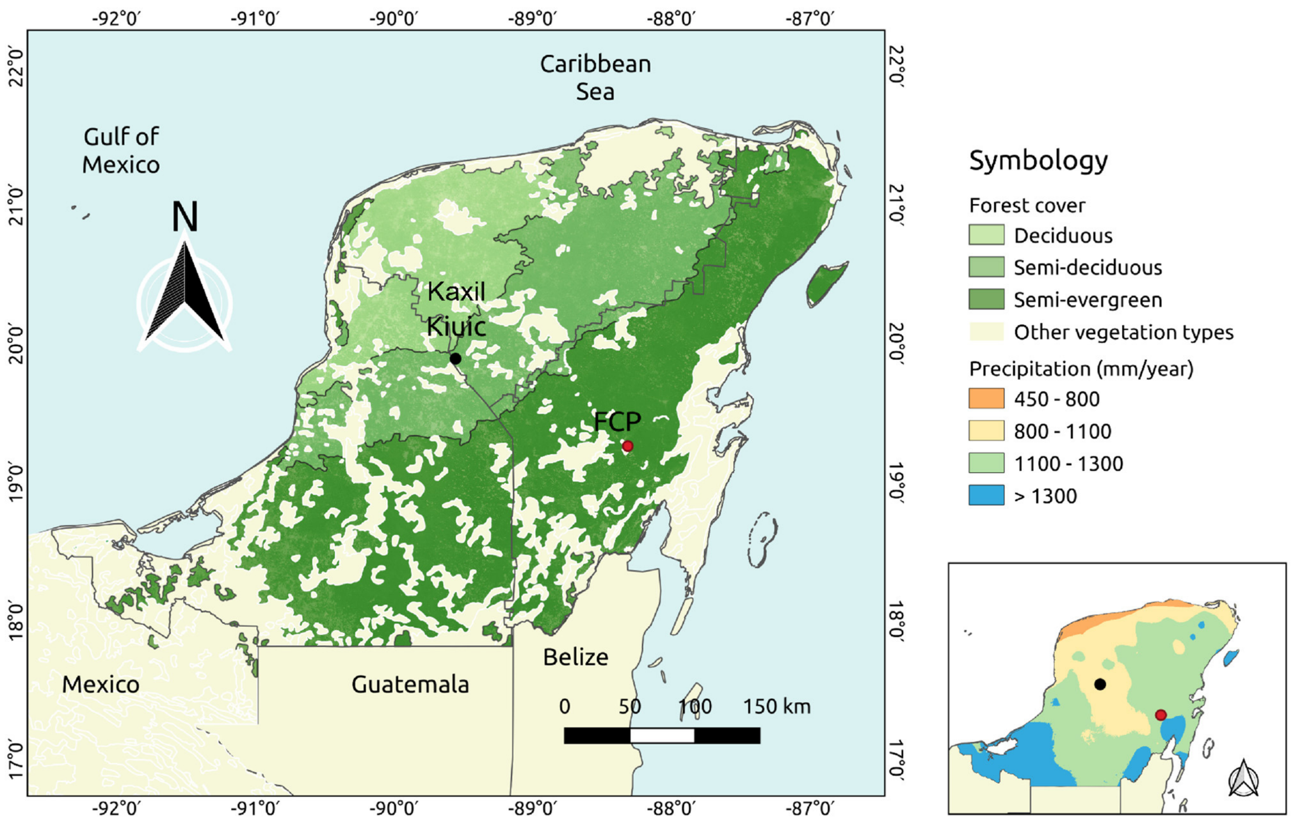

FIGURE 1
Location of study sites Kaxil Kiuic (KK) and Felipe Carrillo Puerto (FCP) land cover distiribution across the Yucatán Peninsula. The panel lower right shows total annual precipitation (mm) in the Yucatán peninsula.

2.2. Ecological data for calibrating the DALEC model

2.2.1. Woody biomass regrowth data

We obtained chronosequence (i.e. space for time substitution) data for 276 semi-deciduous forest plots within KK (Hernández-Stefanoni et al., 2011) and 86 semi-evergreen forest plots within FCP (Miranda-Plaza, 2014). Each plot covers 200 m^2 within which DBH for trees and shrubs $>$ 5 cm in DBH (measured at 1.30 m) were recorded. Total woody biomass was determined from allometric equations (Chave et al., 2005). Plot age was determined from local interviews conducted by Hernández-Stefanoni et al. (2011) and Miranda-Plaza (2014). To provide a temporally consistent time series of wood stock estimates and uncertainties we fitted these data to a logistic curve for each region.

2.3. Climate scenarios and forcing data

2.3.1. Contemporary meteorology

Contemporary meteorological drivers for the two study regions were drawn from the CRU-JRAv1.1 dataset, a 6-hourly 0.5×0.5° reanalysis (Harris, 2019). Atmospheric CO$_2$ concentration is taken from the Mauna Loa global CO$_2$ concentration (www.esrl.noaa.gov/gmd/ccgg/trends/, accessed: 22/08/2020). DALEC is driven by monthly average information on air temperature, short-wave radiation, atmospheric CO$_2$ concentration, vapour pressure deficit, and precipitation (Supplementary Figure 1). To calibrate DALEC using the chronosequence information the contemporary meteorology (2001–2017) was looped to create a time series spanning 119 years. The growth of observed biomass stocks in the chronosequence has necessarily been affected more by recent climate as all plots were measured in 2009 and 2014.

A historical fire regime was imposed on the analyses, driven by MODIS derived burned area products (Giglio et al., 2010) which have monthly and 500 m resolution. Landscape data for KK and FCP for the observational period, 2001–2017, were extracted. Similar to the meteorological drivers these data were looped to create the 119 year time series for the chronosequence simulations.

2.3.2. Future meteorology

To project modeling to 2100, future climate drivers were extracted from the UK Earth System Model (UKESM; Sellar et al., 2019) (Supplementary Figure 1). This study focuses on scenarios spanning a mean global warming of 1.7–5°C (O'Neill et al., 2016) (Supplementary Table 1). A total of six SSPs are simulated to describe the range of ecosystem response to climate change and elevated CO$_2$ concentrations. Future climate is imposed by applying the mean anomaly during the overlap period between the CRU-JRA v1.1 and the UKESM simulated climate. Historical burned area data was used as a driver into all forecasts, hence there were no changes in fire incidence.

2.3.3. Soil carbon

The SoilGrids database provided information on soil carbon stocks and texture (sand / clay fractions) (Hengl et al., 2017). The SoilGrids dataset is temporally undefined, and so is assumed to be nominally valid for the contemporary period. The soil carbon estimate provides an observational constraint on the initial soil carbon stock, i.e. January 2001. We estimated soil C stock uncertainty using the standard deviation of the spatial aggregation to 1 x 1 km (KK = 14%, FCP = 21%). We assumed no limit on rooting depth for any soils.

2.3.4. Leaf area index

Time series information on leaf area index (LAI) magnitude and uncertainty was extracted from the 1×1 km, 8-day Earth Observation (EO) product from the Copernicus Service Information (2020). We applied the maximum uncertainty value reported from the raw data used in the aggregation of each time step. The LAI observations constrained DALEC model dynamics during the observational period 2001–2017 only, to preserve coupled dynamics between LAI variations and meteorology. Based on plot location data, LAI was derived as the mean of observations across the spatial domains covered by mature rather than regrowing forests. We assessed the extracted LAI and determined there were no strong positive trends which could suggest an expanding rather than steady state canopy.

2.4. Calibration and validation of forest (re)growth

2.4.1. DALEC

We use one of the suite of related intermediate complexity terrestrial ecosystem models, DALEC (Data Assimilation Linked Ecosystem Carbon model) (Bloom and Williams, 2015; Smallman et al., 2021). The specific version has been described as M3 in Smallman et al. (2021) and C7 in Famiglietti et al. (2021). This version of DALEC represents the states and fluxes of carbon and water in the ecosystem and their exchanges with the atmosphere. Carbon uptake, via photosynthesis, is allocated to autotrophic respiration (R_a) and plant tissues based on calibrated fixed fractions. DALEC simulates four C pools in live biomass; labile (supports foliage flushing), foliage, wood, and fine roots. Turnover of biomass feeds into two dead organic matter pools (DOM). Each carbon stock and flux within the DALEC model is controlled by one or more parameters which are estimated probabilistically (Supplementary Table 2).

Foliar dynamics are controlled by a day-of-year model determining the timing for both the allocation of labile C to foliage and senescence of the foliar pool (Bloom and Williams, 2015). Plant photosynthesis and ecosystem water cycling in DALEC is simulated by the ACM-GPP-ET sub-model (Smallman and Williams, 2019). Photosynthesis is simulated as a function of leaf area index, meteorology, and soil available water supply. Soil available water supply is determined as a function of root surface area of water uptake (from fine root biomass), rooting depth (linked to woody biomass), and soil moisture content within the rooting zone. The soil water pool dynamics are a function of precipitation, interception and evaporation by the canopy, surface runoff, evaporation, drainage and transpiration by vegetation.

2.4.2. CARDAMOM calibration and validation

We use the CARbon DAta MOdel fraMework (CARDAMOM; Bloom et al., 2016) to retrieve ensembles of DALEC parameters independently for each ecotype. CARDAMOM uses a Bayesian approach within an Adaptive Proposal-Markov Chain Monte Carlo (AP-MCMC; Haario et al., 2001; Roberts and Rosenthal, 2009) to estimate the likelihood of proposed parameter sets by determining the model-observation error weighted by their uncertainties. The AP-MCMC retrieves ensembles of parameters separately for both forest types that are consistent with their observations, meteorology, and model structure. The approach used here is more fully described in Smallman et al. (2017). We use ecological and dynamical constraints (EDCs, Bloom and Williams, 2015) to prevent the acceptance of parameters that result in ecologically unrealistic C dynamics (exponential changes in the absence of disturbance) or trait combinations (e.g., root lifespans > wood lifespan). We adjusted EDCs to allow for rapid regrowth relative to the initial value by loosening the exponential change restrictions (Equation S4 in Bloom et al., 2016) with the following condition which must be met

$$|log(\frac{S_{input-yr1}}{S_{output-yr1}}| - |log(\frac{S_{input-yr2}}{S_{output-yr2}}))| < 0.2 \tag{1}$$

where $S_{input-yr1}$ is the C input to a given pool in the first year, $S_{output-yrx}$ is the C output from a given pool in year x. This test allows a sustained rapid growth but not a rapid growth in the first year followed by an immediate or rapid change to steady state in the second year. The final 17 years of the calibration period nominally correspond to 2001–2017 and include many LAI estimates to calibrate the LAI dynamics in mature forest (Supplementary Figure 2).

A validation process involved several tests including (i) the robustness of the calibrated model estimates of biomass accumulation and LAI dynamics for both forest types; (ii) consistency in identifying the correct leaf life spans; (iii) consistency of calibrations with independent data on leaf traits and litter stocks.

2.5. Analysis of historical forest states and processes (RQ1)

Calibration for the two forest types generated posterior distributions for model parameters. These parameters are linked to ecological traits and processes. The difference between the parameter priors and posteriors indicates the degree of constraint provided by the observational data on the process related to that parameter. We determine the ratio between the 95% confidence interval (CI) for the posterior distribution and the parameter prior range. Subtracting this ratio (fraction) from 1 determines the fractional reduction in the parameter prior generated by data assimilation.

A paired comparison between the two ecosystem types of each posterior parameter distribution was undertaken based on the degree of overlap, using R v3.6.3 and the "overlapping" library (Pastore, 2018). Of the trait overlaps examined, we pick out as a threshold those where overlaps < 0.5 and so are indicative of significant probabilistic differences between traits.

Model simulations, using calibrated parameters and historical climate, provide steady state C cycle estimates for both forest types. Flux and stock estimates are generated as distributions, and summarised by median estimates and 95% CI. A significant difference criteria for comparisons between forest ecotypes was based on whether the median flux and stock estimates for either type were within the 95% CI of the other. Full C cycle estimates are generated with uncertainties for both forest types.

Steady state C stocks determined using data for forest x and local climate drivers are noted as $\overline{C}_x$. To address RQ1, the parameter calibrations and ecosystem states for a forest type x were then forced using the meteorological data from the alternate type y to a new climate steady state C stock $\overline{C}_x^y$. Thus, the semi-deciduous forest calibration was forced with historical FCP climate to a new steady state wood C stock $\overline{C}_{deciduous}^{FCP}$. The shift in steady state wood biomass under each climate swap experiment was then quantified. To aid the understanding and ranking of GPP sensitivity to key traits and their related processes, we determine the parameter specific correlation with GPP (ρGPP, Supplementary Table 2).

2.6. Climate and CO_2 change experiments (RQ2)

The DALEC model with both ecotype calibrations was forced with varied climate and CO_2 projections from UKESM SSPs (Supplementary Figure 1). These experiments investigate the climate sensitivity of future C dynamics and biomass stocks. To understand the independent effects of global change on the wood C stocks of both ecotypes (RQ2), experiments estimated the effect of climate change and the increase in atmospheric CO_2 concentration separately and then combined.

2.7. Disturbance and recovery experiments (RQ3)

We undertook simulations to determine the accumulation rates of biomass during recovery after disturbance, and the effect of varied frequencies of clearance only, and clearance and forest recovery, on mean landscape wood biomass under contemporary climate (RQ3). We generated an ensemble of outputs relating mean biomass 2021–2100 to forest clearances with frequencies spanning 0.15–1.25% per annum, with or without recovery. Generating a large ensemble ensured that varied clearance dates during the 80 year period were included. A clearance resulted in 90% biomass removal imposed on a steady state simulation. An 80-member ensemble was produced by generating model outputs with a single clearance in each of 80 years between 2021 and 2100. The mean biomass of all 80 ensembles provided an estimated mean wood stock for a landscape with random 1.25% per annum cutting frequency. The more infrequent forest % clearance scenarios were then constructed by resampling the 80-member ensemble into a new set of forest landscapes with the appropriate fraction of members undergoing a single cut over the 2021–2100 period. For instance the 0.625% cutting frequency outcome was generated from combining the 80-member ensemble with an 80-member ensemble of the (same) steady state simulation. The process was repeated with and without forest regrowth to span the upper and lower limits of likely impacts.

2.8. Comparison of climate vs. disturbance factors (RQ4)

To address RQ4, we compare the results from climate and climate+CO2 experiments (RQ2, global factor assessment) against results from land use and land use change experiments (RQ3, local factor assessment). For a quantitative comparison, we directly evaluate woody biomass steady state values 2021–2100 simulated under a broad range of climate/CO2 scenarios against those simulated under a range of land use return intervals with and without regrowth. We use analyses across the SSPs to identify and separate the impact of temperature, precipitation and CO2 changes. We use analyses of forest clearances with frequencies spanning 0.15–1.25% per annum with and without regrowth to explore the upper and lower limits to biomass loss related to land use and land use change. The range of SSPs and land use scenarios ensures that uncertainty in these drivers is explicitly included in addressing this research question.

3. Results

3.1. Calibration and validation

The DALEC model calibrations for both forest types simulate C accumulation rates and magnitudes of total wood C which are consistent with estimates from the local chronosequence plot inventory data (Figure 2). The simulated accumulation remains within the age-biomass phase space defined by the chronosequence data. However, the simulated peak rate of biomass accumulation (i.e., slope of the age-biomass curve) is lower than that indicted by the mean of the semi-evergreen forest data. The apparent mean accumulation rate is too rapid for the model to explain based on process constraints. The CARDAMOM calibration process robustly reproduces the magnitudes and seasonal cycles of the LAI earth observation time series over more 17 years (Supplementary Figure 2). Over 2000–2017, at the semi-deciduous forest both satellite observations and the model simulation of LAI range between 1-6, while in semi-evergreen forest the range covered by both is from 3 to 6. The analysis is also consistent with local

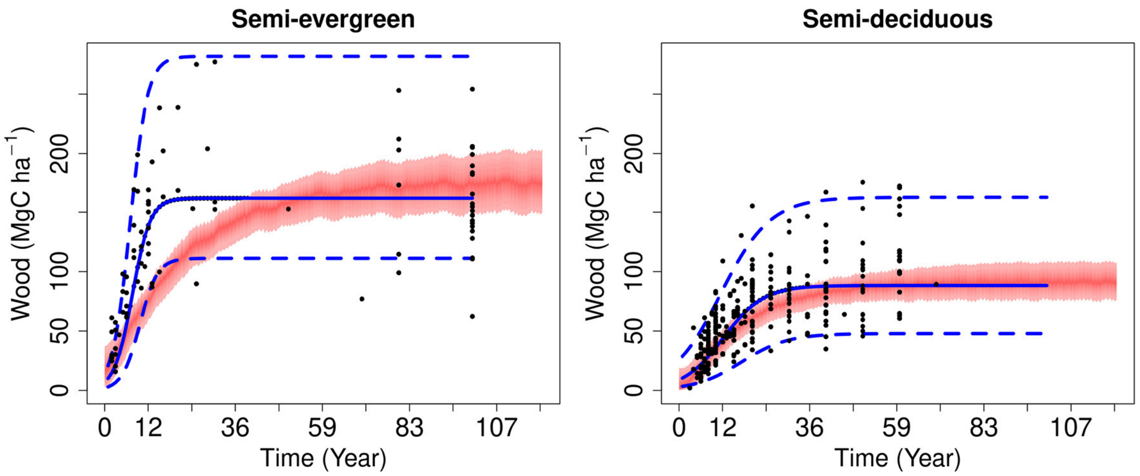

FIGURE 2
Evaluation of the model calibration of total wood C stocks over time for semi-evergreen **(left)** and semi-deciduous **(right)** forests against *in situ* data. Simulations were undertaken over 119 years, but with climate forcing from 2001 to 2017. The shaded red area indicates the 95% confidence interval on the model calibration. Solid point indicate the field data for each plot in the chronosequence. The solid blue line is the logistic function derived from the mean chronosequence data used to provide wood stock estimates to calibrate DALEC. The upper and lower estimates of the logistic curve are shown in dashed blue.

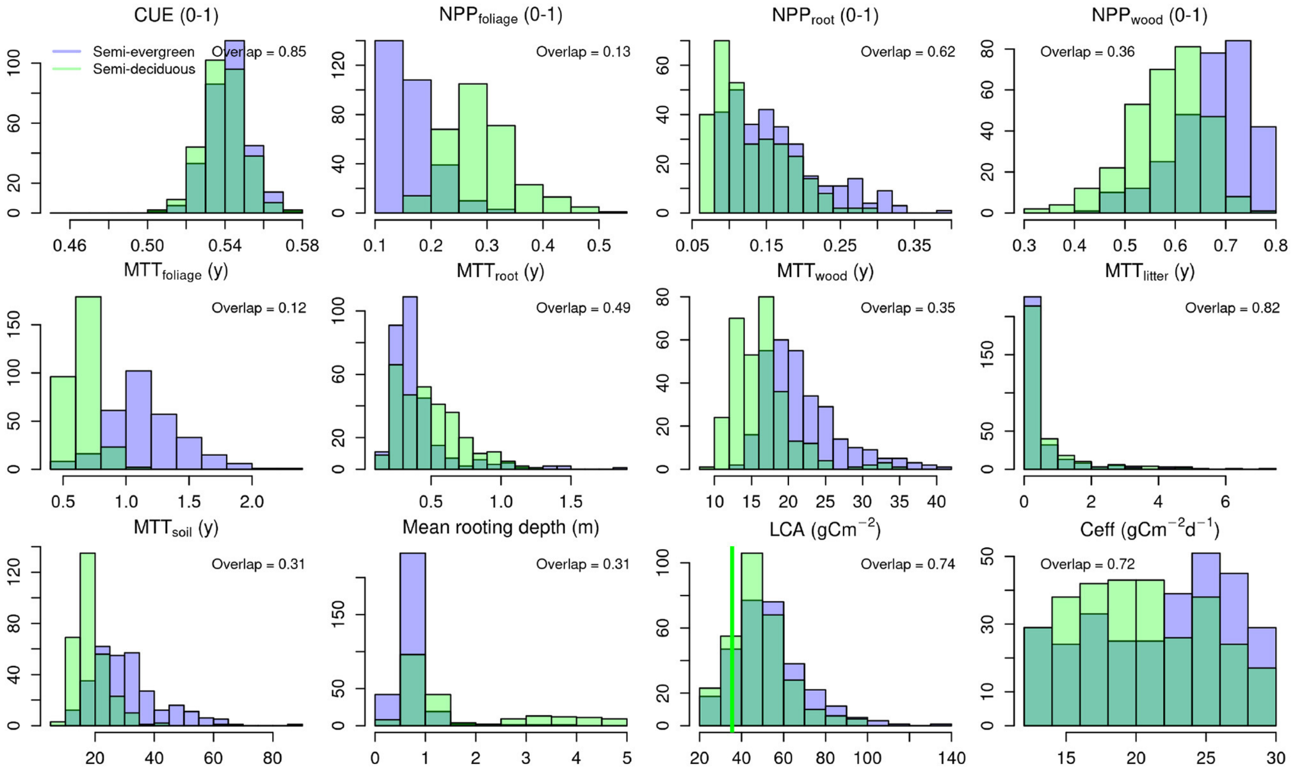

FIGURE 3
Histograms of posterior distributions of parameters and/or ecosystem traits for semi-deciduous (light green) and semi-evergreen forest ecotypes (blue). The dark green indicates overlap between ecotype distributions, quantified by the overlap statistic. Distributions includes carbon use efficiency (CUE = NPP:GPP); fraction of net primary productivity (NPP) allocated to foliage, fine roots and wood; Mean transit time (MTT) for foliage, fine roots, wood, litter and soil organic matter. The x-axis for the maximum rooting depth has been truncated for clarity by excluding 25 ensemble members (out of a sample of 300) from KK with a mean rooting depth > 5 m. The vertical green line for leaf carbon per unit leaf area (LCA) shows an independent field-based estimate of LCA for KK. Ceff is canopy efficiency of photosynthesis.

observations of LAI seasonal amplitudes and minimum values at the semi-deciduous forest (Nafarrate-Hecht et al., 2018).

Leaf C mass per area (LCA), an important leaf trait, is retrieved within CARDAMOM. The retrieved distribution of LCA for semi-deciduous forests (Figure 3) is consistent with an independent estimate of specific leaf area (inversely proportional to LCA) (Sanaphre-Villanueva et al., 2017). The model estimate of median annual aboveground foliar litter fall of 2.82 Mg C ha^{-1} well matched the independently determined values for this forest type measured in trap data (2.46–3.09 Mg C ha^{-1}) (Morffi-Mestre et al., 2020).

3.2. Analysis of historical forest states and processes (RQ1)

3.2.1. Carbon cycling in semi-deciduous and semi-evergreen forest

Both steady-state forest ecotypes have C balances near neutral, with varied levels of confidence at the 95% level (shown in parenthesis). The semi-evergreen forest is estimated to be a marginally stronger net sink (NEE = −56 (−171/ − 2) gC m^{-2} y^{-1}), while the semi-deciduous forest is closer to neutral and with a 95% confidence interval which crosses the source sink boundary (NEE = −6 (−42/5) gC m^{-2} y^{-1}) (see C cycle summaries in Supplementary Figures 3, 4).

The biosphere-atmosphere fluxes are substantively larger in the semi-evergreen forest in nearly all cases. Median gross primary productivity (GPP) is 26% higher (2360 gC m^{-2} y^{-1}) than in semi-deciduous forest (1,880 gC m^{-2} y^{-1}). Net primary production is 27% higher and significantly different in the semi-evergreen forest (NPP median estimates for both forests are not contained within the 95% CI of the other forest). Median heterotrophic respiration is 22% greater in the semi-evergreen forest, but not significantly different. Autotrophic respiration in semi-evergreen forest is 24% higher, but not significantly different. Fire has very small impacts on C exchanges in both forests under historical incidences due to low estimates of burned area recorded by MODIS across the study landscapes.

The stocks and dynamics of the wood pool show clear differences between the two forests. Absolute allocation of NPP to wood is significantly larger (47%) for the semi-evergreen forest. Allocation of NPP to foliage is 45% larger at the semi-deciduous forest but not significantly different. Allocation to the labile C pool is significantly larger (5-fold) the semi-deciduous forest. For median C stocks and mortality only in the wood pool are significant differences are found. The wood stock of the semi-evergreen forests is nearly double that of the semi-deciduous forest. Wood mortality, i.e. wood litter production, is 44% larger at the semi-evergreen forest. During the first five years of regrowth after disturbance, modeled biomass accumulation rates were 4.0 MgC ha^{-1} y^{-1} in the semi-evergreen forest compared to 2.5 MgC ha^{-1} y^{-1} in the semi-deciduous forest.

TABLE 1 Simulated steady state wood C stock estimates (MgC ha^{-1}) generated with climate drivers from either KK (drier) or FCP (wetter), with parameters (functional characteristics) for either semi-deciduous or semi-evergreen forest ecotypes.

		Climate	
		KK (drier)	FCP (wetter)
Parameters	Semi-deciduous	90.9 $\frac{74.5}{108.1}$	125.4 $\frac{103.9}{150.0}$
	Semi-evergreen	114.1 $\frac{94.6}{132.8}$	174.2 $\frac{149.2}{201.1}$

The 2.5% and 97.5% quantiles are shown as fractions.

3.2.2. Trait estimates for semi-deciduous and semi-evergreen forest

Posterior ranges on parameters show a mean 49% reduction in magnitude from the priors for both forest types, but this varies for individual parameters from 4 to 96% reductions. NPP allocation and phenology traits are well constrained (Supplementary Table 2), consistent with these traits' close connections to assimilated data (LAI, biomass time series). Litter and soil organic matter dynamics are less well constrained due to lack of direct observations on these C pools. The model calibration identifies differences in traits between the two forest types relating to allocation of NPP and turnover of C stocks (Figure 3). The semi-evergreen forest has significantly lower proportional NPP allocation to foliage (overlap = 0.13) and higher to wood (overlap = 0.36) and higher foliar residence time (overlap = 0.12) consistent with the expected differences in phenology between forest types (Figure 3). Wood residence time are significantly longer (overlap = 0.35), by 20% for the semi-evergreen forest (medians of 20 years compared to 16 years for semi-deciduous).

Sensitivity tests show that GPP is related most strongly (and positively) to the photosynthetic canopy efficiency (Ceff), maximum root depth, leaf mass per area (LCA) and leaf lifespan in that order (Supplementary Table 2). However, overlap of posterior distributions is high between ecotype Ceff trait posteriors (0.72) suggesting that production differences are not linked to divergence in this trait between forest types. Further there is limited constraint identified on this parameter (Supplementary Table 2). The calibration suggests significantly deeper rooting depths at the drier semi-deciduous forest (overlap 0.31). Estimated rooting depth in the semi-evergreen forest is ≤ 1m, while rooting depth can exceed 5 m in the semi-deciduous forest. Deeper rooting depths might be expected where lower rainfall increases the chance of soil moisture stress. Deeper rooting provides access to a larger pool of soil available moisture and therefore can sustain production in the dry season. The LCA is not significantly different between forest types (overlap 0.74) but leaf lifespans are (overlap 0.12) and this trait controls phenological expression of LAI (Supplementary Figure 2). We conclude that of the rooting depth and leaf lifespan differences between forests are the key traits controlling variation in production.

3.2.3. Sensitivity of steady state wood biomass to climate differences between forest ecotypes

The experimental exchange of climate forcing between forest ecotypes resulted in a convergence in biomass at steady states

(Table 1). With nominal climates, wood C stock in the semi-deciduous forest ($\overline{C}_{deciduous}$) is 48% of that in the semi-evergreen forest ($\overline{C}_{evergreen}$). Using the model to combine the more humid and cooler FCP climate with the semi-deciduous forest parameters increased biomass ($\overline{C}^{FCP}_{deciduous}$) by 38%. Applying the hotter and drier climate of KK to the semi-evergreen forest traits reduced steady state biomass ($\overline{C}^{KK}_{evergreen}$) by 34%. Swapping climate forcing between forests types reduces the difference in steady state biomass by 41% for KK and 72% for FCP. Thus both forest types are highly sensitive to climate change, but semi-evergreen steady biomass is more sensitive than semi-deciduous. On average, climate differences explain 57% of the wood C stock difference between forest types.

3.3. Effect of climate vs CO_2 increase on wood stocks in undisturbed forests, RQ2

Climate change scenarios alone (i.e., without CO_2 changes) reduced modeled steady-state C stocks 2021–2100 (Figure 4). Mean biomass reduction for both forest types 2021–2100 was greater under more intense climate change, increasing from 11 to 14% in SSP1-2.6 to 22-28% in SSP3-7.0 (Supplementary Figure 5). This simulated decline in wood stocks is due to reduced production. Across all six SSPs, the climate impact on mean biomass 2021–2100 was similar for both ecotypes, but slightly larger for semi-deciduous (19%) than semi-evergreen (16%).

Across the climate-only scenarios, the sensitivity of mean biomass 2021–2100 to declines in precipitation and rises in temperature and VPD were linear and of similar magnitude (Figure 5). The future changes in solar radiation were small and had insignificant effects on biomass. Rising CO_2 concentration alone increased modeled wood C stocks in both forest types (Figure 5, Supplementary Figure 5). The degree of increase was linked directly to the magnitude of CO_2 increase, with a 12–14% increase by 2100 in SSP1-2.6 rising to 35–51% in SSP3-7.0.

In full environmental (climate+CO_2) scenarios median steady-state C stocks were maintained to 2100 in the semi-deciduous forest and declined slightly (by 6–11%) in the semi-evergreen forest. There is no clear trend in net response across the gradient of change in the varied SSPs (Figure 4, Supplementary Figure 5). The fertilization of production by CO_2 broadly compensated for the decreased production arising from changing climate, although for semi-evergreen forests the median effect of climate stress outweighed the CO_2 fertilisation effect. However, for neither forest type are net impacts significant at the 95% CI.

3.4. Effect of disturbance, and disturbance and recovery, on median wood stocks, RQ3

Under contemporary climate, increasing frequencies of forest cutting result in a linear decline in mean forest biomass stocks over the period 2021–2100 for both dry forest types (Figure 5). Scenarios without forest recovery (i.e. including land use change) had markedly larger declines in mean wood biomass, three-fold greater in the semi-evergreen forest, and four-fold greater in semi-deciduous forests at clearance rates $\geq$ 0.5% per year. The relative declines without recovery were equivalent for both forest types (e.g., 50% reduction in biomass at the highest loss rate of 1.25%) as carbon stocks were driven entirely by exogeneous processes. But if regrowth was included, then biological processes resulted in a larger relative reduction in biomass for the semi-evergreen forest. The relative difference was non-linear, and varied from 28% greater loss at the highest annual clearance rates (1.25%) to 49% greater loss at clearance rates of 0.625%. More detailed analyses show that in response to a single deforestation event (90% removal) both forest types recover to a steady state consistent with their undisturbed simulations under the same environmental forcing (Supplementary Figure 6).

3.5. Effect of disturbance and climate change on median wood stocks, RQ4

The individual impacts of varied climate changes (temperature, precipitation), altered [CO_2], and disturbance frequencies that span the recent record with and without regrowth, are calculated for both forest types to determine their relative importance for wood biomass stocks across the YP over the rest of this century (2021–2100) (Figure 5). All changes in conditions and land use and land use change result in biomass losses, apart from fertilisation linked to rising [CO_2]. Changes in precipitation and temperature are challenging to evaluate individually, but analysis across the SSPs suggests the expected changes in both will have similar magnitudes of effect in reducing wood C stocks (Figure 5). Forest cutting and regrowth scenarios (up to 1.3% yr^{-1}) lead to reductions in biomass from the steady state which are similar in magnitudes to the climate effects for both forest types. Land use change effects, without forest regrowth, result in the largest overall losses of biomass for the region. Annual clearance rates $\geq$ 0.625% will result in $\geq$ 25% loss in mean biomass 2021–2100, exceeding the mean impact of the climate change scenarios.

4. Discussion

4.1. Controls on tropical dry forest aboveground biomass at steady state (RQ1)

The undisturbed semi-deciduous and semi-evergreen forests of the Yucatán peninsula are approximately carbon neutral. However, there are major differences in vegetation C cycling and stocks between forest types (Supplementary Figures 3, 4). Semi-evergreen forest is more productive (26% greater GPP) and has larger biomass stocks (91% greater). The difference in steady state wood C stock between the two dry forest types was explained primarily by climate (40–70%) with the remainder (30–60%) associated with functional trait variation between the forests (Figure 2). The hypothesis (RQ1) that climate differences would be a small driver of biomass difference is rejected. Flack-Prain et al. (2019) found that climate difference explained only 16% of GPP differences across an Amazon moisture gradient, a much lower fraction than found here for steady state biomass. The difference probably arises because steady

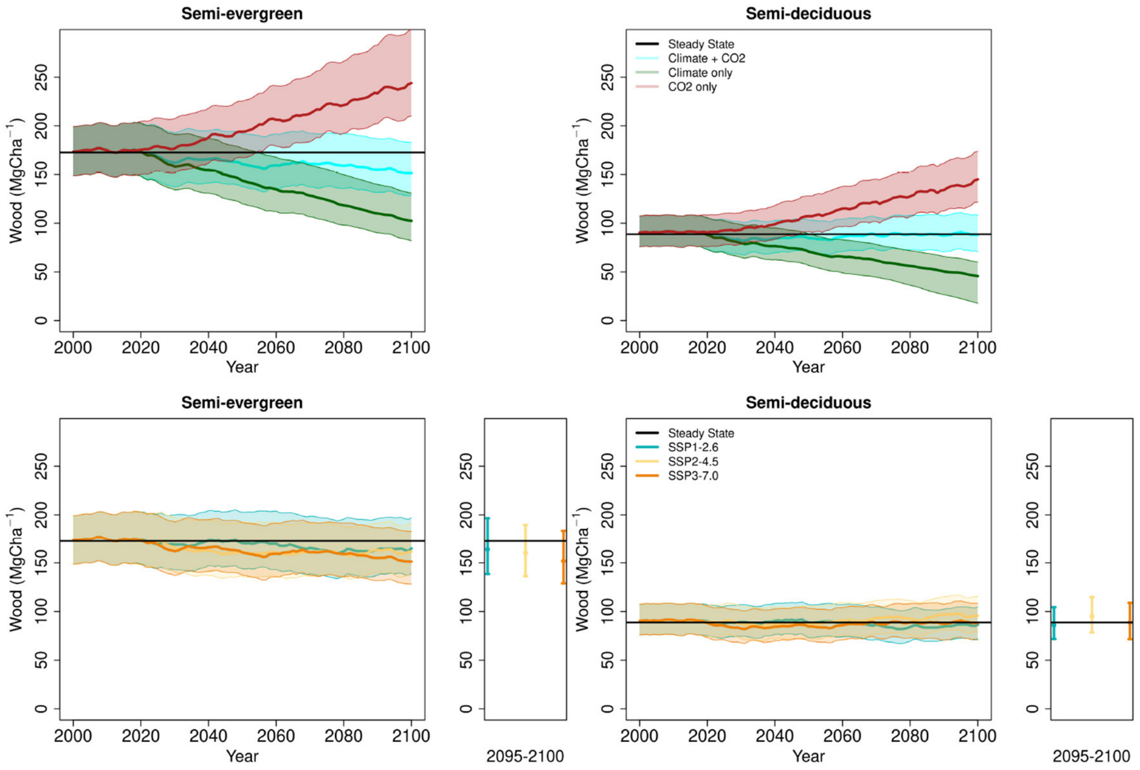

FIGURE 4
Top row, projection of wood stocks under SSP3-7.0 Wm^{-1} partitioning the separate effects of climate change and elevated atmospheric CO_2 concentrations and the combined impact. Bottom row, projections of wood stocks under three SSPs. Solid lines indicate medians and shaded areas indicate the 2.5% and 97.5% quantiles defining the 95% confidence interval. The small sub-panels indicate the stock distributions for 2095–2100.

state biomass is the outcome of decades of cumulative GPP. This long-term outcome amplifies the importance of climate effects for biomass and will be linked to the much larger difference in biomass than GPP between forest types.

For functional characteristics, the analysis indicated that higher rates of woody biomass accumulation in semi-evergreen forests were related to (i) longer leaf lifespans, leading to greater mean LAI and higher annual GPP (as hypothesised), and (ii) greater relative allocation of NPP to wood (Figure 3). These results are consistent with theories that plant traits adjust to maximise canopy carbon export over lifespan of leaves (McMurtrie and Dewar, 2011). The higher biomass steady state was linked to both the higher accumulation rates and also to the 20% longer residence times of wood.

Differences in C stocks and cycling between the two ecotypes were strongly explained (57%) by direct climate effects, but the climate effect was strongest in the more productive semi-evergreen forests (Table 1). We infer that the greater climate sensitivity for semi-evergreen forests is linked to the sensitivity of GPP to maximum rooting depth in the model (Supplementary Table 2). There are significant difference in this parameter between ecotypes, with shallower rooting for semi-evergreen forests (Figure 3) making this forest less resilient to climate stress on water supply and demand. Functional variation is also important in explaining the large divergence in wood biomass between ecotypes (42%). This result suggests functional adjustment amplifies climate sensitivity; more productive (low-risk) climates lead to increased expression of high-reward behaviors (such as retention of leaves in the dry season, reduced investment in roots), and vice versa. This conclusion is dependent on analyses from the two research areas (KK, FCP), and needs broader testing, particularly into the deciduous forests of the YP.

4.2. Sensitivity of steady state aboveground biomass to environmental change (RQ2)

The responses of semi-deciduous and semi-evergreen forest to changes of climate and CO_2 were similar. For both ecotypes there were no clear differences in net response between multiple environmental scenarios (SSPs), with similar biomass trajectories resulting (Supplementary Figure 5). Expected rises in atmospheric CO_2 alone increased biomass (Figure 4). Scenarios of climate change alone reduced biomass stocks in forests, slightly more so proportionally in the semi-deciduous forest. There was no evidence that higher CO_2 emissions combined with climate change led to different outcomes for biomass. Climate change effects arose through direct reductions in photosynthetic carboxylation through higher temperatures exceeding optimum values (i.e. $>30^oC$) and higher VPD

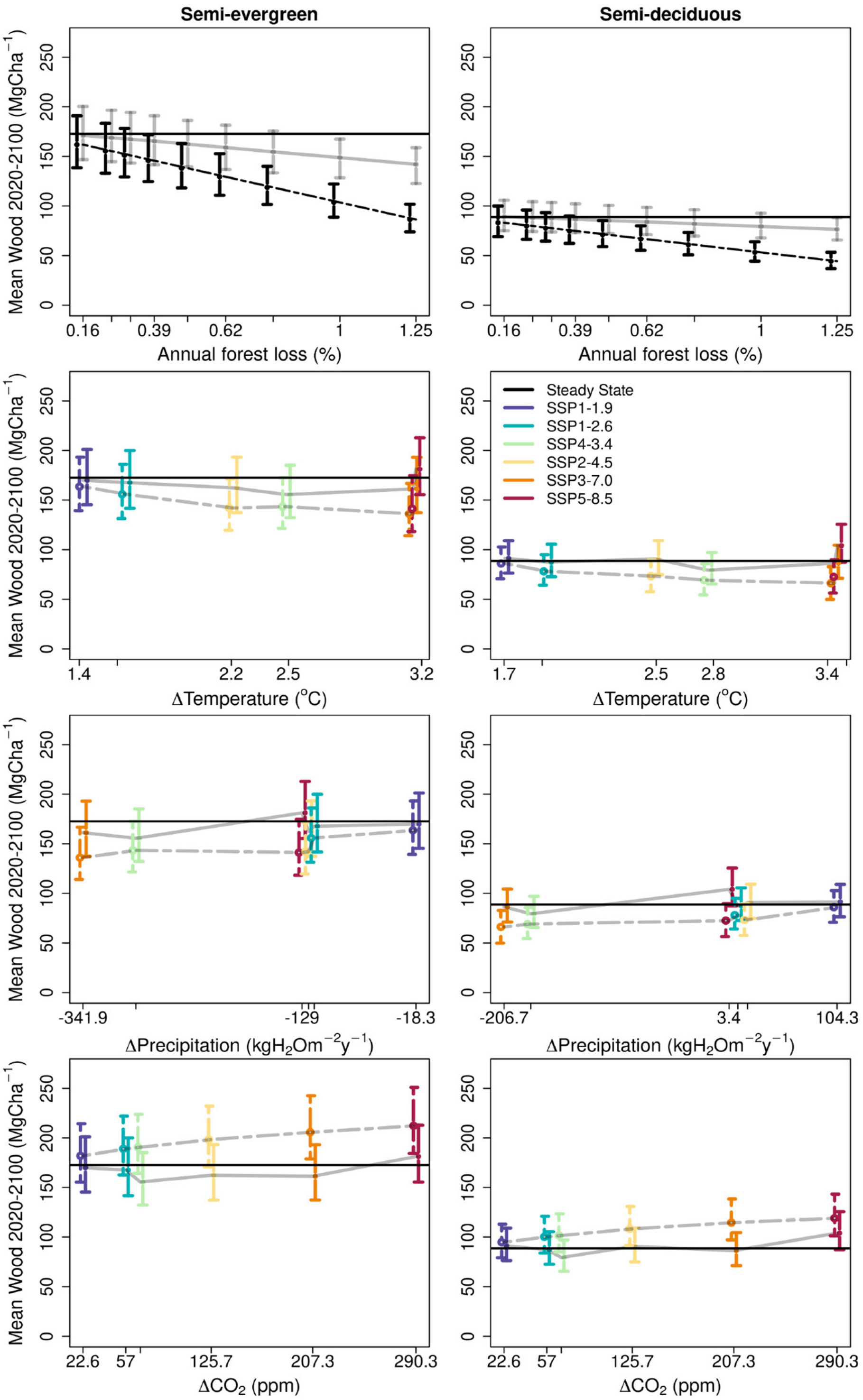

FIGURE 5
Projected impact by varied factors on mean wood C stocks (2021–2100) for two forest ecotypes assessed against current stocks (black lines). Top row: effect of forest clearance rate under contemporary climate, with regrowth (solid gray line) and without (dashed line). 95% CI indicated by error bars. Lower three rows: Environmental change impact assessed using each of 6 SSPs in the absence of disturbance. The impacts of temperature, precipitation and CO_2 enhancement are partitioned across rows. The impact is shown in coloured points (median) and error bars (95% CI) where each colour represents a SSP outcome. A grey line has been added between points to aid identification of trends across intensity. In the temperature and precipitation plots, the isolated climate-only impact is shown using the same colour scheme but using dashed lines. In the CO_2 plots the CO_2-only impact is shown using the same colour scheme but using dashed lines. In all cases the error bars have been "jittered" to reduce overlap, for clarity.

causing stomatal closure. There were also indirect effects of climate through reduced water availability, caused by reduced precipitation and high evapotranspiration, leading to stomatal closure and productivity reductions (Figure 5). Our results were consistent with climate sensitivity studies from secondary forests in latin America which indicated vulnerability to drought through growth rate reductions (de Meira Junior et al., 2020; Elias et al., 2020).

The greater future climate sensitivity for semi-deciduous forests did not match our hypothesis for RQ2, and diverged from the conclusions from RQ1 for current climate sensitivity. We conclude that future climate extremes, higher in the semi-deciduous forests (Supplementary Figure 1), were more damaging and exceeded modeled physiological thresholds more in this ecotype.

Forecasts are dependent on robust simulation of climate and CO_2 responses. The sensitivity to CO_2 is simulated based on responses incorporated in the theory of Farquhar (Farquhar and von Caemmerer, 1982). Down-regulating effects such as developing nutrient limitation (e.g., Thomas et al., 2013) are not simulated in DALEC. Enhancement in mortality in biomass C linked to climate change, particularly weather extremes and increased fire risk, is not modeled within DALEC. The forecast experiments did not specify any functional trait changes (Fisher et al., 2018). But our results suggest that the direct effects of climate change in reducing biomass stocks would be amplified by as much as 70% through indirect effects from trait adjustments (Table 1). Shifts to deciduousness and increased allocation to roots, to reduce risk from extreme climate to production, and declines in wood residence time, would lead to these further reductions in woody biomass. Our results here are consistent with broader analyses showing an acceleration of C turnover rates globally has been linked to land use change and climate change (Wu et al., 2020).

4.3. Response of forest biomass to varying disturbance frequencies (RQ3)

There was linear decline of mean biomass stocks 2021–2100 with increasing disturbance rates for both recovery and land use change scenarios (Figure 5). At typical disturbance frequencies, the effect on mean biomass stocks of land use change was three to four-fold greater than under regrowth scenarios. Supporting our hypothesis, the more productive, high biomass semi-evergreen forest had the larger relative decline in biomass compared to the semi-deciduous in the regrowth scenario. This difference is linked to the modeled rate of forest regrowth and maximum biomass of each ecotype. Our calibration of semi-evergreen forest regrowth was at the lower end of observations (Figure 2). This modeled difference between ecotypes may therefore be related to model bias for semi-evergreen forests. However, the growth rate indicated by the median fit to chronosequence data is difficult to reconcile with theoretical NPP limits in the model. Alternate versions of DALEC including density-dependent feedbacks on woody turnover were calibrated and evaluated for a better fit. However, there was no improvement and we therefore retained the simplest model version for this study, noting that recovery rate is expected to lie within the modeled 95% confidence intervals given in the calibration. While there is evidence that depletion of soil nutrients linked to land use may restrict regrowth rates in the YP (Eaton and Lawrence, 2009), such effects were not modeled here.

4.4. The relative importance of global and local change drivers on the stocks of biomass in Yucatán forests (RQ4)

Multiple independent experiments evaluated the importance to mean wood biomass across the YP of local factors, including forest clearance rates and forest functional characteristics, and global factors, including climate and CO_2 effects (Figure 5). Climate has a significant role in determination of woody biomass, and in explaining the gradients in forest biomass stocks. Climate acts through direct effects of temperature and VPD on physiological C fixation and indirectly through affecting soil moisture constraints on production. Forecast increases in temperature and VPD, and declines in precipitation (Supplementary Figure 1), will degrade the capacity of Yucatán forests to store C over the coming century (Figure 5). Across the six scenarios explored, the reduction in mean wood biomass stocks 2021–2100 ranged from 6.4 to 22.3% for semi-evergreen forests (mean 16.0%) and 5.4-27.5% for semi-deciduous forests (mean 18.2%). These levels match or exceed the estimates of biomass reduction of 5–10% over YP estimated by Sullivan et al. (2020) for a range of land surface models with a 2^{o}C rise in temperature.

Our analysis suggests that rising atmospheric CO_2 will counteract climate effects, so that combined environmental change impacts on wood biomass are small across all SSPs (Figure 4). However, these results represent the high end of expectations. Firstly, we provide evidence that functional characteristics shift towards risk reduction under climate stress. Despite CO_2 fertilisation, the rise in stress linked to temperature extremes and water supply reductions is likely to stimulate composition change and functional trait adjustment (e.g. more deciduous phenology) that will reduce mean production and thus biomass stocks (Muller-Landau et al., 2021). Monitoring of phenological changes in dry forests could provide data to test this hypothesis. Increases in fire, currently at a low level, are likely in warmer conditions and would increase wood mortality, and reduce biomass. Finally, CO_2 fertilisation is modeled at its potential; other physiological factors are likely to be limiting, including rates of nitrogen and phosphorus cycling. CO_2 fertilisation experiments in tropical forests will help to resolve this uncertainty. Our results here would support more robust assessment of land surface models used for regional and global assessment (Fernández-Martínez et al., 2019). Specifically, these results could evaluate for this region (i) the climate and CO2 sensitivity of these models, and (ii) their recovery from disturbance. Most land surface models use plant functional type concepts to simplify their regional parameterisation. Our results here emphasise important functional differences within a single region. Ultimately land surface models have to be adapted to reflect this diversity in ecology.

Forest clearance has direct effects on mean landscape biomass, even with fast biomass recovery rates. Ongoing forest clearance (with subsequent recovery) at historical rates of 0.9% yr^{-1} (Ellis et al., 2020) over the coming century generates substantive reductions in mean biomass over the period 2021–2100 (Figure 5). With annual cutting frequencies of 0.78–1.25%, comparable to contemporary observations, reductions in steady biomass over the period 2021–2100 are forecast to be 11.5–18.7% in the semi-evergreen and 9.8–16.0% for the semi-deciduous forests. Reductions in biomass will be three to four-fold larger without forest regrowth. Historical records indicate that both forestry, swidden agriculture and land use change is active in the YP, so the likely future impact of land use and land use change will be somewhere between the limits of the best-scenario rates of forest clearance modeled with and without regrowth. We conclude that declines in mean wood stocks over YP landscapes linked to likely rates of forest clearance with subsequent regrowth are of similar magnitude to declines independently associated with climate change. Both climate impacts and land use impacts will be larger than these lower bounds due to functional characteristic changes in forests (70% amplification) and land use change (300–400% amplification).

5. Conclusions

Future changes in climate and land use will put biomass C storage of Yucatán's forests at risk. We have identified substantial climate sensitivity of production in these ecosystems. Future climate will lead to temperature optima being exceeded, and higher VPD and reduced soil moisture causing stomatal closure. CO_2 fertilisation may offset the negative effects of changing climate, but modeling here assumes the most optimistic theoretical effects. The detrimental effects of climate change on forest biomass in the Yucatán increase with levels of rising CO_2, because higher CO_2 is linked to extremes of temperature and VPD. Adjustment of forest traits to climate change, particularly shifts to deciduousness and increased allocation to roots, is a likely response to climate change. These shifts will reduce risks to production but also reduce overall production. The result is that climate-change-driven trait changes may magnify direct climate change reductions to production, and therefore generate further reductions in biomass stocks. These results should be used to test the sensitivity and inform the development and calibration of land surface models for dry tropical biomes. Broader testing of these conclusions across other dry tropical forests can further evaluate the role of biodiversity and vegetation composition in ecosystem climate sensitivity (Muller-Landau et al., 2021). Forest clearance and regrowth linked to patterns of historical land use generates reductions in mean biomass C storage over 2021-2100. These changes are similar in magnitude and within the ranges of expected effects of climate change. Hence both these local and global drivers of change must be taken into account in sustaining the biomass of the Yucatán. Land use change will magnify biomass losses three to four-fold if forests cannot recover post-clearance. Maintaining C storage in Yucatán's forests therefore depends both on limiting levels of land use change, and on meeting the objectives of the Paris Climate Agreement to protect biomass against climate change risks.

Data availability statement

Existing datasets are available in a publicly accessible repository: Datasets used in this study can be found here: [https://doi.org/10.7488/ds/3858]. Analysis source codes for CARDAMOM and DALEC source codes are available on request: Access is provided by Github repository (https://github.com/GCEL/CARDAMOM), access will be made available by the authors, without undue reservation.

Author contributions

SG-C: conceptualization, investigation, formal analysis, and writing original draft. TS: conceptualization, methodology, software, visualization, formal analysis, and reviewing and editing. JD and JH-S: investigation, resources, and reviewing and editing. DM: methodology and reviewing and editing. MW: conceptualization, funding acquisition, supervision, formal analysis, and writing original draft. All authors contributed to the article and approved the submitted version.

Funding

Funding was provided by UK Space Agency Forests 2020 and UK National Centre for Earth Observation.

Acknowledgments

We thank Jessie Au and Matus Seci for helpful comments on the manuscript and Tim Green for useful discussions. This work has made use of the resources provided by the Edinburgh Compute and Data Facility (ECDF) (http://www.ecdf.ed.ac.uk/).

Conflict of interest

The authors declare that the research was conducted in the absence of any commercial or financial relationships that could be construed as a potential conflict of interest.

Publisher's note

Supplementary material

The Supplementary Material for this article can be found online at: https://www.frontiersin.org/articles/10.3389/ffgc.2023.1204596/full#supplementary-material

References

Baccini, A., Walker, W., Carvalho, L., Farina, M., Sulla-Menashe, D., and Houghton, R. (2017). Tropical forests are a net carbon source based on aboveground measurements of gain and loss. *Science* 358, 230–234. doi: 10.1126/science.aam5962

Baker, T. R., Phillips, O. L., Malhi, Y., Almeida, S., Arroyo, L., Di Fiore, A., et al. (2004). Increasing biomass in amazonian forest plots. *Philos. Trans. R. Soc. Lond., B, Biol. Sci.* 359:353–365. doi: 10.1098/rstb.2003.1422

Bauman, D., Fortunel, C., Delhaye, G., Malhi, Y., Cernusak, L. A., Bentley, L. P., et al. (2022). Tropical tree mortality has increased with rising atmospheric water stress. *Nature* 608, 528–533. doi: 10.1038/s41586-022-04737-7

Bloom, A., Exbrayat, J.-F., Velde, I. R., Feng, L., and Williams, M. (2016). The decadal state of the terrestrial carbon cycle: global retrievals of terrestrial carbon allocation, pools and residence times. *Proc. Nat. Acad. Sci.* 113, 1285–1290. doi: 10.1073/pnas.1515160113

Bloom, A. A., and Williams, M. (2015). Constraining ecosystem carbon dynamics in a data-limited world: integrating ecological "common sense" in a model-data-fusion framework. *Biogeosciences* 12, 1299–1315. doi: 10.5194/bg-12-1299-2015

Chave, J., Andalo, C., Brown, S., Cairns, M. A., Chambers, J. Q., Eamus, D., et al. (2005). Tree allometry and improved estimation of carbon stocks and balance in tropical forests. *Oecologia* 145, 87–99. doi: 10.1007/s00442-005-0100-x

Chazdon, R. L., Broadbent, E. N., Rozendaal, D. M. A., Bongers, F., Zambrano, A. M. A., Aide, T. M., et al. (2016). Carbon sequestration potential of second-growth forest regeneration in the latin american tropics. *Sci. Adv.* 2, e1501639. doi: 10.1126/sciadv.1501639

Chen, G., Yang, Y., and Robinson, D. (2013). Allocation of gross primary production in forest ecosystems: allometric constraints and environmental responses. *New Phytol.* 200, 1176–1186. doi: 10.1111/nph.12426

Choat, B., Jansen, S., Brodribb, T. J., Cochard, H., Delzon, S., Bhaskar, R., et al. (2012). Global convergence in the vulnerability of forests to drought. *Nature* 491, 752–755. doi: 10.1038/nature11688

Dai, Z., Birdsey, R. A., Johnson, K. D., Dupuy, J. M., Hernandez-Stefanoni, J. L., and Richardson, K. (2014). Modeling carbon stocks in a secondary tropical dry forest in the yucatan peninsula, mexico. *Water, Air, Soil Pollut.* 225, 1–15. doi: 10.1007/s11270-014-1925-x

de Meira Junior, M. S., Pinto, J. R. R., Ramos, N. O., Miguel, E. P., Gaspar, R., d,. O., et al. (2020). The impact of long dry periods on the aboveground biomass in a tropical forest: 20 years of monitoring. *Carbon Balance Manag.* 15:1–14. doi: 10.1186/s13021-020-00147-2

Dupuy, J., Durn Garca, R., Garca Contreras, G., Arellano Morin, J., Acosta Lugo, E., Mndez Gonzlez, M., et al. (2015). *Chapter 8: Conservation and Use*. Cham: Springer.

Eaton, J. M., and Lawrence, D. (2009). Loss of carbon sequestration potential after several decades of shifting cultivation in the southern yucatn. *For. Ecol. Manage.* 258, 949–958. doi: 10.1016/j.foreco.2008.10.019

Elias, F., Ferreira, J., Lennox, G. D., Berenguer, E., Ferreira, S., Schwartz, G., et al. (2020). Assessing the growth and climate sensitivity of secondary forests in highly deforested amazonian landscapes. *Ecology* 101, e02954. doi: 10.1002/ecy.2954

Ellis, E. A., Montero, J., Gmez, I. U. H., Porter-Bolland, L., and Ellis, P. W. (2017). Private property and mennonites are major drivers of forest cover loss in central yucatan peninsula, mexico. *Land Use Policy* 69:474–484. doi: 10.1016/j.landusepol.2017.09.048

Ellis, E. A., Montero, S. A., Gmez, I. U. H., Montero, J. A. R., Ellis, P. W., Rodr-guez-Ward, D., et al. (2019). Reduced-impact logging practices reduce forest disturbance and carbon emissions in community managed forests on the yucatn peninsula, mexico. *For. Ecol. Manage.* 437, 396–410. doi: 10.1016/j.foreco.2019.01.040

Ellis, E. A., Navarro Mart-nez, A., Garc-a Ortega, M., Hernndez Gmez, I. U., and Chacn Castillo, D. (2020). Forest cover dynamics in the selva maya of central and southern quintana roo, mexico: deforestation or degradation? *J. Land Use Sci.* 15, 25–51. doi: 10.1080/1747423X.2020.1732489

Famiglietti, C. A., Smallman, T. L., Levine, P. A., Flack-Prain, S., Quetin, G. R., Meyer, V., et al. (2021). Optimal model complexity for terrestrial carbon cycle prediction. *Biogeosciences* 18, 2727–2754. doi: 10.5194/bg-18-2727-2021

Farquhar, G., and von Caemmerer, S. (1982). "Modeling of photosynthetic response to the environment," in *Encyclopedia of Plant Physiology*. Berlin: Springer-Verlag, p. 549–587.

Fernández-Martínez, M., Sardans, J., Chevallier, F., Ciais, P., Obersteiner, M., Vicca, S., et al. (2019). Global trends in carbon sinks and their relationships with co2 and temperature. *Nat. Clim. Chang.* 9, 73–79. doi: 10.1038/s41558-018-0367-7

Fisher, R. A., Koven, C. D., Anderegg, W. R., Christoffersen, B. O., Dietze, M. C., Farrior, C. E., et al. (2018). Vegetation demographics in earth system models: a review of progress and priorities. *Glob. Chang. Biol.* 24, 35–54. doi: 10.1111/gcb.13910

Flack-Prain, S., Meir, P., Malhi, Y., Smallman, T. L., and Williams, M. (2019). The importance of physiological, structural and trait responses to drought stress in driving spatial and temporal variation in gpp across amazon forests. *Biogeosciences* 16, 4463–4484. doi: 10.5194/bg-16-4463-2019

Giglio, L., Randerson, J. T., van der Werf, G. R., Kasibhatla, P. S., Collatz, G. J., Morton, D. C., et al. (2010). Assessing variability and long-term trends in burned area by merging multiple satellite fire products. *Biogeosciences* 7, 1171–1186. doi: 10.5194/bg-7-1171-2010

Gutiérrez-Granados, G., Prez-Salicrup, D. R., and Dirzo, R. (2011). Differential diameter-size effects of forest management on tree species richness and community structure: implications for conservation. *Biodivers. Conserv.* 20, 1571–1585. doi: 10.1007/s10531-011-0046-8

Haario, H., Saksman, E., and Tamminen, J. (2001). An adaptive metropolis algorithm. *Bernoulli* 7, 223–242. doi: 10.2307/3318737

Hansen, M. C., Potapov, P. V., Moore, R., Hancher, M., Turubanova, S. A., Tyukavina, A., et al. (2013). High-resolution global maps of 21st-century forest cover change. *Science* 342, 850–853. doi: 10.1126/science.1244693

Harris, I. (2019). *Cru jra v1.1: A Forcings Dataset of Gridded Land Surface Blend of Climatic Research Unit (CRU) and Japanese Reanalysis (JRA) Data; Jan.1901–Dec.2017*. Centre for Environmental Data Analysis.

Hengl, T., Mendes de Jesus, J., Heuvelink, G. B., Ruiperez Gonzalez, M., Kilibarda, M., Blagoti, A., et al. (2017). Soilgrids250m: global gridded soil information based on machine learning. *PLoS ONE* 12, e0169748. doi: 10.1371/journal.pone.0169748

Hernández-Stefanoni, J. L., Dupuy, J. M., Tun-Dzul, F., and May-Pat, F. (2011). Influence of landscape structure and stand age on species density and biomass of a tropical dry forest across spatial scales. *Landsc. Ecol.* 26, 355–370. doi: 10.1007/s10980-010-9561-3

Hernández-Stefanoni, J. L., Pineda, J. B., and Valdes-Valadez, G. (2006). Comparing the use of indigenous knowledge with classification and ordination techniques for assessing the species composition and structure of vegetation in a tropical forest. *Environ. Manage.* 37, 686–702. doi: 10.1007/s00267-004-0371-8

Hofhansl, F., Schnecker, J., Singer, G., and Wanek, W. (2015). New insights into mechanisms driving carbon allocation in tropical forests. *New Phytol.* 205, 137–146. doi: 10.1111/nph.13007

Houghton, R. (2005). Aboveground forest biomass and the global carbon cycle. *Glob. Chang. Biol.* 11, 945–958. doi: 10.1111/j.1365-2486.2005.00955.x

Lohbeck, M., Poorter, L., Lebrija-Trejos, E., Mart-nez-Ramos, M., Meave, J. A., Paz, H., et al. (2013). Successional changes in functional composition contrast for dry and wet tropical forest. *Ecology* 94, 1211–1216. doi: 10.1890/12-1850.1

Mäkelä, J., Minunno, F., Aalto, T., Mäkelä, A., Markkanen, T., and Peltoniemi, M. (2020). Sensitivity of 21st century simulated ecosystem indicators to model parameters, prescribed climate drivers, rcp scenarios and forest management actions for two finnish boreal forest sites. *Biogeosciences* 17, 2681–2700. doi: 10.5194/bg-17-2681-2020

Malhi, Y., Doughty, C., and Galbraith, D. (2011). The allocation of ecosystem net primary productivity in tropical forests. *Philos. Trans. R. Soc. Lond., B, Biol. Sci.* 366, 3225–3245. doi: 10.1098/rstb.2011.0062

Markesteijn, L., Poorter, L., Bongers, F., Paz, H., and Sack, L. (2011). Hydraulics and life history of tropical dry forest tree species: coordination of species" drought and shade tolerance. *New Phytol.* 191, 480–495. doi: 10.1111/j.1469-8137.2011.03708.x

McMurtrie, R. E., and Dewar, R. C. (2011). Leaf-trait variation explained by the hypothesis that plants maximize their canopy carbon export over the lifespan of leaves. *Tree Physiol.* 31, 1007–1023. doi: 10.1093/treephys/tpr037

Miranda-Plaza, E. A. (2014). *Factores que afectan la estructura de la vegetacin en dos paisajes del bosque tropical seco de la Pen-nsula de Yucatn (2014–04)* (Master's thesis). Centro de Investigacion Cientifica de Yucatan, Mérida, Mexico. Available online at: https://cicy.repositorioinstitucional.mx/jspui/handle/1003/1027

Mitchard, E. T. (2018). The tropical forest carbon cycle and climate change. *Nature* 559, 527. doi: 10.1038/s41586-018-0300-2

Morffi-Mestre, H., ngeles Prez, G., Powers, J. S., Andrade, J. L., Huechacona Ruiz, A. H., May-Pat, F., et al. (2020). Multiple factors influence seasonal and interannual litterfall production in a tropical dry forest in mexico. *Forests* 11, 12. doi: 10.3390/f11121241

Muller-Landau, H. C., Cushman, K., Arroyo, E. E., Martinez Cano, I., Anderson Teixeira, K. J., and Backiel, B. (2021). Patterns and mechanisms of spatial variation in tropical forest productivity, woody residence time, and biomass. *New Phytol.* 229, 3065–3087. doi: 10.1111/nph.17084

Murphy, P. G., and Lugo, A. E. (1986). Ecology of tropical dry forest. *Annu. Rev. Ecol. Evol. Syst.* 17, 67–88. doi: 10.1146/annurev.es.17.110186.000435

Nafarrate-Hecht, A. C., Dupuy-Rada, J. M., George-Chacon, S. P., and Hernndez-Stefanoni, J. L. (2018). Modeling of seasonal leaf area index values in a tropical dry forest using high resolution satellite imagery. *Madera y bosques* 24, 3. doi: 10.21829/myb.2018.2431666

O'Neill, B. C., Tebaldi, C., Van Vuuren, D. P., Eyring, V., Friedlingstein, P., Hurtt, G., et al. (2016). The scenario model intercomparison project (scenariomip) for cmip6. *Geosci. Model Dev*. 9, 3461–3482. doi: 10.5194/gmd-9-3461-2016

Pan, Y., Birdsey, R. A., Fang, J., Houghton, R., Kauppi, P. E., Kurz, W. A., et al. (2011). A large and persistent carbon sink in the world's forests. *Science* 333, 988–993. doi: 10.1126/science.1201609

Pastore, M. (2018). Overlapping: a r package for estimating overlapping in empirical distributions. *J. Open Source Softw*. 3, 1023. doi: 10.21105/joss.01023

Poorter, L., Bongers, F., Aide, T. M., Almeyda Zambrano, A. M., Balvanera, P., Becknell, J. M., et al. (2016). Biomass resilience of neotropical secondary forests. *Nature* 530, 211–214. doi: 10.1038/nature16512

Roberts, G. O., and Rosenthal, J. S. (2009). Examples of adaptive mcmc. *J. Comput. Graph. Stat*. 18, 349–367. doi: 10.1198/jcgs.2009.06134

Sanaphre-Villanueva, L., Dupuy, J. M., Andrade, J. L., Reyes-Garc-a, C., Jackson, P. C., and Paz, H. (2017). Patterns of plant functional variation and specialization along secondary succession and topography in a tropical dry forest. *Environm. Res. Lett*. 12, 055004. doi: 10.1088/1748-9326/aa6baa

Sellar, A. A., Jones, C. G., Mulcahy, J. P., Tang, Y., Yool, A., Wiltshire, A., et al. (2019). Ukesm1: Description and evaluation of the uk earth system model. *J.Adv. Model. Earth Syst*. 11, 4513–4558.

Smallman, T., Exbrayat, J., Mencuccini, M., Bloom, A., and Williams, M. (2017). Assimilation of repeated woody biomass observations constrains decadal ecosystem carbon cycle uncertainty in aggrading forests. *J. Geophys. Res.: Biogeosci*. 122, 528–545. doi: 10.1002/2016JG003520

Smallman, T. L., Milodowski, D. T., Neto, E. S., Koren, G., Ometto, J., and Williams, M. (2021). Parameter uncertainty dominates c cycle forecast errors over most of brazil for the 21st century. *Earth Syst. Dynam. Discuss*. 2021, 1–52. doi: 10.5194/esd-2021-17

Smallman, T. L., and Williams, M. (2019). Description and validation of an intermediate complexity model for ecosystem photosynthesis and evapotranspiration: Acm-gpp-etv1. *Geosci. Model Dev*. 12, 2227–2253. doi: 10.5194/gmd-12-2227-2019

Sullivan, M. J. P., Lewis, S. L., Affum-Baffoe, K., Castilho, C., Costa, F., Sanchez, A. C., et al. (2020). Long-term thermal sensitivity of earth's tropical forests. *Science* 368, 869–874. doi: 10.1126/science.aaw7578

Thomas, R. Q., Zaehle, S., Templer, P. H., and Goodale, C. L. (2013). Global patterns of nitrogen limitation: confronting two global biogeochemical models with observations. *Glob. Chang. Biol*. 19, 2986–2998. doi: 10.1111/gcb.12281

Williams, M., Schwarz, P., Law, B. E., Irvine, J., and Kurpius, M. R. (2005). An improved analysis of forest carbon dynamics using data assimilation. *Glob. Chang. Biol*. 11, 89–105. doi: 10.1111/j.1365-2486.2004.00891.x

Wright, J., Williams, M., Starr, G., McGee, J., and Mitchell, R. (2013). Measured and modeled leaf and stand"?scale productivity across a soil moisture gradient and a severe drought. *Plant Cell Environ*. 36, 467–483. doi: 10.1111/j.1365-3040.2012.02590.x

Wu, D., Piao, S., Zhu, D., Wang, X., Ciais, P., Bastos, A., et al. (2020). Accelerated terrestrial ecosystem carbon turnover and its drivers. *Glob. Chang. Biol*. 26, 5052–5062. doi: 10.1111/gcb.15224

frontiers | Frontiers in Forests and Global Change

TYPE Original Research
PUBLISHED 14 November 2023
DOI 10.3389/ffgc.2023.1192382

EDITED BY
Donald Mlambo,
National University of Science and Technology, Zimbabwe

REVIEWED BY
Gopal Shukla,
Uttar Banga Krishi Viswavidyalaya, India
Bhupendra Singh,
VCSG Uttarakhand University, India

*CORRESPONDENCE
Nazir A. Pala
✉ nazirpaul@gmail.com

RECEIVED 23 March 2023
ACCEPTED 30 August 2023
PUBLISHED 14 November 2023

CITATION
Saleem I, Mugloo JA, Pala NA, Bhat GM, Masoodi TH, Mughal AH, Baba AA and Mehraj B (2023) Biomass production, carbon stock and sequestration potential of prominent agroforestry systems in north-western Himalaya, India.
Front. For. Glob. Change 6:1192382.
doi: 10.3389/ffgc.2023.1192382

Biomass production, carbon stock and sequestration potential of prominent agroforestry systems in north-western Himalaya, India

Ishrat Saleem[1], J. A. Mugloo[2], Nazir A. Pala[1]*, G. M. Bhat[1], T. H. Masoodi[3], A. H. Mughal[3], Afshan A. Baba[4] and Basira Mehraj[5]

[1]Division of Silviculture and Agroforestry, Faculty of Forestry SKUAST-K, Malangpora, Jammu and Kashmir, India, [2]KVK, Directorate of Research, Malangpora, Jammu and Kashmir, India, [3]Directorate of Research, Malangpora, Jammu and Kashmir, India, [4]Division of FPU, Malangpora, Jammu and Kashmir, India, [5]Division of NRM-SKUAST-Kashmir, Srinagar, Jammu and Kashmir, India

Agroforestry is an age-old practise of integrating farming with practises, preferably on the same unit of land on sustainable basis. There is tremendous scope for Agroforestry because India has achieved self-sufficiency in food production. Now its attention is becoming more focused on the ecological problems and shortage of fuel, fodder and other outputs as well as unemployment. So, agroforestry land use systems offer a better option by serving as carbon sinks and contributing in attaining food safety, subsistence income, and habitat amelioration. The current study was conducted in this context in the south Kashmir area of India with the objective of recognising the capability of various agroforestry systems for biomass estimation and carbon sequestration assessment for mitigating climate variation. The present study entitled "Biomass production, carbon stock and sequestration potential of prominent agroforestry systems in North-western Himalaya, India" was carried out, during 2018–2019. The study site is located between 33° 72′N and 75° 14′E at an altitude ranging from 2,900 to 5,900 M (amsl). Multistage random sampling technique was used for selection of sampled tehsils, blocks, villages and farmers in Anantnag district. The first stage was the random sampling of six tehsils namely Anantnag, Shangus, Kokernag, Dooru, Sallar, and Larnu and blocks per tehsil namely, viz.; Anantnag, Shangus, Sagam, Shahabad, Pahalgam and Larnu. Then four villages within each block like Anantnag (Ruhoo, Dialgam, Wanihama and Donipawa), Shangus (Shangus, Nowgam, Kutheir and Andoora), Sagam (Hiller, Khalhar, Sagam and Bidder), Shahabad (Larkipora, Shankerpora, Nathipora and Bragam), Pahalgam (Yanner, Charigam, Movra and Wahdan) and Larnu (Leesu, Dandipora, Bidhard and Larnu). Ten farmers within each village were selected, thus making a total of 240 farmers, which accounts 25% sampling intensity. Four agroforestry systems including horti-agriculture, agrisilviculture, (boundary planting), agri-horti-silviculture and horti-silvipasture were chosen for the study as the experimental configuration. Maximum biomass was found in horti-silvipastoral contributing 66.55 t ha^{-1} followed by agri-horti-silviculture as 50.18 t ha^{-1}, horti-agriculture as 36.22 t ha^{-1} and agri-silviculture as 34.87 t ha^{-1}. The maximum mean biomass of fruit trees (30.54 t ha^{-1}), forest trees (25.19 t ha^{-1}), grass (7.18 t ha^{-1}) during the first cut and 3.64 t ha^{-1} during the second cut, was calculated in horti-silvipasture system. The overall biomass output of diverse agroforestry systems goes along with the sequence: horti-silvipasture > agri-horti-silviculture > horti-agriculture > boundary plantation, respectively. As a result, estimates of carbon stocks and carbon sequestration for all systems showed the same trend as values for biomass since they are both directly related to the capacity for biomass generation of various plant components. By providing for rural livelihoods and serving as an efficient carbon sink through carbon sequestration, these agroforestry systems in the Himalayas can significantly increase total production and productivity. The results of the current study could have a big impact on how alternative agroforestry systems and tree combinations are chosen for efficient carbon budget management in delicate Himalayan ecosystems.

KEYWORDS

Himalaya, climate, landuse, energy, greenhouse

1. Introduction

In the modern era of global warming, interconnected climate indicators provide a comprehensive view of climate change and the rising threats to the Sustainable Development Goals (SDGs) affecting environmental, social, and economic systems. Carbon dioxide (CO2) is the principal greenhouse gas (GHG) produced as a result of anthropogenic activity and the cumulative impact of humans during the past, along with industrialisation (Malhi et al., 2021; Zandalinas et al., 2021). The well-known "greenhouse effect" is the link between CO2 and global warming that leads to climate change (Anderson et al., 2016). According to the WMO (2021), the amount of CO2 concentration in the earth's atmosphere is around 413.20 0.2 ppm, and 55% of it is absorbed by oceans and land vegetation.

Since the middle of the 20th century, anthropogenic landscape activity has been a significant contributor to climate change, which accelerated in 2020 and 2021 despite a 5.6% decrease in fossil fuel CO2 emissions as a result of COVID-19 pandemic restrictions (WMO, 2021). Climate change and the rise in land-use conflicts necessitate the creation of sustainable land-use systems that balance agricultural production with the provisioning of several ecological services. According to global estimates, land use interventions help reduce emissions by roughly 30% through the process of carbon sequestration and are crucial for achieving the carbon reduction goal set by the COP-25 summit (Aynekulu et al., 2020). According to Mangalassery et al. (2014), carbon capture has been considered as a way to help minimise the rising CO2 accumulation in the environment. The soil and plant biomass that make up the large terrestrial carbon pool have the ability to take in and store atmospheric carbon through photosynthesis (Kaul et al., 2010).

It is well known that forestry can improve carbon sinks and lower CO_2 emissions, thus playing a crucial role in carbon cycling and aids in mitigating climate change (Besar et al., 2020; Sarkar et al., 2021). However, the dynamics of nutrients (carbon and nitrogen) in the terrestrial environment were affected by rapid increases in urbanisation and anthropogenic activity (deforestation, land use change, biodiversity loss, and forest degradation; Dhyani et al., 2021; Mey and Gore, 2021; Kumar et al., 2022). However, it is impossible to ignore the role that trees outside forests (TOFs) play in enhancing human well-being and offering ecosystem services. In addition to supplying the needs for timber, industry, and livelihoods in both agricultural and human-dominated landscapes, the TOFs will successfully and effectively enable carbon dioxide (CO2) emissions to be offset by the forest ecosystems (Chauhan et al., 2020). Since they constitute one of the major C pools that contribute to global carbon (C) cycling, tree-based land use systems, particularly those in non-forested environments like agricultural land, have a important impact on process. Productivity in plantation is higher (3.2 Mg ha/1 year) than productivity of natural forest (1.1 Mg ha/1 year), so it can benefit from better silvicultural techniques than a wild forest (Lal and Singh, 2000). Additionally, resource management through agroforestry may offer a natural way to synchronise the implementation of adaptation and mitigation measures with the satisfaction of forest-based needs (Komal et al., 2022). Agroforestry has been acknowledged as a GHG mitigation strategy under the Kyoto Protocol because it is an integrated approach (Birhane et al., 2020; Das et al., 2020; Sarkar et al., 2021). This recognition is based on carbon capture and utilisation efficiency leading to greater carbon sequestration (Das et al., 2020; Semere et al., 2022).

Agroforestry is the deliberate coexistence of woody vegetation with agricultural crops, grasses, or farm animals on the same plot of land to benefit the environment, the economy, and society (Rapidel et al., 2015; Armengot et al., 2020). Agroforestry systems have different structural and functional compositions depending upon the temperature, elevation, soil structure, and rainfall pattern (Rajput et al., 2017; Chisanga et al., 2018; Singh et al., 2019; Birhane et al., 2020; Salve and Bhardwaj, 2020; Nath et al., 2022; Sharma et al., 2022). Given the significance of this activity, India developed a national agroforestry plan in 2014 to promote the full spread of agroforestry practises. The Green India Mission has also noticed agroforestry interferences. The promise of agroforestry to mitigate climate and assist farmers in adapting to its effects is a key driving force behind India's agroforestry programme. The Green India Mission has also noticed agroforestry interferences. The potential of agroforestry to slow climate change and help farmers adapt to its impacts is a major impetus behind India's agroforestry plan. As evidenced by the multiple-purpose trees (such as fodder, fruit, fuelwood, and timber trees) purposefully retained on farm bunds (Semere, 2019; Chavan et al., 2020), agroforestry has been practised historically for as long as anyone can remember. It also plays a significant role in preserving sustainability in farming systems (Chandra and Singh, 2018). Agroforestry has been identified as having the greatest potential for carbon sequestration among all the land uses that were the subject of the Land-Use, Land-Use Change, and Forestry (LULUCF) report's research (Nair and Garrity, 2012). Agroforestry is receiving increased attention in global initiatives like Reducing Emissions from Deforestation and Forest Degradation (REDD) because of its implication in improving and regulating climate variability (Jose and Bardhan, 2012).

Current study focused on the accurate estimation of carbon stock in the prominent agroforestry systems in the eco-sensitive Himalayan region in order to understand the carbon sequestration potential of agroforestry systems in the region. Keeping this in view, the present investigation was carried out with the objective of quantifying the biomass, carbon stock and carbon sequestration potential of different agroforestry systems in district Anantnag of Kashmir division. The study might be helpful in giving information to decision-framers and agriculturists for efficient and long-term carbon balancing and climate variability mitigation in the temperate region of the Kashmir Himalayan ecosystem.

2. Materials and methods

2.1. Study site

The study area is situated in the southern region of Kashmir covering Anantnag district of Jammu and Kashmir, India. The district is 33 miles (53 km) away from Srinagar (the capital city), and is situated between 33° 20′ and 34°15’ N latitude and 74°30’ and 75°35’ E longitude. There is a mild climate in Anantnag (Koppen climate classification). As per Koppen climate classification, district Anantnag is having a mild climate compared to other regions of Kashmir valley Geographical factors like the Karakoram range to its east and the Pir Panjal range to its south greatly influence its climate. A typical description of the climate is that it is cool in the spring and the autumn season, warm in the summer, and frigid in the winter. The region has a temperate climate, with substantial winter snowfall occurring in the higher elevations. The entire southern sector of the study area, which borders the Jammu province tehsils of Reasi, Banihal, and Kishtwar, as well as the eastern sector, which borders the Ladakh division tehsil of Kargil. Pulwama district borders its northern and western sides, and Kulgam district is located on its western side. Anantnag has the most streams (Nallas) in Kashmir valley including Sandran, Brengi, Arpath, and Lidder,. Lidder, which emerges from Sheshnag Lake and irrigates the largest territory in the district, is the most significant of these. The Anantnag district has a wide intermountain valley and is hilly and mountainous in the north-east and south-west. Productivity is vulnerable in higher ranges and fertile in central regions because soil is poor in steep locations and rich in plain areas. Hapludalf is the name given to the medium- to fine-textured soils that have grown on Karewa tops and upland locations. Clay loam soils, which are dark brown in colour, are typical in plains.

In district Anantnag land use land cover category, there is a total of 341 ha dense built-up, 337 ha mixed built-up, 2,176 ha agriculture, 480 ha plantation, 118 ha water bodies, 60 ha wastelands, 196 ha sparse forests and 95 ha dense forests forming a total of 3,803 ha land (Malik, 2012). Nowadays, agroforestry is considered as the primary route to success for farmers and rural residents in the region, thereby generating work and income, ensuring the security of food and nutrition, satisfying other fundamental human requirements and protecting farmers from the effects of climate change (Figure 1).

2.2. Experimental setup

The current research was performed in year 2018–2019 in district Anantnag of Kashmir division. For conducting this study regarding different land use patterns, field survey of all the agroforestry systems prevalent in selected representative areas was carried. Six tehsils, namely Anantnag, Shangus, Kokernag, Dooru, Sallar, and Larnu, were chosen out of a total of twelve. The blocks were chosen using a multistage stratified random selection procedure *viz.*; Anantnag, Shangus, Sagam, Shahabad, Pahalgam and Larnu. Then four villages within each block like Anantnag (Ruhoo, Dialgam, Wanihama and Donipawa), Shangus (Shangus, Nowgam, Kutheir and Andoora), Sagam (Hiller, Khalhar, Sagam and Bidder), Shahabad (Larkipora, Shankerpora, Nathipora and Bragam), Pahalgam (Yanner, Charigam, Movra and Wahdan) and Larnu (Leesu, Dandipora, Bidhard and Larnu). Ten farmers within each village were selected, thus making a total of 240 farmers to document the land use pattern of district Anantnag. A total of 240 households were selected for the field study from the sample villages with a 25% sampling intensity using a basic random sampling technique. Household heads/eldest members were the respondents interviewed during survey programme.

For different agroforestry systems at different sites, one 20 m × 20 m quadrant was laid for measuring tree biomass and three 1 m × 1 m quadrant were laid within 20 m × 20 m quadrant for measuring crop biomass thus making a total of 240 quadrats for trees and 720 quadrats for crops. During survey across the field, in horti-agriculture system, a total number of 555 trees/ha in combination C_1(Apple + radish-kale), 555 trees/ha in combination C_2(Apple + kale-chilli), 555 trees/ha in combination C_3(Apple + kale-beans) and 80 trees/ha in combination C_4(Walnut + oats-maize) were recorded. In agri-silviculture system (boundary plantation), a total of 138 trees /ha in combination C_1(Poplar + salix + oats-paddy) and 160 trees /ha in combination C_2(Poplar + mustard-paddy) were documented (Table 1).

Also, in agri-horti-silviculture system, a total number of 336 trees/ha (156 fruit trees and 180 forest trees), 380 trees/ha (180 fruit trees and 200 forest trees) and 444 trees/ha (204 fruit trees and 240 forest trees) were recorded in combination C_1(Poplar + apple + kale-beans), C_2(Poplar + apple + kale-chilli) and C_3(Poplar + apple + turnip-kale) respectively. Similarly, in horti-silvipasture system, a total of 753 trees/ha (625 fruit trees and 128 forest trees) and 756 trees/ha (625 fruit trees and 131 forest trees) were recorded in combination C_1(Apple + poplar + grasses) and C_2(Apple + poplar + salix + grasses) respectively (Table 1). All the above-mentioned trees (forest and fruit trees) and crops were further evaluated for biomass, carbon stock and carbon sequestration potential.

3. Methodology adopted

3.1. Biomass production

The study calculated both above- ground and below-ground biomass in trees and crops in all agroforestry systems. The above-ground biomass of several plant components, including stems, branches, leaves, and roots, was estimated. Biomass of forest trees, fruit trees and agricultural crops were calculated separately as below:

3.1.1. Forest tree

Forstem biomass with a diameter tape and a Ravi’s multimeter, the diameter of trees at breast height (dbh) that fell in the

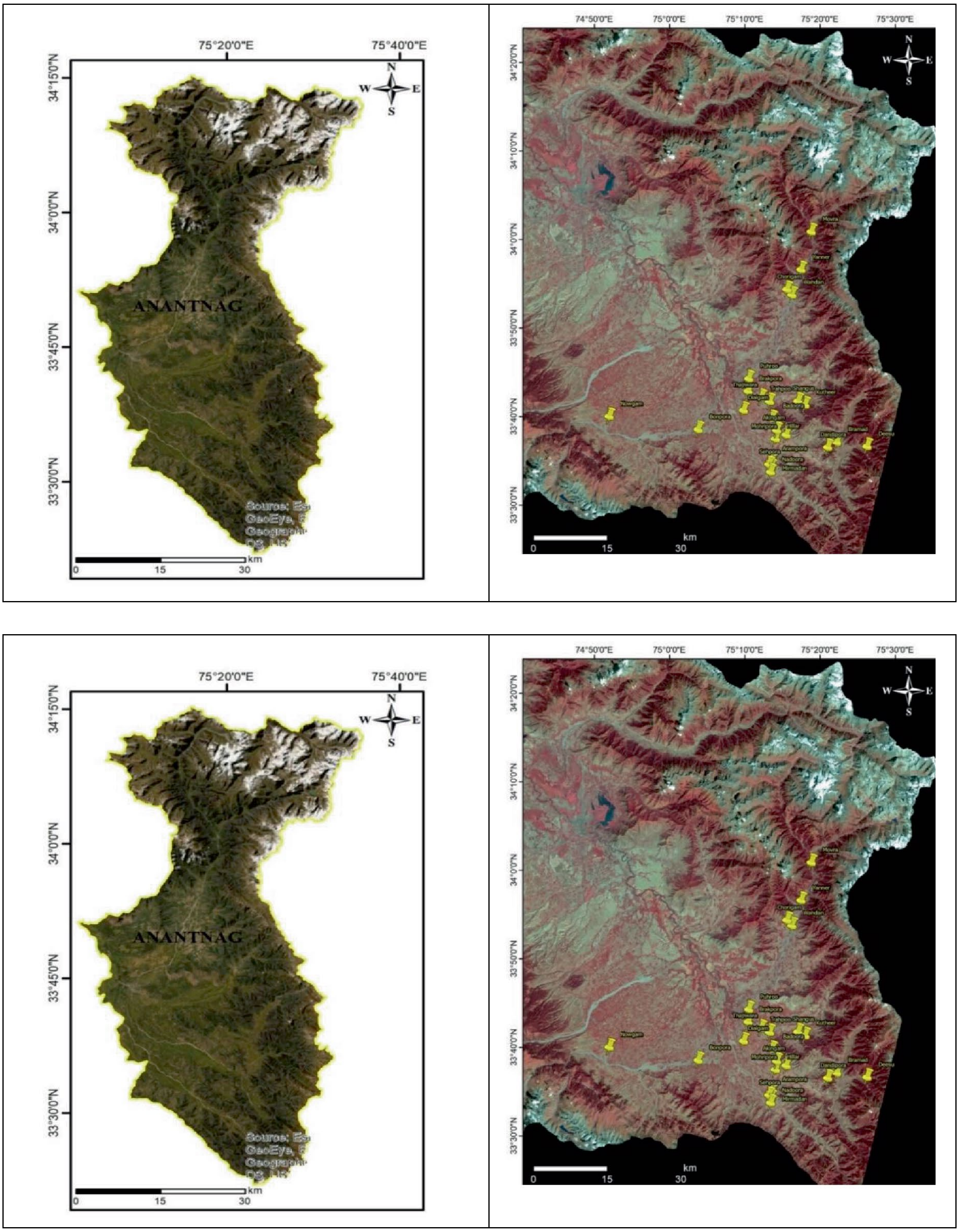

FIGURE 1
Map of sampled villages of district Anantnag, Kashmir.

20 × 20 m quadrat were measured. In order to get the volume using the Pressler (1854) and Bitterlich (1984) formula, the form factor was computed using the Spiegel relascope. Specific gravity was calculated by using formula proposed by Smith (1954). Belowground biomass was measured by using a factor of 0.25 for forest trees (Schulze, 1983). Thus, biomass of stem wood = specific gravity × volume. *For branch biomass* on each sample tree, the aggregate number of branches were calculated regardless of size.

TABLE 1 Inventory of tree-crop combinations in prominent agroforestry systems in study area.

Agroforestry systems	Tree crop combinations	Tree and crop components	Fruit trees			Forest trees		
			Avg. ht. (m) (Mean ± S.E)	Collar dia. (cm) (Mean ± S.E)	Total no. of trees ha^{-1}	Avg. ht. (m) (Mean ± S.E)	dbh (cm) (Mean ± S.E)	Total no. of trees ha^{-1}
Horti-agriculture	C_1	Apple + radish-kale	4.98 ± 0.46	54.5 ± 2.88	555	–	–	–
	C_2	Apple + kale-chilli	4.73 ± 0.41	42.33 ± 2.27	555	–	–	–
	C_3	Apple + kale-beans	4.925 ± 0.41	45.5 ± 3.16	555	–	–	–
	C_4	Walnut + oats-maize	6.85 ± 0.17	50.5 ± 3.0	80	–	–	–
Agri-silviculture (boundary plantation)	C_1	Poplar + salix + oats-paddy	–	–	–	17.66 ± 1.08 7.5 ± 0.74	55.25 ± 1.24 (Poplar) 50.11 ± 1.50 (Salix)	108 + 30 (Poplar + Salix)
	C_2	Poplar + mustard-paddy	–	–	–	17.92 ± 1.33	55.27 ± 0.79	160
Agri-horti-silviculture (homegardens)	C_1	Poplar + apple + kale-beans	4.0 ± 0.34	32.5 ± 2.82	156	22.9 ± 1.09	54.5 ± 1.32	180
	C_2	Poplar + apple + kale-chilli	4.41 + 0.29	40.08 + 2.81	180	18.7 ± 1.61	59.22 ± 0.99	200
	C_3	Poplar + apple + turnip-kale	4.38 ± 0.27	37.63 ± 3.53	204	20.4 ± 0.98	53.1 ± 0.932	240
Horti-silvipasture	C_1	Apple + poplar + grasses	4.71 ± 0.34	39.07 ± 3.5	625	25.36 ± 1.76	58.5 ± 4.86	128
	C_2	Apple + poplar + salix + grasses	4.11 ± 0.22	31.56 ± 3.04	625	19.6 ± 3.11 8.92 ± 1.04	62.77 ± 3.3 56.5 ± 1.84	111 Poplar 20 Salix

Based on the basal diameter, the branches were categorised into three groups: small, medium, and large. Each group's two sampled branches weight was recorded individually. The formula given by Chidumaya (1990) was used to calculate the branch biomass in trees. *Leaf biomass* by dividing the sample tree's branches into three groups based on basal diameter, small, medium, and large, the leaf biomass was calculated. Fresh weight of two sampled branches from each group was recorded separately. Immediately after being severed from the branch, the leaf biomass of each representative branch of the sample trees in each diameter class was counted in 20× 20 m quadrat. The leaf samples from two sampled branches of each group were put in individual bags and oven-dried at 65°C for 72 h, or until the consistent weight is obtained (Chapman, 1964).

3.1.2. Fruit tree

For stem biomass it was calculated by means of the regression equation, prescribed by Brown et al. (1989) and the formula is given as: Y = exp. {−2.4090 + 0.9522 ln (D2HS)}, where, Y = Biomass/tree (kg), D = Tree collar diameter, H = Height of tree (cm), S = Density of wood (g cm-3). *Canopy biomass* Canopy biomass was estimated by multiplying crown volume by specific gravity. Crown volume was estimated by using formula given by Avery and Burkhart (2002) {Crown volume = (db2L)/12, where, db = Crown base diameter (m), L = Length of crown}.

For the purpose of calculating specific gravity, Smith's (1954) maximum moisture method was applied. Fruit samples weighing 1 kg were sun dried followed by oven dried at 60°C until their weight remained constant. Belowground biomass was determined by using formula given by Singh (2010). Then total biomass was computed by summing up of the total above-ground biomass and belowground biomass of the fruit trees.

3.1.3. Crop biomass

Crop (rabi and kharif) and grass biomass were measured by means of (1 × 1) m quadrates. At the time of harvest, the total biomass was determined by uprooting, which was then evaluated to calculate green/fresh weight. The samples were put in individual bags and dried in an oven at 65°C for 72 h, or until the weight remained consistent (Chapman, 1964). *Estimation of carbon*. The calculation of carbon stock was determined by multiplying total biomass by a conversion factor that represents the average carbon content in biomass. The default value of 0.45 for the conversion of biomass to carbon was used (Woomer, 1999). Therefore, the total carbon stock (C) present in the calculated total biomass was equal to C = 0.45 × Biomass (total). The mitigation potential of the system was worked out by calculating equivalent carbon dioxide (eCO_2) as per formula: $CO_2e = C \times 3.67$.

3.2. Data analysis

The data obtained were subjected to the statistical analysis as per procedure given by Gomez and Gomez (1984) using R-software and SAS statistical package. Also, one-way ANOVA was used for analyzing the data of different systems in the present study.

<table>
<tr><td></td><td></td></tr>
<tr><td>Walnut + oatsunder horti-agriculture</td><td>Apple + beans under horti-agriculture</td></tr>
<tr><td></td><td></td></tr>
<tr><td>Poplar + mustard under boundary plantation</td><td>Poplar, salix and paddy under boundary plantation</td></tr>
<tr><td></td><td></td></tr>
<tr><td>Poplar, apple, turnip and kale under homegardens</td><td>Poplar + apple + kale + beans under homegardens</td></tr>
<tr><td></td><td></td></tr>
<tr><td>Apple, poplar and grasses under horti-silvi-pasture</td><td>Apple + poplar + salix + grasses under horti-silvi-pasture</td></tr>
</table>

4. Results

Among four different systems under study, the horti-silvi-pasture system recorded maximum aboveground tree biomass (43.11 t/ha), belowground tree biomass (12.58 t/ha) and total tree biomass (55.73 t/ha) and was significantly greater than all other agroforestry systems. The agri-silvipasture (homegardens) however was found next to horti-silvipasture recording 30.80 t/ha, 8.16 t/ha and 32.76 t/ha as aboveground tree biomass, belowground tree biomass and total tree biomass respectively, while as significantly lowest aboveground tree biomass (15.44 t ha −1), belowground tree biomass (3.84 t ha − 1) and total tree biomass (19.3 t ha −1) were recorded in agri-silviculture system (boundary plantation). Also, maximum total crop biomass was found in agri-silviculture (boundary plantation) as 15.54 $t\,ha^{-1}$, which was significantly higher than all other agroforestry systems. The horti-agriculture system was found next to agri-silviculture (boundary plantation) recording 12.52 t/ha as total crop biomass, while as lowest total crop biomass (10.82 $t\,ha^{-1}$) was recorded in horti-silvipasture system. Total biomass production (tree+ crop component) followed a similar pattern as that seen in above and below ground tree biomass, with horti-silvi-pastoral system contributing maximum as 66.55 $t\,ha^{-1}$ which was significantly higher than all other systems and was followed by agri-horti-silviculture as 50.18 $t\,ha^{-1}$ and horti-agriculture as 36.22 $t\,ha^{-1}$. Minimum value was recorded under agri-silviculture (boundary plantation) as 34.87 $t\,ha^{-1}$ (Table 2).

Since both carbon storage and carbon capture capability of all the systems are directly linked to the biomass production of the various plant components, so they both match their capacity for biomass production. Plant biomass can vary significantly in terms of carbon content in an intricate agroforestry system, and this variation affects production. Productivity is determined by a variety of elements, including age, kind of soil, crop type, growing habits, and management intensity. So, in our study, a similar trend was observed in values of carbon stock and carbon sequestration potential as that of above-mentioned total biomass estimations in agroforestry systems. Horti-silvipasture was having highest values for tree carbon stock (25.07 $t\,ha^{-1}$) and tree carbon sequestration potential (92.04 $t\,ha^{-1}$) and were significantly higher than all other systems. The agri-silvipasture (homegardens) however was found next to horti-silvipasture recording 38.82 $t\,ha^{-1}$ and 64.33 $t\,ha^{-1}$ as tree carbon stock and carbon sequestration potential respectively, while as significantly lowest tree carbon stock and sequestration potential as 8.68 $t\,ha^{-1}$and 31.85 $t\,ha^{-1}$, respectively, were recorded in agri-silviculture system (boundary plantation).Also, maximum total crop carbon stock and carbon sequestration potential was found in agri-silviculture (boundary plantation) as 7.98 $t\,ha^{-1}$ and 25.65 $t\,ha^{-1}$ respectively, which was significantly higher than all other agroforestry systems. The horti-agriculture system was found next to agri-silviculture (boundary plantation) recording 5.63 $t\,ha^{-1}$and 20.62 $t\,ha^{-1}$as total crop carbon stock and sequestration potential, while as lowest total crop carbon stock and sequestration potential (4.86 $t\,ha^{-1}$ and 17.93 $t\,ha^{-1}$ respectively) were recorded in horti-silvipasture system (Tables 3, 4).

The overall comparison of agroforestry systems practised by the farmers of Anantnag district clearly shows that the horti-silvipastoral system outperforms the other agroforestry systems and are most productive in terms of total biomass accumulation (66.55 $t\,ha^{-1}$), carbon stock (29.94 $t\,ha^{-1}$) and carbon dioxide sequestration potential of 104.4 $t\,ha^{-1}$ (Tables 2–4). The involvement of forest trees in the horti-silvipastoral system was 37.83%, fruit trees as 45.86% and crop (rabi and kharif) contributed 16.29% in biomass, carbon stock and carbon sequestration potential. Agri-silviculture, on the other hand, was least productive in terms of total biomass (34.87 $t\,ha^{-1}$), carbon stock (15.67 $t\,ha^{-1}$) and CO_2 sequestration potential (57.58 $t\,ha^{-1}$). The contribution of forest trees in agri-silviculture system was 55.36% and crops contribute 44.61%.

5. Discussion

The horti-silvi-pasture system recorded maximum aboveground tree biomass (43.11 t/ha), belowground tree biomass (12.58 t/ha) and total tree biomass (55.73 t/ha) and was significantly greater than all other agroforestry systems. Also, lowest aboveground tree biomass (15.44 t ha −1), belowground tree biomass (3.84 t ha − 1) and total tree biomass (19.3 t ha −1) was recorded in agri-silviculture system (boundary plantation). In horti-silvi-pasture systems, the density of trees being high and greater average height and dbh values of individual trees will contribute to the higher values of total tree biomass and *vice-versa* (fewer trees per hectare in agri-silviculture). Also, aboveground biomass is a valuable resource in most land use regimes, so more biomass is allocated to aboveground components as it includes biomass from tree's trunk, stump, branch, twig, and leaves, as opposed to the tree's underground biomass, which only includes biomass from its fine and coarse roots. The number of woody plants in a specific agro-forestry system, as well as management strategies, play a vital impact in affecting biomass in a particular agro forestry system (Dar et al., 2019; Siarudin et al., 2021; Kumar et al., 2022). Agroforestry systems are complex and heterogeneous and, the more the heterogeneity, the more efficiently the carbon is sequestered compared to simpler systems (Rai et al., 2021; Tamang et al., 2021). However, the efficiency of Agroforestry systems as carbon sinks is governed by their size, natural site qualities, choice of species and management practises followed, i.e., carbon sequestered by an AFS depends on its structure and composition modified by environmental and socio-economic factors. Moreover, inter- and intra-specific variation in tree diameter, stand age, stand structure and diversity of the system also affect variation in biomass and its carbon (Bajigo et al., 2015; Panwar et al., 2022). Similarly, study conducted by Devagiri et al. (2020) in western Ghats region of peninsular India found that coffee agroforests resembled natural forest and mixed species plantations in terms of biomass production due to presence of tree diversity in this system. Also, study conducted by Panwar et al. (2022) reported that AGB was highest in block plantations (mean = 109.8 Mg ha − 1), followed by plantation crop systems (mean = 88.49 Mg ha − 1), with the lowest AGB observed in boundary plantations (mean = 17.14 Mg ha − 1). BGB was highest in homegardens (mean = 34.68 Mg ha − 1), followed by block plantations (mean = 26.19 Mg ha − 1), and lowest in boundary plantations (mean = 2.67 Mg ha − 1).

Current study also witnessed that agri-silviculture (boundary plantation) contributed maximum crop biomass as 15.54 $t\,ha^{-1}$, which was significantly higher than all other agroforestry systems and minimum was recorded in horti-silvipasture system (10.82 $t\,ha^{-1}$; Table 2). Greater crop biomass observed in case of agri-silviculture system might be due to the consistent and enough solar incidence in open agricultural fields as a result of larger open photosynthetic area, and the absence of competition between

TABLE 2 Aboveground, belowground and total biomass (t ha^{-1}) production in prominent agroforestry systems.

Agroforestry system	Aboveground tree biomass			Belowground tree biomass			Total tree biomass			Total crop biomass			Total biomass
	Fruit tree	Forest tree	Total	Fruit tree	Forest tree	Total	Fruit tree	Forest tree	Total	Rabi	Kharif	Total	
Horti-agriculture	17.8	–	17.8^{c}	5.87	–	5.87^{c}	23.7	–	23.7^{c}	5.20	7.32	12.52^{b}	36.22^{c}
Agri-silviculture (boundary plantation)	–	15.44	15.44^{c}	–	3.84	3.84^{d}	–	19.3	19.3^{d}	5.64	9.9	15.54^{a}	34.87^{c}
Agri-horti-silviculture (homegardens)	5.95	24.85	30.80^{b}	1.95	6.21	8.16^{b}	7.91	24.85	32.76^{b}	5.53	5.62	11.15^{c}	50.18^{b}
Horti-silvipasture	22.96	20.15	43.11^{a}	7.56	5.02	12.58^{a}	30.54	25.19	55.73^{a}	7.18	3.64	10.82^{c}	66.55^{a}
C.D$_{(p \leq 0.05)}$			3.43			0.37			3.73			1.25	3.77
S.E±			1.03			0.10			1.05			0.35	1.07

Letters used as subscript represents variance among the systems and same letters depict non-significant variance among two systems.

TABLE 3 Aboveground, belowground and total carbon stock (t ha^{-1}) in prominent agroforestry systems.

Agroforestry systems	Aboveground tree carbon stock			Belowground tree carbon stock			Total tree carbon stock			Total crop carbon stock			Total carbon stock
	Fruit tree	Forest tree	Total	Fruit tree	Forest tree	Total	Fruit tree	Forest tree	Total	Rabi	Kharif	Total	
Horti-agriculture	8.01	–	8.01^{c}	2.64	–	2.64^{c}	10.66	–	10.66^{c}	2.33	3.29	5.63^{b}	16.28^{c}
Agri-silviculture (boundary plantation)	–	6.95	6.95^{d}	–	1.73	1.73^{d}	–	8.68	8.68^{d}	2.54	5.44	7.98^{a}	15.67^{c}
Agri-horti-silviculture (homegardens)	2.68	11.18	13.86^{b}	0.88	2.79	3.67^{b}	13.97	24.85	38.82^{a}	2.49	2.53	5.02^{c}	22.56^{b}
Horti-silvipasture	10.33	9.06	19.39^{a}	3.40	2.26	5.66^{a}	13.74	11.33	25.07^{b}	3.23	1.63	4.86^{d}	29.94^{a}
C.D$_{(p \leq 0.05)}$			0.49			0.16			1.68			0.56	1.7
S.E±			0.14			0.04			0.47			0.15	0.48

Letters used as subscript represents variance among the systems and same letters depict non significant variance among two systems.

woody perennials and agricultural crops for moisture, light, nutrients, and space, among other factors. Minimum biomass of grass species in case of horti-silvipasture might be because trees and grasses compete for the same resources, such as sunlight, water, and nutrients. Our results are corroborated with Nandal and Singh (2001), Handa et al. (2004), Yadav (2010), and Chauhan et al. (2008) who found that increasing the distance between trees and crops, improved crop performance and production. Chavan et al. (2022) also, reported that the performance of sorghum and wheat crops is strongly influenced by the distance from tree lines and the age of the poplar trees and might be due to significant interaction between distance and aspect that was attributed to small differences in the intensity and duration of shadows cast by the boundary stands. Such study also observed a significant reduction of fodder biomass of sorghum and wheat yield was observed up to 9 m distant from the tree line. The reduction was 10–60% for the kharif season and 7.2–29.5% for rabi crops from the 2nd year to 8 years after planting, respectively. Similarly, Honfy et al., 2023 investigated the tree planting pattern of black locust (*Robinia pseudoacacia* L.) when intercropped with triticale (*x Triticosecale* W.) and observed that more the trees planted on a hectare, the higher the volume of the stand, and the less yield of triticale. Studies carried out by various researchers observed that a significant yield reduction of more than 70% was observed near the tree base (0–3 m) and about a 10–35% reduction up to 9 m away from the tree (Yang et al., 2015).

Total biomass (tree + crop component) followed a similar pattern as in above and below ground tree biomass, with horti-silvi-pastoral system contributing maximum as 66.55 t ha^{-1} which was significantly higher than all other agroforestry systems and was followed by agri-horti-silviculture as 50.18 t ha^{-1} and horti-agriculture as 36.22 t ha^{-1}. Also, minimum total biomass was recorded under agri-silviculture as 34.87 t ha^{-1} (Table 2). This could be attributed to higher tree density and difference in management regimes; for example, in horti-silvipasture system, farmers retain native trees in large numbers to provide them fruit on a large scale and forest trees serve as live fence, thus overcomes fodder scarcity.

TABLE 4 Aboveground, belowground and total carbon sequestration (t ha−1) potential in prominent agroforestry systems.

Agroforestry systems	Aboveground tree carbon sequestration			Belowground tree carbon sequestration			Total tree carbon sequestration			Total crop carbon sequestration			Total carbon sequestration
	Fruit tree	Forest tree	Total	Fruit tree	Forest tree	Total	Fruit tree	Forest tree	Total	Rabi	Kharif	Total	
Horti-agriculture	29.39	–	29.39^c	9.68	–	9.68^c	39.12	–	39.12^c	8.55	12.07	20.62^b	59.83^c
Agri-silviculture (boundary plantation)	–	25.50	25.50^d	–	6.35	6.35^d	–	31.85	31.85^c	9.32	16.33	25.65^a	57.58^c
Agri-horti-silviculture (homegardens)	9.83	41.04	50.87^b	3.23	10.24	13.47^b	13.06	51.27	64.33^b	9.14	9.28	18.42^c	82.8^b
Horti-silvipasture	37.9	33.28	71.18^a	12.5	8.32	20.82^a	50.44	41.60	92.04^a	11.9	6.03	17.93^c	104.4^a
$C.D_{(p \leq 0.05)}$			1.813			0.61			6.17			2.06	6.24
S.E±			0.514			0.17			1.74			0.58	1.77

Letters used as subscript represents variance among the systems and same letters depict non significant variance among two systems.

Similary, carbon stock and carbon sequestration values of different agroforestry systems follows same trend as in above mentioned biomass production being significantly more in horti-silvipasture followed by agri-horti-silviculture (homegardens) and horti-agriculture and minimum values in agri-silviculture (boundary plantation). The inclusion of forest trees in the agroforestry system, which results in continuous carbon locking in woody plants, and the natural accumulation of fallen leaf debris to soil, which assists in the build-up of carbon in soil beds and, consecutively, aids in considerable production of structure, may be the primary causes of the maximum carbon reserve in horti-silvipasture and agri-horti-silviculture (homegardens). However, most of the biomass in horti-agriculture and agri-silviculture (boundary planation) is taken yearly by harvesting, trimming, and felling. The ability to capture carbon dioxide rely on variety of characteristics, involving species type, genetic make-up, maturity, structure, functional components, and number. Tree plantations are a better option for reducing atmospheric carbon since they store more carbon, but due to population pressure and the rising demands for agricultural land, these plantations fail to extend. As a result, the agroforestry system appears to be a better alternative for preserving biodiversity while still providing economic advantages to society. Nair et al. (2009) reported that the capacity for carbon capture in agroforestry land use systems is based on the woody element. Farmlands has greater capacity to sequester carbon with highest woody component than other land use systems (lesser woody components; Sureshbhai et al., 2017; Dar et al., 2019). The ability of different agroforestry systems to store carbon varies greatly, and the amount of carbon stored is mostly influenced by the kind of agroforestry system utilised, its arrangement and role, as well as the surrounding environment and socioeconomic factors. Tree species and system management are two further elements that may influence carbon storage in agroforestry system (Nair et al., 2010).

6. Conclusion

Agroforestry systems has a greater capacity to influence the source or sink role of the trees. It could play an important role in mitigating climate change as it sequesters more atmospheric carbon in plant parts and soil than conventional farming. The present study recognised the capability of various agroforestry systems for biomass estimation and carbon sequestration potential for mitigating climate variation in north-western Himalayas. Agroforestry systems differed in terms of biomass output and carbon sequestration potential. As seen from the data, the horti-silvipasture system recorded maximum values for biomass and carbon sequestration potential, agri-silviculture system (boundary plantation) recorded minimum values. So, the study concluded that horti-silvipasture system outperforms the other agroforestry systems and are most productive in terms of carbon sequestration potential. Thus, adopting these agroforestry systems not only contributes to environmental stability by reducing carbon dioxide emissions, but it also increases farming income, so improving farmer livelihood. As a result, if the carbon trapped by these systems is traded to rich countries, there is a compelling financial incentive for farmers to use them thus, by development of suitable agroforestry systems in diverse agroclimatic zones, not only the area of greenery in the country be increased, but the proportion of greenhouse gases in the environment may also be significantly reduced. Therefore, agroforestry will be a workable method for reducing climate crises if it is encouraged for greater adoption by cultivators in the nation.

Data availability statement

The original contributions presented in the study are included in the article/supplementary material, further inquiries can be directed to the corresponding author.

Author contributions

IS and JAM framed the concept. IS, BM, and AA did the field work. IS, JAM, NAP, GMB, AHM, and THM did the analysis and drafted the manuscript. IS and NAP finalised the manuscript. All authors contributed to the article and approved the submitted version.

Conflict of interest

The authors declare that the research was conducted in the absence of any commercial or financial relationships that could be construed as a potential conflict of interest.

Publisher's note

References

Anderson, T. R., Hawkins, E., and Jones, P. D. (2016). CO2, the greenhouse effect and global warming: from the pioneering work of Arrhenius and Callendar to today's earth system models. *Endeavour* 40, 178–187. doi: 10.1016/j.endeavour.2016.07.002

Armengot, L., Ferrari, L., Milz, J., Velasquez, F., Hohmann, P., and Schneider, M. (2020). Cacao agroforestry systems do not increase pest and disease incidence compared with monocultures under good cultural management practices. *Crop Prot.* 130:105047. doi: 10.1016/j.cropro.2019.105047

Avery, T.E., and Burkhart, H.E. (2002). *Forest Measurements*, *5th*. MCGraw-Hill Series in Forest Resources, New York, USA.

Aynekulu, E., Suber, M., Noordwijk, M., Arango, J., Roshetko, J. M., and Rosenstock, T. S. (2020). Carbon storage potential of silvopastoral systems of Colombia. *Land* 9, 1–12. doi: 10.3390/land9090309

Bajigo, A., Tadesse, M., Moges, Y., and Anjulo, A. (2015). Monitoring of seasonal variation in physicochemical water parameters in Nalasopara region. *J. Ecosyst. Ecography* 5:157.

Besar, N. A., Suaedi, H., Phua, M. H., James, D., Mokhtar, M. B., and Ahmed, M. F. (2020). Carbon stock and carbon sequestration potential of an agroforestry system in Sabah. Malaysia. *Forests* 11, 1–16. doi: 10.3390/f11020210

Birhane, E., Ahmed, S., Hailemariam, M., Negash, M., Rannestad, M. M., and Norgrove, L. (2020). Carbon stock and woody species diversity in homegarden agroforestry along an elevation gradient in southern Ethiopia. *Agrofor. Syst.* 94, 1099–1110. doi: 10.1007/s10457-019-00475-4

Bitterlich, W. (1984). *The Relaskop Idea Slough: Commonwealth Agricultural Bureaux*. Farnham Royal, England pp.242.

Brown, S., Gillespie, A. J. R., and Lugo, A. E. (1989). Biomass estimation methods for tropical forests with application to forest inventory data. *For. Sci.* 35, 881–902.

Chandra, K. K., and Singh, A. K. (2018). Carbon stock appraisal of naturally growing trees on farmlands in plain zone districts of Chhattisgarh. India. *Trop. Ecol.* 59, 679–689.

Chapman, H. D. (1964). Suggested foliar sampling and handling techniques for determining the nutrient status of some field, horticultural and plantation crops. *Indian J Hortic.* 21, 94–105.

Chauhan, V. K., Joshi, A. K., and Dholta, V. K. (2008). Performance of maize (*Zea maize* L.) varieties under different spacings of poplar (*Populus deltoids* M.) in lower western Himalayas. *Indian Forester* 134, 1603–1611.

Chauhan, M., Kumar, M., and Kumar, A. (2020). Impact of carbon stocks of *Anogeissus latifolia* on climate change and socio-economic development: a case study of Garhwal Himalaya, India. *Water Air Soil Pollut.* 231:436. doi: 10.1007/s11270-020-04803-8

Chavan, S. B., Dhillon, R. S., Sirohi, C., Keerthika, A., Kumari, S., Bharadwaj, K. K., et al. (2022). Enhancing farm income through boundary plantation of poplar (*Populus deltoides*): an economic analysis. *Sustainability* 14:8663. doi: 10.3390/su14148663

Chavan, S. B., Newaj, R., Rizvi, R. H., Ajit, P. R., Alam, B., Handa, A. K., et al. (2020). Reduction of global warming potential Vis-a-Vis greenhouse gases through traditional agroforestry systems in Rajasthan, India. *Environ. Dev. Sustain.* 23, 4573–4593. doi: 10.1007/s10668-020-00788-w

Chidumaya, E. N. (1990). Aboveground woody biomass structure and productivity in Zambezian woodland. *For. Ecol. Manag.* 36, 33–46. doi: 10.1016/0378-1127(90)90062-G

Chisanga, K., Bhardwaj, D. R., Pala, N. A., and Thakur, C. L. (2018). Biomass production and carbon stock inventory of high-altitude dry temperate land use systems in North Western Himalayas. *Ecol. Process.* 7, 1–13. doi: 10.1186/s13717-018-0134-8

Dar, M. D., Qaisar, K. N., Masoodi, T. H., Mughal, A. H., and Khan, P. A. (2019). Biomass production and carbon stock potential under home gardens of Kashmir Himalaya. *J. Plant Dev. Sci.* 11, 265–271.

Das, M., Nath, P. C., Reang, D., Nath, A. J., and Das, A. K. (2020). Tree diversity and the improved estimate of the carbon storage for traditional agroforestry systems in north-East India. *Appl Ecol Environ Sci* 8, 154–159.

Devagiri, G. M., Khaple, A. K., Anithraj, H. B., Kushalappa, C. G., Amaresh Kumar, K., and Shashi Bhushan, M. (2020). Assessment of tree diversity and above-ground biomass in coffee agroforest dominated tropical landscape of India's Central Western Ghats. *J For Res* 31, 1005–1015. doi: 10.1007/s11676-019-00885-1

Dhyani, S., Murthy, I. K., Kadaverugu, R., Dasgupta, R., Kumar, M., and Gadpayle, K. A. (2021). Agroforestry to achieve global climate adaptation and mitigation targets: are south Asian countries sufficiently prepared? *Forests* 12:303. doi: 10.3390/f12030303

Gomez, K.A., and Gomez, A.A. (1984). *Statistical Procedure for Agricultural Research*. *2nd*, Willey, Hoboken, 28–192.

Handa, D. P., Jaggis, S., Gill, A. S., and Singh, N. P. (2004). Impact of fruit trees of the yield of wheat crop. *Indian J. For.* 27, 141–144.

Honfy, V., Pödör, Z., Keser, U. Z., Rásó, J., Ábri, T., and Borovics, A. (2023). The effect of tree spacing on yields of alley cropping systems—a case study from Hungary Veronika. *Plan. Theory* 12:595. doi: 10.3390/plants12030595

Jose, S., and Bardhan, S. (2012). Agroforestry for biomass production and carbon sequestration: an overview. *Agrofor. Syst.* 86, 105–111. doi: 10.1007/s10457-012-9573-x

Kaul, M., Mohren, G. M. J., and Dadhwal, V. K. (2010). Carbon storage and sequestration potential of selected tree species in India. *Mitig. Adapt. Strateg. Glob. Chang.* 15, 489–510. doi: 10.1007/s11027-010-9230-5

Komal, N., Zaman, Q., Yasin, G., Nazir, S., Ashraf, K., Waqas, M., et al. (2022). Carbon storage potential of agroforestry systems near brick kilns in irrigated agro-ecosystem. *Agriculture* 12, 1–13. doi: 10.3390/agriculture12020295

Kumar, A., Mishra, S., Pandey, R., Yu, Z., Kumar, M., Khoo, K. S., et al. (2022). Microplastics in terrestrial ecosystems: un-ignorable impacts on soil characterises, nutrient storage and its cycling. *TrAC Trends Anal. Chem.* 158:116869. doi: 10.1016/j.trac.2022.116869

Lal, M., and Singh, R. (2000). Carbon sequestration potential of Indian forests. *Environ Monit Assess* 60, 315–327. doi: 10.1023/A:1006139418804

Malhi, G. S., Kaur, M., and Kaushik, P. (2021). Impact of climate change on agriculture and its mitigation strategies: a review. *Sustainability* 13:1318. doi: 10.3390/su13031318

Malik, M. I. (2012). Analysis of population growth and land use change in Anantnag town of South Kashmir using remote sensing and geographical information system. *J. Exp. Sci.* 3, 23–27.

Mangalassery, S., Dayal, D., Meena, S. L., and Ram, B. (2014). Carbon sequestration in agroforestry and pasture systems in arid northwestern India. *Curr. Sci.* 107, 1290–1293.

Mey, C. B. J., and Gore, M. L. (2021). Biodiversity conservation and carbon sequestration in agroforestry systems of the Mbalmayo Forest reserve. *J For Environ Sci* 37, 91–103.

Nair, P. K. R., and Garrity, D. (2012). "Agroforestry research and development: the way forward" in *Agroforestry – The Future of Global Land Use*. eds. N. PKR and D. Garrity (Dordrecht: Springer), 515–531.

Nair, P. K. R., Kumar, B. M., and Nair, V. D. (2009). Agroforestry as a strategy for carbon sequestration. *J. Plant Nutr. Soil Sci.* 172, 10–23. doi: 10.1002/jpln.200800030

Nair, P. K. R., Nair, V. D., Mohan Kumar, B., and Showalter, J. M. (2010). "Chapter five - carbon sequestration in agroforestry systems" in *Advances in Agronomy*. ed. D. L. Sparks, vol. *108* (Academic Press), 237–307.

Nandal, D. P. S., and Singh, R. R. (2001). Productivity of different cropping sequences in *Dalbergia sissoo* Roxb. Based agroforestry silviculture system. *Indian J. Agroforestry* 24, 433–436.

Nath, P. C., Thangjam, U., Kalita, S. S., Sahoo, U. K., Giri, K., and Nath, A. J. (2022). Tree diversity and carbon important species vary with traditional agroforestry managers in the Indian eastern Himalayan region. *Environ. Sci. Pollut. Res.* 29, 64732–64744. doi: 10.1007/s11356-022-20329-4

Panwar, P., Mahalingappa, D. G., Kaushal, R., Bhardwaj, D. R., Chakravarty, S., Shukla, G., et al. (2022). Biomass production and carbon sequestration potential of different agroforestry systems in India: a critical review. *Forests* 13, 1–15. doi: 10.3390/f13081274

Pressler, M. (1854). *Forest Mensuration and Age Determination*. New York: McGrew Hill Book Co.

Rai, P., Vineeta, , Shukla, G., Manohar, K. A., Bhat, J. A., Kumar, A., et al. (2021). Carbon storage of single tree and mixed tree dominant species stands in a reserve Forest—case study of the eastern sub-Himalayan region of India. *Land* 10:435. doi: 10.3390/land10040435

Rajput, B. S., Bhardwaj, D. R., and Pala, N. A. (2017). Factors influencing biomass and carbon storage potential of different landuse systems along an altitudinal gradient in temperate northwestern Himalayas. *Agrofor. Syst.* 91, 479–486. doi: 10.1007/s10457-016-9948-5

Rapidel, B., Ripoche, A., Allinne, C., Metay, A., Deheuvels, O., Lamanda, N., et al. (2015). Analysis of ecosystem services trade-offs to design agroecosystems with perennial crops. *Agron. Sustain. Dev.* 35, 1373–1390. doi: 10.1007/s13593-015-0317-y

Salve, A., and Bhardwaj, D. R. (2020). Soil carbon stock and nutrient study in different agroforestry systems at Kinnaur district, Himachal Pradesh. *Plant Arch.* 20, 4251–4260.

Sarkar, P. K., Sarkar, P., and Kumar, A. (2021). Carbon storage potential of a waterlogged agroforestry system of Tripura. India. *Water Air Soil Pollut* 232, 232–151. doi: 10.1007/s11270-021-05098-z

Schulze, E. D. (1983). Root shade interaction and plant life forms. *J. Agric. Sci.* 4, 291–303.

Semere, M. (2019). Biomass and soil carbon stocks assessment of agroforestry systems and adjacent cultivated land, in Chehawereda, Gurage zone, Ethiopia. *Int. J. Res. Agric. For.* 6, 17–24.

Semere, M., Cherinet, A., and Gebreyesus, M. (2022). Climate resilient traditional agroforestry systems in Silite district, southern Ethiopia. *J. For. Sci.* 68, 136–144. doi: 10.17221/151/2021-JFS

Sharma, P., Bhardwaj, D. R., and Singh, M. K. (2022). Geospatial technology in agroforestry: status, prospects, and constraints. *Environ. Sci. Pollut. Res.* doi: 10.1007/s11356-022-20305-y

Siarudin, M., Rahman, S. A., Artati, Y., Indrajaya, Y., Narulita, S., Ardha, M. A., et al. (2021). Carbon sequestration potential of agroforestry systems in degraded landscapes in West Java, Indonesia. *Forests* 12:714. doi: 10.3390/f12060714

Singh, B. (2010). Bioeconomic Appraisal and Carbon Sequestration Potential of Different Land Use Systems in Temperate North-Western Himalayas. Ph.D Thesis Dr. Y S Parmar University of Horticulture and Forestry, Nauni, Solan.

Singh, R., Bhardwaj, D. R., Pala, N. A., and Rajput, B. S. (2019). Biomass production and carbon stock potential of natural vegetation, agroforestry and cultivated land use systems along altitudinal gradient in north western Himalayas. *Range Manage. Agroforestry* 40, 94–103.

Smith, D. M. (1954). Maximum Moisture Content for Determining Specific Gravity of Small Wood Samples. Forest Product Laboratory. USDA Forest Service Report pp. 2014.

Sureshbhai, P. J., Thakur, N. S., Jha, S. K., and Kumar, V. (2017). Productivity and carbon sequestration under prevalent agroforestry systems in Navsari District, Gujarat, India. *Int. J. Curr. Microbiol. App. Sci.* 6, 3405–3422. doi: 10.20546/ijcmas.2017.609.419

Tamang, M., Chettri, R., Vineeta, , Shukla, G., Bhat, J. A., Kumar, A., et al. (2021). Stand structure, biomass and carbon storage in *Gmelina arborea* plantation at agricultural landscape in foothills of eastern Himalayas. *Land* 10:387. doi: 10.3390/land10040387

WMO, (2021). *State of the Global Climate. 2021. WMO Provisional Report*. World Meteorological Organization, Geneva, Switzerland, p. 47.

Woomer, P. L. (1999). Impact of cultivation of carbon fluxes in woody savannahs of southern Africa. *Water Air Soil Pollut.* 70, 403–412.

Yadav, A. K. (2010). Carbon sequestration: underexploited environmental benefits of Tarai agroforestry systems. *Indian J. Soil Conserv* 38, 125–131.

Yang, Z. C., Zhao, N., Huang, F., and Lv, Y. Z. (2015). Long-term effects of different organic and inorganic fertilizer treatments on soil organic carbon sequestration and crop yields on the North China plain. *Soil Tillage Res.* 146, 47–52. doi: 10.1016/j.still.2014.06.011

Zandalinas, S. I., Fritschi, F. B., and Mittler, R. (2021). Global warming, climate change, and environmental pollution: recipe for a multifactorial stress combination disaster. *Trends Plant Sci.* 26, 588–599. doi: 10.1016/j.tplants.2021.02.011

Frontiers in
Forests and Global Change

Informs and promotes sustainable management of the world's forests

An innovative journal that places forests at the forefront of attention for scientists, policy makers and the public. It advances our understanding of how forests 'work', spanning from molecules to ecosystems to the biosphere.

Discover the latest Research Topics

See more →

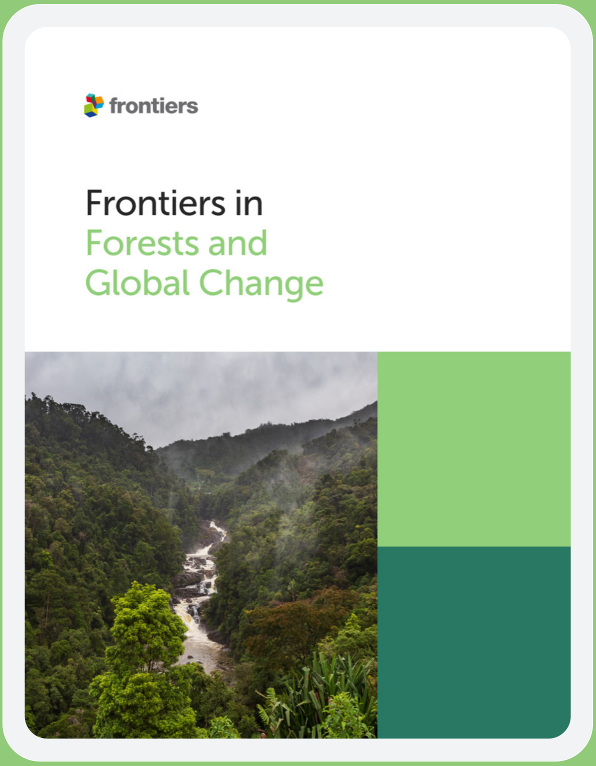
frontiers

Frontiers in
Forests and
Global Change

Frontiers

Avenue du Tribunal-Fédéral 34
1005 Lausanne, Switzerland
frontiersin.org

Contact us

+41 (0)21 510 17 00
frontiersin.org/about/contact